FUNCTIONAL SIGNIFICANCE AND EXPRESSION ANALYSIS OF *N*-ACETYLGALACTOSAMINYLTRANSFERASE-1 IN BREAST CANCER

SIM WEY CHENG

(B.Sc. (Hons), NUS)

A THESIS SUBMITTED

FOR THE DEGREE OF DOCTOR OF PHILOSOPHY

DEPARTMENT OF ANATOMY

NATIONAL UNIVERSITY OF SINGAPORE

2013

DECLARATION

I hereby declare that this thesis is my original work and it has been written by me in its entirety.

I have duly acknowledged all the sources of information which have been used in the thesis.

This thesis has also not been submitted for any degree in any university previously.

_____

Sim Wey Cheng

23 August 2013.

ACKNOWLEDGEMENTS

First of all, I would like to express my deepest gratitude to my Principal Investigator, Associate Professor Yip Wai Cheong, Department of Anatomy, Yong Loo Lin School of Medicine, National University of Singapore (NUS) who had given me the chance to work as a Research Assistant at the same time I had my PhD study as a part-time student. I have learnt a lot in this four and a half year of work and study. A/P Yip's enthusiasm in research and his high self-requirement spirit have enlightened me to excel in my career and study. He has always been helpful and caring when I experienced obstacles and I learnt a lot in problem solving from his valuable advices and critical comments.

My heart-felt thanks extend to the head of Anatomy Department, Professor Bay Boon Huat. Although there is not much interaction between us on work, Prof Bay has always been caring and concerned about my work progress as a staff and student. His spirit of gathering all the members of the department into 'One Anatomy' has always been inspiring.

My great gratitude to Associate Professor Tan Puay Hoon, Head of Pathology Department, Singapore General Hospital (SGH) for her generosity in providing me the tissue microarray and other clinical samples which are needed in my immunohistochemistry staining. My appreciation extends to pathologist Dr Aye Aye Thike for giving me guidance on the scoring of tissue microarray and she has always been patient in teaching me knowledge on histopathology of breast cancer. I would also like to thank Miss Cheok Poh

TABLE OF CONTENTS

SUMMARY

Breast cancer is the top leading cause of cancer and mortality in women worldwide, and it is the top cancer affecting Singapore women. Management and treatment of breast cancer are challenging due to its heterogeneous nature of the disease. Hence, identifying reliable prognostic factors has always been the ultimate goal to the researchers and physicians.

Glycosaminoglycans and proteoglycans are discovered to be involved in human cancer progression and malignancy. In current study, an enzyme, *N*-acetylgalactosaminyltransferase-1, CSGalNAcT-1, which initiates the biosynthesis of chondroitin sulfate/dermatan sulfate was investigated. This gene was found up-regulated in normal breast cell line, MCF-12A, while down-regulated in tested breast cancer cell lines, i.e. MCF7, ZR75-1 and MDA-MB-231. In order to understand the functional role of *CSGalNAcT-1* in breast cancer, this gene was silenced in MCF-12A and over-expressed in MCF7 and MDA-MB-231. The results showed that *CSGalNAcT-1* was involved in regulating cell migration, invasion, viability, apoptosis and adhesion. *CSGalNAcT-1* silenced MCF-12A acquired tumorigenic phenotypes through increased migration and invasion in transwell and Matrigel™ chamber experiments. At the same time, the silenced MCF-12A had significant changes in the cell viability and apoptosis. Cell adhesion to collagen I and fibronectin remained unchanged upon *CSGalNAcT-1* knockdown. The aggressiveness of breast cancer cell lines, MCF7 and MDA-MB-231, was hampered by *CSGalNAcT-1* over-expression in the cells. Migration and invasion of the cells were remarkably reduced. Cell viability of the cancer cell lines were impeded and cell adhesion to fibronectin and collagen I were affected in *CSGalNAcT-1* over-expressed MCF7 and MDA-MB-231.

SUMMARY

Besides, downstream target gene was chosen from microarray result of *CSGalNAcT-1* silenced MCF-12A. Silencing *CSGalNAcT-1* resulted in chemokine *CXCL14* up-regulation. It was hypothesized that *CXCL14* mediated the phenotypic changes downstream of *CSGalNAcT-1* knockdown in MCF-12A. Double knockdown of *CSGalNAcT-1* and *CXCL14* restored the normal phenotypes of MCF-12A, including reduced metastasis and increased adhesion to collagen I and fibronectin. Other than *CXCL14*, silencing *CSGalNAcT-1* in MCF-12A caused the expressional changes in few proto-oncogenes and tumor suppressor genes. Therefore, *CSGalNAcT-1* is hypothesized to interplay with these genes in mediating the signaling pathway of breast cancer progression.

Immunohistochemistry was performed to investigate the expression and localization of CSGalNAcT-1 in microarray clinical samples of invasive ductal carcinoma tissue. It was found that CSGalNAcT-1 was expressed in epithelial cells, stromal cells and diffuse stroma of invasive ductal carcinoma tissue. High expression of CSGalNAcT-1 in stromal cells was negatively associated with increasing histological grade and mitotic index. However, low expression of CSGalNAcT-1 in diffuse stroma along with specific clinicopathological parameters, such as positive estrogen and progesterone receptor, negative lymph node involvement, and lower scoring of tubule formation, was correlated with better survival and longer recurrence free period.

Taken together, the findings of this study had revealed the functional importance of *CSGalNAcT-1* in mediating the phenotypic changes of the

breast cell lines and the potential role of CSGalNAcT-1 as a prognostic factor in invasive ductal carcinoma.

LIST OF TABLES

LIST OF FIGURES

LIST OF ABBREVIATIONS

µg Microgram

µl Microliter

µM Micromolar

ABC Avidin-biotin-complex

ABs Alveolar buds

AJCC American Joint Committee on Cancer

ATM Ataxia telangiectasia mutated homolog

BCA Bicinchoninic acid

BRCA Breast cancer gene

BSA Bovine serum albumin

cDNA Complementary DNA

CDK Cyclin-dependent kinase

CEACAM1 Carcinoembroyonic antigen cell adhesion molecule 1

Chk2 Checkpoint kinase 2

CHPF Chondroitin polymerizing factor

CHST11/C4ST2 Carbohydrate (chondroitin 4) sulfotransferase 11

CHST12/C4ST3 Carbohydrate (chondroitin 4) sulfotransferase 12

CHST13/C4ST1 Carbohydrate (chondroitin 4) sulfotransferase 13

CHST14/D4ST1 Carbohydate (*N*-acetylgalactosamine 4-O) sulfotransferase 14

CHST3/C6ST2 Carbohydrate (chondroitin 6) sulfotransferase 3

CHST7/C6ST1 Carbohydrate (*N*-acetylglucosamine 6-O) sulfotransferase 7

CHSY1 Chondroitin synthase I

CHSY3 Chondroitin sulfate synthase 3

CKI Cyclin-dependent kinase inhibitor

CS Chondroitin sulfate

CS-A Glc-GalNAc-4-sulfate

CS-B Dermatan sulfate

CS-C Glc-GalNAc-6-sulfate

CS-D GlcA (2-O-sulfate)-GalNAc (6-O-sulfate)

CS-E GlcA-GalNAc-(4, 6)-O-disulfate

CSGalNAcT-1 *N*-acetylgalactosaminyl transferase I

CSGalNAcT-II *N*-acetylgalactosaminyltransferase II

CSGlcAT Chondroitin sulfate glucuronyltransferase

CSPGs Chondroitin sulfate proteoglycancs

DAB Diaminobenzidine

DAVID Database for Annotation, Visualization and Integrated Discovery

DCC Deleted in colorectal carcinoma

DCIS Ductal carcinoma in situ

DCN Decorin

DFS Disease free survival

DMSO Dimethyl sulphoxide

DS Dermatan sulfate

DSE Dermatan sulfate epimerase

DSPGs Dermatan sulfate proteoglycans

DTT Dithiothretol

E.coli *Escherichia coli*

ECL Enhanced chemilluminescence

ECM Extracellular matrix

EGF Epidermal growth factor

EGFR Epidermal growth factor receptor

FBS Fetal bovine serum

FFTP First-full-term pregnancy

FGF Fibroblast growth factor

g Gram

GAGs Glycosaminoglycans

GalNAc *N*-acetylgalactosamine

GalNAc4S-6ST Chondroitin 6-O-sulfate sulfotransferase

GalT-I Galactosyltransferase I

GalT-II Galactosyltransferase II

GlcA Glucuronic acid

GlcAT-I Glucuronyltransferase I

GlcNAc *N*-acetylglucosamine

H & E Hematoxylin and Eosin

H$_2$O$_2$ Hydrogen peroxide

HA Hyaluronan

HER2 Human epidermal receptor 2

HRT Hormone replacement therapy

HS Heparan sulfate

HSPGs Heparan sulfate proteoglycans

IDC Invasive ductal carcinoma

IdoA Iduronic acid

IRS Immunoreactivity score

KS Keratan sulfate

Lob 1, 2, 3 Lobule type 1, 2, 3

LPA Lysophosphatidic acid

LYVE-1 Lymphatic vessel endothelial hyaluronan receptor

MAPK Mitogen-activated protein kinase

MCSP Melanoma chondroitin sulfate proteoglycans

MEF Murine embryonic fibroblast

Mel-CAM Melanoma cell adhesion molecule

ml Milliliter

mm Millimeter

MMP Matrix metalloproteinase

MOMP Mitochondrial outer membrane permeabilization

MRI Magnetic resonance imaging

mRNA Messenger RNA

MT3-MMP Membrane type-3 MMP

MTS 3-(4,5-dimethylthiazol-2-yl)-5-(3-carboxymethoxyphenyl)-2-(4-sulfophenyl-2H-tetrazolium, inner salt

NCAM/Ng-CAM Neural cell adhesion molecules

ng Nanogram

nM Nanomolar

OCs Oral contraceptives

OS Overall survival

PAPS 3'-phosphoadenyl 5'-phosphosulphate

PBS Phosphate buffer saline

PCR Polymerase chain reaction

PGs Proteoglycans

PVDF Polyvinyl difluoride

qRT-PCR Quantitative real time polymerase chain reaction

RHAMM Hyaluronan-mediated motility receptor

RISC RNA-induced silencing complex

SAR Survival after recurrence

SDS Sodium dodecyl sulphate

SDS-PAGE Sodium dodecyl sulphate polyacrylamide gel electrophoresis

SLRP Small leucine-rich protein

TBS Tris buffered saline

TBST Tris buffered saline-Tween 20

TBS-Tx Tris buffered saline-Triton X

TEBs Terminal end buds

TEMED Tetramethylelthylenediamine

TGF- β Transforming growth factor-β

TMA Tissue microarray

TNF Tumor necrosis factor

TNFR Tumor necrosis factor receptor

TPS Total percentage score

Trypsin-EDTA Trypsin-ethylenediaminetetraacetic acid

UICC International Union against Cancer

UST Uronyl-2-sulfotransferase

VEGF Vascular endothelial growth factor

WAI Weighted average score

XylT-I Xylosyltransferase I

LIST OF PUBLICATIONS

Meeting Proceeding

1. **Sim Wey Cheng**, Bay Boon Huat, and Yip Wai Cheong George. (2010) Functional analysis of CSGalNAcT-1 in breast cancer in Proceedings of the International Anatomical Sciences and Cell Biology Conference (IASCBC), Singapore.

CHAPTER 1

INTRODUCTION

1. INTRODUCTION

1.1. Breast development and anatomy

The adult mature breasts extend from the second to the sixth ribs and from the sternum to the midaxillary line. Anteriorly, the breast is bounded by the skin; while posteriorly it lies on the pectoralis major, serratus anterior and the superior rectus sheath. Loose connective tissue in the retromammary space enables flexible mobility of the breast on the chest wall (P.O'Malley and E.Pinder, 2006). Each breast possesses a central, erectile nipple with a circular ovoid areola of darker skin. Figure 1.1 shows the gross anatomy of a female breast. Histologically, the parenchymal tree from the central ducts branches out to the lobules which are lined by cuboidal or low columnar epithelial cells. These epithelial cells form the interior lining of the ducts and are surrounded by continuous layer of myoepithelial cells. The lobules are composed of a compact and rounded clump of individual ductules or acini. Ductules or acini are embedded in a specialized myxoid connective tissue, where lymphoid and plasma cells are often present (P.O'Malley and E.Pinder, 2006).

Female breast is a dynamic organ which changes as a female undergoes different stages of life from fetus growth in mother womb, puberty, pregnancy, lactation to menopause (Russo, 2004). The beginning of the breast development takes place in a 5-week old embryo. Mammary gland development in fetus can be divided into the following stages: Ridge, milk hill, mammary disc, G lobule type, cone, budding, indentation, branching, canalization and end-vesicle stage. End-vesicle stage appears during week 34 of gestation. This stage is characterized by the production of colostrums.

However, the breast lacks well-developed lobules, which only become apparent at the end of pregnancy of the fetus, so end-vesicle stage is not a fully differentiated stage. In the newborn, breast is presented in a very primitive structure; it is only composed of ducts ending with short ductules (Russo, 2004).

Puberty in the female starts in between 10 and 12 years old. At this period, glandular tissue and the surrounding stroma of the breasts start to proliferate. The outgrowth of small bundles of primary and secondary ducts increase the glandular mass (Russo, 2004). The ducts continue to grow and divide into terminal end buds (TEBs). Each TEB diverges into two smaller structures of alveolar buds (AB) which may further sprout into ductules. A terminal duct together with four to eleven ductules make up the Lobule type 1 (Lob 1) or virginal lobule (Russo, 2004). The hallmark of breast differentiation is lobule formation, which sets in one to two years after the first menstrual period. The breast tissue of non-pregnant women contains 3 types of lobules, the afore-described Lob 1 and the more developed type 2 (Lob 2) and type 3 (Lob 3) lobules. Transition of Lob 1 to Lob 2 takes place when the gradual sprouting of ductules reaches an average number of 47 per lobules, and transition to Lob 3 happens when at least 80 ductules are found around the terminal duct. In nulliparous women, Lob 1 presents predominantly, Lob 2 presents at minimal number and Lob 3 is barely identifiable. However in parous women, there is a significant increased in Lob 3 until a woman reaches the age of 40 (Russo, 2004).

During pregnancy, the breast reaches its maximum development. In the early stage, ductal lengthening and profuse branching occur rapidly for the progression of Lob 2 to Lob 3. Fully differentiated Lob 4 is formed from the progression of ductules to secretory acini; this indicates the beginning of secretory activity. From mid-pregnancy onwards, milk is secreted into the mammary alveoli and can be expelled from the nipple. No major morphological changes are observed during lactation. Breast regresses after lactation and contain more glandular tissue than breasts of women who have not experienced pregnancy and lactation (Russo, 2004). After menopause, Lob 2 and Lob 3 are predominant in the breasts of both nulliparous and parous women.
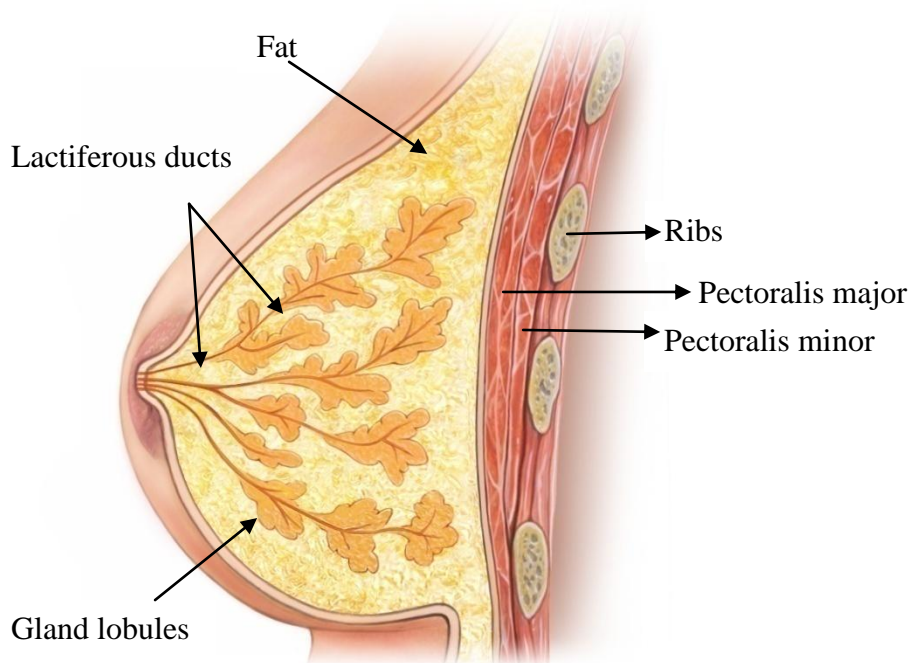
Figure 1.1 The gross anatomy of female breast.

1.2. Epidemiology of breast cancer

According to the report generated from GLOBOCAN 2012 (2012), an estimate of 14.1 million people were diagnosed with cancer and 8.2 million died from the disease. Breast cancer is the most common cancer affecting female worldwide, 25.2% of the total cancer incidence and 14.7% of the cancer deaths in female came from breast cancer. In Singapore, based on data from the Singapore Cancer Registry, breast cancer was the top cancer among the female Singapore residents from 2009 to 2013 (Lee et al., 2014). Besides, breast cancer is the most common cancer affecting females in all three ethnic groups, i.e. Chinese, Malay and Indian. Correspondingly, breast cancer caused the most cancer deaths in Singapore females from 2009 to 2013.

1.3. Risk factors of breast cancer

Since breast cancer is the most common occurring cancer in females worldwide, it is important for each female to be aware of the risk factors of breast cancer. The risk factors of breast cancer can be grouped into non-modifiable and modifiable factors. Most of the well-known breast cancer risk factors are not modifiable, such as age, genetic predisposition, family history, early menarche and late menopause. However, other risk factors such as use of exogenous hormones, consumption of alcohol, diet and physical activity are modifiable.

1.3.1. Age

Most common non-hormone-dependent adult cancers, for example colorectal cancer, increases in incidence with advancing age. While in the case of breast cancer, although the risk of breast cancer rises as a female gets older, the rate of the risk rises significantly after the age of 50. This could be due to the deterioration of the protective machinery critical in preventing the genesis of breast cancer as a female grows older (Roses, 2005).

1.3.2. Family history of breast cancer

Familial clustering of breast cancer is a recognized risk factor in the genesis of breast malignancy. A woman is susceptible to the disease if she has a positive family history of breast cancer; especially when one or a few first-degree relatives are affected. Highly penetrate mutant forms of breast cancer genes, BRACA1 and BRACA2 are inheritable and are responsible for an estimate of 20% of the familial risk for breast cancer (Ponder, 2003). Other genetic abnormalities which contribute lesser cases of familial breast cancer are p53, checkpoint kinase 2 (Chk2) and ataxia telangiectasia mutated homolog (ATM) (Ponder, 2003). However, low penetrating genes could act together and give rise to familial aggregation of cases. Intense research of these genes and other high penetrating genes is still ongoing.

1.3.3. Hormonal factors

The influence of sex steroids estrogen and progesterone on the genesis of breast cancer is largely due to their effects on cell proliferation. Factors that induce cell proliferation can result in introduction of mutations in DNA hence malignant transformation of the cells. The effects of endogenous and exogenous sex hormones on cell proliferation are relevant only in the context of dose and duration but not of ever-never use consideration (Pike et al., 1983).

The growth of normal breast epithelium is under the endocrine control of two important ovarian hormones estrogen and progesterone. Age at menarche and menopause determine the time of exposure to estrogen and progesterone of a female in her lifetime. Late menarche, i.e. after 12 years old, decreases breast cancer risk substantially with an approximate 15% decrease with each year that menarche is delayed (Pike et al., 1983). Hence, the sooner a female develops regular menstrual cycle, the greater the subsequent risk for breast cancer (Henderson et al., 1985). In addition, delayed menopause after age 55 may increase the risk of breast cancer. Ovariectomy before the age of 40 could reduce breast cancer risk by a drastic 45% compared to women who experience normal menopause (Brinton et al., 1988).

Common oral contraceptives (OCs) contain synthetic estrogen ethinylestradiol combined with one of the many available synthetic progestins. Available study showed that level of sex steroids in OCs appeared to promote the same extent of breast cell proliferation as a normal ovulatory cycle (Pike et al., 1993). Although administration of OC predisposes the user to increased risk of breast

cancer, the risk will subside if OCs intake is terminated for more than ten years (1996). Hormone replacement therapy (HRT) is prescribed to post-menopausal women to control menopause symptoms. Long term administration of HRT is associated with higher risk of getting breast cancers; however, the risk will be reduced after a 5-year termination of usage (Boyle, 2005).

1.3.4. Parity and age at first-term pregnancy

Women with a first-full-term pregnancy (FFTP) under the age of 20 years have about 50% reduced breast cancer risk compared with nulliparous women (Collaborative Group on Hormonal Factors in Breast, 2002). Besides, subsequent additional babies exert further protection with an approximate 7% per child birth (Collaborative Group on Hormonal Factors in Breast, 2002). However, the protection from FFTP decreases for women who have an FFTP after the age of 32, and adversely imposes a greater breast cancer risk than nulliparous women (Kelsey and Bernstein, 1996).

1.3.5. Physical activity and diet

Several risk factors of breast cancer are modifiable. These include diet, alcohol consumption and physical activity. Physical activity is proven to decrease risk of breast cancer. It is well proven that exercise before menarche and in premenopausal women decreases risk (Bernstein et al., 1994), and there are evidences showing that exercise is protective in the postmenopausal period too (Patel et al., 2003). The effect of dietary fat on risk of breast cancer is still debatable; there is no significant correlation between intake of fat and an

increase risk of breast carcinogenesis (Mazhar and Waxman, 2006). In contrast, alcohol intake imposes a positive association with increased breast cancer risk (Hamajima et al., 2002, Terry et al., 2006, Zhang et al., 2007). It is proposed that alcohol increases oestrogen level (Singletary and Gapstur, 2001).

In summary, breast cancer is a complex disease that arises from the interplay of many factors. The nature of breast cancer imposes a challenge to treatment and prevention of this disease.

1.4. Changes in cell properties of breast cancer cells

1.4.1. Cell cycle

Cell cycle is tightly regulated to control the correct duplication of genomic DNA. The four phases of cell cycle are G_1, S, G_2 and M phase (Li et al., 2015). S phase is the DNA replication phase; M phase is where the DNA is packaged and ready to be separated to daughter cells. G_1 and G_2 phases separate S phase and M phase to ensure the DNA replication is correct and DNA is packaged appropriately prior to division (Li et al., 2015). Cell cycle progression is positively regulated by cyclin-dependent kinases (CDKs). The activity of CDKs was activated upon association with specific activator called cyclin (Li et al., 2015). Cell cycle progression was activated by distinctive CDK-cyclin at different phases of cell cycle. The inhibition of CDKs could be established by phosphorylation of threonine 14/tyrosine 15 by two enzymes, Wee1 and Myt1 (Baldin and Ducommum, 1995) and this inhibition could be reversed by phosphatases CDC25A, CDC25B and CDC25C (Nilsson and Hoffmann, 2000). In addition to inhibition by phosphorylation, CDKs are negatively

regulated by two families of small-polypeptide inhibitory proteins called CDK inhibitors, or CKIs (Sherr and Robert, 1999). The Ink4 (inhibitors of CDK4) family proteins, which consists of p16^{Ink4a}, p15^{Ink4b}, p18^{Ink4c}, and p19^{Ink4d}, inhibit only CDK4 and CDK6 of G$_1$ phase CDKs. The second family, Cip/Kip family proteins, which includes p21^{Cip1}, p27^{Kip1}, and p57^{Kip2}, bind to a broad range of CDKs but preferentially inhibit CDK2 complexes (Sherr and Robert, 1999).

Mutations or deregulated expressions of CDKs, cyclins, or CKIs are a frequent occurrence in cancer. Cyclin D1, which promotes the progression of G$_1$ phase, is over-expressed in breast and esophageal cancers (Steeg and Zhou, 1998). Gene amplification of CDK4 and CDK2 is a hallmark of large B-cell lymphomas, lung tumors, and cervical carcinomas (Li et al., 2015). The expression of Cip/Kip inhibitors is deregulated in human cancers. Reduced p27^{Kip1} levels and inactivation of p16^{Ink4a} occurs frequently in breast, ovarian, lung, and bladder carcinomas (Serrano et al., 1996).

1.4.2. Apoptosis

Apoptosis is programmed cell death characterized by condensed chromatin, cell membrane blebbing, and cell shrinkage. The apoptotic cells are phagocytosed by macrophages and other cell types through recognition of phosphatidylserine exposed by the apoptotic cells (White et al., 2015). There are two major pathways of apoptosis, the mitochondrial (intrinsic) pathway and the death receptor (extrinsic) pathway. The mitochondrial pathway is initiated with the formation of mitochondrial outer membrane

permeabilization (MOMP), followed by release of cytochrome c, SMAC, and Omi. Cytochrome c activates APAF-1 to oligomerize, and the latter binds and activates initiator caspase, caspase-9 which finally activates executioner caspase, caspase-3 (Wolf and Green, 1999). The regulation of mitochondrial pathway of apoptosis is by pro- and anti-apoptotic members of the Bcl-2 family (Brunelle and Letai, 2009, Letai, 2008, Tait and Green, 2010). BAX and BAK are pro-apoptotic "effectors" proteins which homo-oligomerize to form the MOMP (Wei et al., 2001). Pro-apoptotic "activator" BH3-only proteins, which include BIM, BID, and PUMA, can directly interact with BAX and BAK to activate the pro-apoptotic activity (Willis et al., 2007). Anti-apoptotic Bcl-2 family proteins include Bcl-2, Bcl-XL, Bcl-w, Mcl-1, and Bcl-1. These proteins bind and sequester BAX or BAK protein before they can oligomerize to initiate apoptosis (Certo et al., 2006, Cheng et al., 2001, Letai et al., 2002a). Another subfamily, the pro-apoptotic "sensitizer" BH3-only proteins, which include BAD, BIK, and NOXA competitively inhibit the binding of anti-apoptotic proteins to activators, BAX, or BAK (Letai et al., 2002a). The death receptor (extrinsic) pathway involves a subset of cell surface receptors belonging to the tumor necrosis factor (TNF) receptor (TNFR) superfamily (White et al., 2015). The death receptors include TNFR1, TRAIL receptors, and CD95. When the receptor is engaged by its ligand, the initiator caspase-8 is recruited and activated by the adapter protein, FADD or TRADD, depending on which death receptor is involved (White et al., 2015).

Suppression of apoptosis is one of the hallmarks of cancer progression (Kerr et al., 1994). Tumor cells can evade apoptosis by the expression of anti-apoptotic

protein, Bcl-2; or by down-regulation or mutation of pro-apoptotic protein, BAX (Miyashita et al., 1994). In order to escape immune destruction, expression of Fas receptor has been shown to be down-regulated in tumor cells. Other mechanisms include expression of malfunctioned Fas receptor and secretion of high levels of a soluble form of the Fas receptor which will sequester the Fas ligand from the receptor on the tumor cells (Cheng et al., 1994, Elnemr et al., 2001).

1.4.3. Migration, invasion, and adhesion

Cell migration occurs as the result of coordinated polymerization and depolymerisation of the actin cytoskeleton to create an extended pseudopod at the leading edge of the cells, followed by contraction and disassembly of cell-matrix adhesive contacts from the rear (Wolf and Friedl, 2006). Lamellipodial protrusions at the leading edge are nucleated by Arp2/3 complex, cortactin, and the GTPase Rac. Actin contractility from the rear is however regulated by myosin light-chain kinase and small GTPase, Rho and its effector Rho-kinase (ROCK) (Wolf and Friedl, 2006). Tumor cells can secrete autocrine factor to stimulate motility, such as lysophospholipase D and lysophosphatidic acid (LPA) (Acharyya et al., 2015). Binding of hepatocyte growth factor/scatter factor (HGF/SF) to its receptor, c-met, could induce chemokinetic activity of epithelial cells and result in an invasive phenotype (Acharyya et al., 2015). Chemotaxis gradient formed by the growth factors, chemokines of the CCR and CXC family in ECM could also induce a directional motility to the tumor cells (Acharyya et al., 2015).

Tumor cell invasion is the distinguishing feature of malignancy in which the cells acquire the capacity to disrupt the basement membrane and penetrate the underlying stroma (Acharyya et al., 2015). Tumor invasion involves the loss of cell-cell cadherin adhesion, alterations in cell-matrix adhesion by integrins, proteolysis of the extracellular matrix by proteinases, and organization alterations in the actin cytoskeleton (Acharyya et al., 2015).

Epithelial cell-cell interactions are mediated primarily by epithelial-specific cadherin, E-cadherin, which functions as a tumor and metastatic suppressor (Cavallaro and Christofori, 2004). Transcriptional repression of E-cadherin and proteolytic degradation of the Neural cell adhesion molecule (NCAM), deleted in colorectal carcinoma (DCC), carcinoembryonic antigen CAM1 (CEACAM1), and Mel-CAM (melanoma-CAM), were demonstrated in several tumor types (Cavallaro and Christofori, 2004). The extracellular matrix (ECM) is composed of triple-helical collagens, glycoproteins such as laminins and fibronectin, and proteoglycans. ECM provides a scaffold for the organization of cells and serves as a repository for secreted regulatory proteins and growth factors (Boudreau and Bissel, 1998). Hence, interaction of cells with ECM molecules affects the survival, growth, differentiation, and migration of the cells (Boudreau and Bissel, 1998). Cells adhere to ECM via transmembrane glycoproteins integrins (Hynes, 2002). In tumor development, cancer cells switch to the expression of integrins that promote survival, migration, and proliferation but down-regulate the integrins that mediate adhesion (Guo and Giancotti, 2004). In general integrins $\alpha_2\beta_1$ and $\alpha_3\beta_1$ are

suppressors of tumor progression, whereas $\alpha_v\beta_3$, $\alpha\beta_6$, and $\alpha_6\beta_4$ induce cellular proliferation and migration (Acharyya et al., 2015).

1.5. Types of breast cancer

Breast cancer can be divided into three groups: the in situ breast carcinoma (ductal or lobular), invasive breast carcinoma (ductal or lobular) and less common and unique types of breast malignancies such as phyllodes tumor, Paget disease and inflammatory breast carcinomas (Roses, 2005). As immunohistochemical staining of invasive ductal carcinoma is included in the current study, the pathology of this malignancy will be discussed.

Invasive ductal carcinoma is the most common kind of breast cancer. It is composed of large cancer cells that are liberated from the boundaries of ductolobular system and have infiltrated the fibrous and fatty stroma of the breast, usually in a haphazard manner. The body reacts to this perturbation by producing dense fibrosis, the so-called desmoplastic response, frequently accompanied by variable degrees of chronic inflammation (Roses, 2005). Histological grading of invasive ductal carcinoma is important in determining the prognosis of the patients. The grading schemes largely in use today are based on the findings of Bloom and Richardson and include the assessment of three parameters: amount of tubule formation, degree of nuclear pleomorphism and mitotic rate (Bloom and Richardson, 1957). One difficulty that is encountered with the system is that, mitotic rate of smaller lesions is more difficult to be assessed. So in such instances, histological grading of

invasive ductal carcinoma is based on tubule formation and degree of nuclear pleomorphism.

1.6. Staging and classification of breast cancer

Breast cancer, similar to other malignancies, is staged using a uniform system to ensure accuracy and consistency in classifying groups of patients with similar outcomes and delineating treatment approaches based on the severity of disease. In 1958, International Union against Cancer (UICC) first introduced a staging system based on histologic grounds, namely TNM classification system, representing primary tumor (T), regional nodes (N), and distant metastasis (M) (Roses, 2005). In the late 1980s, American Joint Committee on Cancer (AJCC) and UICC came out with a single TNM staging system. Over time, the TNM staging system has been revised several times to increase accuracy so as to prevent both under-treatment and over-treatment of the disease (Roses, 2005, Edge et al., 2011).

Basically, the TNM staging can be grouped into (Edge et al., 2011):

Stage 0: Early breast cancer cells are still contained within the duct or lobule.

Stage I: Can be sub divided into two groups:

Stage IA: Tumor size of 2 cm or less with no local lymph node metastasis and no distant metastasis of tumor cells.

Stage IB: Primary tumor not detectable or tumor size of 2 cm or less with micrometastases in lymph node only and no distant metastasis of tumor cells.

Stage II: Can be sub divided into two groups:

Stage IIA: Primary tumor not detectable or tumor size up to 5 cm with either no local lymph node metastasis or metastasis in movable ipsilateral axillary lymph nodes; and no distant metastasis of tumor cells.

Stage IIB: Tumor size of more than 2 cm or size of more than 5 cm with either no local lymph node metastasis or metastasis in ipsilateral axillary lymph nodes; and no distant metastasis of tumor cells.

Stage III: Can be sub divided into three groups:

Stage IIIA: Primary tumor not detectable or tumor size larger than 5 cm with metastasis in moveable, fixed or matted ipsilateral axillary lymph nodes; and no distant metastasis of tumor cells.

Stage IIIB: Tumor of any size surfacing to chest wall or skin with either no local lymph node metastasis or with metastasis in moveable, fixed or matted ipsilateral axillary lymph nodes; and no distant metastasis of tumor cells.

Stage IIIC: Tumor of any size and pattern with metastasis in ipsilateral infraclavicular lymph node(s) with or without lymph node involvement; and no distant metastasis of tumor cells.

Stage IV: Tumor of any size and pattern with any lymph node metastasis pattern; and distant metastasis of tumor cells.

1.7. Symptoms and signs of breast cancers

Symptoms and signs of breast cancer include lump in the breast, altered in breast morphology and size, breast pain, nipple retraction, and bleeding or discharge from nipple. However, there are cases where no symptoms are observed, especially in the early stage of breast cancer. This is the stage proven to have most effective treatment responses following early detection.

Therefore, women are highly encouraged to follow the recommended guidelines for routine breast examination and screening (Roses, 2005).

1.8. Breast cancer detection

Mortality of breast cancer could be largely reduced if disease is detected early, as treatment is more effective in early stage of breast cancer. In recent decades, public health campaigns are organized to raise awareness of early detection for breast cancer and encourage females who have reached certain age to undergo periodic examination. Screening test provides acceptable specificity to minimize false-positive examinations. The test imposes low risk to patients and with acceptable cost. Some commonly used screening methods include breast self-examination, mammography tests, ultrasound and magnetic resonance imaging.

1.8.1. Breast self-examination and clinical breast examination

Breast self-examination aids women to be more vigilant and increases awareness of normal breast composition so that changes can be detected and consultation to physicians can be made immediately. Self-examination can be performed monthly. The patients look for lumps, thickening, discharge or any changes in the breast. For menstruating women, the best time to self-examine is a week after the start of the period. Pregnant and lactating women, as well as post-menopausal women are advised to continue perform self-examination monthly (Roses, 2005).

The only difference between clinical breast examination and breast self-examination is that, examiner helps to inspect for abnormalities of breast and detect existence of lumps and any changes in shape and texture of breasts. For women age 40 and above, clinical breast examination is recommended to be taken once a year in complement with mammography examination.

1.8.2. Mammography

Mammography uses low-dose x-ray to visualize the internal structure of the breast. In US and in Singapore, mammography screening is advised for most women beginning at the age of 40 years (Smith et al., 2003). Younger women can benefit from mammography screening only if they are in extremely high-risk group of developing breast cancer at an early age (Smith et al., 2003). It is recommended by many major medical organizations that women from the age of 40 to 49 years old be screened annually (Smith et al., 2003, Feig, 1994). Smaller tumor can be detected by mammography thus the ability of screening mammography to substantially reduce breast cancer mortality is well established and not debatable (Smith et al., 2003, Seidman et al., 1987). A study by Duffy and associates described that among women aged 40 to 69 years, breast cancer mortality was reduced 44% for screened women and 39% for women offered screening compared with the prescreening era (Duffy et al., 2002). However, not all breast cancer can be detected by a mammogram. Besides, like any other diagnostic tests, mammography could also give false-positive test results that lead patients to unnecessary follow-up examinations (Duffy et al., 2010).

1.8.3. Ultrasound

Ultrasound is a highly sensitive technique to evaluate dense breasts and differentiate between cystic and solid masses (Stavros et al., 1995). Tumor masses as small as 5 mm can be localized by ultrasound and physicians may perform subsequent ultrasound-guided aspiration biopsy or core biopsy for further diagnosis.

1.8.4. Magnetic resonance imaging

Unlike mammography, magnetic resonance imaging (MRI) uses magnetic fields instead of x-rays to give the image of cross-sectional body. Patients are injected with a contrast material (usually gadolinium DTPA) before MRI is taken (Duffy et al., 2010). MRI is a useful tool for detecting primary breast carcinoma. MRI could detect microscopic multifocal or multicentric disease in patients. These markers indicate higher risk of local recurrence and identification of these markers could assist physicians in deciding suitable surgical managements to patients. MRI evaluation might help to identify patients who will not benefit from breast conservative therapy, although does not change the overall mastectomy rate. MRI is a technique with high sensitivity but low specificity, so validation by core or excision biopsy of MRI-identified suspicious lesions is necessary before any treatment decision is made (Bedrosian et al., 2003). For women in breast cancer high-risk group, they are recommended to have MRI screening along with a yearly mammogram beginning at age 30. MRI complements mammography screening but is not its replacement.

1.9. Treatment of breast cancer

Treatment decisions are given by physician and under patient's consent with careful consideration. A few considerations of the optimal treatment are the stage and biological characteristic of the cancer, the preferences and conditions of patients, and the pros and cons associated with each treatment protocol.

1.9.1. Surgery

Surgery removal of breast cancer is a primary form of treatment to the disease. The types of surgical procedure include lumpectomy, total mastectomy and modified radical mastectomy (Alteri et al., 2011). In a lumpectomy, only cancerous tissue and circumcised tissues are removed while entire breast is removed in total mastectomy. Lumpectomy is usually followed by duration of 5 to 7 weeks of radiation therapy. Women who chose mastectomy may consider having breast reconstruction after surgery. Patients may also undergo modified radical mastectomy, which involves removal of the entire breast and lymph nodes under the arm. The presence of cancer cells in the lymph nodes can help the physicians to decide subsequent treatment regime (2011).

1.9.2. Radiation therapy

Radiation therapy is recommended to patients after a lumpectomy, before surgery to reduce the size of tumors, or after mastectomy to eliminate remnant cancer cells after surgery (Vogel et al., 2010). There are two types of radiation therapy and each type is given depending on the type, stage, and location of the tumor being treated. External radiation is beamed onto the area affected by

cancer from a machine. External beam radiation is usually administered to patients over a period of 5 to 7 weeks. Internal radiation therapy is an invasive method, which uses a needle, wire, or seed that is sealed with radioactive substance to place into or near the cancer site. Accuracy of radiation therapies has increased dramatically over years to effectively diminish the side effects and also reduce treatment time (2011).

1.9.3. Systemic therapy

Systemic therapy is the use of anti-cancer drugs on patients via oral administration or vein injection. Systemic therapy includes biologic therapy, chemotherapy, and hormone therapy (Freedman et al., 2003). Neoadjuvant therapy is systemic therapy given to patients before surgery. It aims to shrink the tumor size to ease surgical removal and this may allow exemption to total mastectomy in some patients. Neoadjuvant therapy is proven to give better prognosis in terms of survival and recurrence of the disease (Freedman et al., 2003). Conversely, systemic therapy given after surgery is called adjuvant therapy. It is used to eliminate any undetected tumor cells that may have metastasized to distant organs of the body. Systemic therapy is also applied in treating late stage of breast cancer where metastasis has occurred and surgery removal of cancer is not possible anymore (Waters et al., 2010).

1.9.3.1. Biologic therapy

One of the profound key biomarkers of breast cancer is HER2/neu. Approximately 15-30% of breast cancers over-express the growth promoting protein HER2/neu. Tumor growth is accelerated and tumors are more likely to

recur in these cases (Domchek et al., 2010). Monoclonal antibody Herceptin (trastuzumab) specifically targets the HER2 protein and has proven to reduce the risk of relapsing and death of early-stage breast cancer by 52% and 33%, respectively (Domchek et al., 2010). Patients who have become resistant to trastuzumab could benefit from Lapatinib, which was found to be effective in delaying disease progression in women with HER2-positive, late stage breast cancer (Tuttle et al., 2009).

1.9.3.2. Chemotherapy

Multiple factors could affect the efficacy of chemotherapy, including tumor size, lymph nodes involvement, and the biological characteristics of the cancer cells (Tuttle et al., 2009). Research has shown that combination of drugs in chemotherapy brings additive benefits than just using one drug alone for breast cancer treatment (Tuttle et al., 2007). Some of the most commonly used drugs are methotrexate, 5-fluorouracil, doxorubicin and many others. The usual course of adjuvant in chemotherapy is three to six months.

1.9.3.3. Hormone therapy

Estrogen promotes the growth of tumor cells. Women tested with estrogen receptors positivity can be given tamoxifen to block the effects of estrogen on the cancer cells (Recht, 2009). Tamoxifen is administered to both premenopausal and postmenopausal patients who are hormone receptors positive for a recommendation of five years therapy. Tamoxifen therapy has been shown to reduce annual recurrence rate and death rate by 41% and 33%, respectively (Recht, 2009). Aromatase inhibitors, for example anastrozole, are

a class of drugs preferably prescribed to postmenopausal women because these drugs inhibit an enzyme responsible for producing minimal amounts of estrogen in postmenopausal women.

1.10. Glycosaminoglycans

Glycosaminoglycans (GAGs) are linear polymers consisting of alternating units of *N*-acetylgalactosamine (GalNAc) or *N*-acetylglucosamine (GlcNAc) and an uronic acid such as glucuronate or iduronate. GAGs are commonly linked to a protein core via a serine residue to form proteoglycans (PGs) which are ubiquitously distributed at the extracellular and cellular (cell membrane and intracellular) levels. The GAG family consists of hyaluronic acid, keratan sulfate (KS), heparan sulfate (HS) and chondroitin sulfate/ dermatan sulfate (CS/DS) (Yip et al., 2006). The structure of each member is illustrated in Figure 1.2.

Chondroitin sulfate

Dermatan sulfate

Heparan sulfate

Hyaluronan

Keratan sulfate

Key:

- ● Galactose (Gal)
- ⬡ *N*-acetylgalactosamine (GalNAc)
- ▲ Iduronic acid (IdoA)
- ★ Xylose
- ◆ Glucuronic acid (GlcA)
- ⬠ *N*-acetylglucosamine (GlcNAc)
- ⬠ Mannose
- ⋈ Ser-- Protein core with serine residue

GlcA $\overset{\beta1,3}{-----}$ GalNAc

GlcA $\overset{\beta1,4}{-----}$ GlcNAc

GlcA $\overset{\beta1,3}{-----}$ GlcNAc

IdoA $\overset{\alpha1,3}{-----}$ GalNAc

IdoA $\overset{\alpha1,4}{-----}$ GlcNAc

Gal $\overset{\beta1,4}{-----}$ GlcNAc
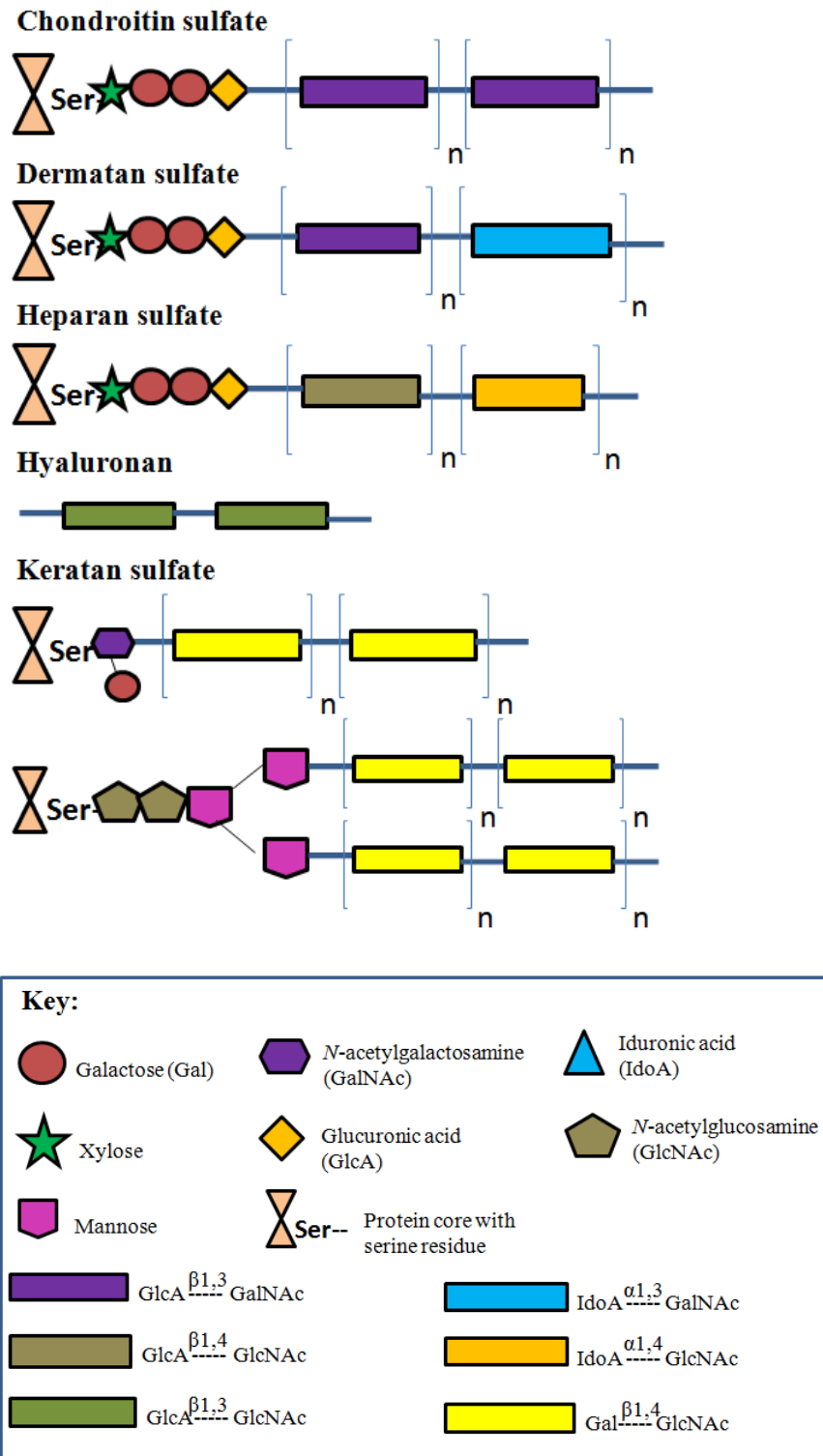
Figure 1.2 The structures of various glycosaminoglycans. Glycosaminoglycans are covalently linked to a protein core via a serine residue to form proteoglycans; except for hyaluronan, which is freely distributed in the extracellular matrix.

Unlike other GAGs, hyaluronan (HA) does not attach to a protein core to form proteoglycan, the repeating dissacharide units are non-sulfated. HA was discovered at a significant amount in tissue regions which were characterized by high cell division and cell mobility (Toole, 2001). HA was found to act as a signaling mediator via binding with CD44, Toll-like receptors 2 and 4, lymphatic vessel endothelial hyaluronan receptor (LYVE-1) and hyaluronan-mediated motility receptor (RHAMM). Among these molecules, CD44 and RHAMM were recently recognized as major receptors implicated in cancer progression (Patel et al., 2007, Turley et al., 2002, Jackson, 2009, Kouvidi et al., 2011).

Keratan sulfate (KS) is distinctively different from other GAGs because the dissacharide units are composed of galactose sugar instead of an uronic acid. KS was found in abundance in cornea to maintain a critical hydration level for corneal transparency (Funderburgh, 2000). KS was also suggested to have potential role in the implantation process whereby cell-associated KS reached a peak abundance when embryo implantation occurred (Graham et al., 1994).

Heparan sulfate (HS) consists of repeating disaccharide units of GlcNAc and hexuronic acid residues [glucuronic acid (GlcA) and iduronic acid (IdoA)] with twelve known sulfation profiles at the hydroxyl groups and the amino groups of glucosamine (Karamanos et al., 1997, Militsopoulou et al., 2002, Malavaki et al., 2011). Sulfated HS chains regulated the interactions of HS with growth factors, cytokines and proteins, therefore affecting the biological roles of these molecules in normal and pathological conditions (Malavaki et al.,

2011). HS chains of heparan sulfate proteoglycans (HSPGs) helped to organize the extracellular matrix through binding with other matrix molecules. Studies showed that presence of HS chains promoted cell adhesion; however their absence caused invasion and migration of malignant cells (Timpl and Brown, 1996, Sanderson, 2001). HS could also act as a 'reservoir' in mediating the bioavailability of selective growth factors and peptides, which are important in regulating tumor progression and angiogenesis (Vlodavsky et al., 1987).

As shown in Figure 1.3, chondroitin sulfate (CS) is composed of repeating disaccharides of *N*-acetylgalactosamine and glucuronic acids while dermatan sulfate (DS) is composed of repeating disaccharides of *N*-acetylgalactosamine and iduronic acid. CS has various sulfation patterns which enable specific interactions with various molecules, including growth factors, cytokines, chemokines, adhesion molecules and lipoproteins (Asimakopoulou et al., 2008). Proteoglycans (PGs) containing CS/DS chains are located at the cellular membrane and at intra- and extra-cellular space. Expression of chondroitin sulfate proteoglycans (CSPGs) was correlated with both normal and pathological conditions. Hence, CSPGs are key regulator in numerous important cellular processes, including proliferation, apoptosis, migration, adhesion and invasion, as well as extracellular matrix (ECM) assembly (Asimakopoulou et al., 2008). Besides, chondroitin sulfate is a well-known supplement to treat degenerative joint disease because of its important role in the maintenance of healthy joint tissues (Kelly, 1998). On the other hand,

dermatan sulfate (DS) was primarily recognized to be involved in wound

healing (Penc et al., 1998, Trowbridge and Gallo, 2002).

A. GlcA β(1→3) GalNAc β(1→4)

B. IdoA β(1→3) GalNAc β(1→4)
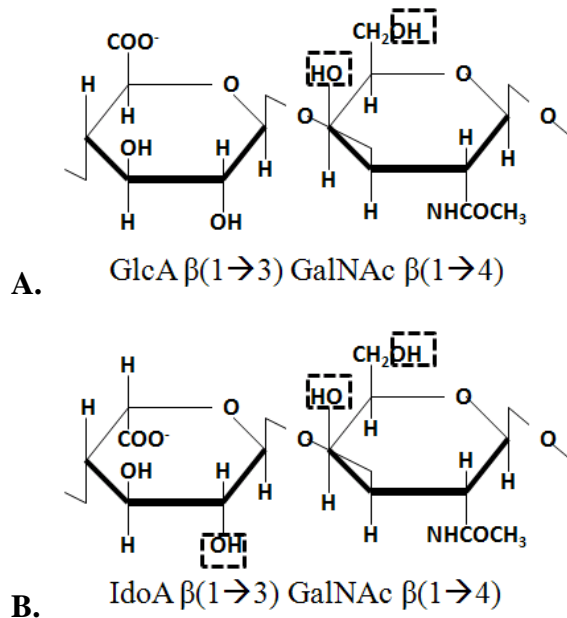
Figure 1.3 The disaccharide units of chondroitin sulfate and dermatan sulfate. (A) The structure of disaccharide units of chondrotin sulfate consists of glucuronic acid (GlcA) covalently conjugated with *N*-acetlygalactosamine (GalNAc). (B) While in the case of dermatan sulfate, iduronic acid (IdoA) instead of GlcA is covalently conjugated with GalNAc. Dashed lines denote the sulfation positions.

1.10.1. Biosynthesis of chondroitin sulfate/ dermatan sulfate and the respective

proteoglycans

The biosynthesis of chondroitin sulfate/ dermatan sulfate

(galactosaminoglycans) is a highly complex process that occurs mainly in the

lumen of the golgi. A high number of biosynthetic enzymes are co-

coordinately involved in the generation of these chains. The complex

biosynthesis process of chondroitin sulfate/ dermatan sulfate is illustrated in

Figure 1.4. First of all, the linker tetrasaccharide is synthesized sequentially by

the addition of xylose, two galactoses, and glucuronic acid catalyzed by

xylosyltransferase I (XylT-I), galactosyltransferase I (GalT-I), galactosyltransferase II (GalT-II) and glucuronyltransferase I (GlcAT-I), respectively (Nicola, 2006). Linker tetrasaccharide is conjugated to core protein via a serine residue to form proteoglycan. It is conserved and common for heparin, heparan sulfate, chondroitin sulfate and dermatan sulfate.

Post-translational modifications of the linkage region regulate the type of glycan chain to be synthesized. Sulfation at position O-4 and/or O-6 of the galactose residues is only found in linkage region of CS/DS, but does not occur in heparin/HS (de Waard et al., 1992, Sugahara and Kitagawa, 2000, Sugahara et al., 1988), even when these two GAGs are attached to the same protein core (Ueno et al., 2001). However, 2-phosphorylation in xylose residue was found in all types of GAG chains (Fransson et al., 1985, Moses et al., 1997). Phosphorylation of xylose is most prominent after the addition of two galactose residues (Moses et al., 1999) but is rapidly dephosphorylated after glucuronic acid is added (Moses et al., 1997). The role of C2-phosphorylation in xylose remains unclear, although it is postulated that it might provide a signal for secretory transport of PGs or for further modifications of the growing GAGs (Moses et al., 1999).

After completion of the linker tetrasaccharide synthesis, the addition of galactosamine by chondroitin sulfate *N*-acetylgalactosaminyltransferase I (CSGalNAcT-1) determines the GAG chain to CS/DS but not HS (Prydz and Dalen, 2000). Elongation of chondroitin sulfate is mediated by the alternate transfer of GalNAc and GlcA by galactosaminyltransferases and

glucuronyltransferases, chondroitin sulfate *N*-acetylgalactosaminyltransferase II (CSGalNAcT-II) (Sato et al., 2003, Uyama et al., 2003), chondroitin synthase 1 (CHSY1) (Kitagawa et al., 2001), chondroitin sulfate synthase 3 (CHSY3) (Yada et al., 2003), chondroitin polymerizing factor (CHPF) (Kitagawa et al., 2003) and chondroitin sulfate glucuronyltransferase (CSGlcAT) (Gotoh et al., 2002b, Izumikawa et al., 2008). In dermatan sulfate, epimerization of glucuronic acid to iduronic acid is catalyzed by the dermatan sulfate epimerase (DSE) (Maccarana et al., 2006).

The sulfation of GAGs also occurs in the Golgi compartment and is catalyzed by sulfotransferases. Sulfate group from the universal donor 3'-phosphoadenyl 5'-phosphosulphate (PAPS) is transferred to hydroxyl group of a specific position of the sugar residue. Sulfation at 6-O position is catalyzed by carbohydrate (*N*-acetylglucosamine 6-O) sulfotransferase 7 (CHST7/C6ST1) (Fukuta et al., 1998), carbohydrate (chondroitin 6) sulfotransferase 3 (CHST3/C6ST2) (Kitagawa et al., 2001), and chondroitin 6-O-sulfate sulfotransferase (GalNAc4S-6ST) (Ohtake et al., 2001). Three sulfotransferases i.e. carbohydrate (chondroitin 4) sulfotransferase 13 (CHST13/C4ST1) (Yamauchi et al., 2000, Hiraoka et al., 2000), carbohydrate (chondroitin 4) sulfotransferase 11 (CHST11/C4ST2) (Hiraoka et al., 2000), and carbohydrate (chondroitin 4) sulfotransferase 12 (CHST12/C4ST3) (Kang et al., 2002) are involved in 4-O sulfation of GalNAc units. Finally, sulfation at position 2 of the GlcA involves Uronyl-2-sulfotransferase (UST) (Kobayashi et al., 1999). In dermatan sulfate, the GAG chain is sulfated by Carbohydate (N-acetylgalactosamine 4-O) sulfotransferase 14

(CHST14/D4ST1) (Evers et al., 2001). Thus, based on the different sulfation patterns, CS chains are classified as CS-A [Glc-GalNAc-4-sulfate], CS-C [Glc-GalNAc-6-sulfate], CS-D [GlcA (2-O-sulfate)-GalNAc (6-O-sulfate) or CS-E [GlcA-GalNAc-(4, 6)-O-disulfate]. Dermatan sulfate is formerly designated as CS-B. Sulfation of DS may involve IdoA (2-O-sulfate) and/or GalNAc (4-O-sulfate and/or 6-O-sulfate) (Afratis et al., 2012).

A.

B.

C.
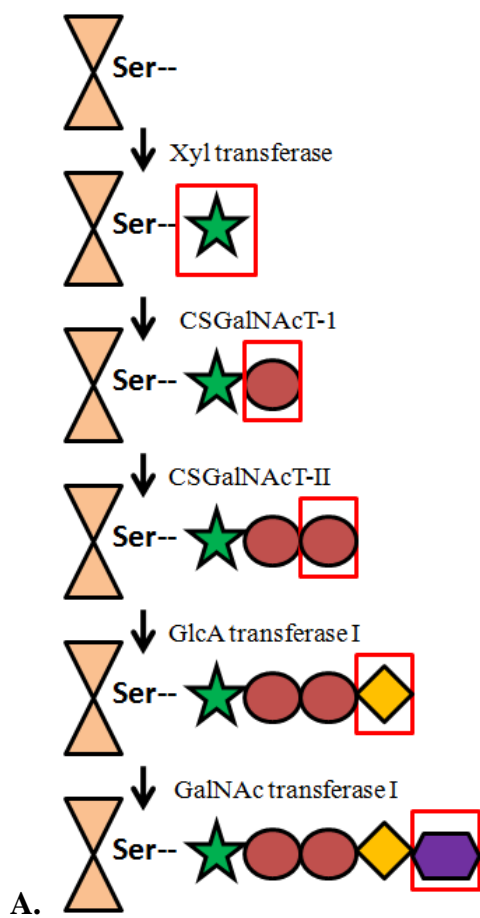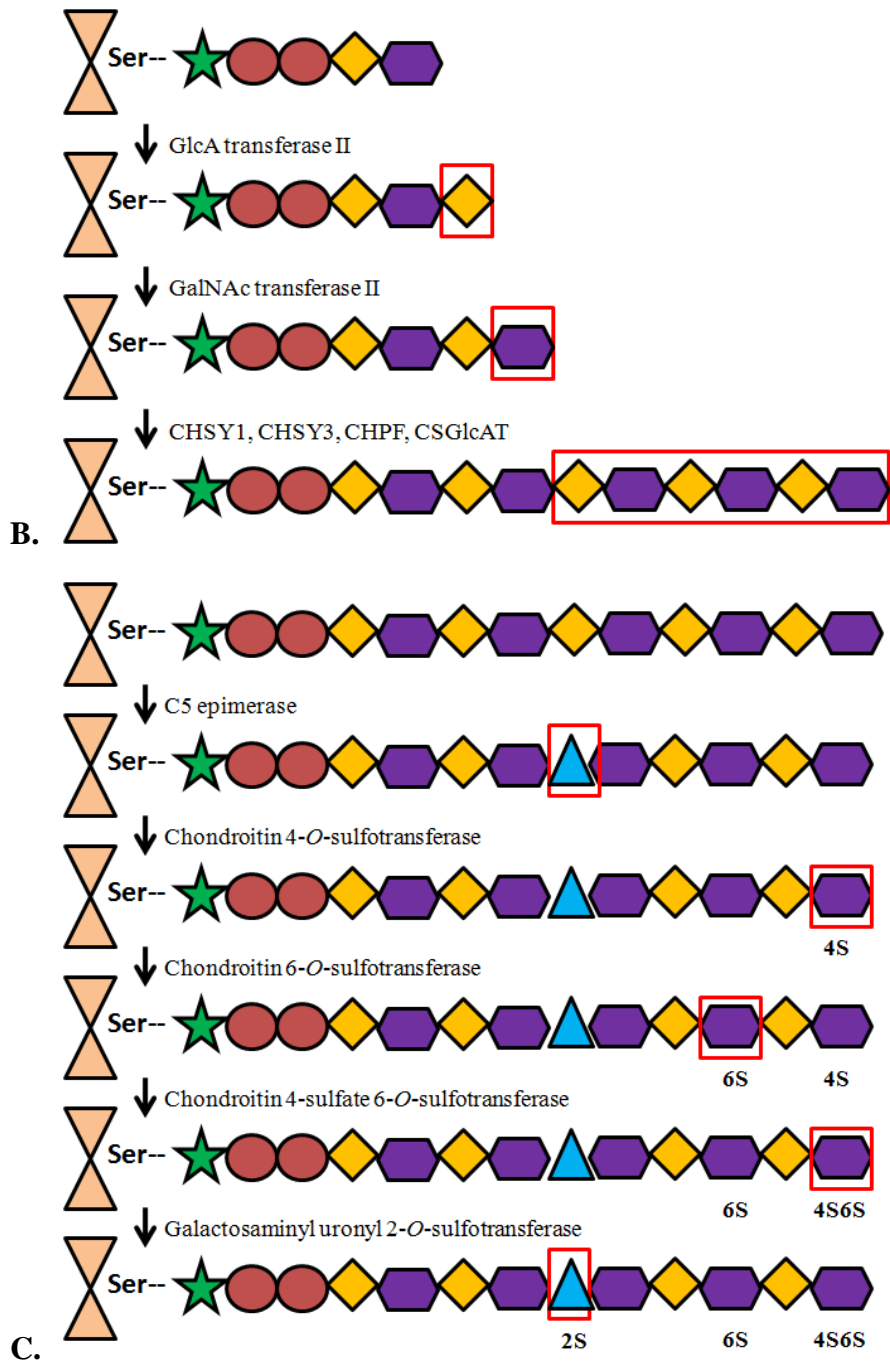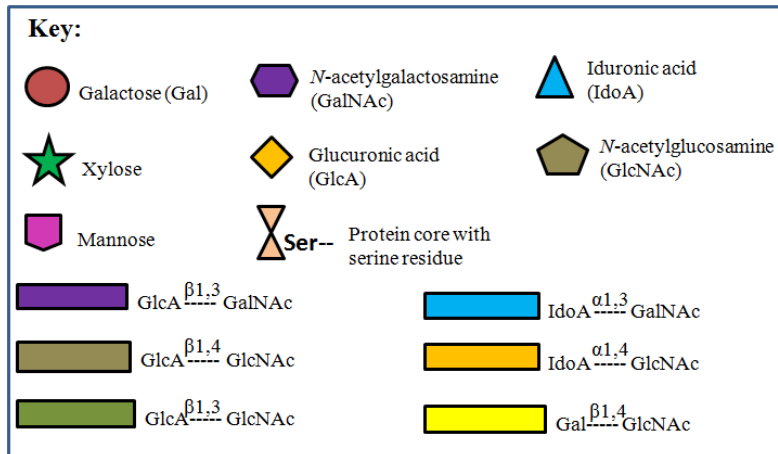
Figure 1.4 The biosynthesis of galactosaminoglycans (GalAGs). (A) The synthesis of the linkage region. CSGalNAcT-1 commits the nascent chain to GalAG formation. Linker tetrasaccharide is conjugated to core protein via serine residue to form proteoglycans. (B) Chain polymerization is mediated by a variety of enzymes. (C) Chain modification such as sulfation and epimerization involved different sulfotransferases and epimerase.

1.10.1.1. *N*-acetlygalactosaminyltransferase (CSGalNAcT-1) enzyme family: CSGalNAcT-1 and CSGalNAcT-2

The cDNA of CSGalNAcT was cloned and described by two groups of researchers from Japan (Gotoh et al., 2002a, Uyama et al., 2002). CSGalNAcT-1 and -2 enzymes are ubiquitously expressed in various tissues and cell types and especially highly expressed in thyroid and placenta (Gotoh et al., 2002a). The amino acid sequences of CSGalNAcT-1 and CSGalNAcT-2 are highly homologous (Sato et al., 2003). Assay of CSGalNAcT activity revealed that CSGalNAcT-1 is involved in initiation of chondroitin sulfate synthesis and in elongation of the chondroitin sulfate chain. In contrast, CSGalNAcT-2 showed stronger elongation activity by enhancing the transfer of *N*-acetylgalactosamine to glucuronic acid of chondroitin poly- and oligosaccharides, and to chondroitin sulfate poly- and oligosaccharides harbouring β1-4 linkage (Sato et al., 2003). CSGalNAcT-1 was proven to

favor elongation of chondroitin instead of chondroitin sulfate poly- and oligosaccharide (Gotoh et al., 2002a).

Chondroitin sulfate is commercially available in pharmacy as a health supplement for patients suffering from cartilage degenerative diseases, osteoarthritis and spinal disorders with back pain (Sakai et al., 2007). Aggrecan is the major proteoglycan found in the extracellular matrix of cartilage and consists of approximately 100 chains of chondroitin sulfate attached to the protein core (Doege et al., 1994, Plaas et al., 1997). Study showed that expression of CSGalNAcT-1 was the highest among other glycosyltransferases in developing cartilage of mouse embryo by in-situ hybridization and real time qPCR techniques (Sakai et al., 2007). Aggrecan generated from CSGalNAcT-1 over-expressing chondrocytic cell line revealed a greater number of chondroitin sulfate chains attached to aggrecan core proteins (Sakai et al., 2007). Hence, this enzyme is shown to be important in chondroitin sulfate synthesis in cartilage. A non-redundant role of CSGalNAcT-1 in chondroitin sulfate synthesis was also demonstrated in a vivo study analyzing CSGalNAcT-1-null mice. These mice expressed 50% reduction of chondroitin sulfate synthesis during embryonic stage, and demonstrated defects in skeletal and cartilage development (Watanabe et al., 2010).

Chondroitin sulfate proteoglycans (CSPGs) was shown to be important in the healing process of injured spinal cord and in the recovery of the motor function during the acute phase after injury (English, 2005). A study revealed

the possible association between missense mutations of CSGalNAcT-1 with neuropathies. Poor productivity of CSPGs due to defective CSGalNAcT-1 enzymatic activity impaired the effectiveness of the healing of injured peripheral nervous system (Saigoh et al., 2011).

The role of CSGalNAcT-1 in breast cancer and other cancer types have not been investigated thus far. However, since CSGalNAcT-1 enzyme determines the biosynthesis of chondroitin/ dermatan sulfate GAG chains; and these molecules are intensively investigated in cancers, it is highly possible that CSGalNAcT-1 is implicated, if not, indirectly, in breast cancer.

1.10.2. Major species of CSPGs/DSPGs

Aggrecan is the major proteoglycan found in cartilage and also presents in a number of other connective tissues such as tendon, ligament, joint capsule, and neural tissue (Nicola, 2006). Aggrecan helps to maintain the hydration of the cartilage by attracting and binding to water and in doing so gives the tissue its ability to resist compression (Maroudas et al., 1969).

Versican is the most common PG present in the ECM of most connective tissues as well as smooth muscle, the nervous system and the kidney (Nicola, 2006). Versican is the largest PG in the family due to the large core protein of the size of 400 kDa; and four splice variants of versican has been identified in mammalian tissues and are termed V0, V1, V2, and V3 (Dours-Zimmermann and Zimmermann, 1994). Similar to aggrecan, versican is important for the maintenance of the hydration of ECM (LeBaron et al., 1992). Versican is

likely to be involved in the organization of the ECM through its interaction with a number of extracellular macromolecules and cell surface receptors (Aspberg et al., 1999). Study showed that the V0 and V1 splice variants inhibited the adherence of cells to Type I collagen, fibronectin, and laminin, probably due to the CS chains associated with these PGs (Yamagata et al., 1993) . Abundance of versican expressed by rapidly growing cells could imply the involvement of versican in regulating cell proliferation and migration (Zimmermann et al., 1994). Versican is also essential in development because knockout mice did not survive in utero (Mjaatvedt et al., 1998).

Neurocan and brevican are two CSPGs expressed specifically by the nervous system. Neurocan is synthesized by neural cells. It mediates the adhesion and outgrowth of neural cells as it specifically interacts with neural cell adhesion molecules (Ng-CAM and NCAM) and tenascin-C. It has been shown that the presence of CS chains was critical for these interactions (Margolis and Margolis, 1997). Brevican is expressed by astrocytes in the central nervous system. Brevican deficient mice showed some changes in the brain development and acquired a poor memory (Brakebusch et al., 2002).

Decorin and biglycan are members of the small leucine-rich family of PGs. Decorin is predominantly presents in dense connective tissues such as tendon and ligaments (Vogel and Heinegard, 1985). Decorin has been found to interact with Type I and II collagens and influence collagen fibrillogenesis resulting in thinner collagen fibrils (Vogel et al., 1984). Decorin was involved in the regulation of cell proliferation by interacting directly with cells or with

growth factors (Nicola, 2006). The core protein of decorin could bind to transforming growth factor-β (TGF- β) and control the level of availability of this growth factor in cell signaling; thus affecting a number of cellular function including cell division, differentiation, adhesion, and organization of ECM (Yamaguchi et al., 1990). Biglycan is found in a number of tissues that include capillary endothelium, skeletal muscle, cartilage, bone, and tendon (Fisher et al., 1989). In biglycan-knockout mice, the rate of bone growth was affected and the animals showed signs of early osteoporosis, which indicated that biglycan was essential in cell division and regeneration of bone marrow stromal cells (Xu et al., 1998).

NG2 is one of the important CS transmembrane PGs and is known as high-molecular weight melanoma-associated antigen or cell surface CSPG. NG2 was identified due to its expression in most human melanoma cell lines as tumor-associated antigen (Paulus et al., 1996). NG2 is expressed in numerous embryonic and non-differentiated cell types (Nishiyama et al., 1991, Ozerdem et al., 2001) and is widely distributed in central and peripheral nervous system (Petrini et al., 2003). NG2 was primarily studied in melanoma progression, but the expression of this PG was also discovered in different nervous system tumors (Chekenya et al., 1999), basal cell, breast cancer (Kageshita et al., 1985, Walter-Yohrling et al., 2003, Smith et al., 1996), and leukemia of different origins (Smith et al., 1996).

1.10.3. The roles of chondroitin sulfate/ dermatan sulfate and the respective

proteoglycans in cancer

Chondroitin sulfate/ dermatan sulfate is widely expressed intercellularly (in

extracellular matrix), at the cell membrane and intracellularly. Incorporation

of synthesizing and post-modification enzymes gives rise to the huge

repertoire of diverse structures found in chondroitin sulfate/ dermatan sulfate.

Besides, post-modification of the protein backbones and numbers and varieties

of GAG chains attached to the protein cores also contribute to the complexity

of the glycoproteins. The functions of proteoglycans derived primarily from

the types of GAG chains attached and the modification patterns, such as

sulfation pattern on the GAG chains (Asimakopoulou et al., 2008, Yip et al.,

2006).

Changes in expression of CSPGs/DSPGs are correlated with pathological

conditions. Versican and decorin were over-expressed in the stroma of

malignant tumors, including osteosarcoma, testicular tumors, breast,

pancreatic and colon cancer (Theocharis et al., 2006, Labropoulou et al., 2006,

Skandalis et al., 2011). Over-expression of versican in melanoma cells was

shown to correlate with poor prognosis and cancer relapse in breast and

prostate cancers (Ricciardelli et al., 2002, Ricciardelli et al., 1998). Expression

of CS chains predominantly consist of 6-O-sulfated and non-sulfated

disaccharide was enhanced in pancreatic, rectal and gastric carcinomas

(Theocharis et al., 2006, Skandalis et al., 2006, Theocharis et al., 2003).

Enzymes that involve in the biosynthesis of CS determine the CS chain profile

in a malignant environment. For example, chondroitin-polymerizing factor,

glucuronyltransferase and chondroitin synthase III were expressed at much higher levels in colorectal cancer tissue compared with adjacent normal tissue, the expression of these enzymes increased as the cancer stage advanced (Kalathas et al., 2011).

As mentioned earlier, the sulfation pattern of CS determines the function of the GAG chains; thus, sulfation pattern is a critical factor in cancer progression (Theocharis et al., 2006). CS-E and CS-A chains acted as a 'growth-factors reservoir' for FGF2 by regulating the storage and release of the growth factors; binding to FGF2 led to activation of the mitogen-activated protein kinase (MAPK) pathway and eventually malignant transformation (Nikitovic et al., 2008, Deepa et al., 2002). CS-E was found highly expressed in ECM of ovarian adenocarcinoma, mediating VEGF binding and promoting tumor progression (ten Dam et al., 2007). The importance of sulfation pattern in CS/DS chains could also be seen in their specific selection of binding to cell membrane receptors such as L- and P-selectins and CD44, leading to malignant transformation of tumor cells (Asimakopoulou et al., 2008, Kawashima et al., 2000, Monzavi-Karbassi et al., 2007). In melanoma cells, CS-A chains of melanoma chondroitin sulfate proteoglycans (MCSP) specifically enhanced formation of a complex with membrane type-3 MMP (MT3-MMP) and pro-MMP2, leading to activation of MMP3, which is the primary extracellular matrix degrading enzyme in the metastatic cascade (Iida et al., 2007).

1.10.3.1. Chondroitin sulfate/ dermatan sulfate and the respective

proteoglycans in breast cancer

The roles of chondroitin sulfate/ dermatan sulfate were reported to implicate in breast cancer tumorigenesis. In a paper published earlier (Alini and Losa, 1991), comparison of biochemical composition of proteoglycans in invasive mammary carcinoma and benign lesions of the breast was made. In neoplastic tissue, there was an increased level of chondroitin sulfate but dermatan sulfate level was lower compared with tissue from benign lesions. Similar alteration in proteoglycans composition was detected by another group of researchers when comparing proteoglycans composition in breast cancer tissue with normal tissue. Extracted proteoglycans from breast cancer tissue could stimulate endothelial cells proliferation by 1.3- to 1.5-fold, and the proliferative action was the consequent of the increased chondroitin sulfate content (Vijayagopal et al., 1998). Decorin was shown to possess anti-proliferative property. Decorin is a ligand for EGF receptor. In breast cancer, the ectopic expression of decorin inhibited EGF signaling through interaction with EGF receptor (Iozzo, 1998, Wegrowski and Maquart, 2004), leading to the down-regulation of ErbB2 and MAP kinases (Santra et al., 2000) and upregulation of p21^{Cip1}/WAF1 CDK inhibitor (De Luca et al., 1996), causing an inhibition of cell proliferation and specific induction in transformed cells (Tralhao et al., 2003). In invasive breast carcinoma, reduced expression of lumican, another member of SLRP family, was demonstrated to correlate with cancer progression (Troup et al., 2003). In patients with node-negative invasive breast cancer, reduced expression of decorin and lumican were associated with poor prognosis. Low decorin was shown to predict recurrence

and poor survival from multivariate cox regression analysis model (Troup et al., 2003). One explanation for this observation was that as both decorin and lumican were important in maintaining normal collagen organization, the reduced expressions of these proteoglycans dampened the strength of extracellular matrix as physical barrier to tumor spread (Peyrol et al., 1997). Besides, stroma with lower expression of decorin was unable to sequester TGF-β effectively, thus led to poor disease outcome in later stages of epithelial tumors (Akhurst and Balmain, 1999, Reiss and Barcellos-Hoff, 1997, Arteaga et al., 1996).

Versican is a high molecular mass stroma PG decorated with CS chains. In breast cancer, versican expression was found positively correlated with recurrence and more advanced disease (Wilson et al., 1983). Versican was demonstrated as a potential prognostic marker in predicting recurrence in node-negative primary breast cancer (Ricciardelli et al., 2002). Cox analyses from the study showed that patients with low peritumoral versican level had lower relapse rate than those with high versican levels.

Chondroitin sulfate chains containing sulfation pattern of [GlcA-GalNAc (4, 6-O-disulfate)] and [IdoA-GalNAc (4, 6-O-disulfide)] binds P-selectin with high affinity (Kawashima et al., 2002). It was demonstrated in a study that CSPGs on the surface of a metastatic breast cancer cell line, 4T1, were major P-selectin ligands and this interaction promoted pro-metastatic heterotypic adhesion of tumor cells to platelets and endothelial cells (Monzavi-Karbassi et al., 2007). The same group of researchers further extended the experiment to

indicate that the expression of CHST11 gene controlled the construction of CS-A chains. In aggressive breast cancer cells, CHST11 gene expression was associated with metastatic phenotypes and synthesis of P-selectin ligands (Cooney et al., 2011). In addition, expression of CHST11 and CSPG4 were assessed by qRT-PCR in primary invasive breast cancer clinical specimens. Both of these genes were over-expressed in tumor-containing tissues compared with normal tissues. The significance of interaction between CS chains and P-selectin was further evident when CS chains in highly metastatic mammary cell line were removed by enzymatic methods. The formation of lung metastases was significantly impeded.

1.11. Objectives of project

To the best of my knowledge, this is the first study conducted to investigate the functional role of *CSGalNAcT-1* in breast cancer. *CSGalNAcT-1* was hypothesized to mediate the phenotypic changes of the breast cell lines.

The objectives of this study are as follows:

1. To determine the expression of *CSGalNAcT-1* in different breast cell lines and investigate the functions of this gene in affecting cellular behaviors by silencing *CSGalNAcT-1* in normal breast cell line, MCF-12A; and over-expressing *CSGalNAcT-1* in breast cancer cell lines, MCF7 and MDA-MB-231.

2. To investigate if *CXCL14* is a downstream target of *CSGalNAcT-1*.

3. To determine the localization and expression of CSGalNAcT-1 in clinical samples of breast invasive ductal carcinoma by immunohistochemistry and to study the association of CSGalNAcT-1 with clinicopathological parameters and its value in predicting clinical outcome.

CHAPTER 2

MATERIALS AND

METHODS

2. MATERIALS AND METHODS

2.1. *In vitro* cell culture

2.1.1. Cell lines

A few breast cell lines were used in this project. A non-tumorigenic human breast cell line, MCF-12A (ATCC: CRL-10782) and breast cancer cell lines, MCF-7 (ATCC: HTB-22), MDA-MB-231 (ATCC: HTB-26), and ZR75-1 (ATCC: CRL 1500) were obtained from American Type Culture Collection (ATCC, Manassas, VA, USA). MCF-12A was propagated in DMEM/F12 (Invitrogen, Carlsbad, CA, USA) supplemented with 20 ng/ml human epidermal growth factor (EGF) (Sigma-Aldrich, Missouri, USA), 100 ng/ml cholera toxin (Sigma-Aldrich, Missouri, USA), 0.01 mg/ml bovine insulin (Sigma-Aldrich, Missouri, USA), 500 ng/ml hydrocortisone (Sigma-Aldrich, Missouri, USA) and 5% fetal bovine serum (FBS) (Hyclone, Logan, Utah). MCF-7, a poorly invasive human breast adenocarcinoma cell line was cultured in DMEM supplemented with 10% FBS. ZR75-1 is a less invasive breast cancer cell line and MDA-MB-231 is a highly invasive human breast adenocarcinoma cell line. These two cell lines were cultivated in RPMI 1640 supplemented with 10% FBS. All cell lines were incubated in a humidified incubator at 37 ℃ in a 5% CO_2, 95% air atmosphere.

2.1.2. Thawing of human breast cell lines

The frozen vial of human breast cell lines was thawed immediately in 37 ℃ water bath upon removal from liquid nitrogen storage tank. Cryopreserved cells were neutralized with 4 ml of culture medium and centrifuged at 125 x *g* for 5 minutes to remove the cytotoxic, cryoprotectant dimethyl sulphoxide

44

(DMSO) (Sigma-Aldrich, Missouri, USA). Cell pellet was resuspended in 5 ml of culture medium and transferred into a 25 cm^2 culture flask and incubated at 37 ℃, 5% CO_2 incubator.

2.1.3. Subculture of human breast cell lines

Cells were ready to be subcultured when cell confluency of 80% was reached. Culture medium was decanted from the culture flasks and washed with 1X PBS to remove any cell debris. MCF7, ZR75-1 and MDA-MB-231 were detached from the surface of the flask with 1X pre-warmed trypsin-ethylenediaminetetraacetic acid (trypsin-EDTA) (Invitrogen, Carlsbad, CA, USA) for 5 minutes at 37 ℃ inside incubator. However, the highly adherent MCF-12A cells need to be trypsinized using 5X pre-warmed trypsin-EDTA for 10 minutes at 37 ℃ inside incubator. The detached cells were then resuspended with complete medium at 3X the volume of added trypsin to inactivate the trypsin activity. The cell suspension was centrifuged at 125 x g for 5 minutes and resuspended with fresh complete medium before dividing into culture flasks at ratio of 1:3.

2.1.4. Cryopreservation of human breast cell lines

The cryopreservation medium used for the various breast cell lines comprised of culture medium supplemented with 20% FBS and 5% DMSO. The cells were transferred to cryovials and placed in freezing container Mr. Frosty (Nalgene, Rochester, NY) for overnight at -80 ℃ before long-term storage in liquid nitrogen.

2.2. RNA extraction, cDNA synthesis, quantitative real time polymerase chain

reaction (qRT-PCR) of human breast cell lines

Total RNA was extracted from breast cell lines grown in culture flasks and 6-well plates using RNeasy Mini kit (Qiagen, Hilden, Germany), as according to manufacturer protocol. RNA yield was quantified using Nanodrop ND-100 spectrophotometer (Thermo Fisher Scientific, Wilmington, USA). The purity of extracted RNA was determined using the absorbance ratio of A_{260}/A_{280}, which should range from 1.8 to 2.1. cDNA synthesis from total RNA was performed using the Superscript III First-strand cDNA synthesis kit (Invitrogen, Carlsbad, USA), following the manufacturer protocol. The cDNA was used for quantitative real-time PCR using the QuantiTect SYBR Green PCR kit (Qiagen, Hilden, Germany) on the Roche LightCycler 2 machine (Roche Diagnostics Corporation, Roche Applied Science). Primers used for qRT-PCR are listed in Table 2.1 (1st Base, Singapore). Program settings used for qRT-PCR is as described: An initial activation step at 95 ℃ for 15 minutes, followed by 45 cycles of a 3 three-step process of denaturation at 94 ℃ for 15 seconds, annealing at 60 ℃ for 25 seconds, and extension at 72 ℃ for 12 seconds. Melting curve analysis followed by cooling of samples was performed last.

Table 2.1 Sequences of qRT-PCR primers used

Gene symbol	Forward primer	Reverse primer	Product size
β-actin	tggcaccacaccttctacaat	gatagcacagcctggatagca	166
CSGalNAcT-1	gagatgtgcattgagcagga	gaagttggcagctttggaag	114
CSGalNAcT-2	tccccttggagagaaactga	cggaagagggtcacatgtct	141
CXCL14	accaagagcgtgtccaggta	ttgcacaagtctcccaactg	175
GAPDH	gaaggtgaaggtcggagtcaacg	tgccatgggtggaatcatattgg	157
T7, BGH	taatacgactcactataggg	cttatgagtatttcttccagggta	177

2.3. Gene silencing in MCF-12A

2.3.1. Single siRNA silencing

ON-TARGET*plus* SMARTpool *CSGalNAct-1* siRNA, negative control ON-TARGET*plus* si*CONTROL* Non-targeting pool siRNA and positive control ON-TARGET*plus* si*CONTROL GAPDH* SMARTpool siRNA as the positive control were used (Dharmacon Inc, Colorado, United States of America). The sequences of *CSGalNAcT-1* siRNA are listed in Table 2.2. Before transfection, MCF-12A cells were trypsinized and resuspended in Opti-MEM I Reduced Serum Medium (Invitrogen, Carlsbad, CA, USA). For each well in a 6-well plate, 30 nM of siRNA was diluted in 96.25 μl of Opti-MEM I and a mixture of 8 μl siPORT Amine transfection reagent (Ambion, Inc/Applied Biosystems, Texas, USA) with 92 μl of Opti-MEM I were incubated for 25 minutes at room temperature. The two diluents that made up a total volume of 200 μl were mixed gently and incubate for 15 minutes at room temperature to allow transfection complexes to form. After that, 2×10^5 MCF-12A cells in 2.3 ml of Opti-MEM I were seeded into each well and 200 μl of siRNA complex was added into the cell suspension. The 6-well plate was swirled gently to mix the complexes and cells evenly. Finally, incubate the 6-well plate at 37 ℃ in 5% CO_2 incubator for 8 hours.

Following incubation, transfection complexes were totally replaced with 2.5 ml complete DMEM/F12 in every well. After 24 hours post transfection, every well was replaced with fresh 2.5 ml complete medium again. Silenced cells were harvested at either 48 hours or 72 hours post transfection for further experiments. The silencing efficiencies of transfected MCF-12A cells were determined using qRT-PCR.

Table 2.2 ON-TARGET*plus* SMARTpool *CSGalNAcT-1* siRNA sequence

Sequence	Anti-sense	Sense
1	5'PUGACACGAUAUUUAUG GUUUU	AACCAUAAAUAUCGUGU CAUU
2	5'PUAUUGAUGAAGUCUG ACCGUU	CGGUCAGACUUCAUCAA UAUU
3	5'PAUACCUUCUUCCCUGG CUGUU	CAGCCAGGGAAGAAGGU AUUU
4	5'PAUACUUGCGAUAAAGG UGCUU	GCACCUUUAUCGCAAGU AUUU

Same transfection protocol was applied in silencing MCF-12A with Ambion Silencer® Select *CXCL14* siRNA (Ambion, Inc / Applied Biosystems, Texas, USA). A final concentration of 10 nM siRNA and 8 μl siPORT Amine transfection reagent (Ambion, Inc / Applied Biosystems, Texas, USA) were added to each well. Table 2.3 listed the sequences of *CXCL14* siRNA used. Ambion Silencer® Select siRNA Negative Control was used as negative control while Ambion Silencer® Select *GAPDH* siRNA was used as positive control.

Table 2.3 Ambion Silencer Select® *CXCL14* siRNA sequences

siRNA ID	Anti-sense	Sense
s18333	AUUUGGACCCGUCCACACGcg	CGUGUGGACGGGUCCAAAUtt
S18332	AUGAUAACCAUCUUCUCCUcg	AGGAGAAGAUGGUUAUCAUtt

2.3.2. Double siRNA silencing

The same transfection method as above was adopted in double siRNA silencing. Four experimental groups were included: double silenced group 30 nM *CSGalNAcT-1* siRNA + 10 nM *CXCL14* siRNA; double negative group 30 nM ON-TARGET*plus* si*CONTROL* Non-targeting pool siRNA + 10 nM Ambion Silencer® Select siRNA Negative Control siRNA; *CSGalNAcT-1* single silenced group 30 nM *CSGalNAcT-1* siRNA + 10 nM Ambion Silencer® Select siRNA Negative Control siRNA and *CXCL14* single silenced group 10 nM *CXCL14* siRNA + 30 nM N-TARGET*plus* si*CONTROL* Non-targeting pool siRNA.

2.4. Microarray analysis

CSGalNAcT-1 silenced MCF-12A cells were harvested 48 hours post transfection as described in section 2.3.1. Total RNA was extracted using RNeasy Mini kit (Qiagen, Hilden, Germany) and RNA purity and concentration was obtained as described in section 2.2. Sample RNA was confirmed to have good quality before sending to Origen Labs (Origen Laboratories, Singapore) for hybridization to Affymetrix Human U133 Plus version 2.0 array. Raw microarray data was processed using GeneSpring software (Agilent Technologies, United States). MultiExperiment Viewer

(TM4 Microarray Software Suite) was used to perform further data visualization. Gene ontology grouping was performed using The Database for Annotation, Visualization and Integrated Discovery (DAVID) version 6.7 (NIH, Maryland, United States).

2.5. Stable over-expression of *CSGalNAcT-1* in MCF-7 and MDA-MB-231

The plasmid was kindly provided by Prof Hideto Watanabe from Institute for Molecular Science of Medicine, Aichi Medical University, Nagakute, Aichi (Sakai et al., 2007) and pcDNA 3.1 empty vector was kindly provided by Associate Professor Ann Lee Siew Gek from National Cancer Centre, Singapore. Full *CSGalNAcT-1* mRNA sequence was cloned into pcDNA 3.1 vector (Invitrogen, Carlsbad, USA). The plasmid contains both Ampicillin and Neomycin (G418) resistant gene for selection purpose. The details of *CSGalNAcT-1* cloning were described in Sakai et al., 2007.

2.5.1. Plasmid transformation

Competent *Escherichia coli* (*E.coli*) (Sigma-Aldrich, Missouri, USA) were used for plasmid transformation. 20 ng of plasmid was added to the competent cells. The cells were placed on ice for 20 minutes followed by heating up to 42°C for 90 seconds and then placed back on ice for 2 minutes. After heat shock, 1 ml of LB broth was added to the cells and the culture was placed on shaker at 300 rpm for 1 hour. After that, the cells were streaked onto agar plates containing 100 µg/ml of Ampicillin (Sigma-Aldrich, Missouri, USA). The agar plates were placed in oven at 37°C overnight.

2.5.2. Colony polymerase chain reaction (PCR)

Several colonies were picked up partially for colony PCR. This is to ensure the gene of interest remains in the plasmids during the transformation. *CSGalNAcT-1* primers were used in the PCR; while T7 forward primer and BGH reverse primer were used to bind to empty vector in the PCR. The PCR setup is as follows: initial denaturation at 94 ℃ for 3 minutes, followed by 44 cycles of 94 ℃ 30 seconds, 55 ℃ 30 seconds and 72 ℃ 1 minute, and final extension step of 72 ℃ 10 minutes. Taq PCR Core Kit from Qiagen, Hilden, Germany was used in the PCR. Subsequently, the PCR products were run on a 2% DNA gel electrophoresis to verify the correct product size. The DNA gel electrophoresis was run at 90 V for one hour.

2.5.3. Colony expansion and plasmid extraction

After colony PCR, the remaining part of the colonies were picked up and inoculated into LB broth containing 100 ug/ml Ampicillin and left on shaker to shake overnight again at 37 ℃ at speed of 300 rpm. The next day the cultures were used for plasmid extraction using Qiagen Mini-prep kit (Qiagen, Hilden, Germany), following the manufacturer protocol. Plasmid yield was quantified using Nanodrop ND-100 spectrophotometer (Thermo Fisher Scientific, Wilmington, USA). The purity of extracted plasmid was determined using the absorbance ratio of A_{260}/A_{280}, which should range from 1.8 to 2.0.

2.5.4. *CSGalNAcT-1* plasmid stable transfection in MCF-7 and MDA-MB-231

MCF-7 (8×10^4 cells) and MDA-MB-231 (5×10^4 cells) were seeded in 24-well plate to reach a confluency of 80-90% the next day. 0.2 μg of *CSGalNAcT-1* plasmid and 0.5 μg of the plasmid were transfected into MCF7 and MDA-MB-231 respectively using Lipofectamine 2000 reagent (Invitrogen, Carlsbad, USA), according to the manufacturer protocol. 24 hours later, each well was replaced with complete medium. To achieve optimal condition for antibiotic selection, transfected cells were reseeded at 2×10^4 cells per well for Neomycin (Invitrogen, Carlsbad, USA) selection. MCF-7 cells were added with 700 μg/ml of Neomycin while MDA-MB-231 cells were added with 450 μg/ml of Neomycin. Two weeks later, colonies were picked up for expansion. The over-expression level of *CSGalNAcT-1* in MCF-7 and MDA-MB-231 were determined by qRT-PCR.

2.6. Cell migration assay

Cell migration assay was performed in Transwell Inserts (Corning Incorporated, New York) of polycarbonated membrane with 8.0 μm pore size. To improve cell attachment, the transwell inserts were hydrated with medium overnight at 4 ℃. The transwell inserts were placed in incubator at 37 ℃ for an hour before use. After 48 hours of siRNA transfection, MCF-12A cells were trypsinized and reseeded at a density of 5×10^4 into the chamber. *CSGalNAcT-1* over-expressed MCF-7 and MDA-MB-231 were seeded at a seeding density of 5×10^4 cells per well. The chambers were incubated for 24 hours in the humidified incubator at 37 ℃, 5% CO_2.

Following incubation, cell suspension was removed from the Transwell Inserts and washed with 1X PBS. Migrated cells were fixed by methanol for 15 minutes. Subsequently, the inserts were rinsed with 1X PBS again and left to air dry. The inserts were then stained aqueous crystal violet (0.5% w/v) for 30 minutes. Excessive stain was removed by clean tap water. Non-migrated cells on the upper surface of the membrane insert were removed with a cotton swab. Migrated cells on the underneath surface of the inserts were visualized at 10X objective under stereo microscope (Nikon SMZ 1500) coupled to a digital camera (Nikon DXM1200F). Images of five random fields per insert were captured for quantification.

2.7. Cell invasion assay

In vitro cell invasion was assayed using BD BioCoat™ Cell Environments, Matrigel™ Invasion Chambers inserts (BD, Franklin Lakes, NJ, USA) on a 24-well format. The invasion chambers were dehydrated by medium overnight at 4 ℃. The invasion chambers were placed in incubator at 37 ℃ for 1 hour before use. After 48 hours of siRNA transfection, MCF-12A cells were trypsinized and reseeded at a density of 5 x 10^4 into the chamber. *CSGalNAcT-1* over-expressed MCF-7 and MDA-MB-231 were seeded at a density of 1 x 10^5 cells per well. The wells were filled with medium supplemented with different concentration of FBS. The chambers were incubated for 24 hours in the humidified incubator at 37 ℃, 5% CO_2. The subsequent fixation and quantification procedure was the same as described in section 2.6.

2.8. Cell viability assay

Cell viability was analyzed using a colorimetric technique CellTiter 96 Aqueous Non-radioactive cell proliferation assay (Promega, Madison, USA) 72 hours post transfection. The reagent contains a novel tetrazolium compound, [3-(4,5-dimethylthiazol-2-yl)-5-(3-carboxymethoxyphenyl)-2-(4-sulfophenyl-2H-tetrazolium, inner salt; MTS). MTS is bioreduced into formazan by living cell mitochondrial dehydrogenase. The quantity of formazan is directly proportional to the amount of living cells in culture. The samples were incubated for 4 hours before measuring absorbance at 490 nm in a TECAN plate reader (GENios, Austria).

2.9. Cell apoptosis assay

Cell apoptosis was assayed using a fluorescent technique Apo-ONE® Homogenous Caspase-3/7 Assay (Promega, Madison, USA). 48 hours post siRNA transfection, MCF-12A cells were reseeded into 96-well black opaque plate at a seeding density of 1×10^4 cells per well and the cells were incubated overnight. Caspase profluorescent substrate and Apo-ONE® Caspas-3/7 buffer were thawed and mixed in 1:100 ratios before use. 100 µl of Apo-ONE® Caspase-3/7 reagent was added to each well. The plate was placed at room temperature for one hour. Subsequently, fluorescence was measured at excitation wavelength of 499 nm and emission wavelength of 521 nm.

2.10. Cell adhesion assay

96-well plate was pre-coated with collagen Type I (BD, Franklin Lakes, NJ, USA) or fibronectin (BD, Franklin Lakes, NJ, USA) overnight at 4 ℃. the plate was blocked with 1% bovine serum albumin (Sigma-Aldrich, St. Louis, MO, USA) for one hour the next day. Transfected cells were reseeded at 1 x 10^4 cells per well (for Collagen Type I coated plate) or 3 x 10^4 cells per well (for Fibronectin coated plate). Each treatment group consists of washed and unwashed group. The washed group has to be washed with 1X PBS thrice before 1 hour incubation and no washing is done to the unwashed group. MTS assay was performed to compare the amount of adhered cells. Absorbance was taken at 490 nm 4 hours after MTS was added.

2.11. Western blotting

2.11.1. Protein extraction

Cells were harvested 48 hours post siRNA transfection. Protein was extracted using M-PER Mammalian Protein Extraction Reagent (Pierce, Illinois, USA) with Halt Protease Inhibitor cocktail and EDTA (Pierce, Illinois, USA) added at 10 μl/ml to produce a 1X final concentration. The protein extraction buffer was added to the wells and waited for 5 minutes on ice. Adherent cells were scrapped with cell scrapper (TPP, Switzerland) and centrifuged at 13000 rpm for 10 minutes at 4 ℃. The supernatant which contained protein was aspirated and stored at -80 ℃.

2.11.2. Protein quantification

The protein concentration was quantified using a colorimetric method, bicinchoninic acid (BCA) protein assay kit (Piece, Illinois, USA). The protein reduced Cu^{+2} to Cu^+ in the alkaline medium. The concentration of protein is directly proportional to the amount of reduction which is presented in a purple coloration. 25 μl of protein sample was added into a 96-well plate along with BCA working reagent containing 50 parts of BCA solution and 1 part of 4% of cupric sulphate solution. Samples were incubated at 37 ℃ for 30 minutes before absorbance reading at 562 nm. The final absorbance values were recorded after subtracting away blank absorbance readings. A standard curve was plotted using the final absorbance values of serial diluted bovine serum albumin standards. Protein concentration of each sample was derived from the standard curve.

2.11.3. Sodium dodecyl sulphate polyacrylamide gel electrophoresis (SDS-
          PAGE)

10% resolving gel was casted. The resolving gel contained deionised water, 30% acrylamide mix, Tris (1.5 M, pH 8.8), 10% sodium dodecyl sulfate, 10% ammonium persulfate, and tetramethylelthylenediamine (TEMED). Gel liquid was allowed to polymerize in 30 minutes. After that 5% stacking gel was prepared and added on top of polymerized resolving gel. Stacking gel contained deionised water, 30% acrylamide mix, Tris (1.0 M, pH 6.8), 10% SDS, 10% ammonium persulfate and TEMED.

30 µg of protein was diluted in 5X SDS loading buffer containing Tris-Cl (250 mM, pH 6.8, 30% glycerol, 5% dithiothretol (DTT) and 0.02% bromophenol blue. The diluted samples were heated at 95°C for 5 minutes and cooled at room temperature. Samples and Precision Plus Protein dual color marker (Biorad, CA, USA) were loaded into wells and electrophoresis was performed at 80V with 1X SDS Tris-glycine buffer for 2.5 hours.

2.11.4. Semi-dry electroblotting

Polyvinyl difluoride (PVDF) membrane (Biorad, CA, USA) was activated by sequential rinsing of PVDF in methanol for 15 seconds, followed by deionised water and lastly 1X transfer buffer (Biorad, CA, USA). The gel was removed and equilibrated in 1X transfer buffer upon completion of electrophoresis run. In addition, two thick filter pads were pre-wetted in 1X transfer buffer as well. A gel-sandwich was assembled by placing a filter pad at the bottom, following the PVDF membrane, gel and lastly, another filter pad. Protein transfer was performed via Trans-Blot Semi-Dry Transfer Cell (Biorad, CA, USA) at 15V for 1 hour.

2.11.5. Western blot

Once the transfer was completed, the PVDF membrane was rinsed twice with 1X TBS in 0.1% Tween-20 (1X TBST) for 5 minutes and blocked with 5% non-fat milk (Biorad, CA, USA) in 1X TBST for 1 hour. Subsequently, the membrane was probed with primary antibody in 5% non-fat milk with 1X TBST at 4°C overnight. The membrane was washed thrice with 1X TBST for 10 minutes in each wash, followed by incubation with secondary antibody for

1 hour at room temperature. The dilutions of primary and secondary antibodies used are listed in Table 2.4. After secondary antibody, membrane was washed thrice again with 1X TBST and bound antibodies were detected by enhanced chemilluminescence (ECL) using Femto Substrate System (Pierce, Illinois, USA). Equal volumes of stable peroxide solution and luminal solution were mixed and added carefully on to the membrane. X-ray films were exposed to the membrane in the dark and developed using an automatic film processor. The same protocol was used in CSGalNAcT-1 western blot except that the washing buffer and buffer for blocking was 1X PBS in 0.05% Tween-20 (1X PBST) and the primary and secondary antibody was diluted in 1X PBST with 5% non-fat milk. CSGalNAcT-1 band intensity was captured and analysed by ChemiDoc^{TM} MP imager.

Table 2.4 Dilution of primary and secondary antibodies used in western blotting

Primary antibody	Catalogue number	Dilution	Secondary antibody	Catalogue number	Dilution
CSGalNAcT-1	Abcam rabbit polyclonal ab83071	1:1000	Polyclonal goat anti-rabbit HRP	Dako P0448	1:10,000
BAD	Cell Signaling Rabbit IgG #9268	1: 500	Polyclonal goat anti-rabbit HRP	Dako P0448	1: 5000
Phosphorylated BAD	Cell Signaling Rabbit IgG #5284	1: 500	Polyclonal goat anti-rabbit HRP	Dako P0448	1: 5000
β-actin	Sigma Aldrich A2228	1:10,000	Anti-mouse IgG HRP	GE Healthcare NA9310	1:15,000

2.11.6. Densitometric analysis

The protein band intensities were scanned and evaluated by densitometry (GS-800 Calibrated Imaging Densitometer, BioRad, CA, USA). The intensities of the bands were processed and measured using Quantity-One Image Analysis Software version 4.6.9 (Biorad, CA, USA). Protein band intensity for each sample was normalised against band intensity of loading control, β-actin. CSGalNAcT-1 band intensity was captured and analysed by ChemiDoc^{TM} MP imager.

2.12. Immunofluorescence

2.12.1. F-actin immunofluorescence

Cells were seeded on coverslips in a 6-well plate. *CSGalNAcT-1* over-expressed MCF-7 and MDA-MB-231 were seeded directly while silenced MCF-12A was assayed 48 hours post-transfection. Coverslips were rinsed thrice with 1X PBS. Fixation was performed using 4% paraformaldehyde for 15 minutes. Subsequently, coverslips were washed thrice with 1X PBS-Triton X. Blocking was performed using 1% bovine serum albumin (BSA) for an hour followed by incubation with Alexa Fluor 488 Phalloidin for F-actin (Invitrogen, Carlsbad, CA, USA) at 1:40 dilution in 1% BSA for 20 minutes. After that, coverslips were washed thrice with 1X PBS for 5 minutes in each wash and mounted with VECTASHIELD mounting medium with DAPI (Vector Laboratories, CA, United States). Fluorescence was viewed and captured using Leica DM6000 M microscope (Leica Microsystems, Wetzlar, Germany). Fluorescence intensity was measured using ImageJ software version 1.42q (National Institutes of Health).

2.12.2. CXCL14 immunofluorescence

CSGalNAcT-1 over-expressed MCF-7 and MDA-MB-231 were seeded directly on 6-well plate while silenced MCF-12A was assayed 48 hours post-transfection. Coverslips were rinsed thrice with 1X PBS. Fixation was performed using 4% paraformaldehyde for 15 minutes. Subsequently, coverslips were washed thrice with 1X PBS-Triton X. Blocking was performed using 1% bovine serum albumin (BSA) for an hour. Incubation of CXCL14 antibody (ab46010, Abcam, CA, USA) was done at a dilution of 1:100 overnight at 4 °C. The next day, coverslips were washed thrice with 1X PBS-Tx for 5 minutes in each wash. Secondary antibody Alexa Fluor 488 goat anti-rabbit IgG (Invitrogen, Carlsbad, CA, USA) diluted at 1:400 was incubated for another one hour at room temperature in the dark and followed by three washes of 1X PBS-Tx for 5 minutes in each wash. Finally, coverslips were mounted with VECTASHIELD mounting medium with DAPI (Vector Laboratories, CA, United States). Fluorescence was viewed and captured using Leica DM6000 M microscope (Leica Microsystems, Wetzlar, Germany). Fluorescence intensity was measured using ImageJ software version 1.42q (National Institutes of Health).

2.12.3. CSGalNAcT-1 immunofluorescence in over-expressed MCF-7 and MDA-MB-231 cells

CSGalNAcT-1 over-expressed MCF-7 and MDA-MB-231 were seeded directly on 6-well plate. Coverslips were rinsed thrice with 1X PBS. Fixation was performed using 4% paraformaldehyde for 15 minutes. Subsequently, coverslips were washed thrice with 1X PBS-Triton X. Blocking was

performed using 1% bovine serum albumin (BSA) for an hour. Incubation of CSGalNAcT-1 antibody (ab67128, Abcam, CA, USA) was done at a dilution of 1:36 for 2 hours at room temperature. After that, coverslips were washed thrice with 1X PBS-Tx for 5 minutes in each wash. Secondary antibody Alexa Fluor 568 goat anti-mouse IgG (Invitrogen, Carlsbad, CA, USA) diluted at 1:200 was incubated for another one hour at room temperature in the dark and followed by three washes of 1X PBS-Tx for 5 minutes in each wash. Finally, coverslips were mounted with VECTASHIELD mounting medium with DAPI (Vector Laboratories, CA, United States). Fluorescence was viewed and captured using Leica DM6000 M microscope (Leica Microsystems, Wetzlar, Germany). Fluorescence intensity was measured using ImageJ software version 1.42q (National Institutes of Health).

2.13. Tissue microarray samples and clinicopathological data

Tissue microarray blocks of paraffin-embedded invasive ductal cancer specimens were constructed by the Department of Pathology, Singapore General Hospital. Briefly, specific regions representative of the breast tumours are selected and punched out from the donors' blocks. Cores of invasive ductal carcinomas (IDCs) (2 mm diameter) were inserted sequentially into different recipient blocks. Control tissues (e.g. colon, liver and testis) of 1 mm diameter were included in the series of tissue microarray on invasive ductal carcinomas. 4 µm sections were cut from these recipient blocks and mounted on pre-coated poly-lysine slides. A total of 297 cases of breast invasive ductal carcinomas dated from year 1998 to 2004 were included in the tissue microarrays. Clinicopathological information of patients diagnosed with breast invasive

ductal carcinomas included patient age, race, tumor size, staging, histological grade, lymph node status, DCIS grade, steroid hormone receptors, HER2 status, Bloom-Richardson scoring, tumor tubule formation, pleomorphism and mitotic index are obtained.

2.14. Immunohistochemistry

2.14.1. CSGalNAcT-1 immunohistochemistry

Formalin-fixed, paraffin-embedded tissue microarray sections of 4 μm thickness were deparaffinized in 2 changes of histoclear, followed by rehydration in a graded series of ethanol. The sections were washed with 1X Tris buffered saline (TBS) for 5 minutes before endogenous peroxidase activity was quenched with 3% hydrogen peroxide (H_2O_2) for 30 minutes. Antigen retrieval was performed by microwaving the sections in 0.1 M citric acid buffer and 0.1 M sodium citrate buffer at 100 ℃ for 20 minutes. The slides were washed in 1X TBS-Triton X (TBS-Tx) thrice and 5 minutes each prior to 1 hour incubation of blocking serum at room temperature. Next, the sections were incubated overnight with the mouse CSGalNAcT-1 polyclonal primary antibody (Abnova, Taipei, Taiwan) at a dilution of 1:100 at 4 ℃. Negative controls were assessed by replacing primary antibody with 1X TBS-Tx. After rinsing with 1X TBS-Tx, biotinylated secondary antibody was added for 1 hour at room temperature. Visualisation was achieved by the avidin-biotin-complex technique (ABC kit, Vector Laboratories) using diaminobenzidine (DAB) as the substrate, followed by counterstaining with hematoxylin. The sections were dehydrated in graded series of ethanol and histoclear before mounted in permount.

2.14.2. Semi-quantitative analysis of CSGalNAcT-1 immunostaining in breast

invasive ductal carcinomas (IDCs)

Every tissue microarray case was examined using ImageScope software

version 10.2.1.2314 for Windows (Aperio Technologies, Inc, CA, USA).

Assessment of CSGalNAcT-1 staining was scored independently by one

individual, followed by verification by a pathologist from Singapore General

Hospital. Any discordant in immunoscoring will be re-evaluated until

consensus was reached. Prior knowledge of the clinical data was not known

during the immunoscoring of the TMA sections to avoid any bias in scoring.

The scoring criteria of CSGalNAcT-1 in the stroma and epithelial components

of invasive ductal carcinomas were divided into different categories as follows:

staining intensities of $0 =$ no staining; $1+ =$ weak staining; $2+ =$ moderate

staining; $3+ =$ intense staining and the percentage immune-positivity.

Weighted average intensity (WAI) is the semi-quantitative measurement of the

amount of a molecule being expressed. Total percentage score (TPS) is the

total percentage of cells stained. A final immunoreactivity score (IRS) is the

multiplication of WAI and TPS.

2.14.3. Statistical Analysis

The results of CSGalNAcT-1 immunostaining in invasive ductal carcinomas

were analysed using SPSS 17.0 for Windows (SPSS Inc, Chicago, IL, USA).

The   association   of   CSGalNAcT-1   immunostaining   with   other

clinicopathological parameters was evaluated using Fisher's exact test, while

correlation with ordinal parameters was evaluated using Kendall's tau-b and c

test. Statistical significance was defined as a P-value of <0.05. Besides,

multivariate analysis was performed to investigate the confounding effect in these parameters with CSGalNAcT-1 immunoscoring.

Timeline analyses were then carried out to assess the recurrence and survival of the malignant IDC cases. The timeline measurements used were: (1) Overall Survival (OS) = Date of Death − Date of Diagnosis; (2) Disease Free Survival (DFS) = Date of Recurrence − Date of Diagnosis; (3) Survival After Recurrence (SAR) = Date of Death − Date of Recurrence. Analyses were done using the Log Rank (Mantel-Cox) test and Kaplan-Meier graphs were constructed. Statistical significance was also defined as a *P*-value of <0.05.

CHAPTER 3

FUNCTIONAL ANALYSIS OF

CSGALNACT-1

IN

BREAST CELL LINES

3. FUNCTIONAL ANALYSIS OF *CSGALNACT-1* IN BREAST CELL LINES

The objective of this section of study is to determine the functional role of *CSGalNAcT-1* in breast cell lines. The expression of *CSGalNAcT-1* in different breast cell lines was investigated. Subsequently, the functional impact of this gene was determined by knocking it down in normal breast cell line, MCF-12A; and over-expressing it in breast cancer cell lines, MCF7 and MDA-MB-231. The functional properties of *CSGalNAcT-1* were assessed by examining the changes in migration, invasion, survival and adhesion of the cells. Microarray analysis was done to identify downstream targets of the *CSGalNAcT-1* signaling pathway. *CXCL14* was subsequently selected for double knockdown experiments to determine if *CXCL14* works downstream of *CSGalNAcT-1* in mediating the phenotypic changes of MCF-12A cells.

3.1. *CSGalNAcT-1* expression in different breast cell lines

The expression of *CSGalNAcT-1* was measured by qRT-PCR in breast cancer cell lines (MCF7, ZR75-1 and MDA-MB-231) in relative to MCF-12A, the normal breast cell line. The result is shown in Figure 3.1. Expression level of *CSGalNAcT-1* in breast cancer cell lines is significantly lower in normal breast cell line, MCF-12A.

Expression Level of *CSGalNAcT-1* in Breast Cell Lines
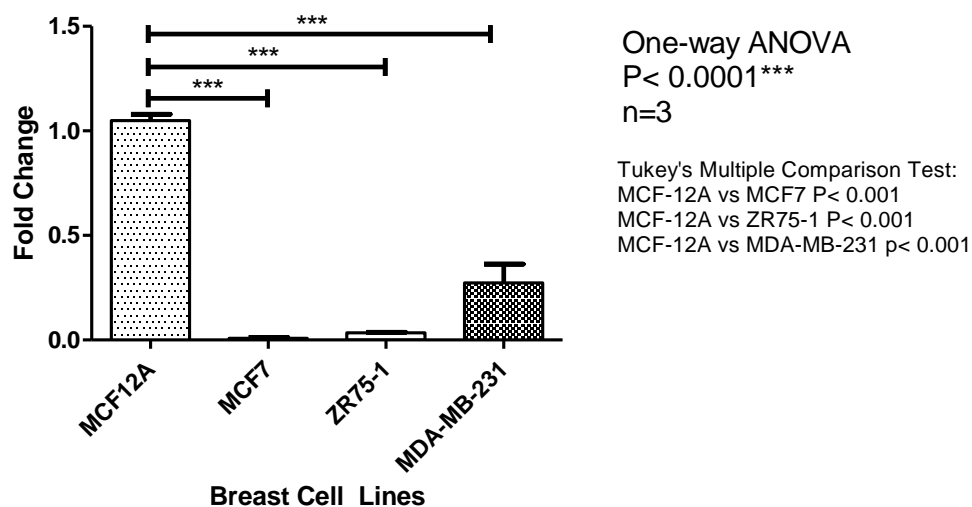
One-way ANOVA
P< 0.0001***
n=3

Tukey's Multiple Comparison Test:
MCF-12A vs MCF7 P< 0.001
MCF-12A vs ZR75-1 P< 0.001
MCF-12A vs MDA-MB-231 p< 0.001

Figure 3.1 Expression level of *CSGalNAcT-1* in breast cancer cell lines (MCF7, ZR75-1 and MDA-MB-231) and MCF-12A, the normal breast cell line. Data shows that expression of *CSGalNAcT-1* is lower in breast cancer cell lines as compared with MCF-12A normal breast cell line. Error bar represents standard error.

3.2.   Knockdown of *CSGalNAcT-1* in MCF-12A cells

CSGalNAcT-1 gene was silenced in MCF-12A with Dharmacon ON-TARGET*plus* SMARTpool *CSGalNAcT-1* siRNA. After optimization, *CSGalNAcT-1* was successfully knockdown by 76.42% as shown in Figure 3.2.

Silencing Efficiency of *CSGalNAcT-1* in MCF-12A

Unpaired T-test
P< 0.0001***
n= 3
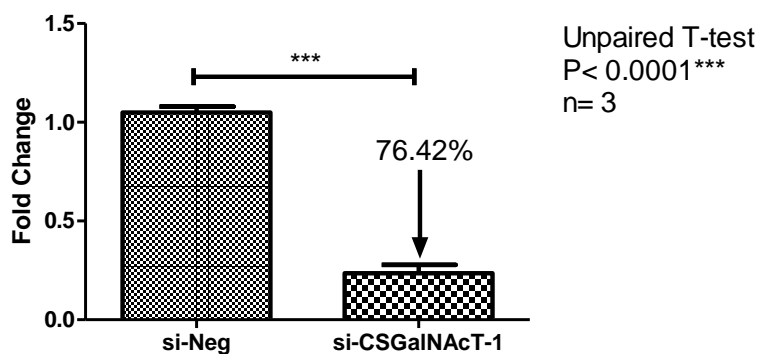
Figure 3.2 Silencing efficiency of *CSGalNAcT-1* gene in MCF-12A normal breast cell line. *CSGalNAcT-1* was successfully knockdown by 76.42%. Error bar represents standard error.

3.2.1. Knockdown of *CSGalNAcT-1* expression in MCF-12A is specific

To confirm that Dharmacon ON-TARGET*plus* SMARTpool *CSGalNAcT-1* siRNA specifically knockdown *CSGalNAcT-1* only but not its isoform *CSGalNAcT-2*, qRT-PCR was performed to analyze the expression level of *CSGalNAcT-2* in *CSGalNAcT-1* silenced MCF-12A cells. As shown in Figure 3.3, there is no significant change in mRNA expression of *CSGalNAcT-2* after MCF-12A cells were transfected with *CSGalNAcT-1* siRNA.
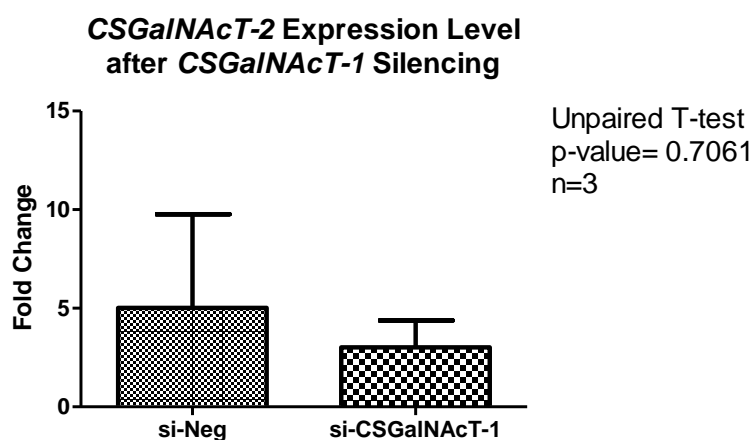
Figure 3.3 Transfection of *CSGalNAcT-1* in MCF-12A cells did not cause a change in the expression of its isoform *CSGalNAcT-2*, indicating the specificity of the siRNA. Error bar represents standard error.

3.2.2. Assessment of *CSGalNAcT-1* protein expression in MCF-12A cells after silencing

The CSGalNAcT-1 protein level was examined 48 hours post silencing and the expression level was assessed by western blotting. As shown in Figure 3.4A, band intensity of protein extracted from *CSGalNAcT-1* silenced MCF-12A (61 kDa) was markedly reduced compared to negative control group. Figure 3.4B indicates the expression of the housekeeping gene, β-actin (41 kDa), as the reference gene. In Figure 3.4C, quantification of the band

intensity was performed and the result showed that expression of

CSGalNAcT-1 was significantly decreased after silencing.

A.

B.

C.
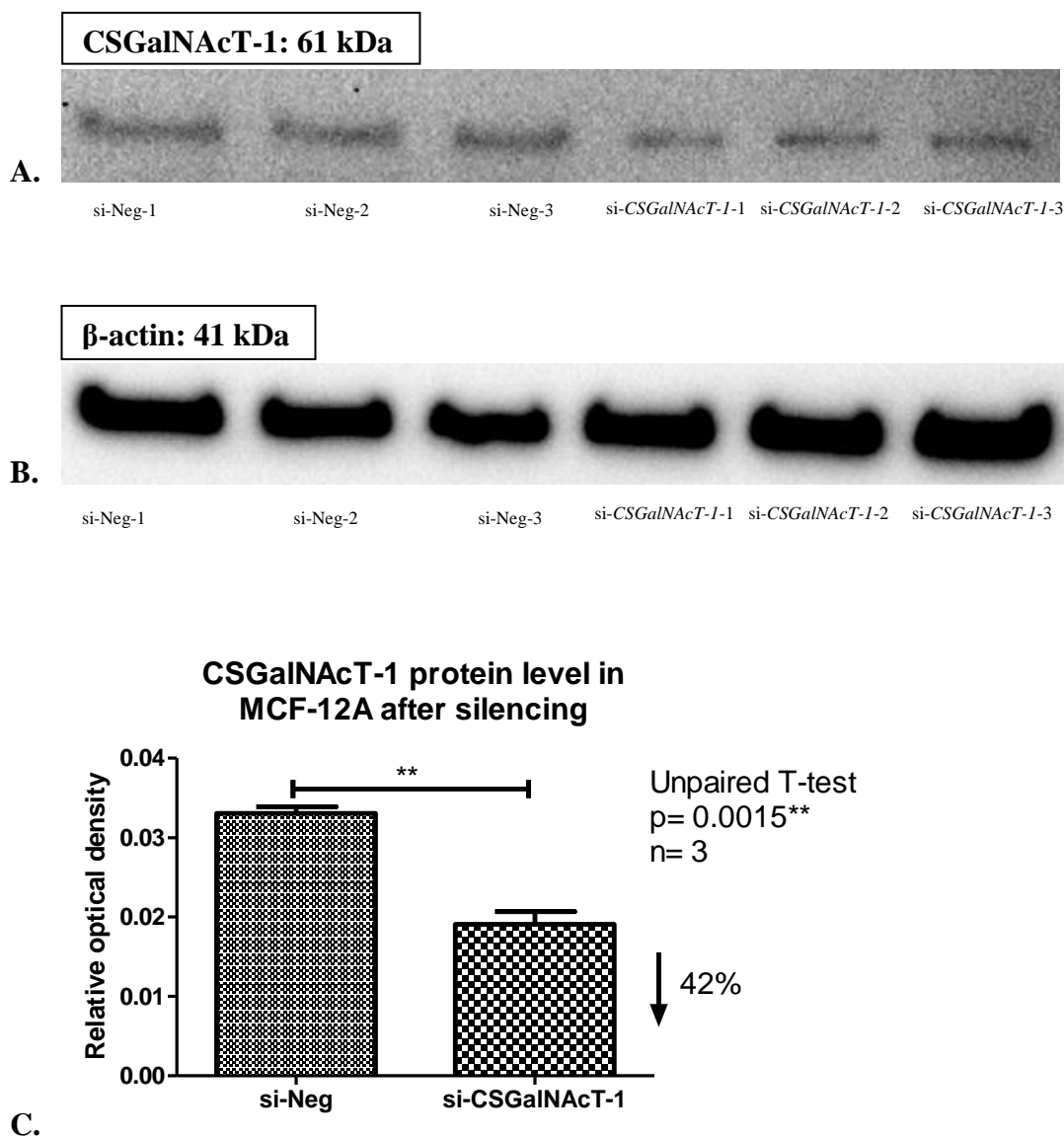
Figure 3.4 Western blot analysis of CSGalNacT-1 protein level 48 hours post transfection in MCF-12A cells. (A) Band intensity of CSGalNAcT-1 in silenced cells was reduced as compared with si-Neg. (B) β-actin protein acts as a normalizer and the expression was unaffected in the silencing process. (C) Densitometric analysis of protein bands revealed that CSGalNAcT-1 protein level is significantly reduced by 42% in silenced cells as compared with the si-Neg. Error bar represents standard error.

3.2.3. Analysis of cell motility in *CSGalNAcT-1* silenced MCF-12A cells

3.2.3.1. Transwell migration assay

Cell migration assay was performed in transwell inserts to study the migratory behavior of MCF-12A cells after *CSGalNAcT-1* silencing. A chemoattractant gradient was created by supplementing medium with 15% FBS in the bottom chamber while no FBS is added to the cell suspension seeded into the top insert. Figure 3.5 shows that a remarkable increase in the migration of MCF-12A cells was observed when *CSGalNAcT-1* is suppressed.

A.

B.

C.
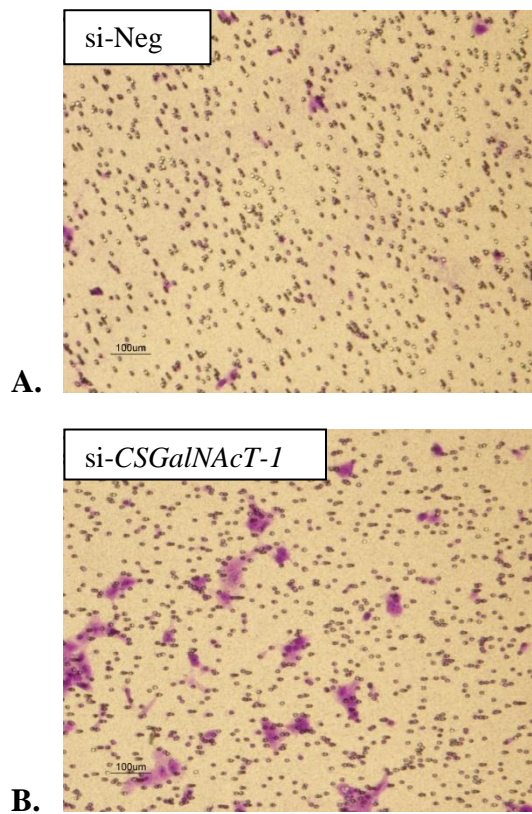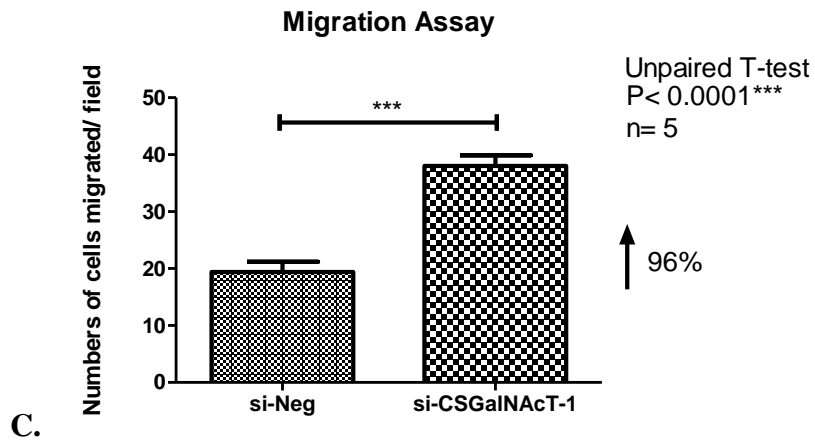
Figure 3.5 Silencing of *CSGalNAcT-1* in MCF-12A promoted cell migration. (A) and (B) showed migrated cells in chambers. (C) Cells treated with *CSGalNAcT-1* siRNA exhibited almost a double fold of increase in migration as compared with si-Neg. Error bar represents standard error.

3.2.3.2.   F-actin immunofluorescence

F-actin is an indicator of cell motility. Generally, fluorescence intensity of F-actin in *CSGalNacT-1* silenced MCF-12A was greater than the negative control, as shown in Figure 3.6A and 3.6B. This result agrees with that of transwell migration assay in section 3.2.3.1, indicating that stronger F-actin staining is consistent with the increased motility in migration assay (Figure 3.6C).

A.

B.

C.
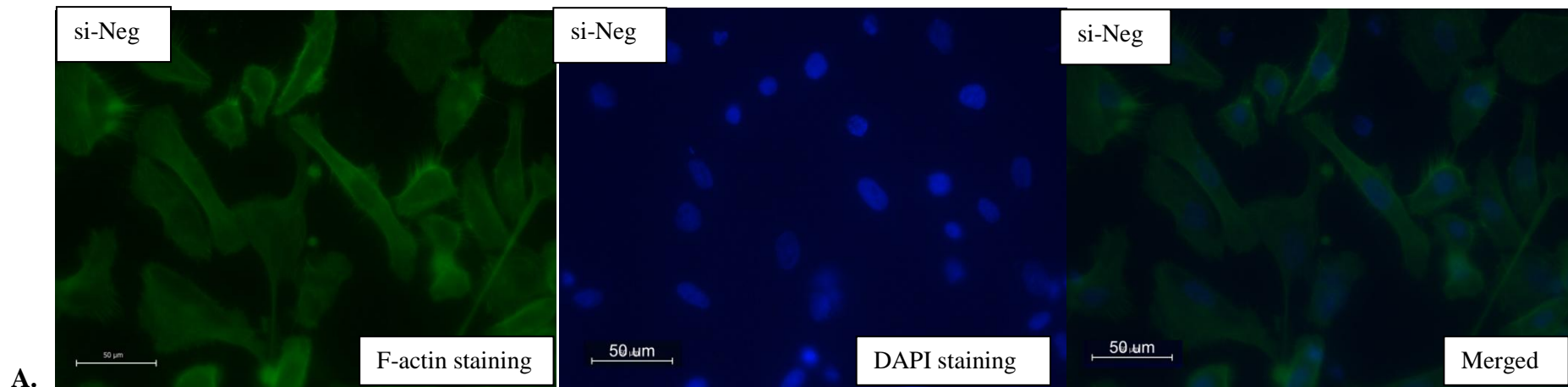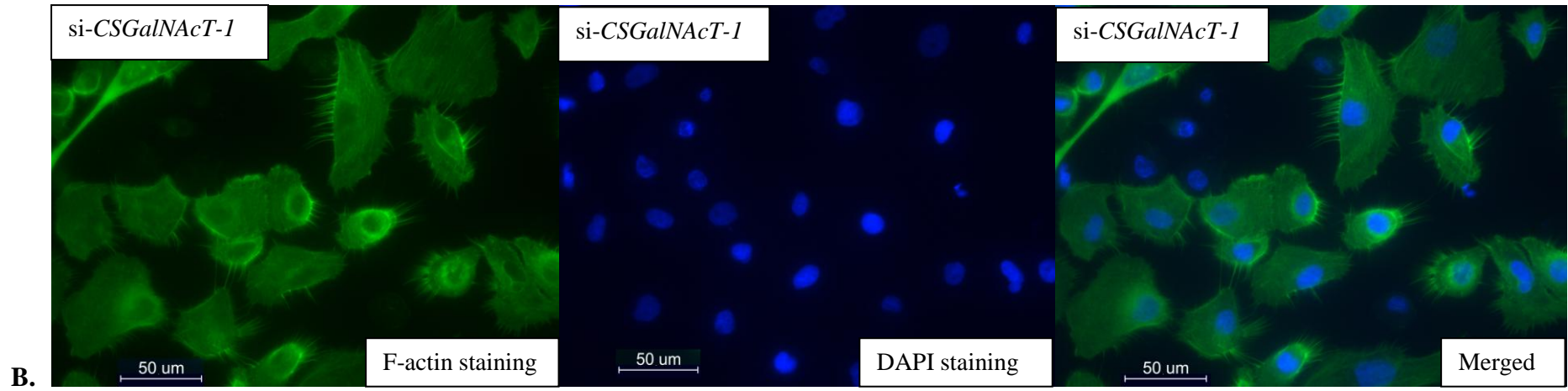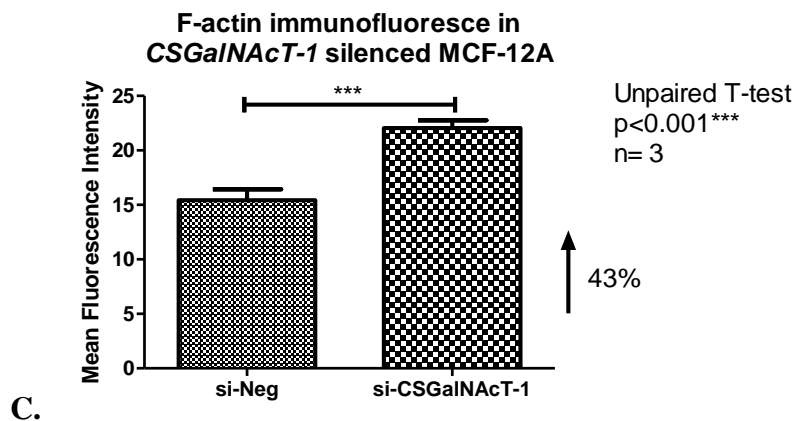
Figure 3.6 Changes in F-actin polymerization after *CSGalNAcT-1* knockdown in MCF-12A. (A, B) Immunofluorescence images stained with F-actin (left), DAPI in nucleus (DAPI blue, middle) and merged figures (right) of si-Neg and *CSGalNAcT-1* silenced group. Mean fluorescence intensity is measured by the ImageJ software. (C) Statistically, F-actin intensity increased significantly upon *CSGalNAcT-1* silencing in MCF-12A. Error bar represents standard error.

3.2.4. Assessment of the cell invasiveness of *CSGalNAcT-1* silenced MCF-

12A using Matrigel assay

In vitro cell invasion was assayed in BD Biocoat invasion chambers of PET membrane with 8.0 μm pore size. Lower wells were added with medium supplemented with 15% FBS to serve as chemoattractant. A profound increase in *CSGalNAcT-1* suppressed cells invading across the Matrigel coated membrane was observed in Figure 3.7A and 3.7B. The invasive capability was increased by 87.8% in *CSGalNAcT-1*-silenced group as shown in Figure 3.7C.

A.

B.

C.
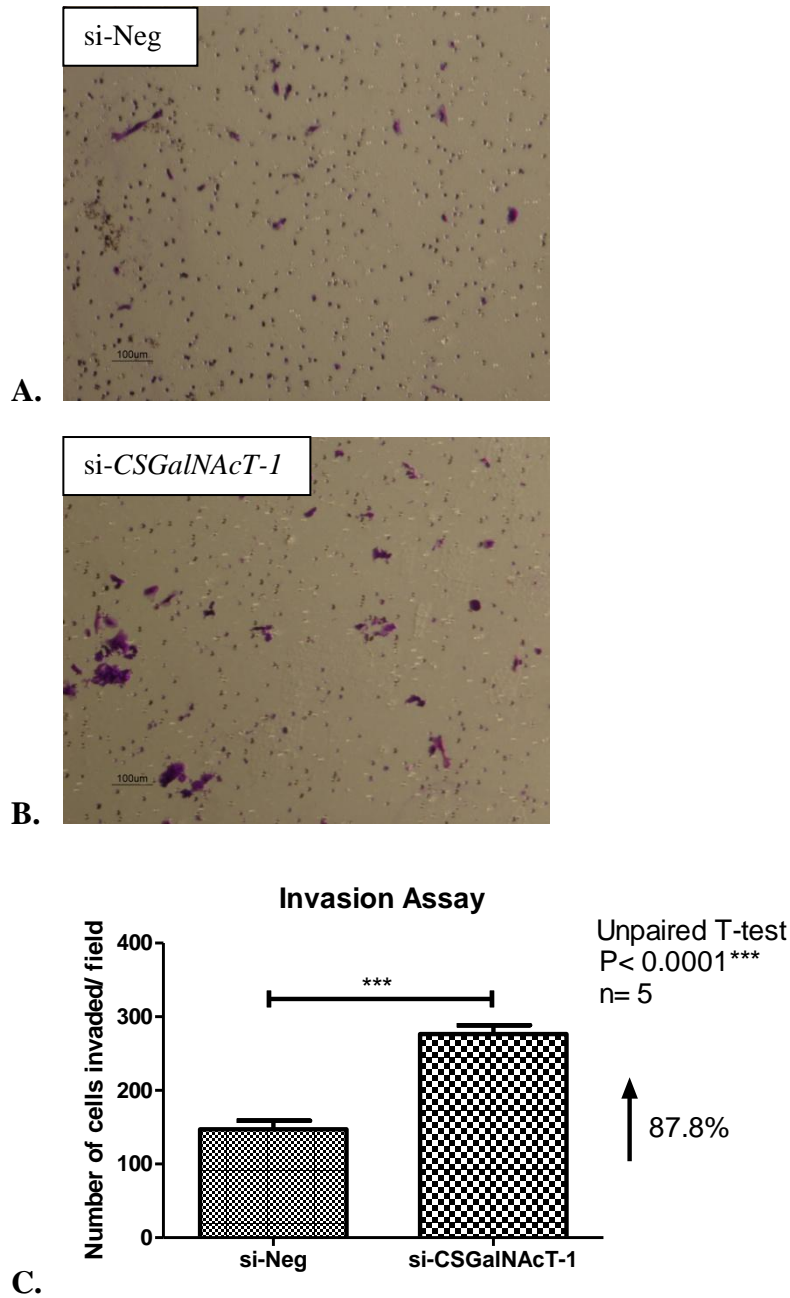
Figure 3.7 Down-regulation of *CSGalNAcT-1* induced MCF-12A cells invasion across matrigel membrane. (A) and (B) showed the invaded cells in chambers. (C) The invasive capability of *CSGalNAcT-1* silenced cells was significantly increased by 87.8% compared to si-Neg. Error bar represents standard error.

3.2.5. *CSGalNAcT-1* silencing promotes cell viability in MCF-12A

To test whether silencing of *CSGalNAcT-1* brings any effect on the MCF-12A cell viability, the cell viability was measured by CellTiter 96 Aqueous Non-radioactive cell proliferation assay 72 hours later after transfection. In Figure 3.8, the analysis showed slight but significant increase in viability after *CSGalNAcT-1* was silenced.
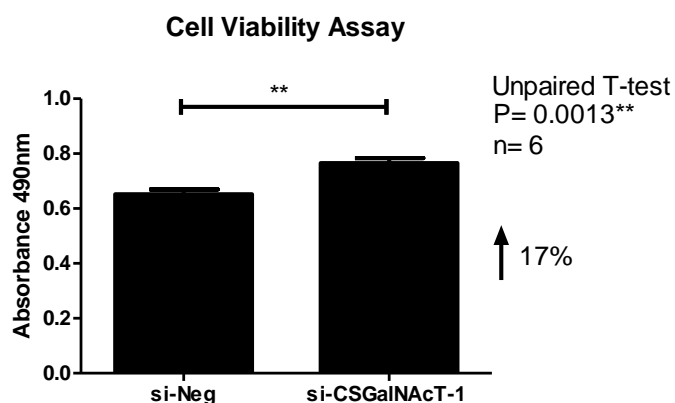
Figure 3.8 Cell viabilities were measured based on absorbance of formazan produced by MCF-12A cells 48 hours after transfection. *CSGalNAcT-1* silenced group has significant 17% increase of proliferation as compared to the si-Neg group. Error bar represents standard error.

3.2.6. Assessment of cell apoptosis in *CSGalNAcT-1* silenced MCF-12A

3.2.6.1. Caspase-3/7 apoptosis assay

Caspase-3/7 apoptosis assay measured the activities of caspase-3 and -7, which are the members of the cystein aspartic acid-specific protease (caspase) family that play key effector roles in apoptosis in mammalian cells. The result in Figure 3.9 shows that there were significantly more apoptotic cells following the silencing of *CSGalNAcT-1* in MCF-12A as compared to negative control group.
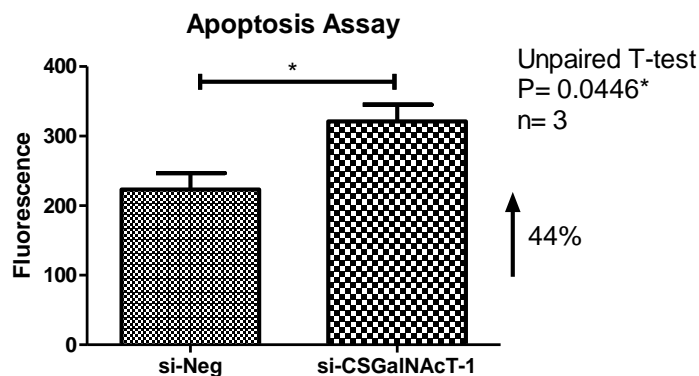
Figure 3.9 Apo-ONE Homogenous Caspase-3/7 assay was performed for the assessment of apoptosis in *CSGalNAcT-1* silenced MCF-12A. There was a significant increase in apoptosis after *CSGalNAcT-1* was silenced in MCF-12A cells. Error bar represents standard error.

3.2.6.2. Phosphorylated BAD (pBAD) protein expression

BAD interacts with anti-apoptotic Bcl-2 and Bcl- X_L and sequesters this two protein away from the Bax-like proteins thus promotes apoptosis. However, phospohorylated BAD (pBAD) indirectly promote cell survival, due to the consequence of its inability to bind Bcl-2 or Bcl-X_L. *CSGalNAcT-1* silenced MCF-12A cells had increased apoptosis; this is reflected in reduced protein expression of pBAD (25kDa) in *CSGalNAcT-1* silenced MCF-12A (Figure 3.10B and 3.10E). Although total BAD protein (25kDa) expression had no significant differences between knockdown and negative control group (Figure 3.10A and 3.10D), relative pBAD protein level is still significantly reduced in *CSGalNAcT-1* silenced group (Figure 3.10F).

Total Bad: 25kDa

A.

si-Neg-1   si-Neg-2   si-Neg-3   si-*CSGalNAcT-1*-1 si-*CSGalNAcT-1*-2 si-*CSGalNAcT-1*-3

Phosphorylated Bad (pBAD): 25kDa

B.

si-Neg-1   si-Neg-2   si-Neg-3   si-*CSGalNAcT-1*-1 si-*CSGalNAcT-1*-2 si-*CSGalNAcT-1*-3

β-actin: 41kDa

C.

si-Neg-1   si-Neg-2   si-Neg-3   si-*CSGalNAcT-1*-1 si-*CSGalNAcT-1*-2 si-*CSGalNAcT-1*-3

Total Bad protein level in
***CSGalNAcT-1* silenced MCF-12A**

Unpaired T-test
p= 0.1514
n= 3

D.

pBAD protein protein level in
***CSGalNAcT-1* silenced MCF-12A**

Unpaired T-test
p= 0.0498*
n= 3

↓ 37%

E.

F.

Figure 3.10 Western blot analysis of total BAD and phosphorylated BAD (pBAD) in *CSGalNAcT-1* silenced MCF-12A. (A, D) No significant change in total BAD (25 kDa) protein expression level was found in between si-Neg and silenced group. (B, E) pBAD (25 kDa) protein level was significantly reduced by 37% in *CSGalNAcT-1* silenced MCF-12A, indicating reduced survival in silenced cells. (F) Relative total BAD to pBAD protein level also showed a significant reduction pattern. (C) β-actin protein level (41 kDa) acts as normalizer and the expression level was unaffected in the silencing process. Error bar represents standard error.

3.2.7.   Cell adhesion analysis in *CSGalNAcT-1* silenced MCF-12A

In addition to cell migration and invasion, adhesion is one of the most important factors in tumorigenesis. This assay was done to investigate the effect of *CSGalNAcT-1* silencing on the adhesion of MCF-12A cells to extracellular matrix (ECM). Two major components of ECM, which are collagen I and fibronectin were used to mimic ECM environment in the assay. The negative control and silenced group did not adhere differently to collagen I (Figure 3.11A) and fibronectin (Figure 3.11B).

Adhesion Assay (Collagen I coated)

Unpaired T-test
P= 0.1013
n= 10

A.

Adhesion Assay (Fibronectin coated)

Unpaired T-test
p= 0.2046
n= 8

B.
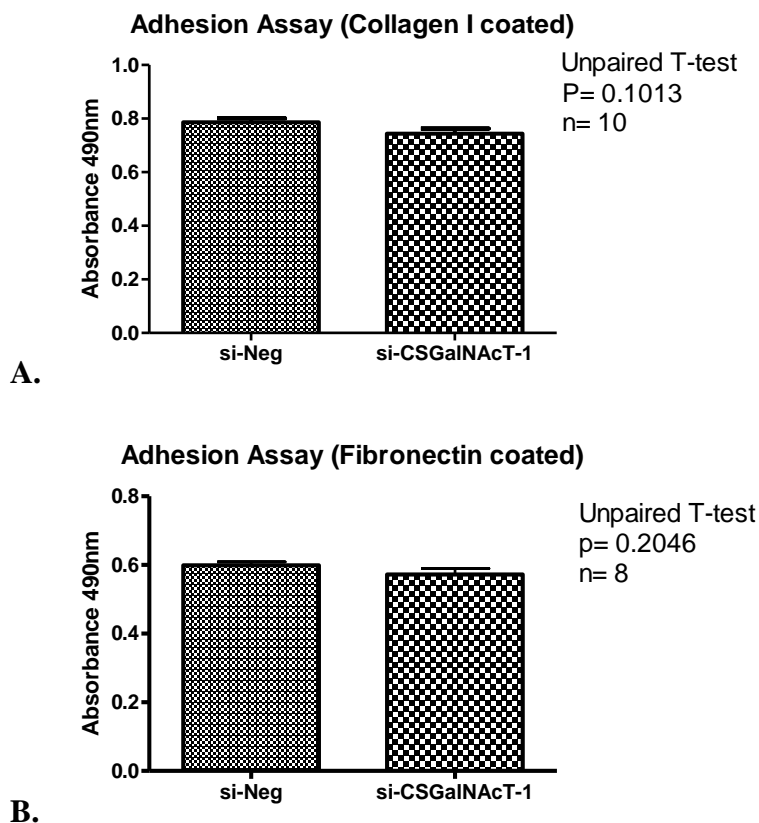
Figure 3.11 Analysis of adhesiveness of *CSGalNAcT-1* silenced MCF-12A to collagen I and fibronectin. Absorbance of each group (negative control and *CSGalNAcT-1* silenced group) was normalized based on the ratio of washed wells to unwashed wells. (A and B) No significant changes in adhesion to collagen I and fibronectin were observed upon *CSGalNAcT-1* silencing in MCF-12A cells. Error bar represents standard error.

3.3.   Microarray analysis of *CSGalNAcT-1* silenced MCF-12A

To understand the mechanisms of *CSGalNAcT-1* in mediating cellular behavior, a microarray analysis using Affymetrix Human U133 Plus version 2.0 array was performed. MCF-12A cells were transfected with non-targeting siRNA and *CSGalNAcT-1* siRNA as described in section 3.2. Total RNA was extracted and sent to Origen Labs to determine the good quality of the RNA samples. The RNA samples had OD 260/280 ratios of 1.779 to 2.201 and concentration range from 66.89 ng/μl to 149.41 ng/μl, as shown in Table 3.1.

Quality of the RNA was assessed based on the electrophoretic trace (Figure 3.12) of the RNA sample and the RNA integrity number (Table 3.1). As determined by the Agilent Bioanalyzer, all the samples had RNA integrity values of 10, indicating good quality of RNA samples.

For each sample, 100 ng total RNA was used for the 3' IVT Express assay according to Origen Labs SOP. RNA was reverse transcribed to cDNA and subsequently used as a template to create a biotinylated labeled amplified RNA (aRNA). aRNA was then fragmented and hybridized to Affymetrix Human U133 Plus version 2.0 array. CEL files were generated from GeneChip Operating Software (GCOS) and imported into Expression Console (EC) 1.1 software for quality control of arrays. GeneSpring software was used for raw data analysis.

Table 3.1 RNA purity and quality used for microarray analysis

Sample	OD260 nm	OD280 nm	OD320 nm	Ratio 260/280	Conc. (ng/ul)	RIN
CSGalNAcT-1 silenced #1	0.0149	0.0076	0.0000	1.779	66.89	10
CSGalNAcT-1 silenced #2	0.0323	0.0154	0.0000	2.094	129.88	10
CSGalNAcT-1 silenced #3	0.0286	0.0153	0.0000	1.872	114.26	10
Negative #1	0.0286	0.0153	0.0000	1.852	115.72	10
Negative #2	0.0282	0.0135	0.0000	1.968	119.14	10
Negative #3	0.0377	0.0173	0.0004	2.201	149.41	10
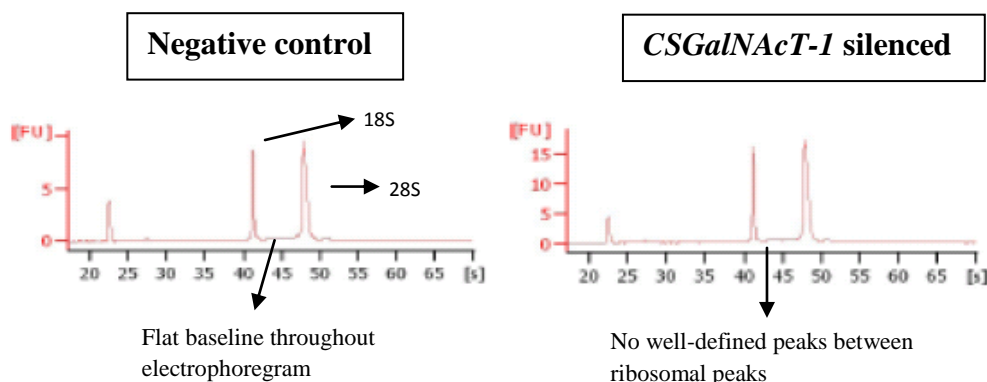
Figure 3.12 Electrophoregrams of RNA samples determined by Agilent Bioanalyzer. RNA samples with good quality are typified by intact 18S and 28S ribosomal subunit peaks, flat baseline throughout electrophoregrams and no well-defined peaks between 18S and 28S peaks.

3.3.1. Microarray table of genes and heat map

Results from GeneSpring software analysis indicate a total of 30 genes that were significantly up and down regulated between the negative control and silenced group. The change of each gene was at least 1.5 fold. These genes are represented along with fold change and p-value in Table 3.2. Heat map was plotted in Figure 3.13 to display list of genes that were significantly up- and down-regulated between the negative control and *CSGalNAcT-1* silenced group. Heat map adopted color-coding method, i.e. green and red color, to represent direction of expression and the color gradient represents increasing or decreasing expression value.

Table 3.2 List of genes that were significantly up- and down-regulated at least by 1.5 fold following the silencing of *CSGalNAcT-1* in normal breast cell line MCF-12A.

Number	Gene symbol	Probe set ID	p-value	Fold change	Regulation
1	*ATL3*	224893_at	9.32E-04	1.7441963	Down
2	*C6orf120*	221786_at	6.52E-05	2.0711255	Down
		221787_at	0.001319238	1.5095084	Down
3	*CMAS*	218111_s_at	0.005513553	1.5049442	Down
4	*CPOX*	204172_at	6.71E-04	1.7968925	Down
5	*CSGalNAcT-1*	219049_at	7.20E-08	10.77752	Down
6	*EXOC2*	226270_at	0.004970458	1.6187352	Down
7	*LYPLA2*	202292_x_at	8.52E-04	1.8298787	Down
		215566_x_at	4.31E-04	2.0218742	Down
8	*LYPLA2P1*	216606_x_at	2.29E-05	1.819549	Down
9	*MAPRE1*	200713_s_at	2.57E-05	2.2625957	Down
10	*NCAM1*	212843_at	0.004154318	1.5822985	Down
11	*PLEKHA8*	227247_at	2.56E-05	2.0324197	Down
12	*RAB28*	227003_at	0.002662569	1.5219765	Down
13	*RCBTB1*	218352_at	8.06E-05	2.1755447	Down
14	*TRAPPC2*	219351_at	3.98E-05	1.873583	Down
15	*APOL6*	1557236_at	0.011513989	1.6276952	Up
16	*CALB1*	205625_s_at	0.039278515	1.5815449	Up
		205626_s_at	0.011313328	1.5016893	Up
17	*CDKN1C*	213182_x_at	4.55E-04	1.6526825	Up
		213348_at	3.17E-04	1.5226234	Up
		216894_x_at	0.001148584	1.6225524	Up
		219534_x_at	1.89E-04	1.6592742	Up
18	*CXCL14*	218002_s_at	2.94E-04	1.904126	Up
		222484_s_at	1.95E-04	1.8966751	Up
19	*GAS1*	204457_s_at	0.005914766	1.519408	Up
20	*HIVEP3*	235122_at	0.04710484	1.6094921	Up
21	*HOPX*	211597_s_at	0.031734325	1.5025384	Up
22	*HSPB3*	206375_s_at	0.016321188	1.5295488	Up
23	*KIAA0774*	214961_at	0.027066868	1.9408674	Up
24	*KIF26A*	232069_at	4.86E-04	1.666597	Up
25	*NIPBL*	242352_at	0.018583402	1.5061634	Up
26	*ONECUT2*	233446_at	0.032158457	1.552688	Up
27	*RRAD*	204803_s_at	0.005861233	1.538713	Up
28	*SULT1E1*	219934_s_at	1.32E-05	1.5776308	Up
		222940_at	0.001612507	1.5213795	Up
29	*TNFSF10*	202687_s_at	0.003737635	1.5123925	Up
		202688_at	0.015174521	1.5859073	Up
30	*TRIM59*	235476_at	0.012354963	1.9657407	Up
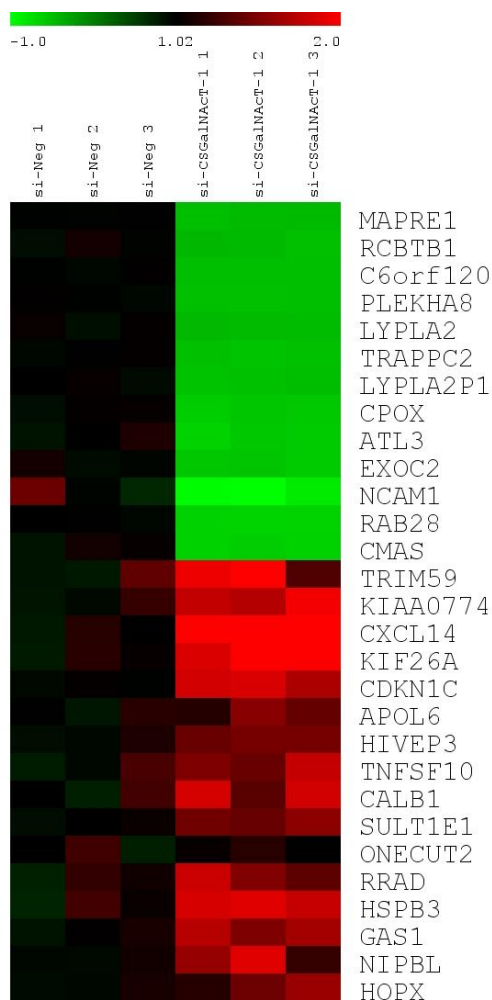
Figure 3.13 Heat map displaying list of 29 genes (excluding *CSGalNAcT-1*) that were significantly up- and down-regulated between the negative control and *CSGalNAcT-1* silenced groupd. Down-regulated genes are presented in green color whereas up-regulated genes are presented in red color.

3.3.2. Functional gene ontology classification

The list of 29 genes (excluding *CSGalNAcT-1*) in Table 3.2 was classified based on their functional ontologies by using a sophisticated software Database for Annotation, Visualization and Integrated Discovery (DAVID). The functional gene ontology of up-regulated and down-regulated genes is displayed in Figure 3.14 and the list of genes from each gene ontology group is listed in Table 3.3.
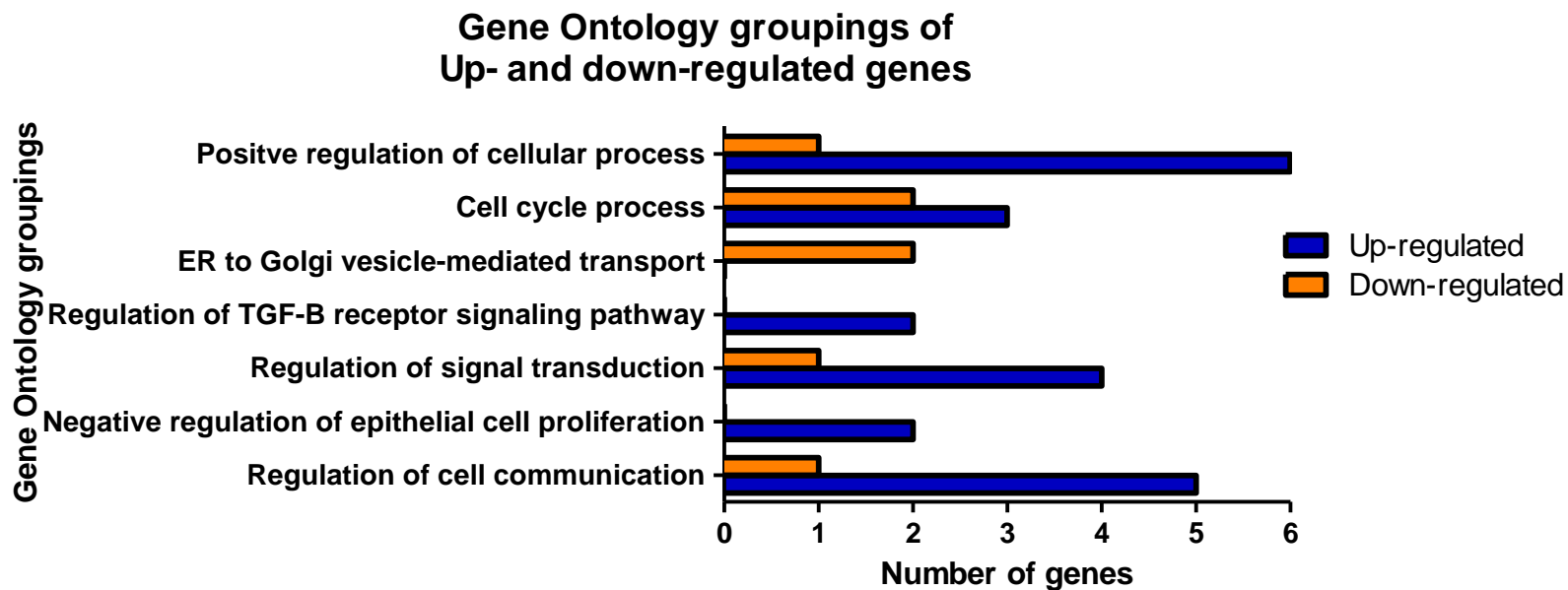
Figure 3.14 Functional ontology classifications of genes that were significantly up- and down-regulated by DAVID software.

Table 3.3 List of genes that are functionally grouped into each ontology group

Gene ontology groupings	Genes	
	Up-regulated	**Down-regulated**
Positive regulation of cellular process	*CDKN1C* *GAS1* *HIVEP3* *HOPX* *ONECUT2* *TNFSF10*	*NCAM1*
Cell cycle process	*CDKN1C* *GAS1* *NIPBL*	*MAPRE1* *RCBTB1*
ER to Golgi vesicle-mediated transport		*ATL3* *TRAPPC2*
Regulation of TGF-β receptor signaling pathway	*CDKN1C* *ONECUT2*	
Regulation of signal transduction	*CDKN1C* *GAS1* *ONECUT2* *TNFSF10*	*NCAM1*
Negative regulation of epithelial cell proliferation	*CDKN1C* *GAS1*	
Regulation of cell communication	*CALB1* *CDKN1C* *GAS1* *ONECUT2* *TNFSF10*	*NCAM1*

3.3.3. Selection of *CXCL14* as a candidate gene for *CSGalNAcT-1* downstream signaling investigation

Among the 16 genes which were up-regulated in Table 3.2, *CXCL14* was selected for the investigation of *CSGalNAcT-1* downstream signaling pathway. The selection criterion was based on the literatures that indicated the role of *CXCL14* in promoting tumorigenesis in various types of cancer.

3.3.3.1. *CXCL14* expression was up-regulated by *CSGalNAcT-1* silencing in MCF-12A

Figure 3.15 shows that *CXCL14* expression level was significantly increased by 2-fold in *CSGalNAcT-1* silenced MCF-12A as compared with negative control from the microarray results.
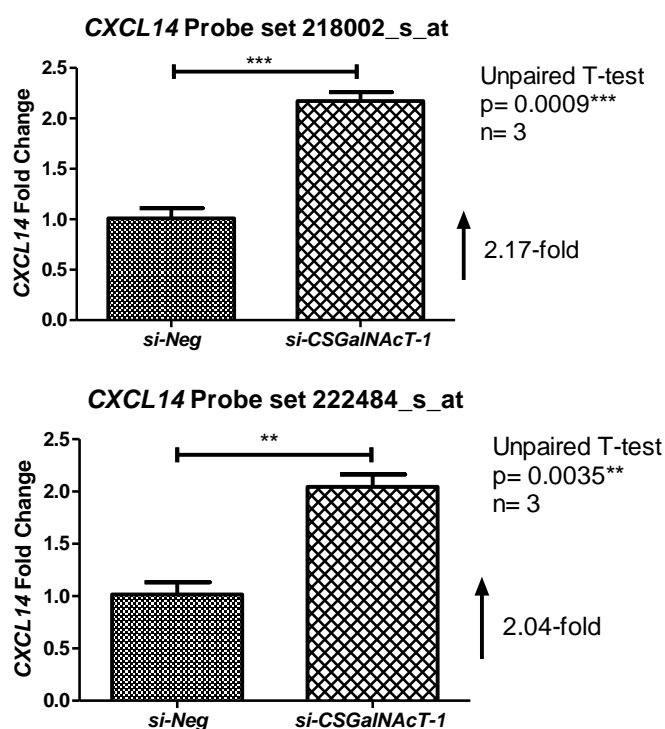
Figure 3.15 Both *CXCL14* probe sets were significantly up-regulated in *CSGalNAcT-1* silenced MCF-12A compared to the negative control MCF-12A cells from the microarray results. Error bar represents standard error.

Validation of *CSGalNAcT-1* expression was carried out by qRT-PCR as well, as shown in Figure 3.16A. In Figure 3.16 B-D, up-regulation of CXCL14 protein in *CSGalNAcT-1* silenced MCF-12A was verified by immunofluorescence.

A.

CXCL14 immunofluorescence in
***CSGalNAcT-1* silenced MCF-12A**

Unpaired T-test
p= 0.0194*
n= 3

26%

D.
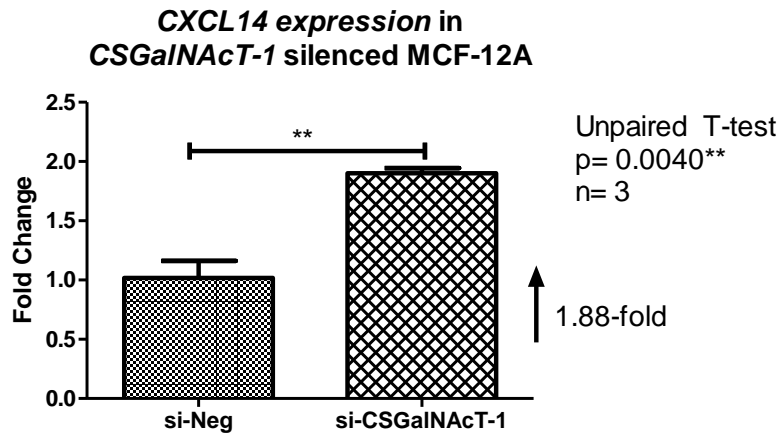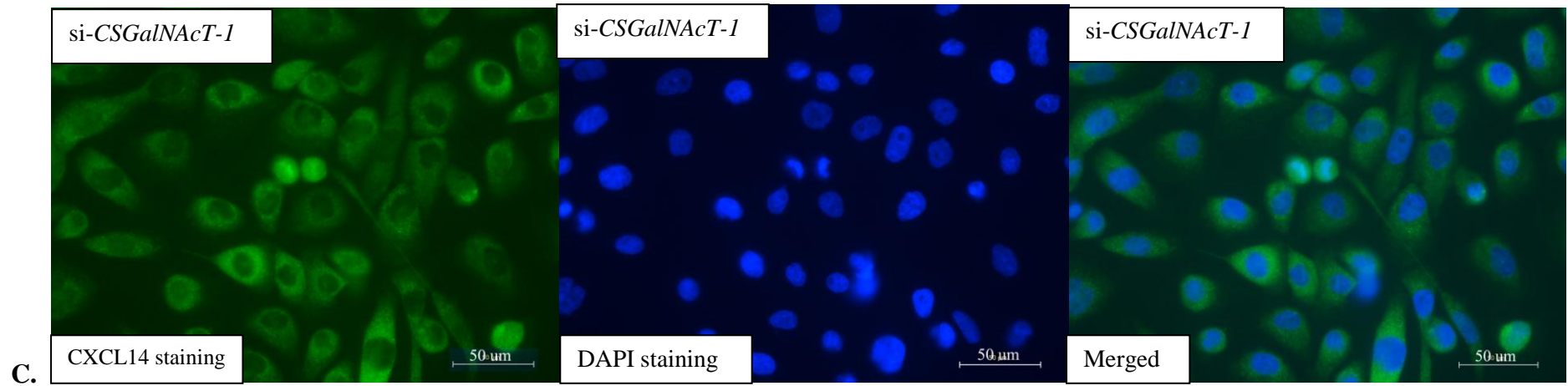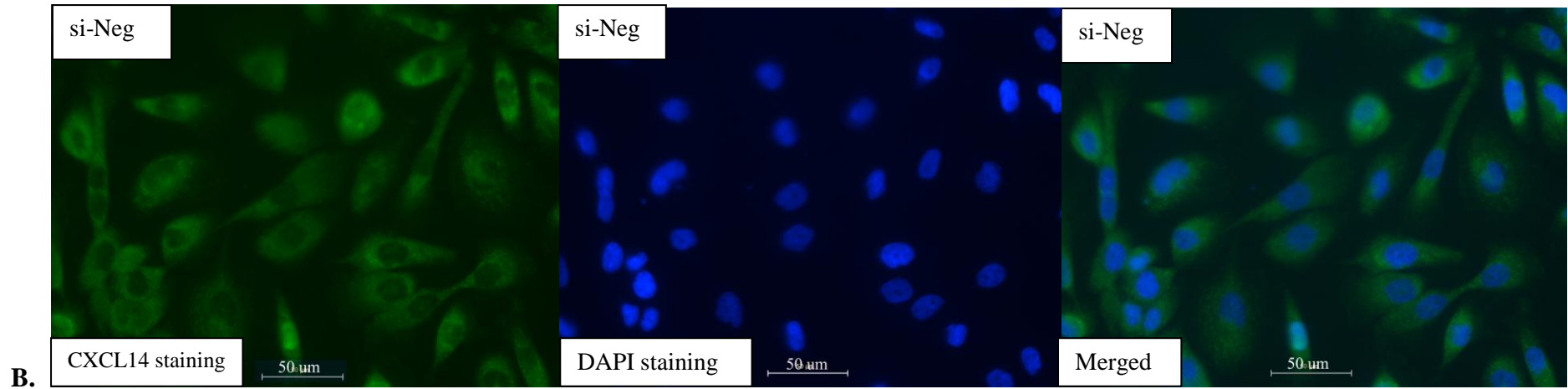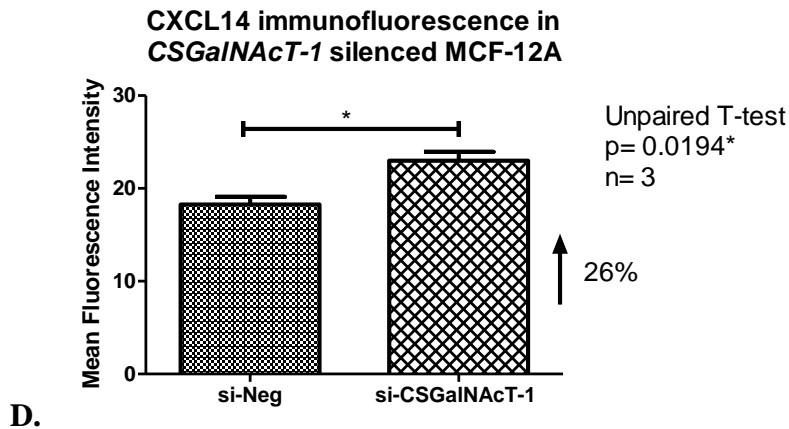
Figure 3.16 Transcript level and protein level of *CXCL14* was up-regulated in *CSGalNAcT-1* silenced MCF12A. (A) qRT-PCR validation of *CXCL14* in *CSGalNAcT-1* silenced MCF-12A showed an up-regulation of the gene in the silenced group. (B, C) *CXCL14* was stained green (left), nucleus was stained blue with DAPI (middle) in immunofluorescence and the merged figure is on the right. Mean fluorescence intensity was measured by the ImageJ software. *CXCL14* protein level in the presentation of immunofluorescence (D) and transcript level (A) were significantly up-regulated. Error bar represents standard error.

3.3.3.2.   Silencing of *CXCL14* in MCF-12A

CXCL14 was silenced in MCF-12A using 10 nM of Ambion Silencer® Select

siRNA. Two siRNAs (sequence ID s18332 and s18333) were employed for

the validation of silencing efficiency. *CXCL14* was knockdown by 98% with

both siRNAs. The siRNA with sequence ID s18333 was selected to be

silenced with *CSGalNAcT-1* in double knockdown experiment in MCF-12A.

Silencing efficiencies of both *CXCL14* siRNAs are shown in Figure 3.17. The

CXCL14 siRNA with sequence ID s18333 was used for subsequent double

silencing experiment. Knockdown of *CXCL14* in return did not affect the

expression of *CSGalNAcT-1* in MCF-12A. qRT-PCR result of *CSGAlNAcT-1*

expression in *CXCL14* (sequence ID s18333) silenced MCF-12A is shown in

Figure 3.18.
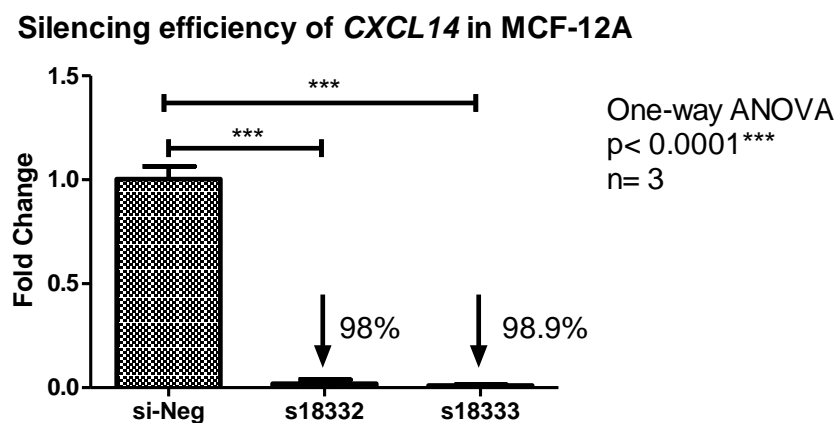
Figure 3.17 Successful knockdown of both *CXCL14* siRNA sequences in MCF-12A. Both siRNAs gave 98% and 98.9% silencing efficiency in MCF-12A. Error bar represents standard error.
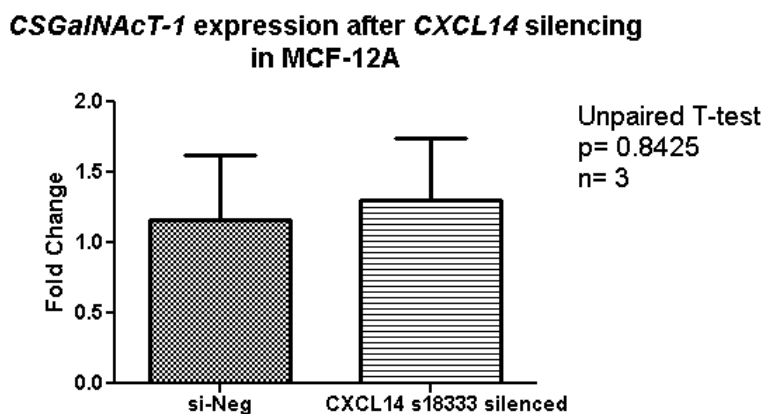
Figure 3.18 *CSGalNAcT-1* expression was not affected in *CXCL14* silenced MCF-12A. Result showed that silencing of *CXCL14* does not affect expression of *CSGalNAcT-1* by qRT-PCR. Error bar represents standard error.

3.3.3.3.   Double knockdown of *CSGalNAcT-1* and *CXCL14* in MCF-12A

Based on results from Section 3.3.3.1, *CXCL14* expression was up-regulated by *CSGalNAcT-1* silencing in MCF-12A. The aim of double knockdown experiment is to prevent the up-regulation of *CXCL14* when *CSGalNAcT-1* was silenced. Thus, it is expected that double silencing will result in down-regulation of *CSGalNAcT-1* and reduce the impact of *CXCL14* up-regulation thereafter. Double silencing of *CSGalNAcT-1* and *CXCL14* was successful as shown in Figure 3.19A and 3.19B.

**Silencing efficiency of *CSGalNAcT-1*
in double knockdown**

One-way ANOVA
p= 0.0002***
n= 3

A.

**Silencing efficiency of *CXCL14*
in double knockdown**

One-way ANOVA
p<0.0001***
n= 3

B.
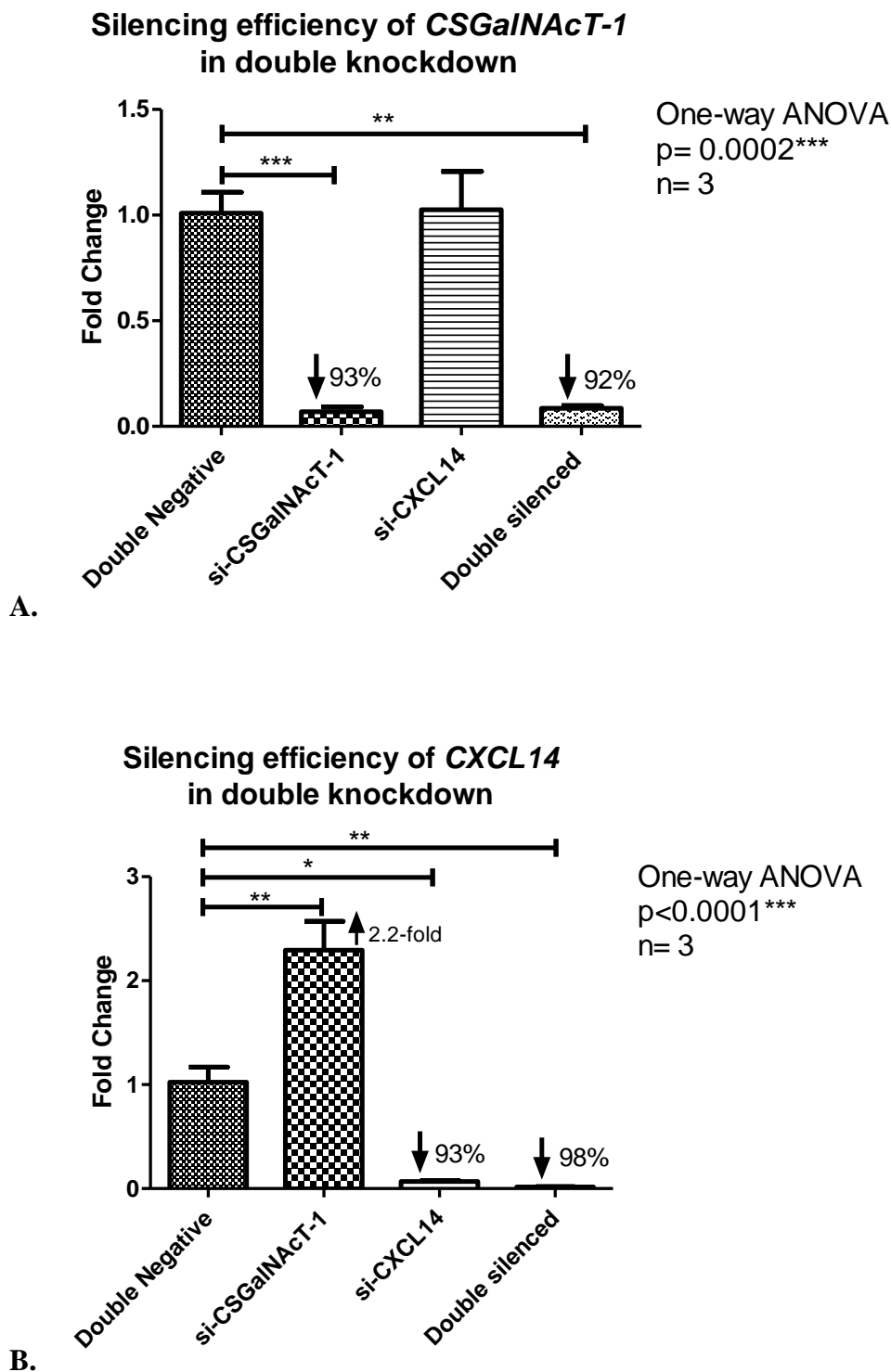
Figure 3.19 Successful double knockdown of *CSGalNAcT-1* and *CXCL14* in MCF-12A. (A) *CSGalNAcT-1* was successfully silenced in both single silenced (93% knockdown) and double silenced (92% knockdown) groups; silencing *CXCL14* did not affect the expression of *CSGalNAcT-1* in feedback loop. (B) Similarly, *CXCL14* was successfully silenced in both the single silenced (93% knockdown) and double silenced (98% knockdown) samples; the expression of *CXCL14* was up-regulated by 2.2 fold in *CSGalNAcT-1* single silenced sample. Error bar represents standard error.

3.3.3.4.   Impact of *CSGalNAcT-1* and *CXCL14* double silencing on MCF-12A cell migration

Cell motility of the siRNA transfected cells were assessed using transwell migration method as mentioned in section 3.2.3.1. As Figure 3.20 shows, MCF-12A cells silenced with *CSGalNAcT-1* significantly increased migration by 34.4% as compared with negative siRNA transfected cells. In contrast, silencing *CXCL14* brought down the migration of the cells by 23.3%. While when MCF-12A was double silenced with *CSGalNAcT-1* and *CXCL14*, cell migration dropped below basal level (double negative). Thus, double silencing of these two transcripts abolishes the cell migration initially observed in *CSGalNAcT-1* silenced MCF-12A; this result implies the impact of *CXCL14* in controlling the migration of cells.
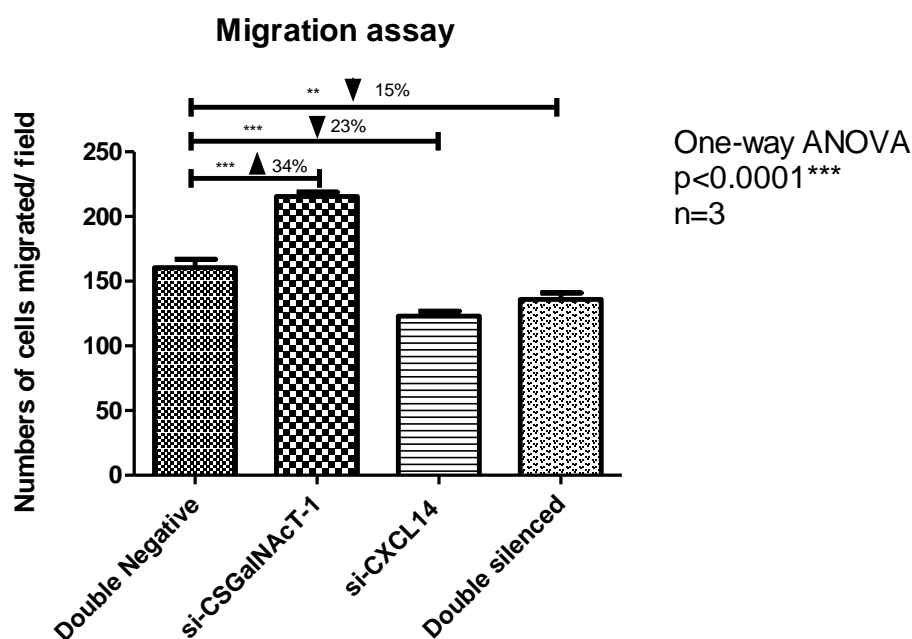
Figure 3.20 Cell motility changes as a result of double knockdown of *CSGalNAcT-1* and *CXCL14* in MCF-12A. *CSGalNAcT-1* silenced MCF-12A significantly increased migration by 34.4%. *CXCL14* silenced MCF-12A had significant reduction in migration. Double silencing of both *CSGalNAcT-1* and *CXCL14* reduced the migration of MCF-12A which was initially increased by silencing *CSGalNAcT-1*. Error bar represents standard error.

3.3.3.5.   Impact of *CSGalNAcT-1* and *CXCL14* double silencing on MCF-12A cell invasion

Cell invasion was assessed by the ability of cells to invade through the basement membrane of Matrigel invasion chambers as mentioned in section 3.2.4. As shown in Figure 3.21, knockdown of *CSGalNAcT-1* increased MCF-12A cell invasion by 21%; while there was a remarkable decrease in cell invasion of *CXCL14* silenced MCF-12A by 40.4%. However, when MCF-12A was silenced simultaneously with *CSGalNAcT-1* and *CXCL14*, the effect of increase in invasion by silencing *CSGalNAcT-1* was neutralized by *CXCL14* knockdown, cell invasion dropped below baseline level. This finding once again shows the positive impact of *CXCL14* in cell invasion.
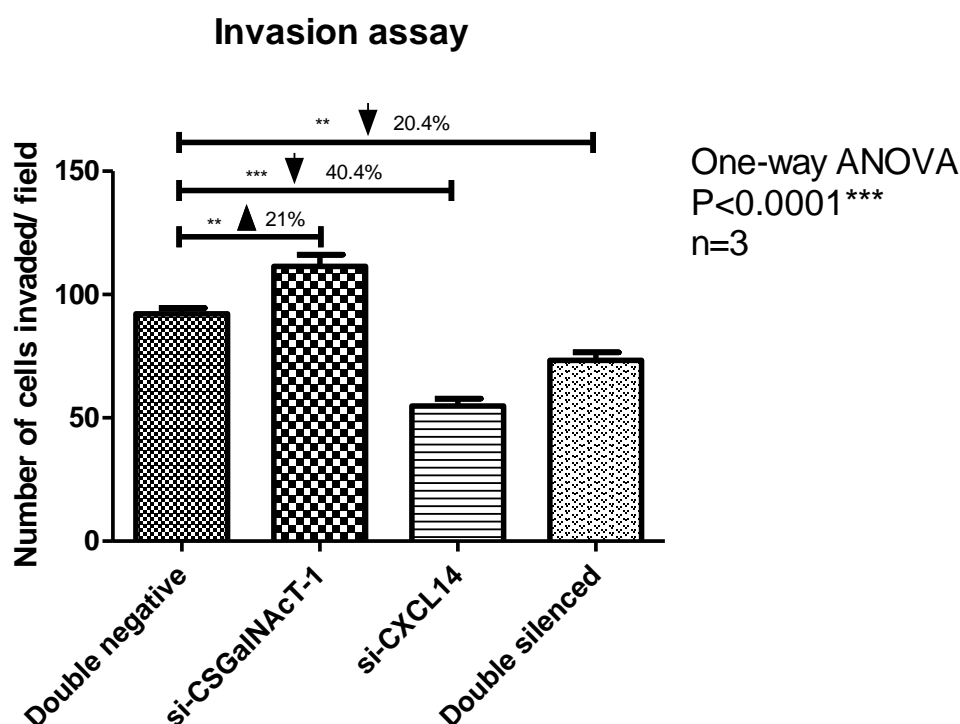
Figure 3.21 Changes in MCF-12A cell invasiveness in double knockdown of *CSGalNAcT-1* and *CXCL14*. Knockdown of *CSGalNAcT-1* significantly increased invasiveness of MCF-12A by 21% while *CXCL14* silenced MCF-12A had reduced invasiveness in the cells. *CSGalNAcT-1* and *CXCL14* double

silenced MCF-12A had reduced cell invasion below the baseline level. Error bar represents standard error.

3.3.3.6.   Impact of *CSGalNAcT-1* and *CXCL14* double silencing on MCF-12A cell viability

Cell viability of siRNA transfected cells were measured 72 hours post transfection by the MTS assay method as described in section 3.2.5. In Figure 3.22, *CSGalNAcT-1* silenced MCF-12A had more cells that are viable but the difference was not significant. In *CXCL14* silenced MCF-12A, the cell viability dropped but was not significant too. No significant difference in cell viability was observed when MCF-12A was double silenced with both genes.
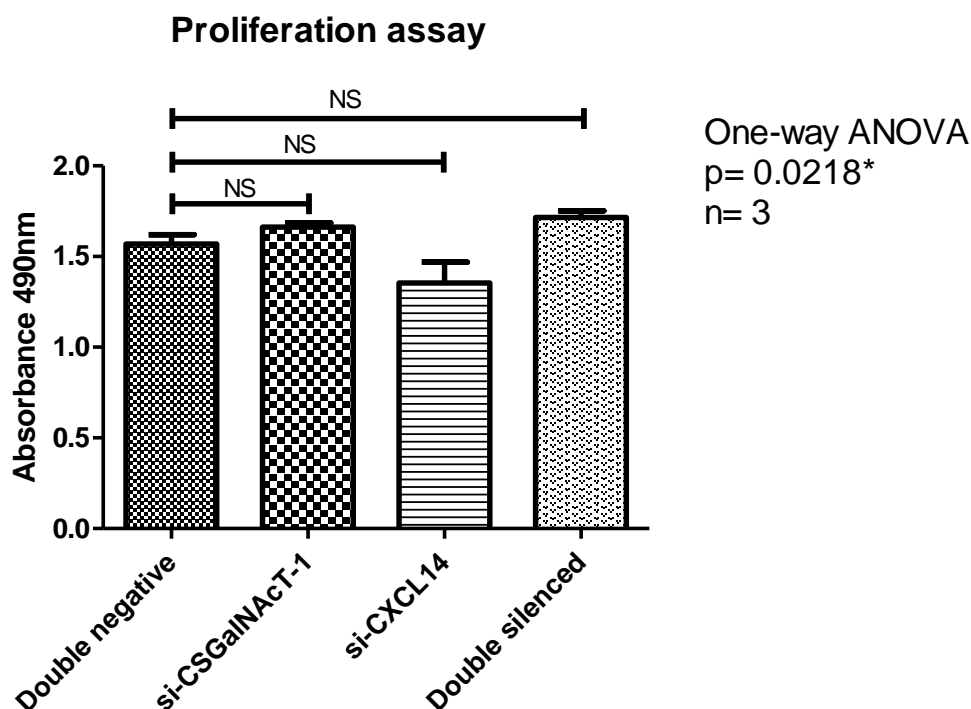
Figure 3.22 No significant changes in cell viability were seen in MCF-12A silenced with *CSGalNAcT-1* and *CXCL14*. Error bar represents standard error.

3.3.3.7.   Impact of *CSGalNAcT-1* and *CXCL14* double silencing on MCF-12A cell adhesion

Cell adhesion to major extracellular matrix constituents, collagen I and fibronectin, was analyzed. As shown in Figure 3.23A, knockdown of both *CSGalNAcT-1* and *CXCL14* individually had no significant changes in adhesion to collagen I of the cells. However, when MCF-12A cells were double silenced with both genes, cells significantly became more adhesive to collagen I.

Similarly, adhesion to fibronectin was not significant in *CSGalNAcT-1* silenced MCF-12A, as shown in Figure 3.23B. However, adhesion to fibronectin was significantly improved upon *CXCL14* silencing in the cells. Moreover, double silenced of these two genes brought back the adhesiveness to baseline level.

A.

Fibronectin adhesion Assay

One-way ANOVA
p= 0.0109*
n= 7

B.
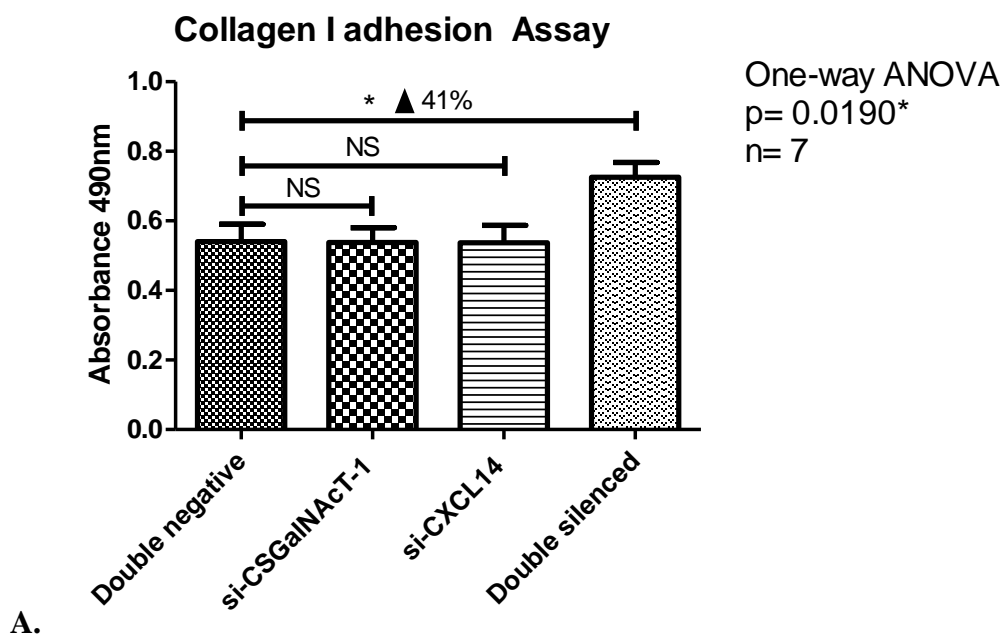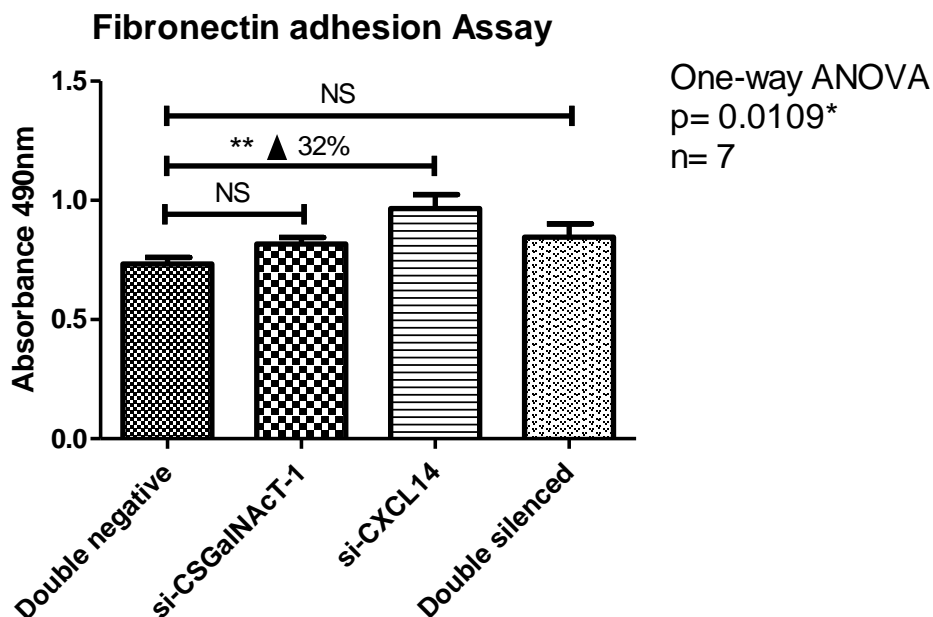
Figure 3.23 Adhesion to collagen and fibronectin in *CSGalNAcT-1* and *CXCL14* double knockdown MCF-12A. (A) No significant changes in adhesion to collagen after *CSGalNAcT-1* and *CXCL14* was silenced individually in MCF-12A. However, double silenced MCF-12A had increased adhesiveness to collagen. (B) *CSGalNAcT-1* silenced MCF-12A did not have significant change in fibronectin adhesion. Knockdown of *CXCL14* increased adhesion to fibronectin significantly but was brought back to baseline level when the cells were double silenced with both *CSGalNAcT-1* and *CXCL14*. Error bar represents standard error.

3.4. Over-expression and functional analysis of *CSGalNAcT-1* in breast cancer cell line MCF7 and MDA-MB-231

3.4.1. *CSGalNAcT-1* over-expression in breast cancer cell line MCF7 and MDA-MB-231

Figure 3.1 showed that expression level of *CSGalNAcT-1* in breast cancer cell lines MCF-7 and MDA-MB-231 was lower as compared with normal breast cell line MCF-12A. Hence, it would be interesting to find out the implications of *CSGalNAcT-1* to the behavioral changes of the cells after being over-expressed in MCF7 and MDA-MB-231. *CSGalNAcT-1* plasmid was transfected to the cells to establish stable cell lines after Neomycin antibiotic selection. Two *CSGalNAcT-1* over-expression clones were generated in MCF7 and were abbreviated OE1 and OE3. One empty vector clone was generated in MCF7, and was given the name EV2. One *CSGalNAcT-1* over-expression clone was generated in MDA-MB-231, and was abbreviated OE2. One empty vector clone was also generated in MDA-MB-231, and was abbreviated EV3. Over-expression level of the *CSGalNAcT-1* in MCF7 and MDA-MB-231 was determined by qRT-PCR and immunofluorescence as shown in Figure 3.24 (A-E) and Figure 3.25 (A-D).

A.

MCF7 EV2

MCF7 EV2

MCF7 EV2

CSGalNAcT-1 staining

50 µm

DAPI staining

50 µm

Merged

50 µm

B.

MCF7 OE1

MCF7 OE1

MCF7 OE1

50 µm

CSGalNAcT-1 staining

50 µm

DAPI staining

50 µm

Merged

C.

D.

CSGalNAcT-1 immunofluorescence in over-expressed MCF7

One-way ANOVA
P< 0.0001***
n= 3
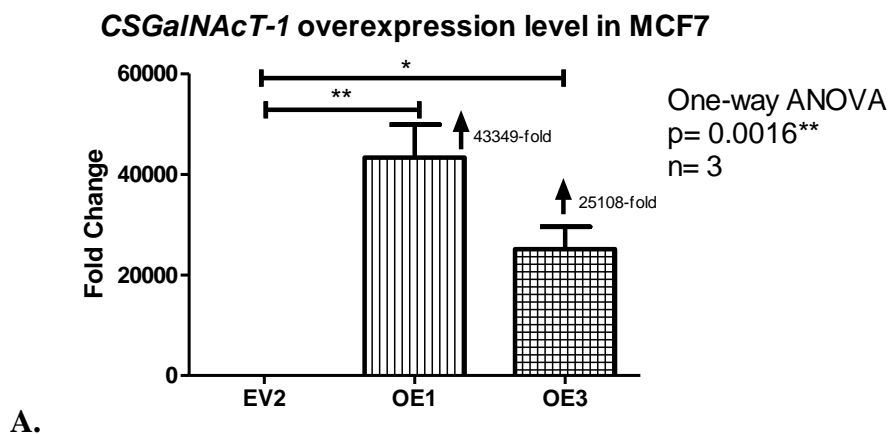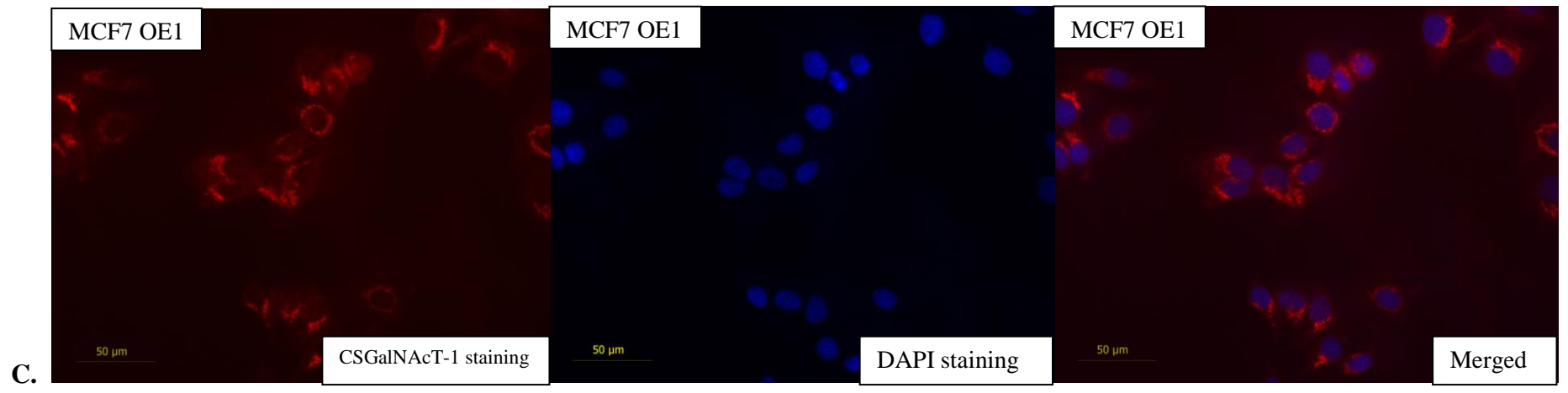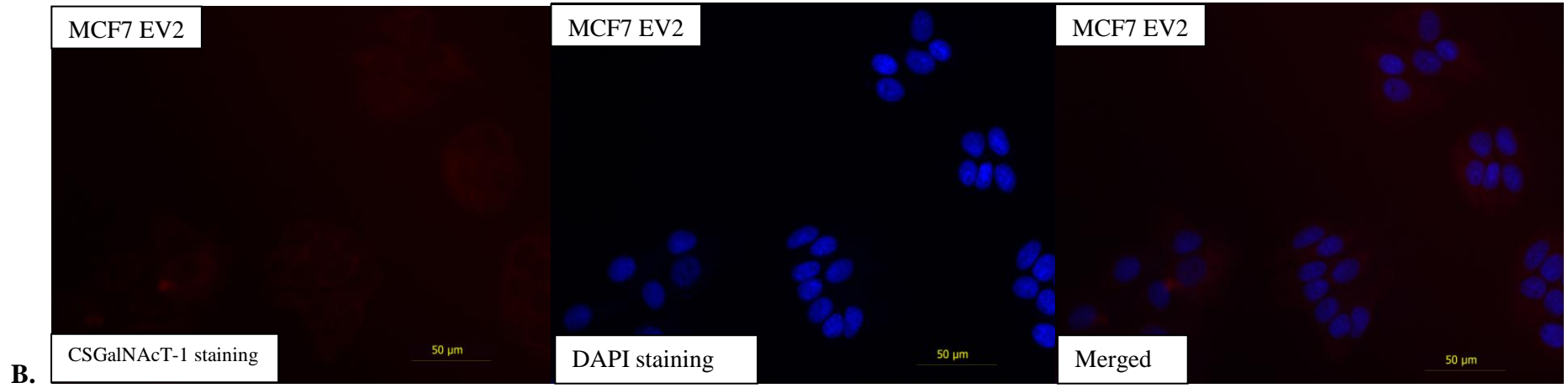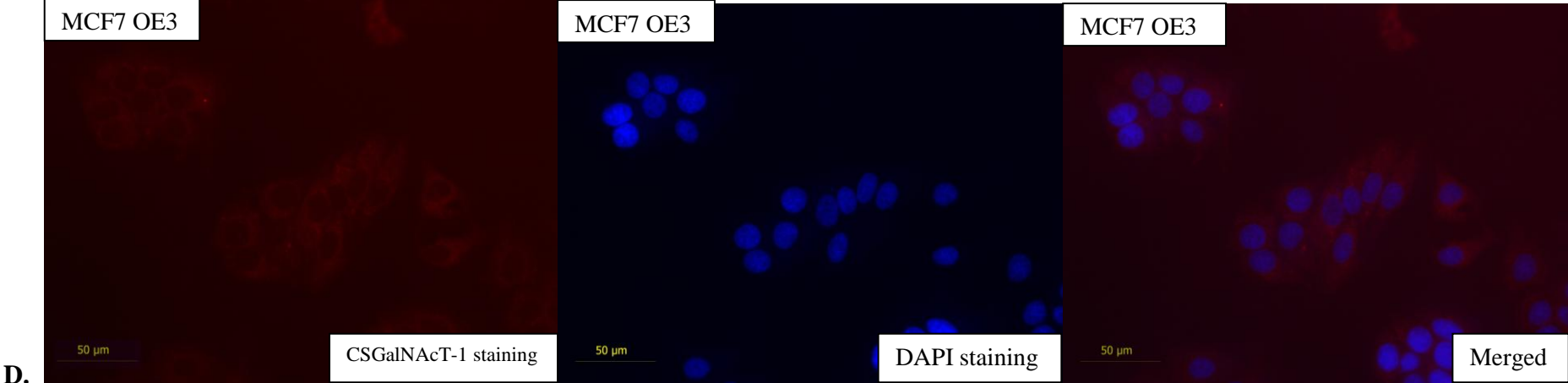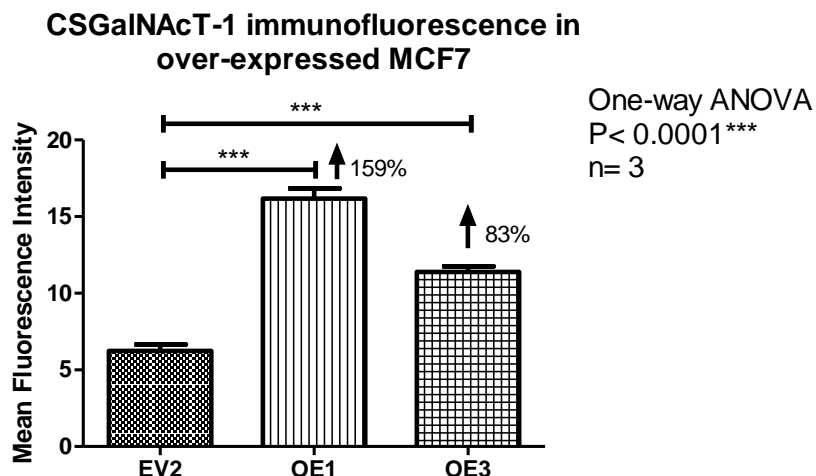
E.

Figure 3.24 Over-expression transcript and protein level of *CSGalNAcT-1* in MCF7. (A) Two MCF7 *CSGalNAcT-1* over-expression clones were generated. EV2 being empty vector clone 2; OE1 and OE3 are over-expression clones 1 and 3 respectively. Both clones exhibited more than 20,000 fold increased in *CSGalNAcT-1*. (B-D) CSGalNAcT-1 was stained red (left), nucleus was stained blue by DAPI (middle) and merged figure is on the right. (E) CSGalNAcT-1 protein level showed significant up-regulation in the over-expression clones. Mean fluorescence intensity was measured by ImageJ software. Error bar represents standard erorr.

CSGalNAcT-1 overexpression level in MDA-MB-231

Unpaired T-test
p= 0.0001***
n= 3

A.

CSGalNAcT-1 immunofluorescence in over-expressed MDA-MB-231

Unpaired T-test
p= 0.0021**
n= 3
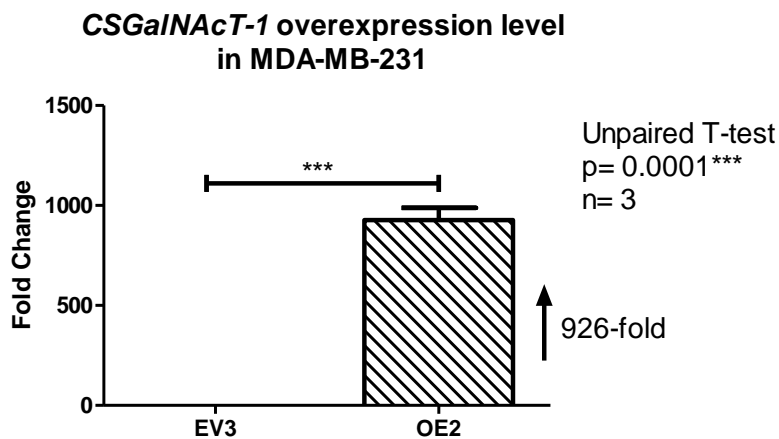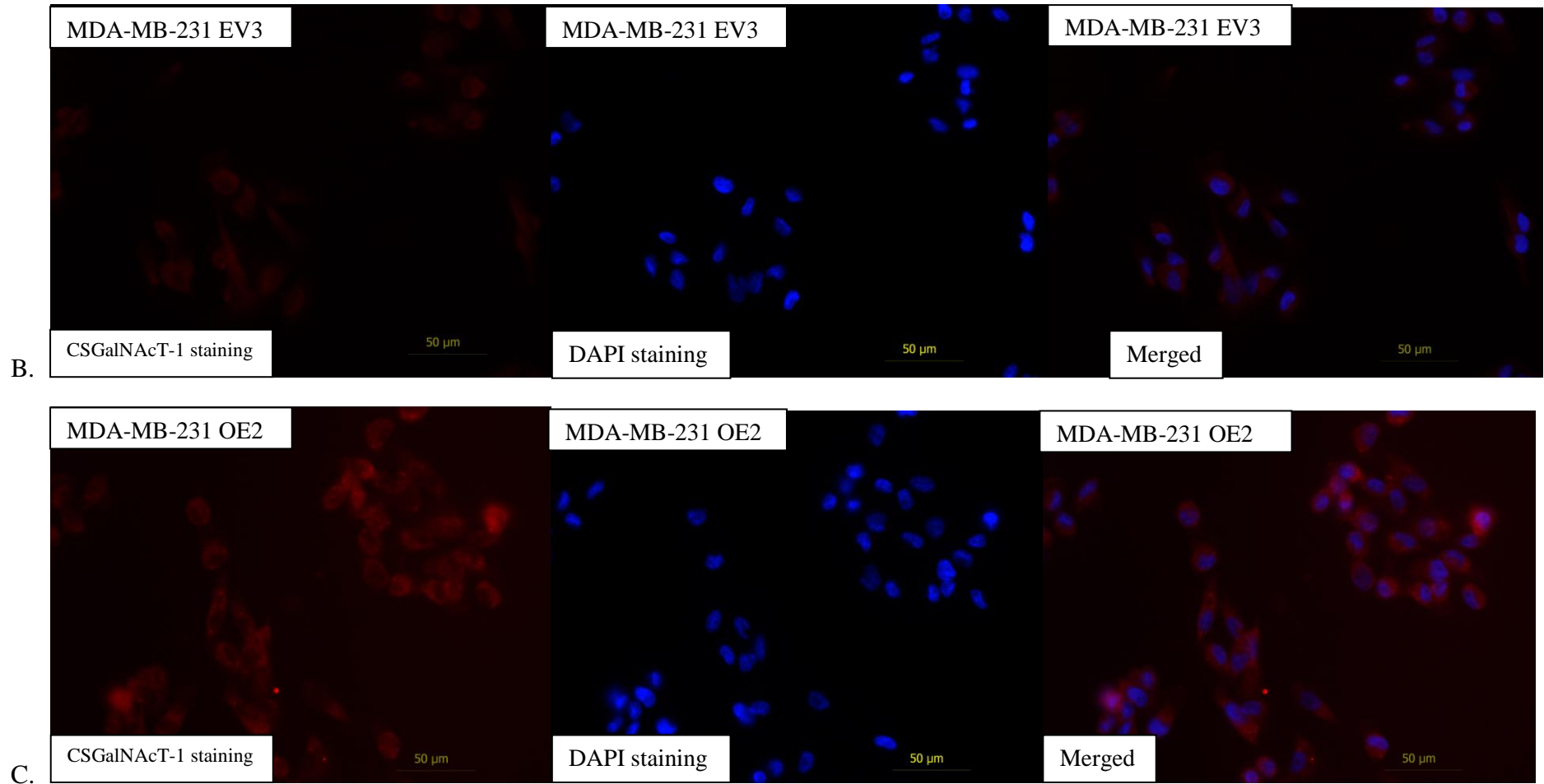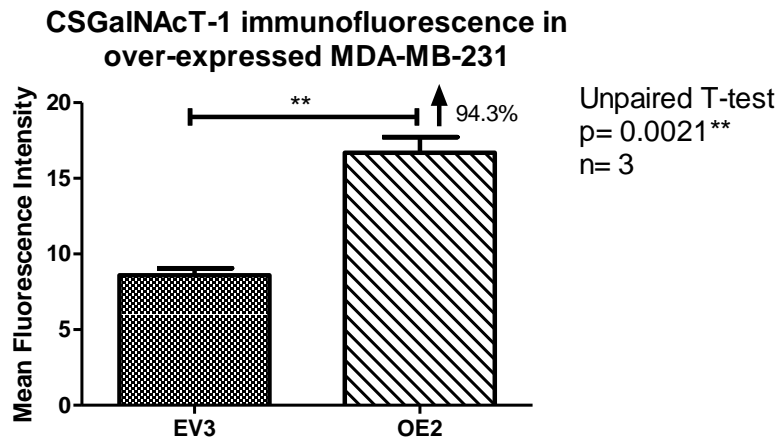
D.

Figure 3.25 Over-expression transcript and protein level of *CSGalNAcT-1* in MDA-MB-231. (A) *CSGalNAcT-1* was over-expressed at 926-fold in MDA-MB-231. EV3 being empty vector clone 3 and OE2 is over-expression clone 2. (B, C) CSGalNAcT-1 protein was stained red (left), nucleus was stained blue by DAPI (middle) and merged figure is on the right. (D) Protein level of CSGalNAcT-1 showed significant up-regulation by 94.3% in the over-expression clones. Mean fluorescence intensity was measured by ImageJ software. Error bar represents standard erorr.

3.4.2. Transcript and protein level of CXCL14 in *CSGalNAcT-1* over-expressed MCF7 and MDA-MB-231

Expression level of *CXCL14* was investigated in the over-expression clones. As illustrated in Figure 3.26 (A-E) and Figure 3.27 (A-C), transcript level of *CXCL14* was examined by qRT-PCR while protein level of CXCL14 was investigated by immunofluorescence technique. Indeed, there were reciprocal down-regulation of CXCL14 transcript and protein level in *CSGalNAcT-1* over-expressed MCF7 and MDA-MB-231.

A.

D.

One-way ANOVA
p= 0.0128*
n= 3

E.
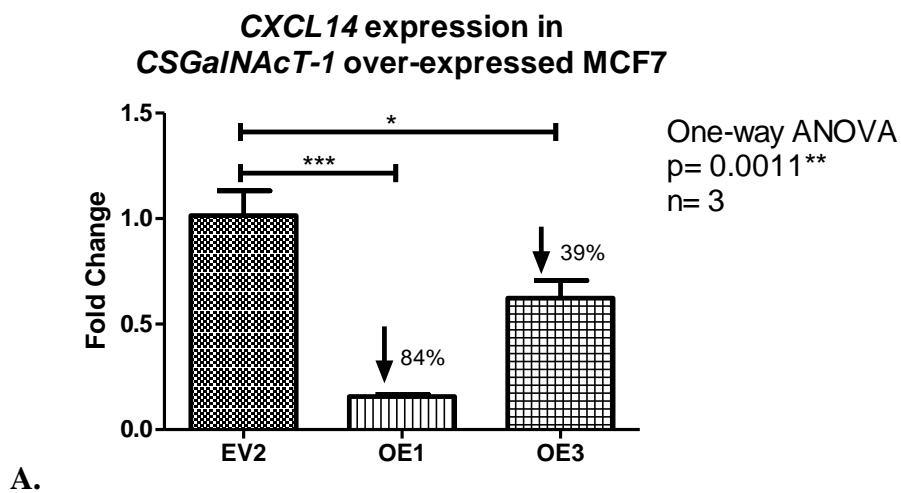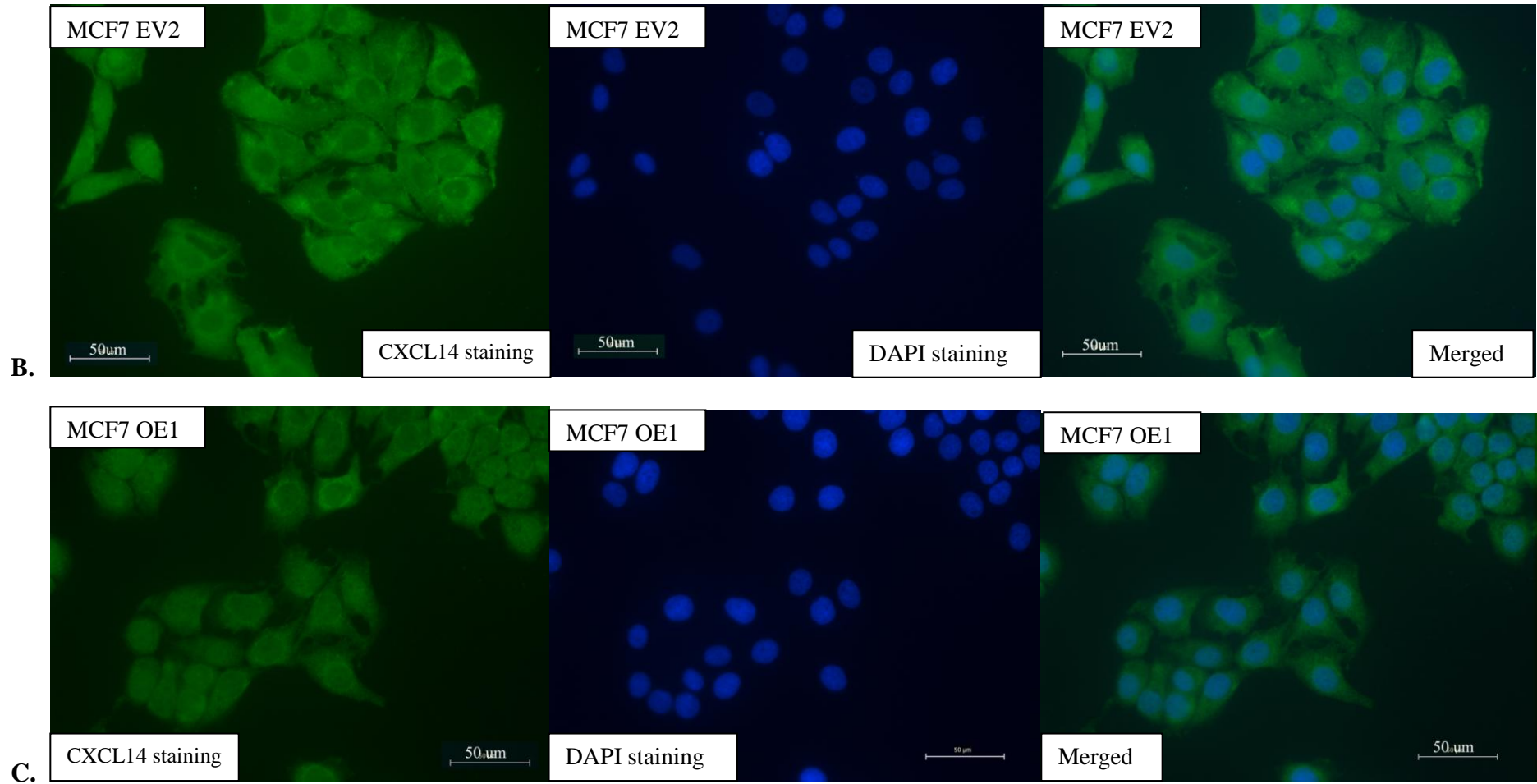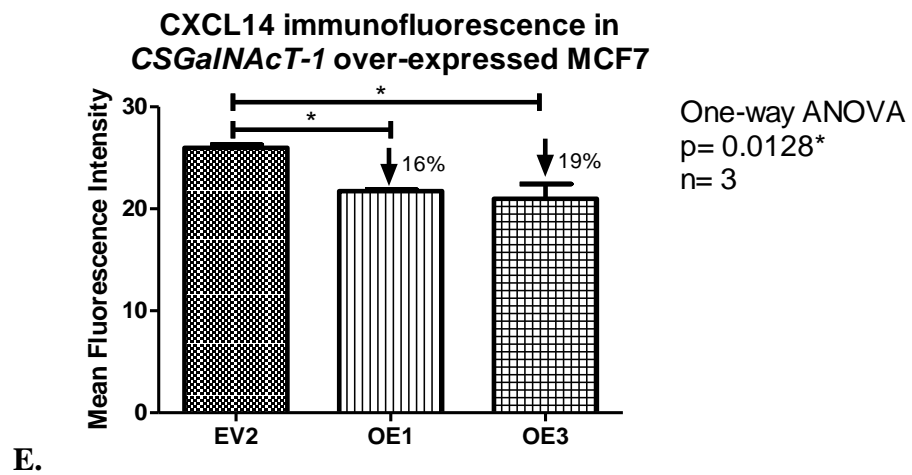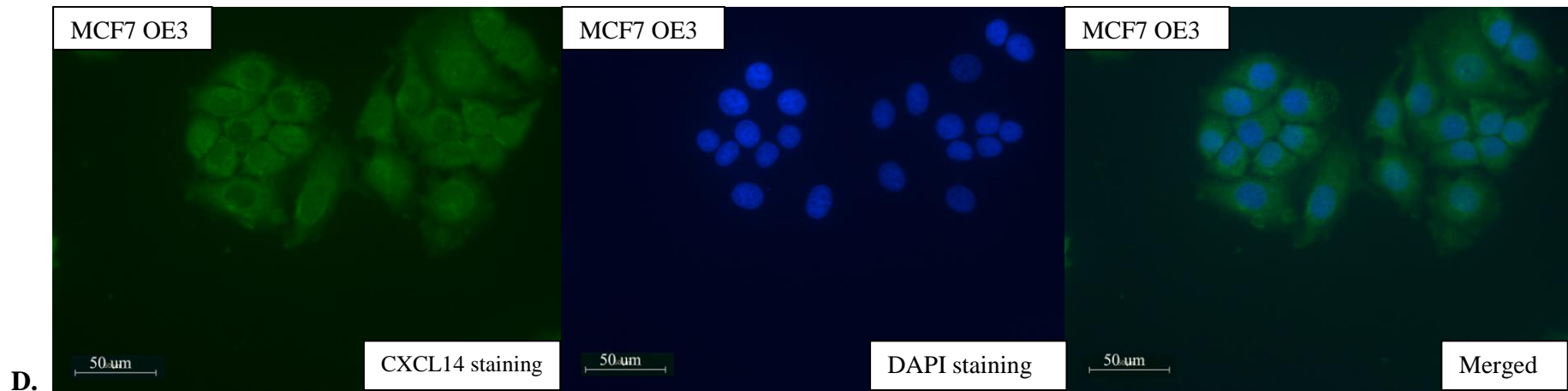
Figure 3.26 Transcript and protein level of CXCL14 were significantly down-regulated in *CSGalNAcT-1* over-expressed MCF7. (A) *CXCL14* transcript level was significantly down-regulated in MCF7 over-expression clones. (B-D) CXCL14 was stained green (left), nucleus was stained blue by DAPI (middle) and merged figure is on the right. (E) Protein level of CXCL14 also showed significant down-regulation in the clones. Mean fluorescence intensity is measured by the ImageJ software. Error bar represents standard error.

B.

MDA-MB-231 OE2 — CXCL14 staining — 50 μm
MDA-MB-231 OE2 — DAPI staining — 50 μm
MDA-MB-231 OE2 — Merged — 50 μm

C.
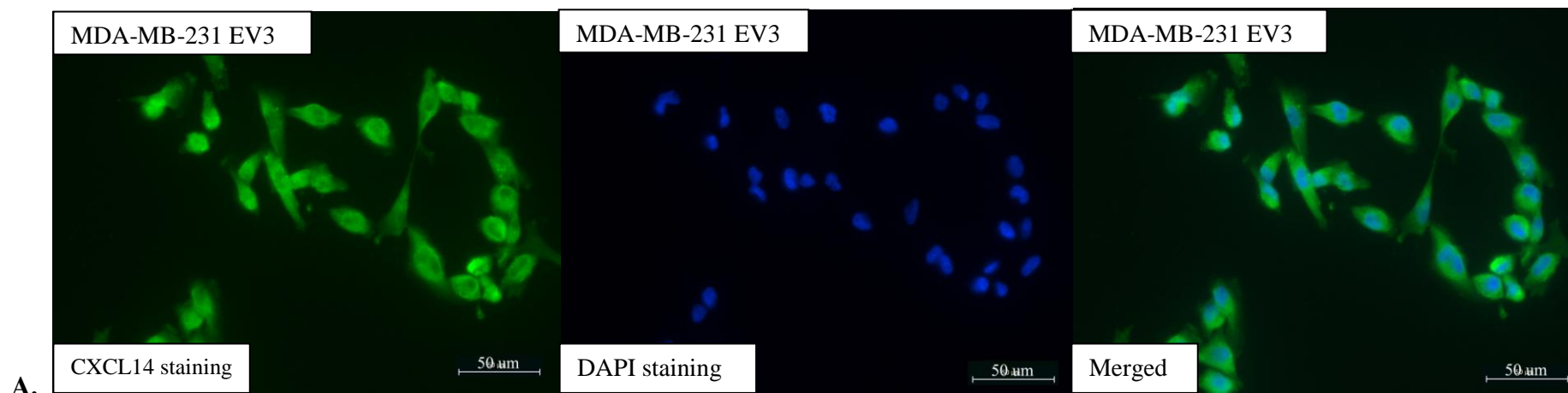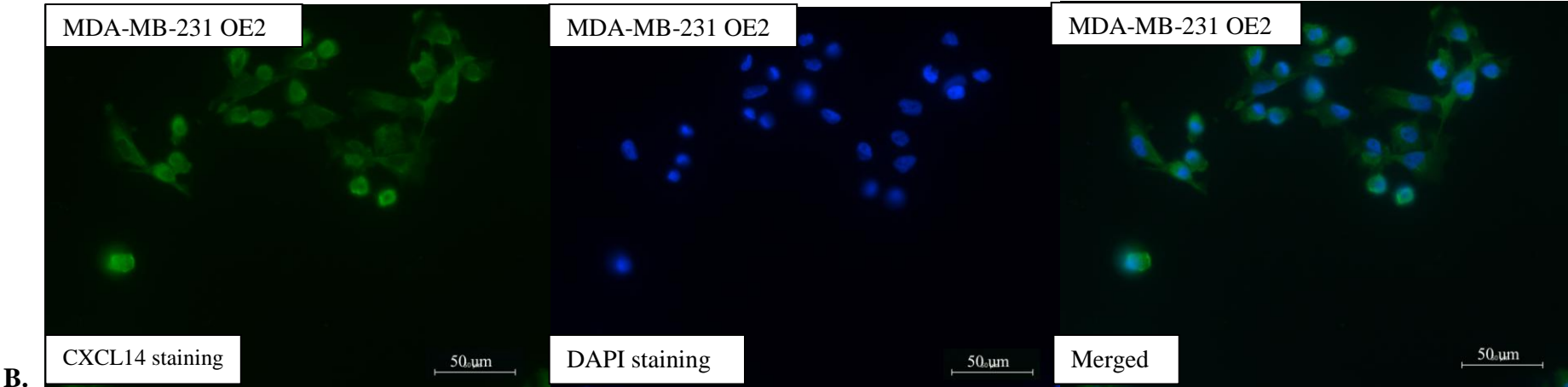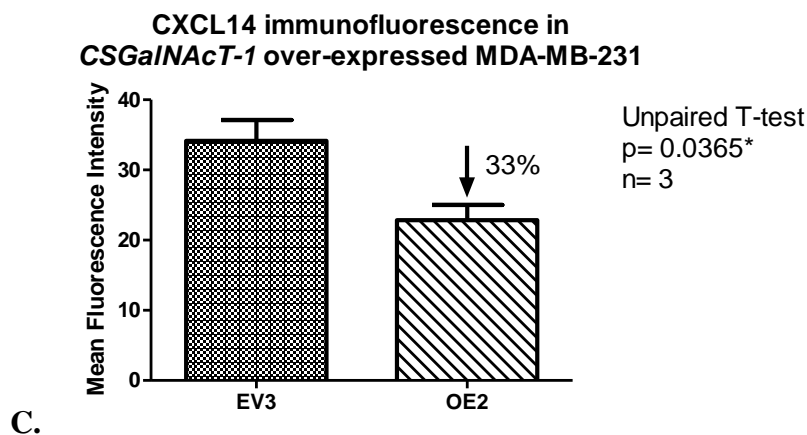
Figure 3.27 Protein level of CXCL14 was significantly down-regulated in *CSGalNAcT-1* over-expressed MDA-MB-231. (A, B) CXCL14 was stained green (left), nucleus was stained blue by DAPI (middle) and merged figure is on the right. (C) Protein level of CXCL14 showed significant down-regulation in the MDA-MB-231 over-expression clones. Mean fluorescence intensity is measured by the ImageJ software. Error bar represents standard error.

3.4.3. Cell migration analysis in *CSGalNAcT-1* over-expressed MCF7 and

MDA-MB-231

3.4.3.1. Transwell migration assay

Cell migration assay using transwell method was performed on *CSGalNAcT-1*

over-expressed MCF7 and MDA-MB-231 clones. A chemoattractant gradient

was created by supplementing medium with 15% FBS in the bottom chamber

while no FBS is added to the cell suspension seeded into the top insert. From

Figure 3.28, both MCF7 and MDA-MB-231 breast cancer cell lines had

reduced migratory capability when *CSGalNAcT-1* was over-expressed in the

cells.

CSGalNAcT-1 over-expressed MCF7 Migration Assay

One-way ANOVA
p= 0.0005***
n= 4

A.

CSGalNAcT-1 over-expressed MDA-MB-231 Migration assay

Unpaired T-test
p= 0.0002***
n= 3

B.
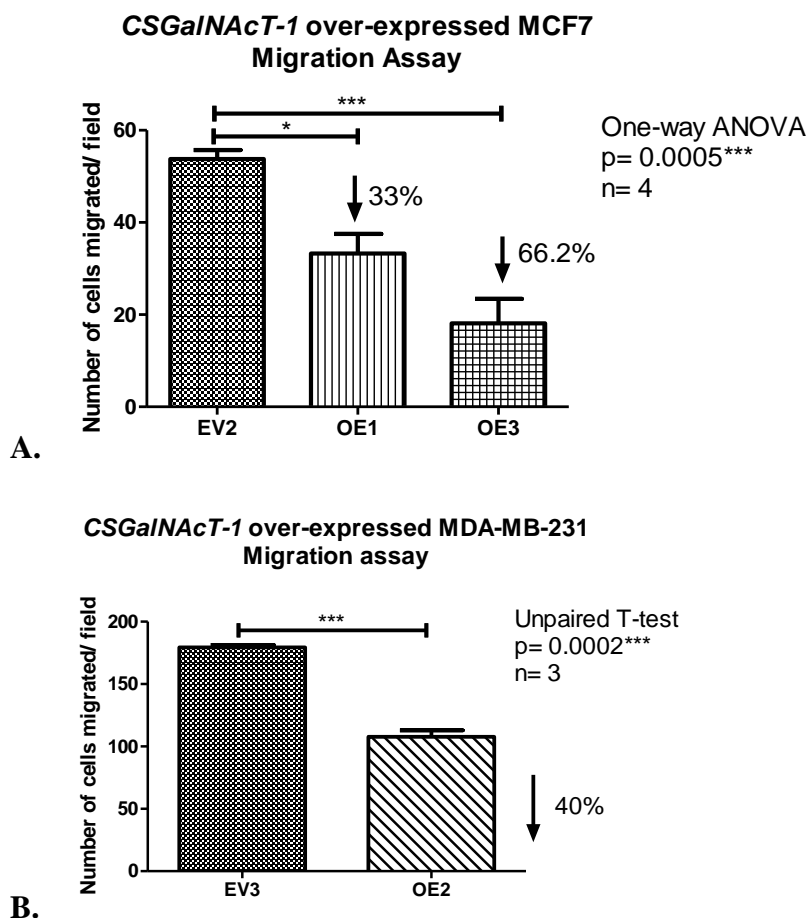
Figure 3.28 Transwell migration assay of *CSGalNAcT-1* over-expressed MCF7 and MDA-MB-231. Migration of both MCF7 and MDA-MB-231 breast cancer cell lines was reduced after *CSGalNAcT-1* gene was over-expressed as presented in (A) and (B). The changes were statistically significant. Error bar represents standard error.

3.4.3.2.   F-actin immunofluorescence

As shown in Figure 3.29 (A-D) and Figure 3.30 (A-C), cell motility of *CSGalNAcT-1* over-expressed MCF7 and MDA-MB-231 was presented in F-actin immunofluorescence staining as well. In general, *CSGalNAcT-1* over-expression reduced F-actin staining intensity in both MCF7 and MDA-MB-231.

A.

B.

C.

D.
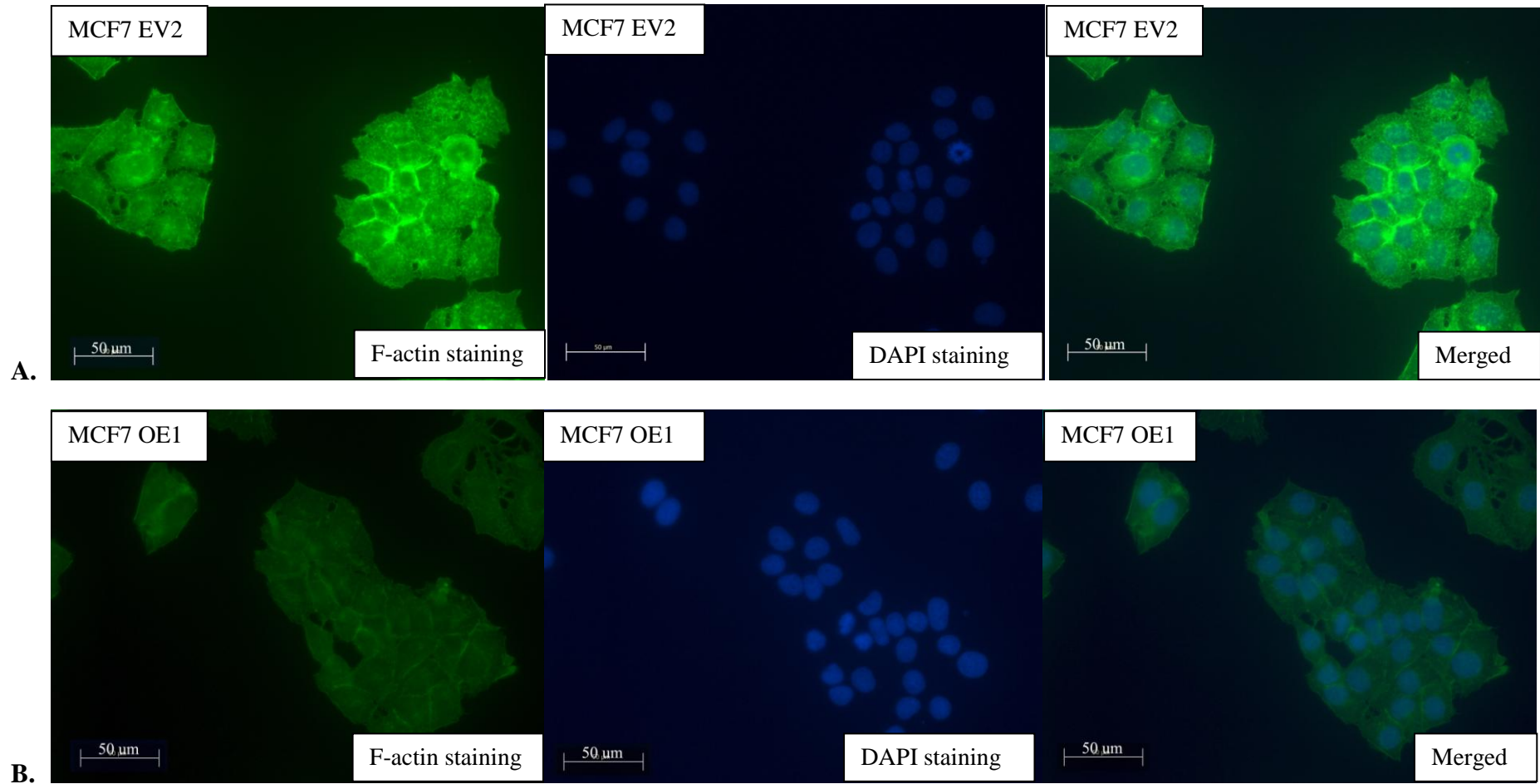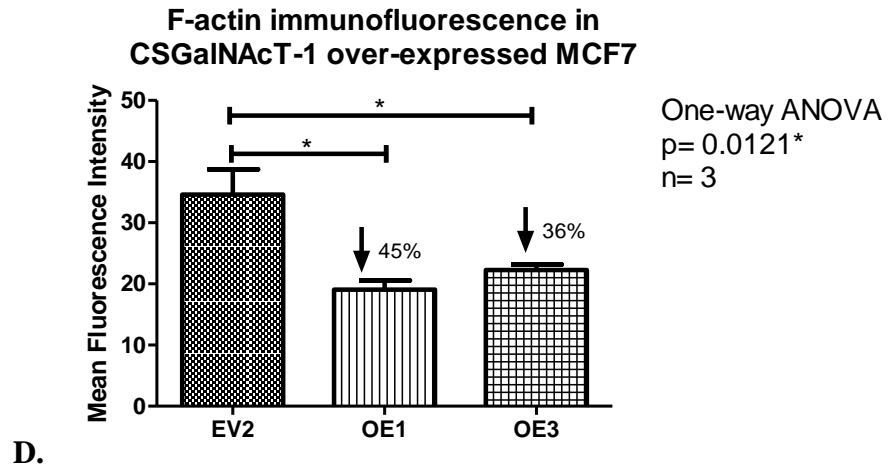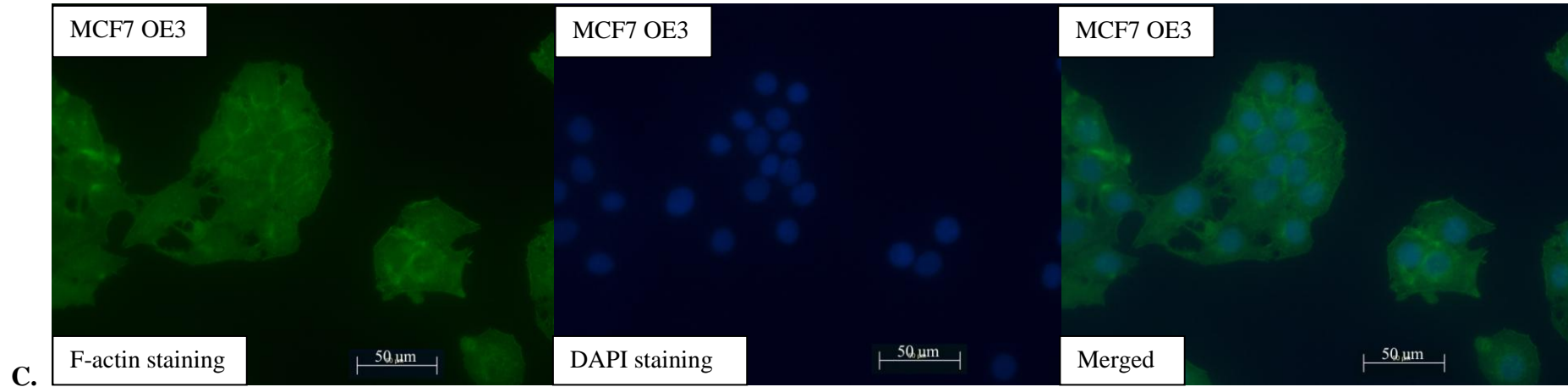
Figure 3.29 Changes in F-actin polymerization after *CSGalNAcT-1* over-expression in MCF7. (A-C) F-actin was stained green (left), nucleus was stained blue by DAPI (middle) and merged figure is on the right. (D) F-actin intensity was decreased in MCF7 after *CSGalNAcT-1* over-expression. Mean fluorescence intensity is measured by the ImageJ software. Error bar represents standard error.

B.

F-actin immunofluoresce in
CSGalNAcT-1 **over-expressed MDA-MB-231**

Unpaired T-test
p= 0.0382*
n= 3

20%

C.
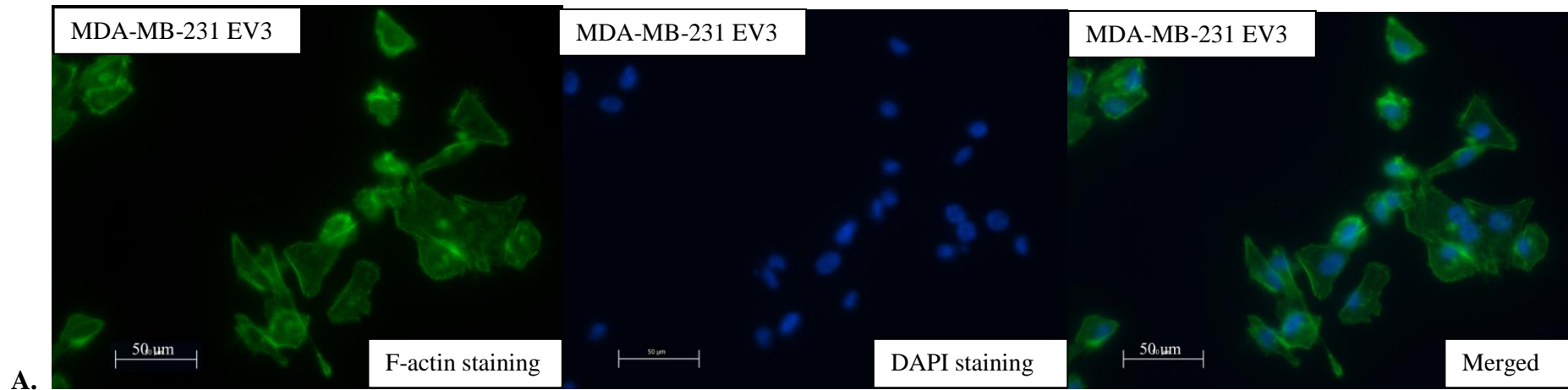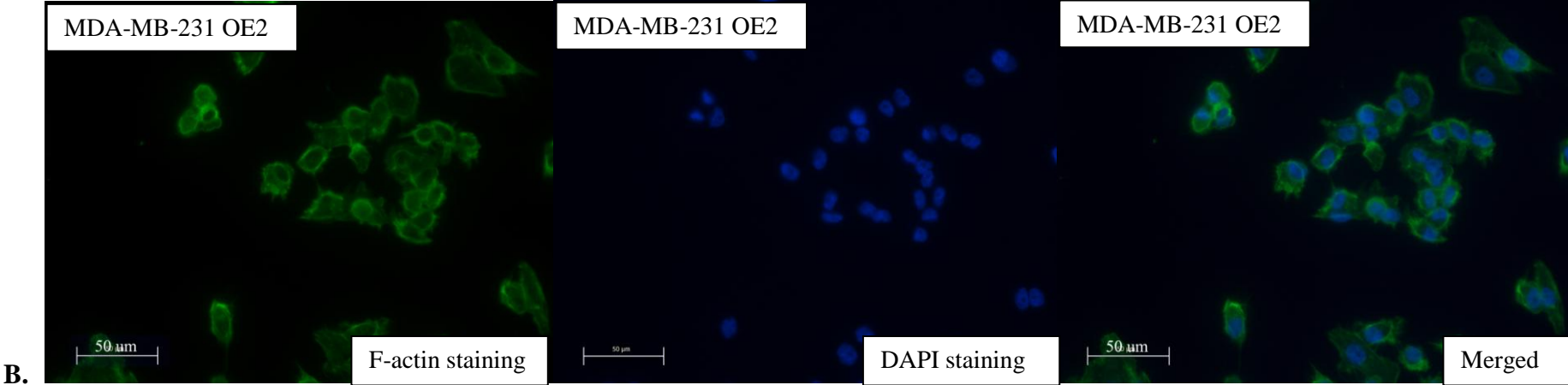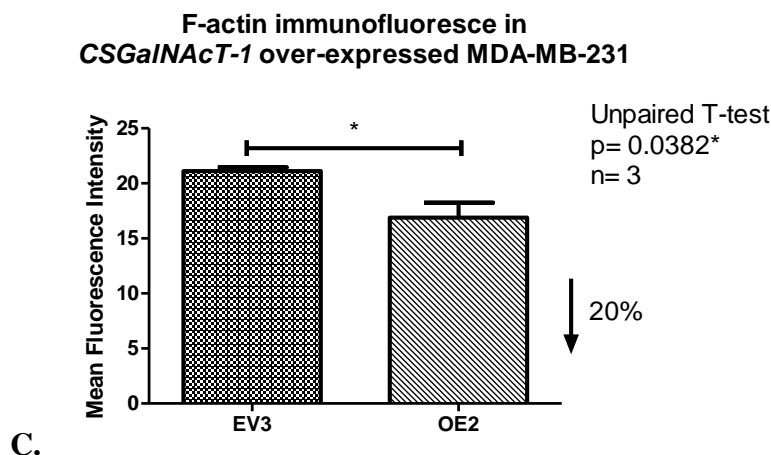
Figure 3.30 Changes in F-actin polymerization after *CSGalNAcT-1* over-expression in MDA-MB-231. (A, B) F-actin was stained green (left), nucleus was stained blue by DAPI (middle) and merged figure is on the right. (C) F-actin intensity was decreased in *CSGalNAcT-1* over-expressed MDA-MB-231. Mean fluorescence intensity is measured by the ImageJ software. Error bar represents standard error.

3.4.4. Assessment of cell invasiveness in *CSGalNAcT-1* over-expressed

MCF7 and MDA-MB-231 by Matrigel chamber

In vitro cell invasion was assayed in BD Biocoat invasion chambers as described earlier in 3.2.4. Lower wells were added with medium supplemented with 15% FBS to serve as chemoattractant. Similar to cell migration, cell invasion was reduced in both MCF7 and MDA-MB-231 cell lines after *CSGalNAcT-1* gene was over-expressed (Figure 3.31).

A. MCF7 EV2

B. MCF7 OE1

C. MCF7 OE3

D.

CSGalNAcT-1 over-expressed MCF7 Invasion assay

One-way ANOVA
p= 0.0030**
n= 4

E.

F.

G.
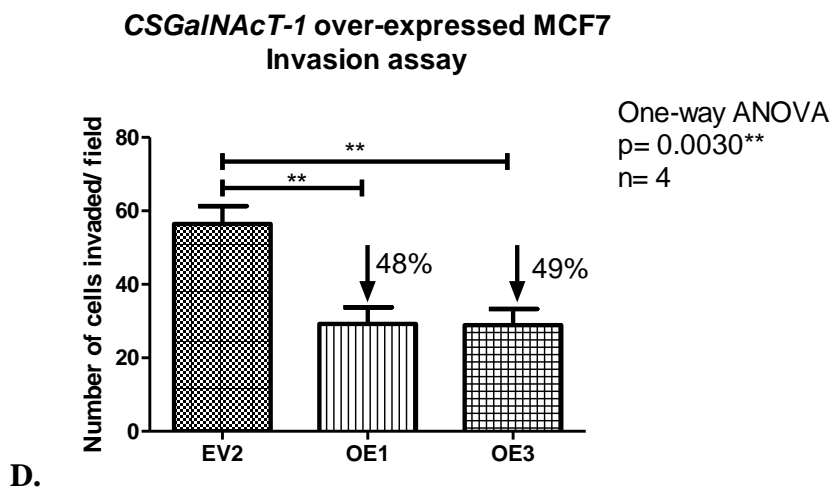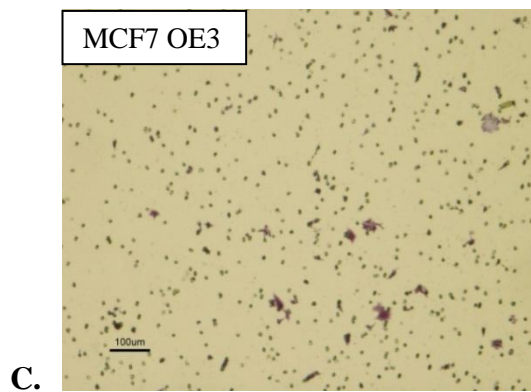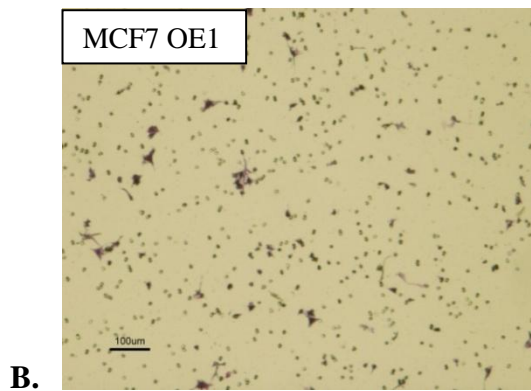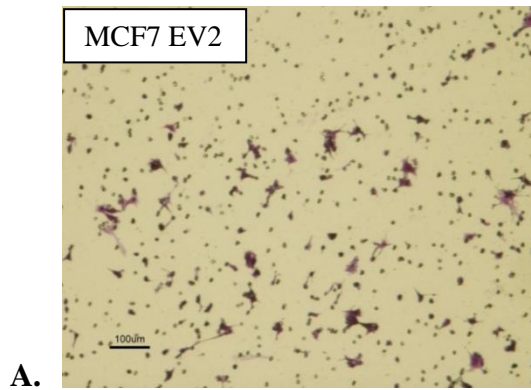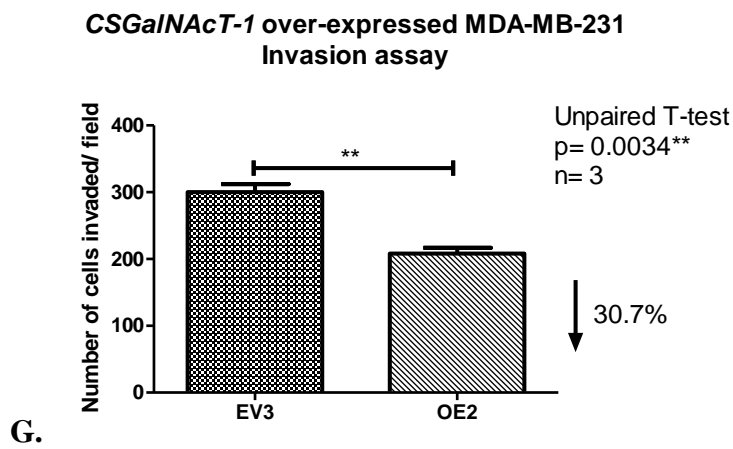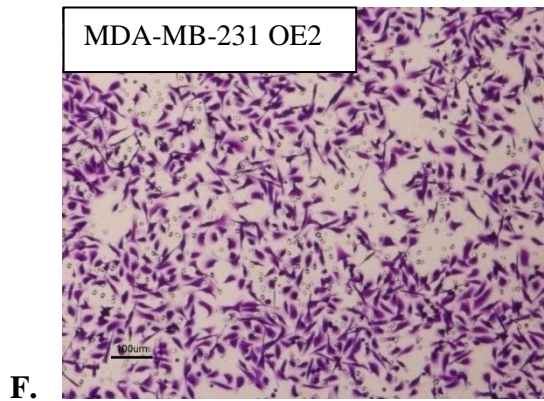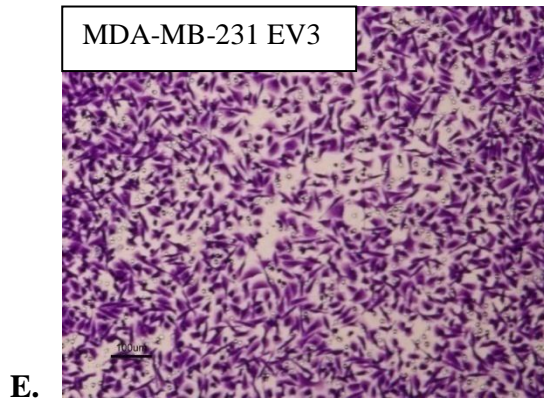
Figure 3.31 Invasion assay in *CSGalNAcT-1* over-expressed MCF7 and MDA-MB-231. *CSGalNAcT-1* over-expression MCF7 and MDA-MB-231 clones exhibited reduced invasion as displayed in both (D) and (G). The reduction in invasion as compared with corresponding empty vector is significantly different. Figure A, B, C, E, and F showed the cells invaded through the chambers. Error bar represents standard error.

3.4.5. Over-expressing *CSGalNAcT-1* impedes cell viability in MCF7 and MDA-MB-231

Cell viability of the *CSGalNAcT-1* over-expression clones was determined by using CellTiter 96 Aqueous Non-radioactive cell proliferation assay. Figure 3.32 shows that both MCF7 and MDA-MB-231 *CSGalNAcT-1* over-expression clones exhibited reduced viability as compared with the respective empty vector clones.

A.

B.
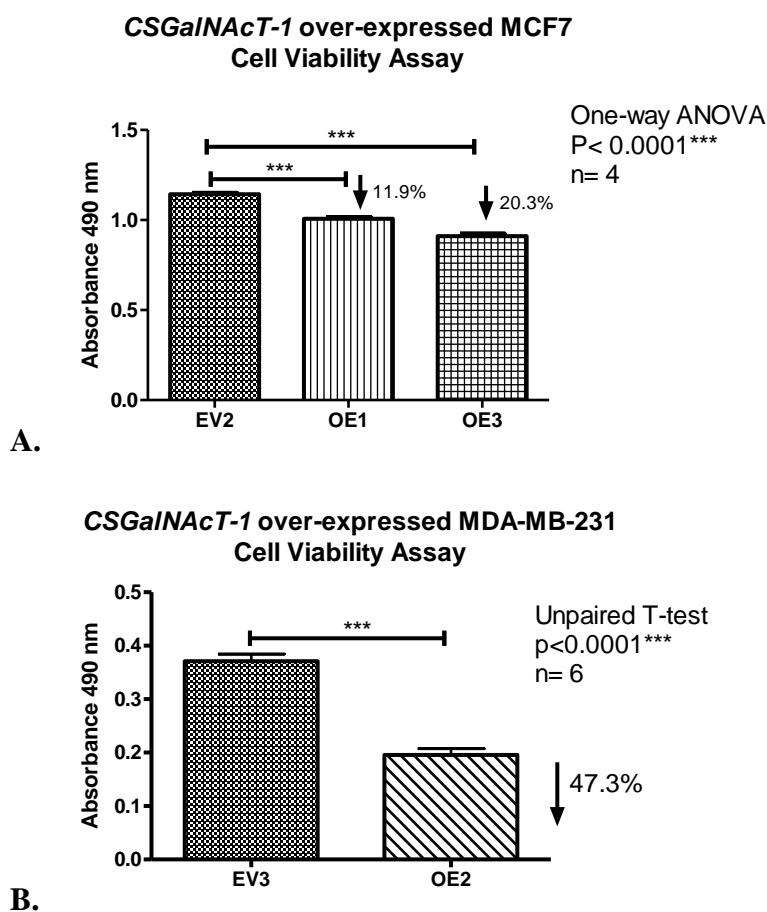
Figure 3.32 Viability assay in *CSGalNAcT-1* over-expressed MCF7 and MDA-MB-231. MCF7 and MDA-MB-231 over-expression clones had significant reduction in viability as compared with empty vectors. Results are displayed in figures (A) and (B). Error bar represents standard error.

3.4.6. Assessment of *CSGalNAcT-1* over-expressed MCF7 and MDA-MB-231 cell adhesion to collagen I

Collagen adhesion assay was done to examine the adhesiveness of *CSGalNAcT-1* over-expression clones to the collagen I which is one of the major and ubiquitous constituents in extracellular matrix. Over-expressing *CSGalNAcT-1* in MCF7 and MDA-MB-231 caused the cells to be less adhesive to collagen I, as shown in Figure 3.33.
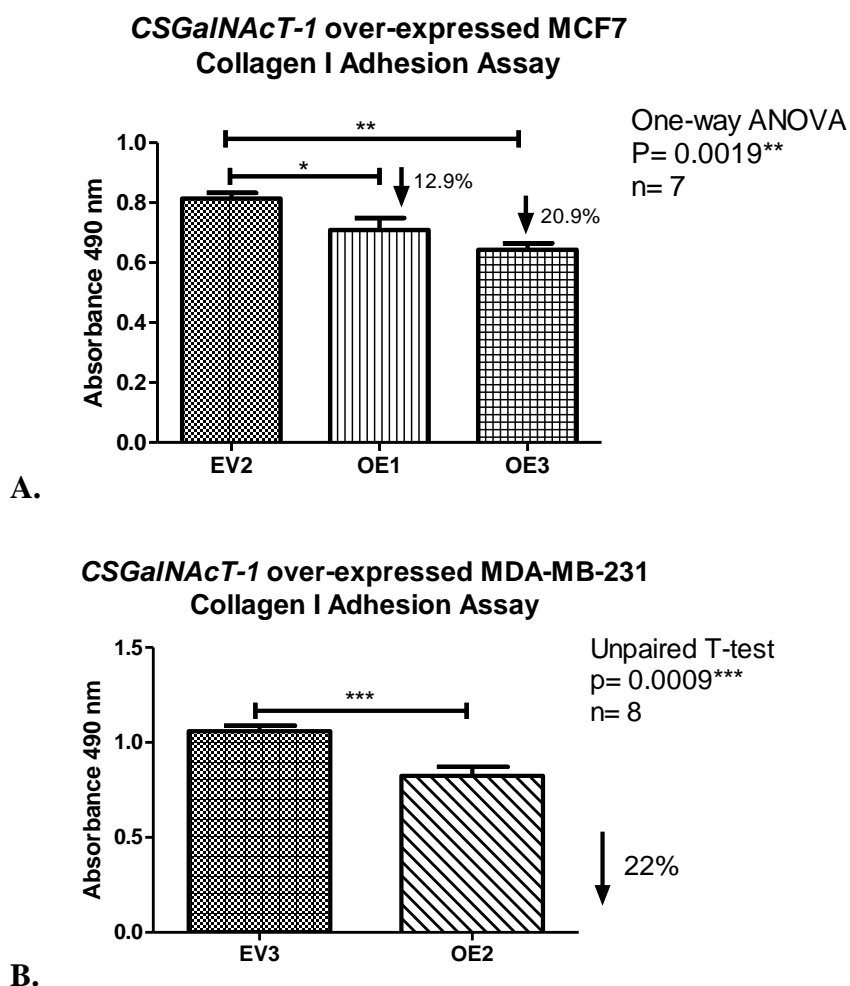
Figure 3.33 Collagen I adhesion assay in *CSGalNAcT-1* over-expressed MCF7 and MDA-MB-231. The adhesiveness of MCF7 and MDA-MB-231 over-expression clones to collagen I reduced significantly as seen in figures (A) and (B). Error bar represents standard error.

3.4.7. Assessment of *CSGalNAcT-1* over-expressed MCF7 and MDA-MB-231 cell adhesion to fibronectin

Besides collagen I adhesion assay, fibronectin adhesion assay was also carried out on *CSGalNAcT-1* over-expressed MCF7 and MDA-MB-231. MCF7 clones exhibited decreased adhesion to fibronectin (Figure 3.34A) while MDA-MB-231 clones had increased adhesion to fibronectin (Figure 3.34B) after *CSGalNAcT-1* over-expression.

A.

B.
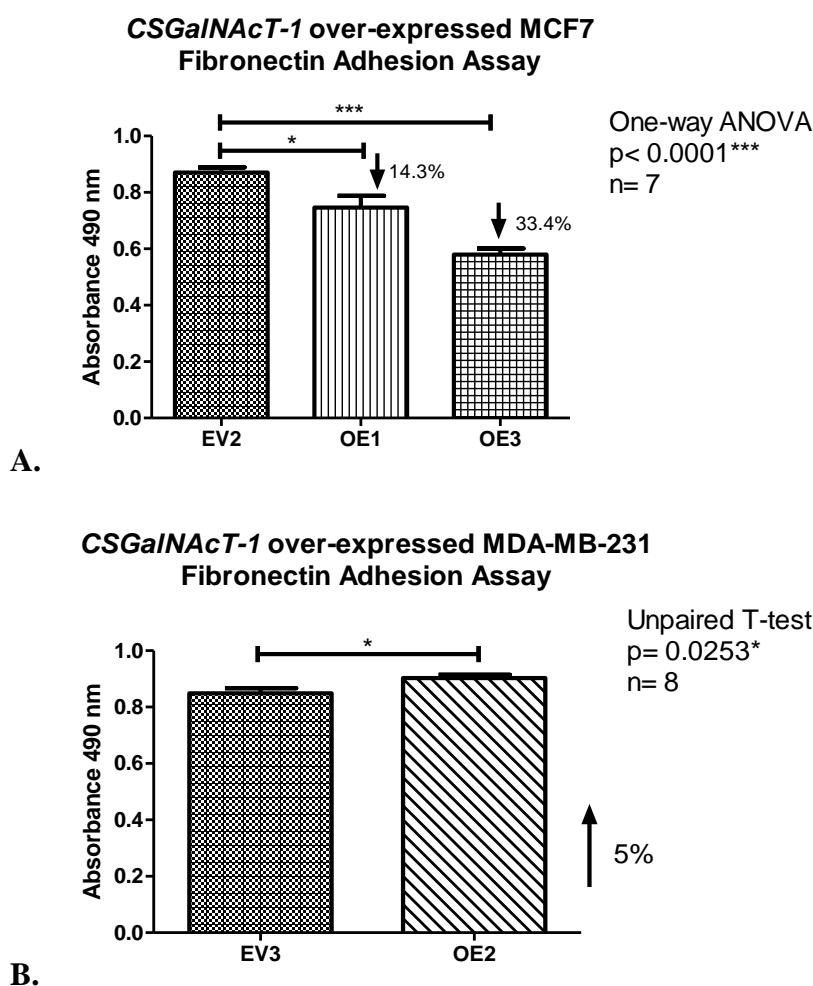
Figure 3.34 Fibronectin adhesion assay in *CSGalNAcT-1* over-expressed MCF7 and MDA-MB-231. (A) MCF7 *CSGalNAcT-1* over-expression clones had reduced adhesion to fibronectin. (B) However, MDA-MB-231 clones increased the adhesion to fibronectin after *CSGalNAcT-1* was over-expressed. Error bar represents standard error.

CHAPTER 4

EXPRESSION ANALYSIS OF

CSGALNACT-1

IN

INVASIVE DUCTAL

CARCINOMA

In this chapter, the expression and localization of CSGalNAcT-1 was detected by immunohistochemistry in breast invasive ductal carcinoma clinical samples. The aim is to determine if there is any association between the expression patterns of CSGalNAcT-1 in different compartments of breast invasive ductal carcinoma clinical samples and their clinicopathological parameters. At the same time, survival analysis was done to determine the prognosis value of CSGalNAcT-1 in breast invasive ductal carcinoma patients.

4.1.   Clinical and demographic data of breast IDC patients

A total of 297 breast IDC tissue microarrays (TMAs) from 1998 to 2004 were included in this study, consisting of 52 normal and 245 IDC cases. Among the 245 IDC cases, 52 cases had enough normal tissue to be dissected and stained for comparison. Among the 245 IDC cases, 52 cores were dropped or folded during immunohistochemical procedure, so these cases were excluded from the analysis with the remaining of 193 cases. Whilst 23 cases from the 52 cases of normal cases were eliminated from analysis due to dropped off or folded during immunohistochemical procedure. The clinicopathological data of IDC patients were summarized in Table 4.1. All of these cases were female origin. The age of patients ranged from 23 to 89 years old.

Table 4.1 Clinicopathological features and distribution of invasive carcinoma tissue sections. The numbers in the brackets represent the percentage of cases in a particular pathological feature against the total number of IDC cases.

Clinical Feature			
Number of patients	193		
Age (mean, in years)	56.76		
Age (median, in years)	56		
Tumor size (mean, in mm)	34.60		
Tumor size (median, in mm)	30		
Clinicopathological feature	**Number of cases (%)**	**Clinicopathological feature**	**Number of cases (%)**
Race		*Bloom-Richardson score*	
Chinese	127 (65.8)	≤5	10 (5.2)
Malay	11 (5.7)	>5	101 (52.3)
Indian	7 (3.6)	Not available	82 (42.5)
Others	8 (4.1)		
Not available	40 (20.7)	*Lymph node involvement*	
		Negative	82 (42.5)
Histological grade		Positive	54 (28.0)
Grade 1 and 2	89 (46.1)	Not available	57 (29.5)
Grade 3	96 (49.7)		
Not available	8 (4.1)	*Lymph node stage*	
		1-9 LN metastasis	139 (72.0)
Staging		≥10 LN metastasis	41 (21.2)
Stage 1 and 2	100 (51.8)	Not available	13 (6.7)
Stage 3	11 (5.7)		
Not available	82 (42.5)	*ER status*	
		Negative	98 (50.8)
Nuclear pleomorphism		Positive	83 (43.0)
Grade 1 and 2	60 (31.1)	Not available	12 (6.2)
Grade 3	63 (32.6)		
Not available	70 (36.3)	*PR status*	
		Negative	79 (40.9)
Tumor tubule formation		Positive	101 (52.3)
Score 1 and 2	42 (21.8)	Not available	13 (6.7)
Score 3	81 (42.0)		
Not available	70 (36.3)	*HER2 status*	
		Negative	126 (65.3)
Mitotic index		Positive	44 (22.8)
Grade 1 and 2	65 (33.7)	Not available	23 (11.9)
Grade 3	58 (30.1)		
Not available	70 (36.3)		

4.2.   Localization of CSGalNAcT-1 in breast IDC

Expression of CSGalNAcT-1 was observed in epithelial cells, stromal cells and diffuse stroma components in breast IDC samples as these three compartments were stained brown immunohistochemically. Weak to strong staining can be detected in the cytoplasm of IDC epithelial cells with score of 1+ to 3+. Expression of CSGalNAcT-1 in diffuse stroma was weak or moderate with score of 1+ and 2+ whereas stromal cells staining was predominantly weak with score of 1+ and with a few cases that have 2+ staining. Immunostaining of CSGalNAcT-1 in various components are shown in Figure 4.1. Diffuse stroma is also known as the extracellular matrix, which comprises of cell types such as fibroblast, epithelial cells, immune inflammatory cells, endothelial cells, pericytes, and adipocytes (Mao et al., 2013, Hanahan and Weinberg, 2011). Cells in diffuse stroma are collectively called stromal cells. Under the guidance of Singapore General Hospital pathologist, only CSGalNAcT-1 staining in fibroblasts were scored in current immunohistochemical study. Hence, the stromal cells in this study only refer to fibroblasts.

A. Epithelial cells
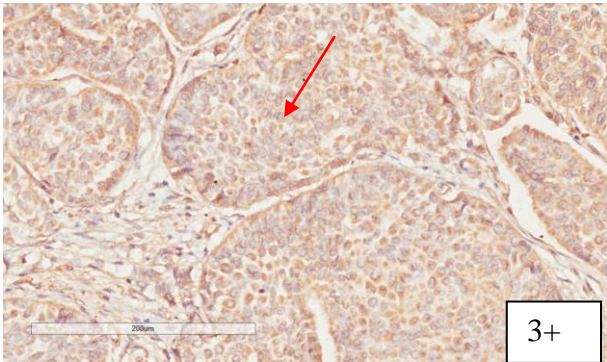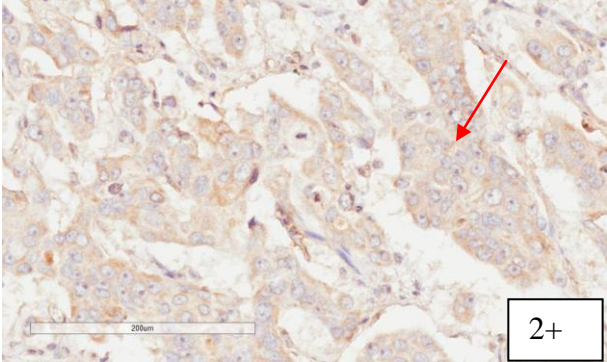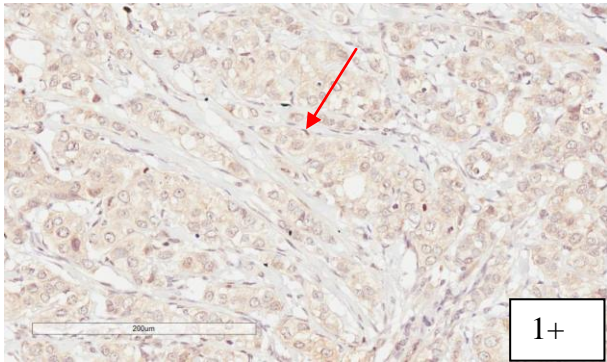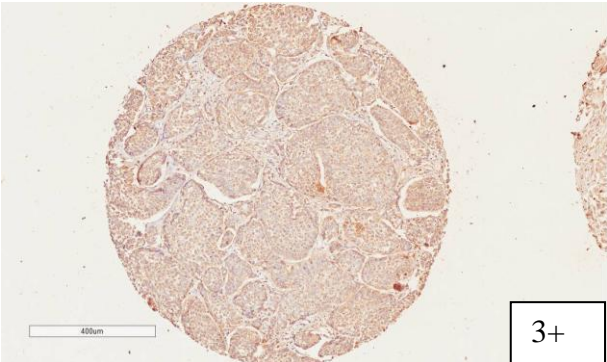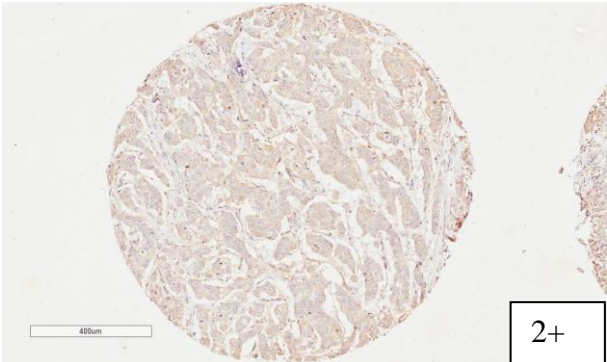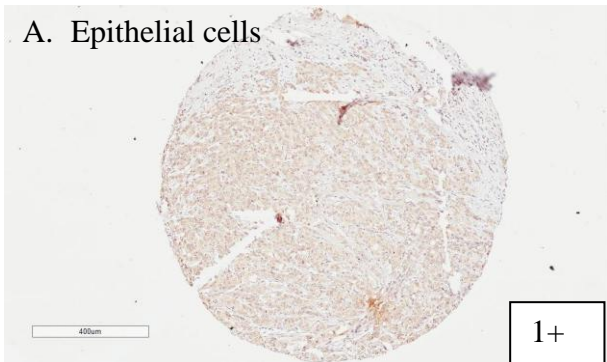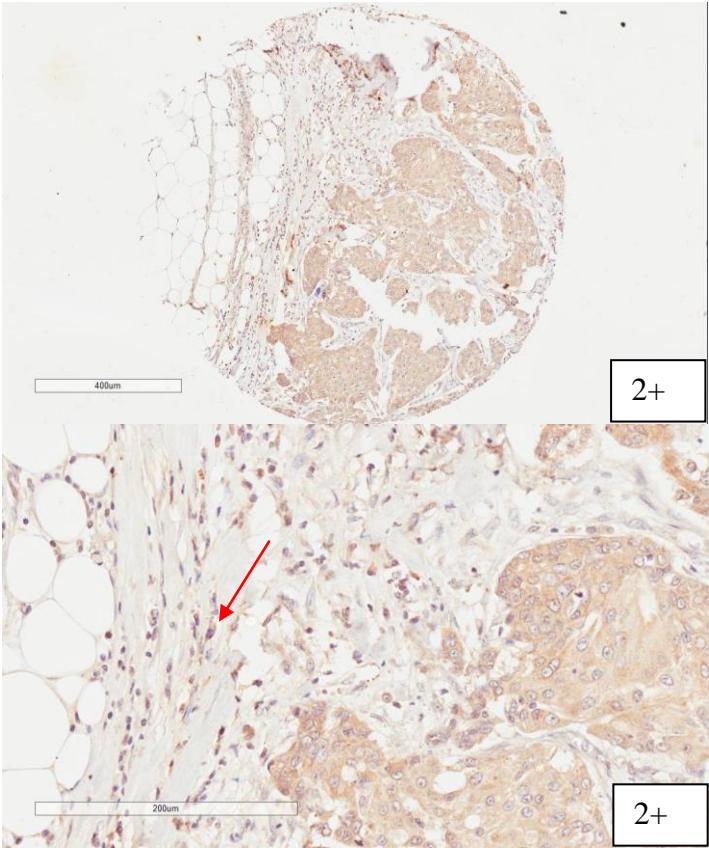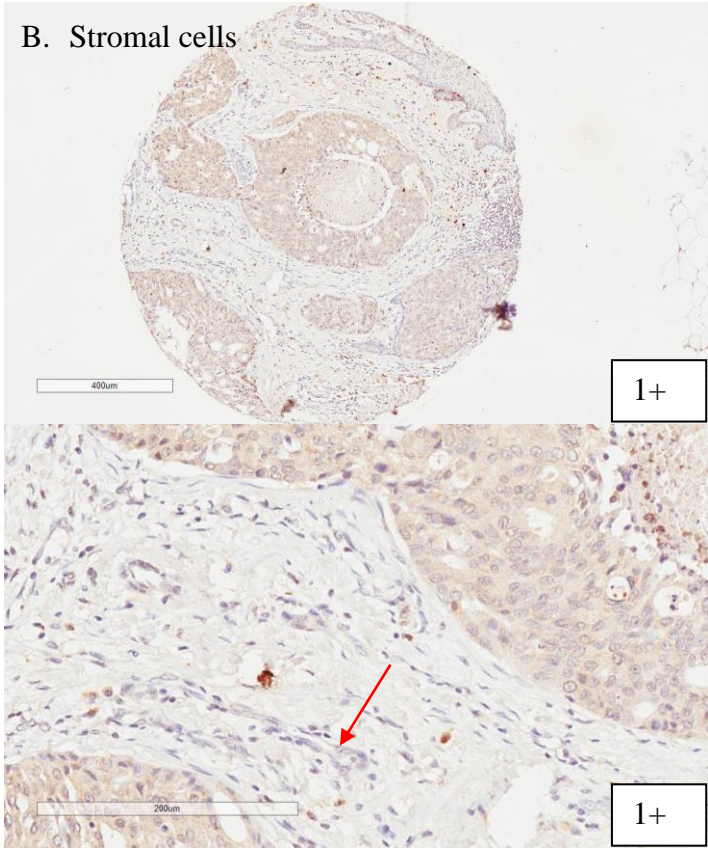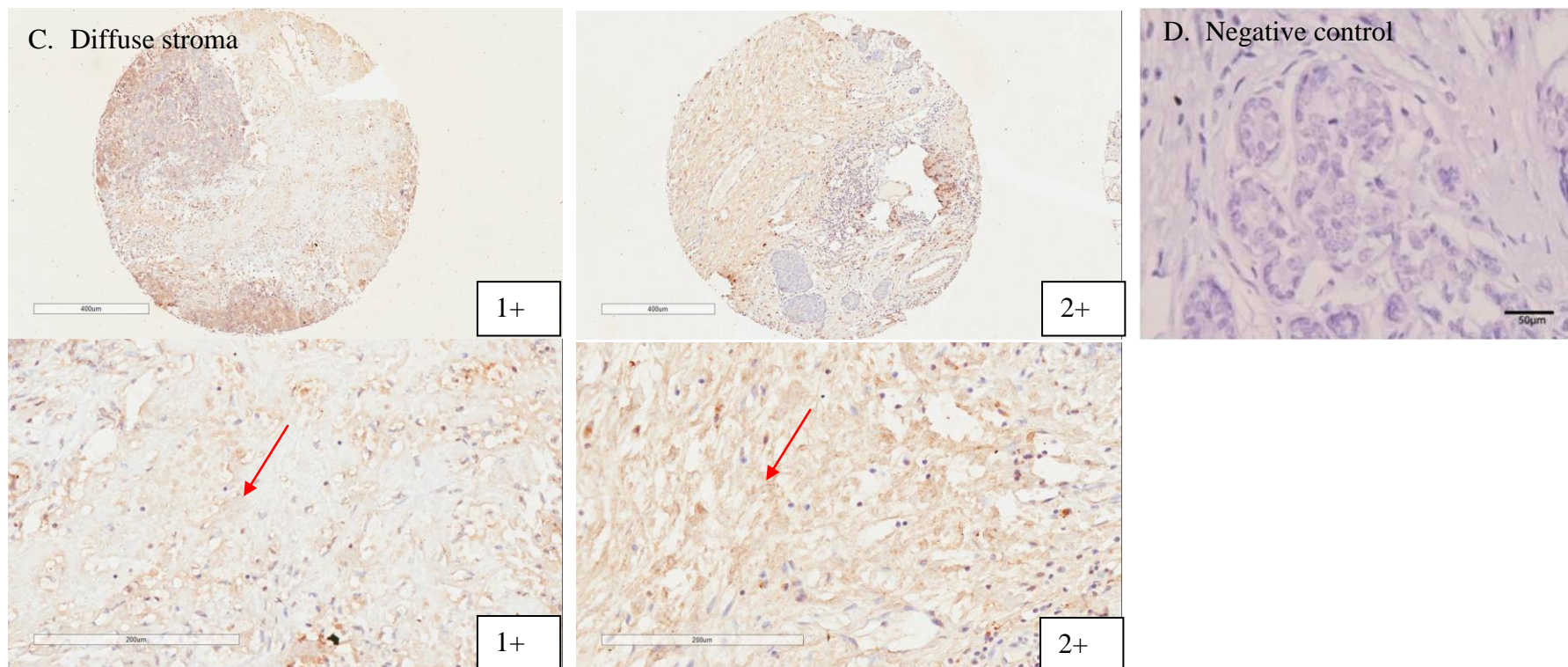
B. Stromal cells

Figure 4.1 CSGalNAcT-1 staining was detected in breast epithelial cells, stromal cells and diffuse stroma. (A) Weak (1+), moderate (2+) and strong (3+) immunostaining of CSGalNAcT-1 in breast epithelial cells. Red arrows indicate the different staining intensity of the immunopositive epithelial cells. (B) Weak (1+) and moderate (2+) immunostaining of CSGalNAcT-1 in stromal cells. Red arrows indicate the different staining intensity of the immunopositive stromal cells. (C) Diffuse stroma was stained weakly (1+) and moderately (2+) with CSGalNAcT-1. Red arrows indicate the different staining intensity of the immunopositive diffuse stroma. (D) No background immunoreactivity detected in negative control which was done by omitting CSGalNAcT-1 primary antibody.

4.3. Comparison of CSGalNAcT-1 staining in normal breast tissue and breast IDC

A total of 21 available paired normal and IDC cases were compared for the CSGalNAcT-1 immunostaining in epithelial cells, stromal cells and diffuse stroma, respectively, using non-parametric Wilcoxon matched pairs test for statistical analysis. Generally, in stromal cells, CSGalNAcT-1 immunostaning in normal cases was significantly weaker than in IDC cases (Figure 4.2B). However, in diffuse stroma, significant stronger expression of CSGalNAcT-1 was found in normal cases as compared to IDC cases (Figure 4.2C). All comparisons from each component were displayed in Figure 4.2.

A. Epithelial cells
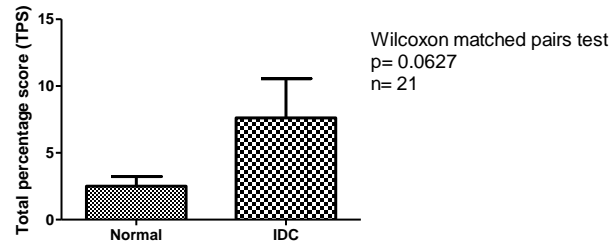
B. Stromal cells
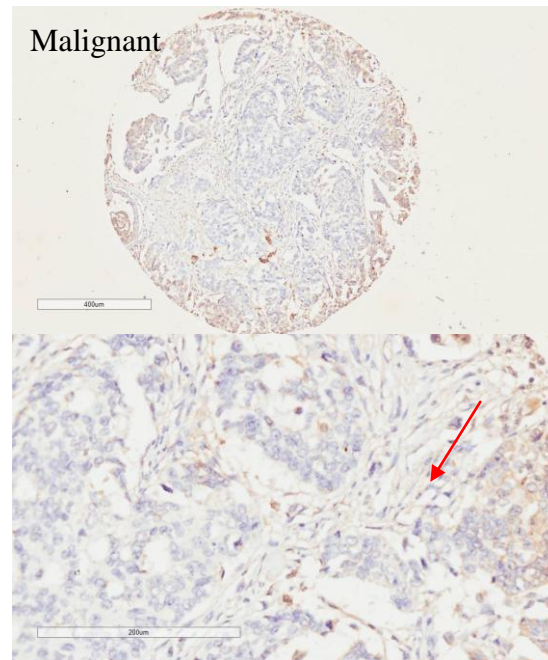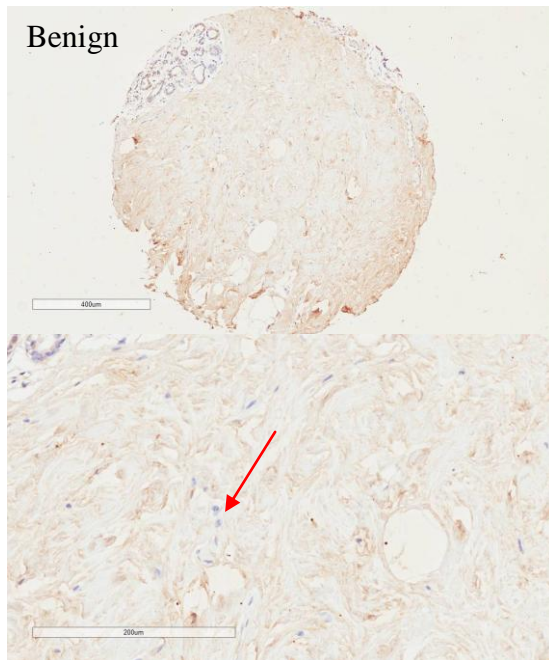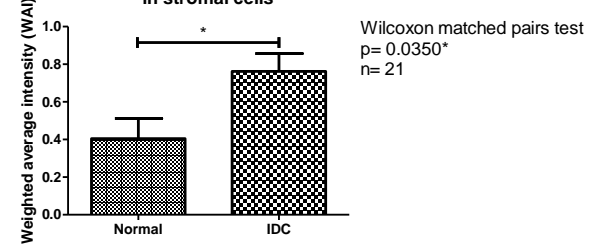
C. Diffuse stroma
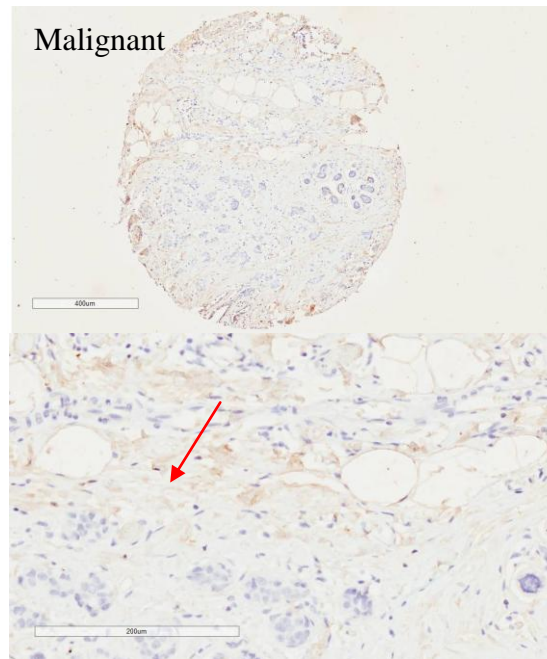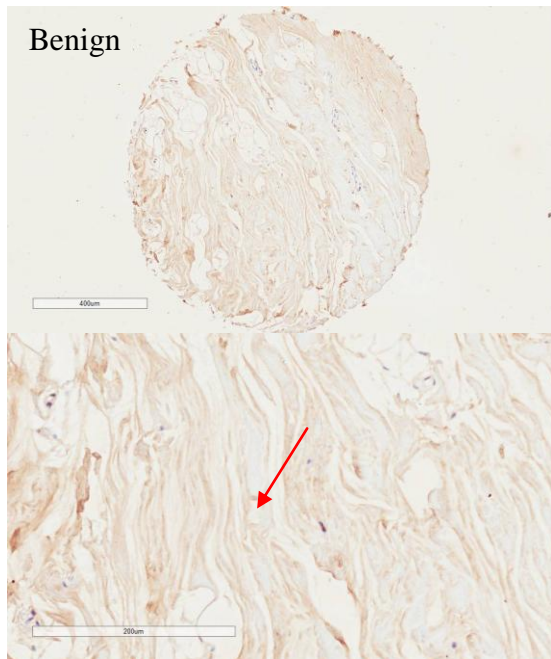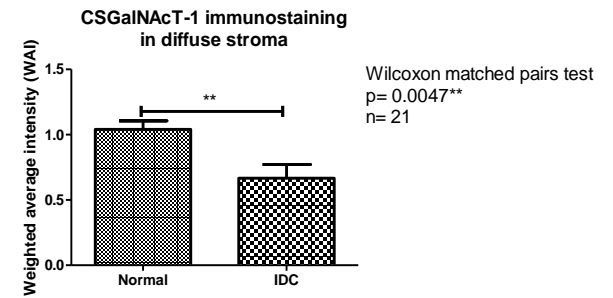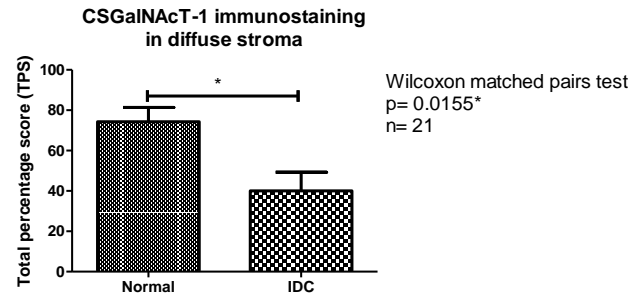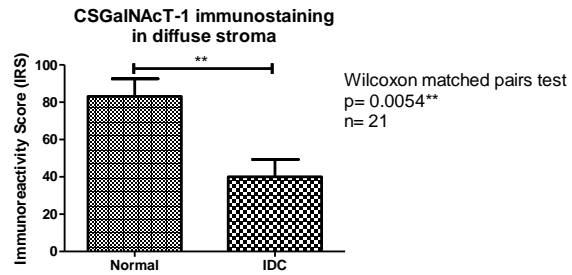
Figure 4.2 Graphs and figures showing the immunoscores comparisons of CSGalNAcT-1 expression in normal and IDC cases in three stained components. (A) No significant difference in CSGalNAcT-1 immunostaining was detected in epithelial cells of normal and IDC cases. (B) The expression of CSGalNAcT-1 in stromal cells was stronger in malignant cases. Figures indicate the stromal cells in IDC cases have higher staining intensity than in normal cases. Red arrows indicate the CSGalNAcT-1 immunopositive stromal cells. (C) However, expression of CSGalNAcT-1 in diffuse stroma was stronger in normal cases. Figures indicate the diffuse stroma in normal cases have higher staining intensity than in IDC cases. Red arrows indicate the CSGalNAcT-1 immunopositive diffuse stroma. The results were expressed in mean±SE.

4.4. Comparison of CSGalNAcT-1 staining in low grade and high grade breast IDC

Among the 193 malignant IDC cases, 89 cases belongs to low grade IDC (histological grade 1 and 2) and 96 cases are high grade IDC

(histological grade 3), whilst eight cases with no available data. Comparisons of CSGalNAcT-1 immunostaining in epithelial cells, stromal cells

and diffuse stroma were made between low grade and high grade IDC (Figure 4.3). Only stromal cells WAI showed significant difference

(Figure 4.3B); but overall, low grade IDC cases had stronger expression of CSGalNAcT-1 than high grade IDC.

A. Epithelial cells
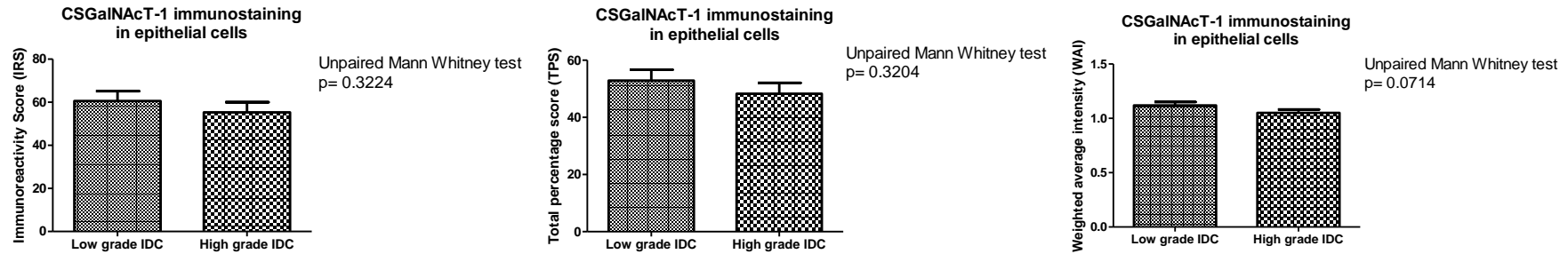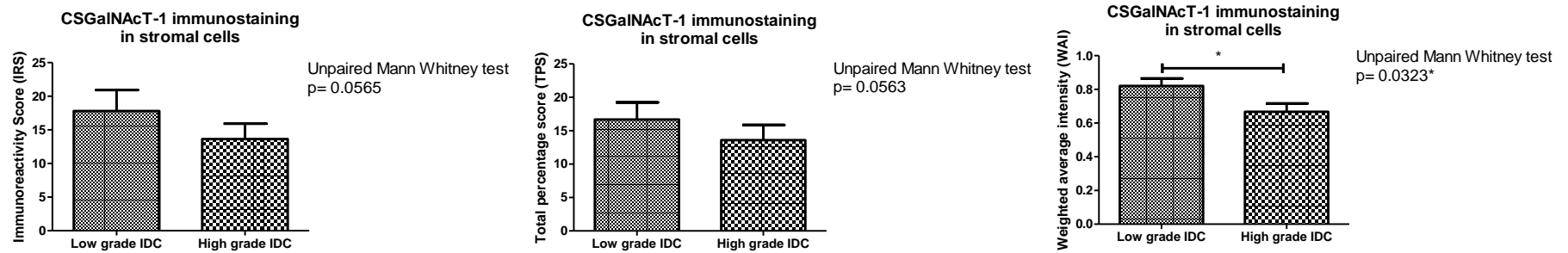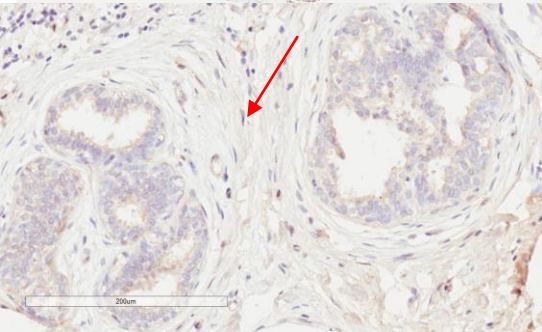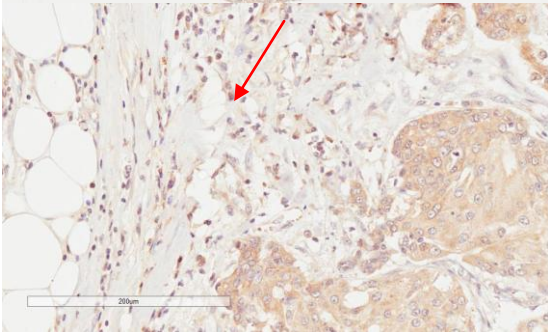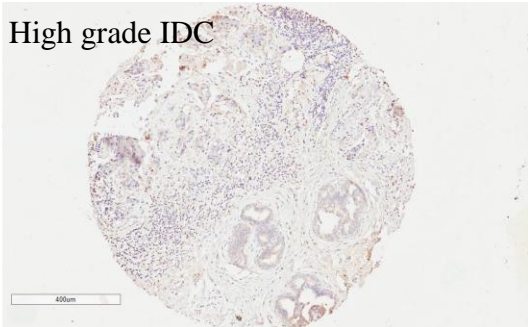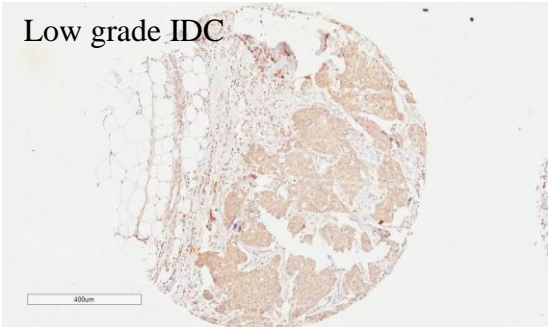
B. Stromal cells
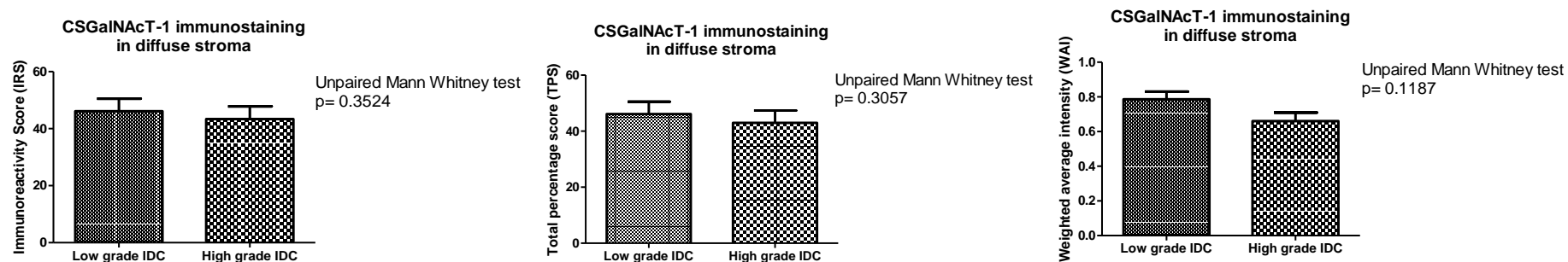
C. Diffuse stroma

Figure 4.3 Immunostaining of CSGalNAcT-1 in low grade and high grade IDC. Expression of CSGalNAcT-1 in epithelial cells (A), stromal cells (B) and diffuse stroma (C) is generally higher in low grade IDC than in high grade IDC. (B) Only the comparison in WAI of stromal cells is significant. Figures indicate that stromal cells in low grade IDC have stronger expression of CSGalNAcT-1 than in high grade IDC. Red arrows indicate the CSGalNAcT-1 immunopositive stromal cells. The results were expressed in mean±SE.

4.5. Associations of CSGalNAcT-1 immunoreactivity in breast IDC with clinicopathological parameters

The banding of each immunoscoring measurement (i.e. IRS, TPS, WAI) in all three stained components and the number of each cases in each banded category were shown in Table 4.2. The cut-off points were used throughout the following analysis. This is an exploratory study to investigate the expression of CSGalNAcT-1 in IDC cases. As nothing is known about the use of CSGalNacT-1 to differentiate between IDC patients with good and bad prognosis, different cut-offs were examined to find a suitable value to differentiate between the two groups. In future, a different set of IDC samples can be used to validate this cut-off value. The associations of clinicopathological parameters with CSGalNAcT-1 immunostaining in all three components, i.e. epithelial cells, stromal cells and diffuse stroma, were presented in following sections.

Table 4.2 Different types of CSGalNAcT-1 immunoscoring in epithelial cells, stromal cells and diffuse stroma and their cut-offs in each immunoscoring factor.

Components	Immunoscores	Cut-offs	Number of cases (%)
Epithelial cells	IRS	≤150	188 (97.4)
		>150	5 (2.6)
	TPS	≤90	156 (80.8)
		>90	37 (19.2)
	WAI	≤1.7	182 (94.3)
		>1.7	11 (5.7)
Stromal cells	IRS	≤50	172 (89.1)
		>50	21 (10.9)
	TPS	≤50	172 (89.1)
		>50	21 (10.9)
	WAI	≤0.9	51 (26.4)
		>0.9	142 (73.6)
Diffuse stroma	IRS	≤100	189 (97.9)
		>100	4 (2.1)
	TPS	≤20	97 (50.3)
		>20	96 (49.7)
	WAI	≤1.0	187 (96.9)
		>1.0	6 (3.1)

4.5.1. Epithelial cells

CSGalNAcT-1 was stained in epithelial cells of IDC. The following tables show the associations between IDC clinicopathological parameters and IRS (Table 4.3), TPS (Table 4.4), and WAI (Table 4.5) of CSGalNAcT-1 in epithelial cells.

Table 4.3 Correlation of clinicopathological parameters of IDC with CSGalNAcT-1 immunoreactivity score (IRS) of epithelial cell. No significant correlation was found.

Clinicopathological parameters		Immunoreactivity score (IRS)				P-value
		≤150	>150	Valid cases (%)	Missing cases (%)	
		Number of cases (%)	Number of cases (%)			
Age	≤50	73 (96.1%)	3 (3.9%)	192 (99%)	1 (1%)	0.386
	>50	114 (98.3%)	2 (1.7%)			
Race	Chinese	123 (96.9%)	4 (3.1%)	153 (78.9%)	40 (21.1%)	0.840
	Malay	11 (100%)	0			
	Indian	7 (100%)	0			
	Others	8 (100%)	0			
Tumor size	≤30mm	101 (97.1%)	3 (2.9%)	189 (97.4%)	4 (2.6%)	1.000
	>30mm	83 (97.6%)	2 (2.4%)			
Histological grade	Grade 1 and 2	87 (97.8%)	2 (2.2%)	185 (95.4%)	8 (4.6%)	0.939
	Grade 3	94 (97.9%)	2 (2.1%)			
Staging	Stage 1 and 2	96 (96%)	4 (4%)	111 (57.2%)	82 (42.8%)	0.070

	Stage 3	11 (100%)	0			
DCIS nuclear grade	None and low	65 (97%)	2 (3%)	174 (89.7%)	19 (10.3%)	0.650
	Intermediate and high	105 (98.1%)	2 (1.9%)			
Lymph node involvement	Negative	80 (97.6%)	2 (2.4%)	136 (70.1%)	57 (29.9%)	0.649
	Positive	52 (96.3%)	2 (3.7%)			
Lymph node stage	1-9 LN metastasis	135 (97.1%)	4 (2.9%)	180 (92.8%)	13 (7.2%)	0.875
	10 and above LN metastasis	40 (97.6%)	1 (2.4%)			
ER	Negative	96 (98%)	2 (2%)	181 (93.3%)	12 (6.7%)	1.000
	Positive	81 (97.6%)	2 (2.4%)			
PR	Negative	78 (98.7%)	1(1.3%)	180 (92.8%)	13 (7.2%)	0.632
	Positive	98 (97%)	3 (3%)			
HER2	Negative	123 (97.6%)	3 (2.4%)	170 (87.6%)	23 (12.4%)	0.605
	Positive	42 (95.5%)	2 (4.5%)			
BloomRichardson	≤5	10 (100%)	0	111 (57.2%)	82 (42.8%)	NA
	>5	101 (100%)	0			
Mitotic index	Grade 1 and 2	65 (100%)	0	123 (63.4%)	70 (36.6%)	NA
	Grade 3	58 (100%)	0			
Nuclear pleomorphism	Grade 1 and 2	60 (100%)	0	123 (63.4%)	70 (36.6%)	NA
	Grade 3	63 (100%)	0			
Tumor tubule formation	Score 1 and 2	42 (100%)	0	123 (63.4%)	70 (36.6%)	NA
	Score 3	81 (100%)	0			

Table 4.4 Correlation of clinicopathological parameters of IDC with CSGalNAcT-1 total percentage score (TPS) of epithelial cell. No significant correlation was found.

Clinicopathological parameters		Total percentage score (TPS)				P-value
		≤90	>90	Valid cases (%)	Missing cases (%)	
		Number of cases (%)	Number of cases (%)			
Age	≤50	57 (75%)	19 (25%)	192 (99%)	1 (1%)	0.134
	>50	98 (84.5%)	18 (15.5%)			
Race	Chinese	101 (79.5%)	26 (20.5%)	153 (78.9%)	40 (21.1%)	0.562
	Malay	9 (81.8%)	2 (18.2%)			
	Indian	7 (100%)	0			
	Others	7 (87.5%)	1 (12.5%)			
Tumor size	≤30mm	82 (78.8%)	22 (21.2%)	189 (97.4%)	4 (2.6%)	0.585
	>30mm	70 (82.4%)	15 (17.6%)			
Histological grade	Grade 1 and 2	70 (78.7%)	19 (21.3%)	185 (95.4%)	8 (4.6%)	0.533
	Grade 3	79 (82.3%)	17 (17.7%)			
Staging	Stage 1 and 2	76 (76%)	24 (24%)	111 (57.2%)	82 (42.8%)	0.817
	Stage 3	8 (72.7%)	3 (27.3%)			
DCIS nuclear grade	None and low	53 (79.1%)	14 (20.9%)	174 (89.7%)	19 (10.3%)	0.724
	Intermediate and high	87 (81.3%)	20 (18.7%)			
Lymph node involvement	Negative	65 (79.3%)	17 (20.7%)	136 (70.1%)	57 (29.9%)	0.834
	Positive	10 (18.5%)	44 (81.5%)			
Lymph node stage	1-9 LN metastasis	112 (80.6%)	27 (19.4%)	180 (92.8%)	13 (7.2%)	0.729
	10 and above LN	32 (78%)	9 (22%)			

	metastasis					
ER	Negative	78 (79.6%)	20 (20.4%)	181 (93.3%)	12 (6.7%)	1.000
	Positive	67 (80.7%)	16 (19.3%)			
PR	Negative	63 (79.7%)	16 (20.3%)	180 (92.8%)	13 (7.2%)	1.000
	Positive	81 (80.2%)	20 (19.8%)			
HER2	Negative	97 (77%)	29 (23%)	170 (87.6%)	23 (12.4%)	0.278
	Positive	38 (86.4%)	6 (13.6%)			
BloomRichardson	≤5	9 (90%)	1 (10%)	111 (57.2%)	82 (42.8%)	0.684
	>5	81 (80.2%)	20 (19.8%)			
Mitotic index	Grade 1 and 2	53 (81.5%)	12 (18.5%)	123 (63.4%)	70 (36.6%)	0.663
	Grade 3	49 (84.5%)	9 (15.5%)			
Nuclear pleomorphism	Grade 1 and 2	34 (56.7%)	26 (43.3%)	123 (63.4%)	70 (36.6%)	0.252
	Grade 3	42 (66.7%)	21 (33.3%)			
Tumor tubule formation	Score 1 and 2	35 (83.3%)	7 (16.7%)	123 (63.4%)	70 (36.6%)	0.931
	Score 3	67 (82.7%)	14 (17.3%)			

Table 4.5 Correlation of clinicopathological parameters of IDC with CSGalNAcT-1 weighted average intensity (WAI) of epithelial cell. No significant correlation was found.

Clinicopathological parameters		Weighted average intensity (WAI)				P-value
		≤1.70	>1.70	Valid cases (%)	Missing cases (%)	
		Number of cases (%)	Number of cases (%)			
Age	≤50	72 (94.7%)	4 (5.3%)	192 (99%)	1 (1%)	1.000
	>50	110 (94.8%)	6 (5.2%)			
Race	Chinese	119 (93.7%)	8 (6.3%)	153 (78.9%)	40 (21.1%)	0.757
	Malay	10 (90.9%)	1 (9.1%)			
	Indian	7 (100%)	0			
	Others	7 (87.5%)	1 (12.5%)			
Tumor size	≤30mm	98 (94.2%)	6 (5.8%)	189 (97.4%)	4 (2.6%)	1.000
	>30mm	80 (94.1%)	5 (5.9%)			
Histological grade	Grade 1 and 2	83 (93.3%)	6 (6.7%)	185 (95.4%)	8 (4.6%)	0.258
	Grade 3	93 (96.9%)	3 (3.1%)			
Staging	Stage 1 and 2	92 (92%)	8 (8%)	111 (57.2%)	82 (42.8%)	0.904
	Stage 3	10 (90.9%)	1 (9.1%)			
DCIS nuclear grade	None and low	64 (95.5%)	3 (4.5%)	174 (89.7%)	19 (10.3%)	0.553
	Intermediate and high	100 (93.5%)	7 (6.5%)			
Lymph node involvement	Negative	76 (92.7%)	6 (7.3%)	136 (70.1%)	57 (29.9%)	1.000
	Positive	51 (94.4%)	3 (5.6%)			
Lymph node stage	1-9 LN metastasis	130 (93.5%)	9 (6.5%)	180 (92.8%)	13 (7.2%)	0.687
	10 and above LN	39 (95.1%)	2 (4.9%)			

	metastasis					
ER	Negative	93 (94.9%)	5 (5.1%)	181 (93.3%)	12 (6.7%)	1.000
	Positive	79 (95.2%)	4 (4.8%)			
PR	Negative	76 (96.2%)	3 (3.8%)	180 (92.8%)	13 (7.2%)	0.733
	Positive	95 (94.1%)	6 (5.9%)			
HER2	Negative	121 (96%)	5 (4%)	170 (87.6%)	23 (12.4%)	1.000
	Positive	42 (95.5%)	2 (4.5%)			
BloomRichardson	≤5	10 (100%)	0	111 (57.2%)	82 (42.8%)	1.000
	>5	96 (96%)	4 (4%)			
Mitotic index	Grade 1 and 2	62 (95.4%)	3 (4.6%)	123 (63.4%)	70 (36.6%)	0.353
	Grade 3	57 (98.3%)	1 (1.7%)			
Nuclear pleomorphism	Grade 1 and 2	58 (96.7%)	2 (3.3%)	123 (63.4%)	70 (36.6%)	0.960
	Grade 3	61 (96.8%)	2 (3.2%)			
Tumor tubule formation	Score 1 and 2	39 (92.9%)	3 (7.1%)	123 (63.4%)	70 (36.6%)	0.157
	Score 3	80 (98.8%)	1 (1.2%)			

4.5.2. Stromal cells

CSGalNAcT-1 was expressed in IDC stromal cells. The following tables show the correlation between clinicopathological parameters and and IRS (Table 4.6), TPS (Table 4.7, and WAI (Table 4.8) of CSGalNAcT-1 in stromal cells. There were significant correlation between CSGalNAcT-1 WAI in stromal cells with patients' age, histological grade and mitotic index (Table 4.9).

Table 4.6 Correlation of clinicopathological parameters of malignant IDC with CSGalNAcT-1 immunoreactivity score (IRS) of stromal cells. No significant correlation was found.

Clinicopathological parameters		Immunoreactivity score (IRS)				P-value
		≤50	>50	Valid cases (%)	Missing cases (%)	
		Number of cases (%)	Number of cases (%)			
Age	≤50	66 (86.8%)	10 (13.2%)	192 (99%)	1 (1%)	0.482
	>50	105 (90.5%)	11 (9.5%)			
Race	Chinese	113 (89%)	14 (11%)	153 (78.9%)	40 (21.1%)	0.694
	Malay	9 (81.8%)	2 (18.2%)			
	Indian	7 (100%)	0			
	Others	7 (87.5%)	1 (12.5%)			
Tumor size	≤30mm	90 (86.5%)	14 (13.5%)	189 (97.4%)	4 (2.6%)	0.234
	>30mm	79 (92.9%)	6 (7.1%)			
Histological grade	Grade 1 and 2	80 (89.9%)	9 (10.1%)	185 (95.4%)	8 (4.6%)	0.768

	Grade 3	85 (88.5%)	11 (11.5%)			
Staging	Stage 1 and 2	85 (85%)	15 (15%)	111 (57.2%)	82 (42.8%)	0.534
	Stage 3	10 (90.9%)	1 (9.1%)			
DCIS nuclear grade	None and low	60 (89.6%)	7 (10.4%)	174 (89.7%)	19 (10.3%)	0.814
	Intermediate and high	97 (90.7%)	10 (9.3%)			
Lymph node involvement	Negative	72 (87.8%)	10 (12.2%)	136 (70.1%)	57 (29.9%)	1.000
	Positive	48 (88.9%)	6 (11.1%)			
Lymph node stage	1-9 LN metastasis	127 (91.4%)	12 (8.6%)	180 (92.8%)	13 (7.2%)	0.187
	10 and above LN metastasis	34 (82.9%)	7 (17.1%)			
ER	Negative	87 (88.8%)	11 (11.2%)	181 (93.3%)	12 (6.7%)	0.811
	Positive	75 (90.4%)	8 (9.6%)			
PR	Negative	72 (91.1%)	7 (8.9%)	180 (92.8%)	13 (7.2%)	0.628
	Positive	89 (88.1%)	12 (11.9%)			
HER2	Negative	111 (88.1%)	15 (11.9%)	170 (87.6%)	23 (12.4%)	0.784
	Positive	40 (90.9%)	4 (9.1%)			
BloomRichardson	≤5	10 (100%)	0	111 (57.2%)	82 (42.8%)	0.595
	>5	91 (90.1%)	10 (9.9%)			
Mitotic index	Grade 1 and 2	60 (92.3%)	5 (7.7%)	123 (63.4%)	70 (36.6%)	0.851
	Grade 3	53 (91.4%)	5 (8.6%)			
Nuclear pleomorphism	Grade 1 and 2	56 (93.3%)	4 (6.7%)	123 (63.4%)	70 (36.6%)	0.560
	Grade 3	57 (90.5%)	6 (9.5%)			
Tumor tubule formation	Score 1 and 2	38 (90.5%)	4 (9.5%)	123 (63.4%)	70 (36.6%)	0.694
	Score 3	75 (92.6%)	6 (7.4%)			

Table 4.7 Correlation of clinicopathological parameters of malignant IDC with CSGalNAcT-1 total percentage score (TPS) of stromal cells. No significant correlation was found.

Clinicopathological parameters		Total percentage score (TPS)				P-value
		≤50	>50	Valid cases (%)	Missing cases (%)	
		Number of cases (%)	Number of cases (%)			
Age	≤50	66 (86.8%)	10 (13.2%)	192 (99%)	1 (1%)	0.482
	>50	105 (90.5%)	11 (9.5%)			
Race	Chinese	113 (89%)	14 (11%)	153 (78.9%)	40 (21.1%)	0.694
	Malay	9 (81.8%)	2 (18.2%)			
	Indian	7 (100%)	0			
	Others	7 (87.5%)	1 (12.5%)			
Tumor size	≤30mm	90 (86.5%)	14 (13.5%)	189 (97.4%)	4 (2.6%)	0.234
	>30mm	79 (92.9%)	6 (7.1%)			
Histological grade	Grade 1 and 2	80 (89.9%)	9 (10.1%)	185 (95.4%)	8 (4.6%)	0.768
	Grade 3	85 (88.5%)	11 (11.5%)			
Staging	Stage 1 and 2	85 (85%)	15 (15%)	111 (57.2%)	82 (42.8%)	0.534
	Stage 3	10 (90.9%)	1 (9.1%)			
DCIS nuclear grade	None and low	60 (89.6%)	7 (10.4%)	174 (89.7%)	19 (10.3%)	0.814
	Intermediate and high	97 (90.7%)	10 (9.3%)			
Lymph node involvement	Negative	72 (87.8%)	10 (12.2%)	136 (70.1%)	57 (29.9%)	1.000
	Positive	48 (88.9%)	6 (11.1%)			
Lymph node stage	1-9 LN metastasis	127 (91.4%)	12 (8.6%)	180 (92.8%)	13 (7.2%)	0.187
	10 and above LN	34 (82.9%)	7 (17.1%)			

	metastasis					
ER	Negative	87 (88.8%)	11 (11.2%)	181 (93.3%)	12 (6.7%)	0.811
	Positive	75 (90.4%)	8 (9.6%)			
PR	Negative	72 (91.1%)	7 (8.9%)	180 (92.8%)	13 (7.2%)	0.628
	Positive	89 (88.1%)	12 (11.9%)			
HER2	Negative	111 (88.1%)	15 (11.9%)	170 (87.6%)	23 (12.4%)	0.784
	Positive	40 (90.9%)	4 (9.1%)			
BloomRichardson	≤5	10 (100%)	0	111 (57.2%)	82 (42.8%)	0.595
	>5	91 (90.1%)	10 (9.9%)			
Mitotic index	Grade 1 and 2	60 (92.3%)	5 (7.7%)	123 (63.4%)	70 (36.6%)	0.851
	Grade 3	53 (91.4%)	5 (8.6%)			
Nuclear pleomorphism	Grade 1 and 2	56 (93.3%)	4 (6.7%)	123 (63.4%)	70 (36.6%)	0.560
	Grade 3	57 (90.5%)	6 (9.5%)			
Tumor tubule formation	Score 1 and 2	38 (90.5%)	4 (9.5%)	123 (63.4%)	70 (36.6%)	0.694
	Score 3	75 (92.6%)	6 (7.4%)			

Table 4.8 Correlation of clinicopathological parameters of malignant IDC with CSGalNAcT-1 weighted average intensity (WAI) of stromal cells. P-value with asterisk represents statistically significant results.

Clinicopathological parameters		Weighted average intensity (WAI)				P-value
		≤0.90	>0.90	Valid cases (%)	Missing cases (%)	
		Number of cases (%)	Number of cases (%)			
Age	≤50	29 (38.2%)	47 (61.8%)	192 (99%)	1 (1%)	**0.004***
	>50	22 (19%)	94 (81%)			
Race	Chinese, Malay and Indian	37 (25.5%)	108 (74.5%)	153 (78.9%)	40 (21.1%)	**0.007***
	Others	6 (75%)	2 (25%)			
Tumor size	≤30mm	25 (24%)	79 (76%)	189 (97.4%)	4 (2.6%)	0.328
	>30mm	26 (30.6%)	59 (69.4%)			
Histological grade	Grade 1 and 2	17 (19.1%)	72 (80.9%)	185 (95.4%)	8 (4.6%)	**0.025***
	Grade 3	32 (33.3%)	64 (66.7%)			
Staging	Stage 1 and 2	12 (12%)	88 (88%)	111 (57.2%)	82 (42.8%)	0.287
	Stage 3	3 (27.3%)	8 (72.7%)			
DCIS nuclear grade	None and low	15 (22.4%)	52 (77.6%)	174 (89.7%)	19 (10.3%)	0.328
	Intermediate and high	31 (29%)	76 (71%)			
Lymph node involvement	Negative	17 (20.7%)	65 (79.3%)	136 (70.1%)	57 (29.9%)	0.834
	Positive	12 (22.2%)	42 (77.8%)			
Lymph node stage	1-9 LN metastasis	38 (27.3%)	101 (72.7%)	180 (92.8%)	13 (7.2%)	0.146
	10 and above LN metastasis	7 (17.1%)	34 (82.9%)			

ER	Negative	23 (23.5%)	75 (76.5%)	181 (93.3%)	12 (6.7%)	0.245
	Positive	26 (31.3%)	57 (68.7%)			
PR	Negative	21 (26.6%)	58 (73.4%)	180 (92.8%)	13 (7.2%)	1.000
	Positive	27 (26.7%)	74 (73.3%)			
HER2	Negative	32 (25.4%)	94 (74.6%)	170 (87.6%)	23 (12.4%)	0.177
	Positive	16 (36.4%)	28 (63.6%)			
BloomRichardson	≤5	3 (30%)	7 (70%)	111 (57.2%)	82 (42.8%)	0.691
	>5	22 (21.8%)	79 (78.2%)			
Mitotic index	Grade 1 and 2	14 (21.5%)	51 (78.5%)	123 (63.4%)	70 (36.6%)	**0.027***
	Grade 3	23 (39.7%)	35 (60.3%)			
Nuclear pleomorphism	Grade 1 and 2	14 (23.3%)	46 (76.7%)	123 (63.4%)	70 (36.6%)	0.106
	Grade 3	23 (36.5%)	40 (63.5%)			
Tumor tubule formation	Score 1 and 2	9 (21.4%)	33 (78.6%)	123 (63.4%)	70 (36.6%)	0.113
	Score 3	28 (34.6%)	53 (65.4%)			

Table 4.9 Summary of statistically significant correlation between CSGalNAcT-1 WAI in stromal cells and clinicopathological parameters.

Immunoscores	Parameters	Remarks
WAI 0.90	Race	Higher expression was found in Chinese, Malay and Indian
	Age cut off at 50	WAI increases with age
	Histological grade	Higher expression – lower histological grade
	Mitotic index	Higher expression – lower mitotic index

4.5.3. Diffuse stroma

CSGalNAcT-1 expression was located in IDC diffuse stroma. The following tables show the correlation between clinicopathological parameters

and and IRS (Table 4.10), TPS (Table 4.11), and WAI (Table 4.12) of CSGalNAcT-1 in diffuse stroma.

Table 4.10 Correlation of clinicopathological parameters of malignant IDC with CSGalNAcT-1 immunoreactivity score (IRS) of diffuse stroma. No significant correlation was found.

Clinicopathological parameters		Immunoreactivity score (IRS)				P-value
		≤100	>100	Valid cases (%)	Missing cases (%)	
		Number of cases (%)	Number of cases (%)			
Age	≤50	74 (97.4%)	2 (2.6%)	192 (99%)	1 (1%)	0.649
	>50	114 (98.3%)	2 (1.7%)			
Race	Chinese	125 (98.4%)	2 (1.6%)	153 (78.9%)	40 (21.1%)	0.347
	Malay	10 (90.9%)	1 (9.1%)			
	Indian	7 (100%)	0			
	Others	8 (100%)	0			
Tumor size	≤30mm	103 (99%)	1 (1%)	189 (97.4%)	4 (2.6%)	0.328
	>30mm	82 (96.5%)	3 (3.5%)			
Histological grade	Grade 1 and 2	89 (100%)	0	185 (95.4%)	8 (4.6%)	0.153
	Grade 3	94 (97.9%)	2 (2.1%)			
Staging	Stage 1 and 2	98 (98%)	2 (2%)	111 (57.2%)	82 (42.8%)	0.179

	Stage 3	11 (100%)	0			
DCIS nuclear grade	None and low	66 (98.5%)	1 (1.5%)	174 (89.7%)	19 (10.3%)	0.750
	Intermediate and high	106 (99.1%)	1 (0.9%)			
Lymph node involvement	Negative	80 (97.6%)	2 (2.4%)	136 (70.1%)	57 (29.9%)	0.518
	Positive	54 (100%)	0			
Lymph node stage	1-9 LN metastasis	136 (97.8%)	3 (2.2%)	180 (92.8%)	13 (7.2%)	0.917
	10 and above LN metastasis	40 (97.6%)	1 (2.4%)			
ER	Negative	98 (100%)	0	181 (93.3%)	12 (6.7%)	0.209
	Positive	81 (97.6%)	2 (2.4%)			
PR	Negative	79 (100%)	0	180 (92.8%)	13 (7.2%)	0.505
	Positive	99 (98%)	2 (2%)			
HER2	Negative	124 (98.4%)	2 (1.6%)	170 (87.6%)	23 (12.4%)	0.276
	Positive	42 (95.5%)	2 (4.5%)			
BloomRichardson	≤5	10 (100%)	0	111 (57.2%)	82 (42.8%)	1.000
	>5	99 (98%)	2 (2%)			
Mitotic index	Grade 1 and 2	64 (98.5%)	1 (1.5%)	123 (63.4%)	70 (36.6%)	0.935
	Grade 3	57 (98.3%)	1 (1.7%)			
Nuclear pleomorphism	Grade 1 and 2	58 (96.7%)	2 (3.3%)	123 (63.4%)	70 (36.6%)	0.150
	Grade 3	63 (100%)	0			
Tumor tubule formation	Score 1 and 2	42 (100%)	0	123 (63.4%)	70 (36.6%)	0.154
	Score 3	79 (97.5%)	2 (2.5%)			

Table 4.11 Correlation of clinicopathological parameters of malignant IDC with CSGalNAcT-1 total percentage score (TPS) of diffuse stroma. No significant correlation was found.

Clinicopathological parameters		Total percentage score (TPS)				P-value
		≤20	>20	Valid cases (%)	Missing cases (%)	
		Number of cases (%)	Number of cases (%)			
Age	≤50	41 (53.9%)	35 (46.1%)	192 (99%)	1 (1%)	0.464
	>50	56 (48.3%)	60 (51.7%)			
Race	Chinese	60 (47.2%)	67 (52.8%)	153 (78.9%)	40 (21.1%)	0.464
	Malay	6 (54.5%)	5 (45.5%)			
	Indian	3 (42.9%)	4 (57.1%)			
	Others	6 (75%)	2 (25%)			
Tumor size	≤30mm	52 (50%)	52 (50%)	189 (97.4%)	4 (2.6%)	1.000
	>30mm	43 (50.6%)	42 (49.4%)			
Histological grade	Grade 1 and 2	44 (49.4%)	45 (50.6%)	185 (95.4%)	8 (4.6%)	0.827
	Grade 3	49 (51%)	47 (49%)			
Staging	Stage 1 and 2	41 (41%)	59 (59%)	111 (57.2%)	82 (42.8%)	0.763
	Stage 3	4 (36.4%)	7 (63.6%)			
DCIS nuclear grade	None and low	38 (56.7%)	29 (43.3%)	174 (89.7%)	19 (10.3%)	0.197
	Intermediate and high	50 (46.7%)	57 (53.3%)			
Lymph node involvement	Negative	35 (42.7%)	47 (57.3%)	136 (70.1%)	57 (29.9%)	0.726
	Positive	25 (46.3%)	29 (53.7%)			
Lymph node stage	1-9 LN metastasis	68 (48.9%)	71 (51.1%)	180 (92.8%)	13 (7.2%)	0.987
	10 and above LN	20 (48.8%)	21 (51.2%)			

	metastasis					
ER	Negative	53 (54.1%)	45 (45.9%)	181 (93.3%)	12 (6.7%)	0.458
	Positive	40 (48.2%)	43 (51.8%)			
PR	Negative	39 (49.4%)	40 (50.6%)	180 (92.8%)	13 (7.2%)	0.764
	Positive	53 (52.5%)	48 (47.5%)			
HER2	Negative	64 (50.8%)	62 (49.2%)	170 (87.6%)	23 (12.4%)	1.000
	Positive	22 (50%)	22 (50%)			
BloomRichardson	≤5	3 (30%)	7 (70%)	111 (57.2%)	82 (42.8%)	0.507
	>5	47 (46.5%)	54 (53.5%)			
Mitotic index	Grade 1 and 2	31 (47.7%)	34 (52.3%)	123 (63.4%)	70 (36.6%)	0.523
	Grade 3	31 (53.4%)	27 (46.6%)			
Nuclear pleomorphism	Grade 1 and 2	26 (43.3%)	34 (56.7%)	123 (63.4%)	70 (36.6%)	0.122
	Grade 3	36 (57.1%)	27 (42.9%)			
Tumor tubule formation	Score 1 and 2	19 (45.2%)	23 (54.8%)	123 (63.4%)	70 (36.6%)	0.408
	Score 3	43 (53.1%)	38 (46.9%)			

Table 4.12 Correlation of clinicopathological parameters of malignant IDC with CSGalNAcT-1 weighted average intensity (WAI) of diffuse stroma. No significant correlation was found.

Clinicopathological parameters		Weighted average intensity (WAI)				P-value
		≤1.0	>1.0	Valid cases (%)	Missing cases (%)	
		Number of cases (%)	Number of cases (%)			
Age	≤50	74 (97.4%)	2 (2.6%)	191 (98.5%)	2 (1.5%)	1.000
	>50	112 (97.4%)	3 (2.6%)			
Race	Chinese	124 (98.4%)	2 (1.6%)	152 (78.4%)	41 (21.6%)	0.351
	Malay	10 (90.9%)	1 (9.1%)			
	Indian	7 (100%)	0 (0%)			
	Others	8 (100%)	0			
Tumor size	≤30mm	103 (99%)	1 (1%)	188 (96.9%)	5 (3.1%)	0.174
	>30mm	80 (95.2%)	4 (4.8%)			
Histological grade	Grade 1 and 2	88 (100%)	0	184 (94.8%)	9 (5.2%)	0.078
	Grade 3	93 (96.9%)	3 (3.1%)			
Staging	Stage 1 and 2	98 (98%)	2 (2%)	110 (57.2%)	83 (43.3%)	0.183
	Stage 3	10 (100%)	0			
DCIS nuclear grade	None and low	66 (98.5%)	1 (1.5%)	173 (89.2%)	21 (10.8%)	0.843
	Intermediate and high	104 (98.1%)	2 (1.9%)			
Lymph node involvement	Negative	35 (42.7%)	47 (57.3%)	135 (69.6%)	58 (30.4%)	0.726
	Positive	25 (46.3%)	29 (53.7%)			
Lymph node stage	1-9 LN metastasis	79 (97.5%)	2 (2.5%)	179 (92.3%)	14 (7.7%)	0.516
	10 and above LN	54 (100%)	0			

	metastasis					
ER	Negative	98 (100%)	0	180 (92.8%)	13 (7.2%)	0.093
	Positive	79 (96.3%)	3 (3.7%)			
PR	Negative	78 (98.7%)	1 (1.3%)	179 (92.3%)	14 (7.7%)	1.000
	Positive	98 (98%)	2 (2%)			
HER2	Negative	123 (97.6%)	3 (2.4%)	170 (87.6%)	23 (12.4%)	0.605
	Positive	42 (95.5%)	2 (4.5%)			
BloomRichardson	≤5	10 (100%)	0	110 (56.7%)	83 (43.3%)	1.000
	>5	98 (98%)	2 (2%)			
Mitotic index	Grade 1 and 2	64 (98.5%)	1 (1.5%)	122 (62.9%)	71 (37.1%)	0.926
	Grade 3	56 (98.2%)	1 (1.8%)			
Nuclear pleomorphism	Grade 1 and 2	57 (96.6%)	2 (3.4%)	122 (62.9%)	71 (37.1%)	0.150
	Grade 3	63 (100%)	0			
Tumor tubule formation	Score 1 and 2	41 (100%)	0	122 (62.9%)	71 (37.1%)	0.154
	Score 3	79 (97.5%)	2 (2.5%)			

Immunoscores of CSGalNAcT-1 in epithelial cells, stromal cells and diffuse stroma were associated with clinicopathological parameters. Significant associations were only found in stromal cells between WAI and race, age cut off at 50, histological grade and mitotic index, as summarized in Table 4.9. Higher expression of CSGalNAcT-1 was found generally in older population; and in Chinese, Malay and Indian as compared to races of other kinds. On the other hand, stronger CSGalNAcT-1 expression was significantly associated to lower histological grade and mitotic index.

4.6. Multivariate analysis in breast IDC

By considering the presence and effect of other parameters simultaneously, multivariate test was performed to search for further meaningful and more in depth association in breast IDC cases. From Table 4.13, it shows that in the case of CSGalNAcT-1 staining in stromal cells, race of Chinese, Malay and Indian once again significantly correlated with CSGalNAcT-1 immunoscore WAI 0.90 after adjusting for age, histological grade, and mitotic index. Hence it can be interpreted that race may affect the expression pattern of CSGalNAcT-1 in stromal cells.

Table 4.13 Multivariate analysis for association of multiple clinicopathological parameters and CSGalNAcT-1 staining in stromal cells. P-value with asterisk represents statistically significant results, after adjusting confounders (parameters).

Dependent variable	P-value	Clinicopathological parameters	Total number of cases	Standardized coefficients (Beta)	P-value for standardized coefficient (Beta)
WAI 0.90	0.018*	Race Chinese, Malay and Indian vs Others	153	-0.196	0.028*
		Histological grade Grade 1 and 2 vs Grade 3	185	-0.054	0.621
		Mitotic index Grade 1 and 2 vs Grade 3	123	-0.125	0.252
		Age ≤50 vs >50	192	0.159	0.074

4.7.   Survival and tumor recurrence data for survival analysis

In this survival analysis, the data was available in 186 out of 193 cases and the

patients' follow-up period ranged from 0.5 month to 134.47 months. The three

timelines that were used to measure the mortality and recurrence of IDC

patients are overall survival (OS), disease free survival (DFS), and survival

after recurrence (SAR). Figure 4.4 illustrates the interpretation of these three

parameters. Table 4.14 shows that death from breast cancer occurred in 25

patients and 44 patients had tumor recurrence, of which six death from

recurrence were reported. The remaining cases were censored cases, indicating

no tumor recurrence and death was found at the end of follow-up period.
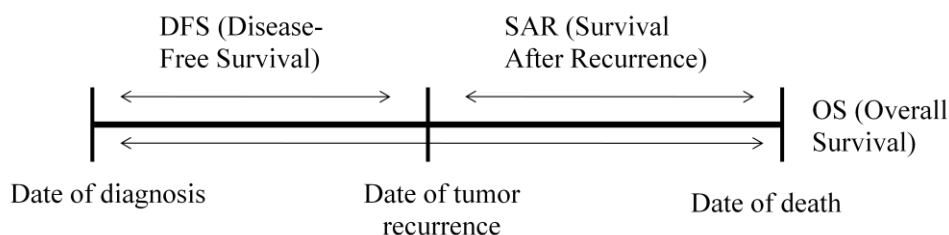
Figure 4.4 The interpretation of overall survival (OS), disease free survival
(DFS), and survival after recurrence (SAR) based on the date of diagnosis,
date of tumor recurrence and date of death.

Table 4.14 Descriptive statistics of OS, DFS and SAR in terms of mean,
median and range of period in malignant IDC. The unit used is in month.

	OS	DFS	SAR
Number of cases	186	186	186
Missing cases	7	7	7
Number of events	25	44	6
Mean (months)	39.9412	41.4177	17.43
Median (months)	31.27	34.615	15.75
Range (months)	4.90 to 104.53	4.90 to 111.90	1.16o 48.72

4.8.   Timeline analysis of mortality due to disease in patients with breast

invasive ductal carcinoma

Mortality due to breast IDC is investigated for any correlation with the

immunoscores of CSGalNAcT-1 using Kaplan-Meier analysis. The timelines

that were investigated were overall survival (OS) and survival after recurrence

(SAR). In summary, Table 4.15 and 4.20 show that there was no significant

correlation between CSGalNAcT-1 immunoscoring with the mortality of

patients in terms of overall survival (OS) and survival after recurrence (SAR)

in Kaplan-Meier analysis.

4.8.1.   Overall survival (OS)

Table   4.15   Summary   of   the   correlation   between   CSGalNAcT-1
immunohistochemical staining and mortality in breast IDCs. There is no
significant correlation.

Epithelial cells			
Parameters	IRS 150	TP 90	WAI 1.70
Log Rank (Mantel-Cox)	0.588	0.952	0.668
Stromal cells			
Parameters	IRS 50	TP 50	WAI 0.90
Log Rank (Mantel-Cox)	0.986	0.986	0.440
Diffuse stroma			
Parameters	IRS 100	TP 20	WAI 1.0
Log Rank (Mantel-Cox)	0.351	0.479	0.354

To exclude the confounding effect from the other clinicopathological

parameters, survival analysis was carried out for different patient sub-strata.

This was done for every stained component, i.e. epithelial cells, stromal cells,

and diffuse stroma, with timeline OS for the mortality data. The data was

presented in Table 4.16 to Table 4.18 Significant correlation was found

between IRS and WAI of CSGalNAcT-1 in diffuse stroma and patients who are ER positive, and have no lymph node involvement. The summary of the significant correlation is presented in Table 4.19 and results were presented in Kaplan-Meier graphs in Figure 4.5 to 4.8.

4.8.1.1. Epithelial cells

Table 4.16 Summary of the correlation between CSGalNAcT-1 epithelial cells immunohistochemical staining (IRS, TPS, WAI) and mortality in every stratum of parameters in breast IDC. There is no significant correlation.

Clinicopathological parameters	Stratum	Immunoscoring		
		IRS 150	TPS 90	WAI 1.70
		P-value		
Age	≤50	0.572	0.935	0.508
	>50	0.115	0.847	0.354
Tumor size	≤30 mm	0.701	0.544	0.582
	>30mm	0.285	0.983	0.512
Histological grade	Grade 1 and 2	0.636	0.302	0.398
	Grade 3	0.191	0.569	0.088
Staging	Stage 1 and 2	0.484	0.846	0.881
	Stage 3	NA	0.400	0.074
DCIS grade	None and low	0.159	0.620	0.053
	Intermediate and high	0.614	0.347	0.369
Lymph node involvement	Negative	0.560	0.938	0.305
	Positive	0.183	0.913	0.050
Lymph node stage	1-9 LN metastasis	0.204	0.508	0.221
	10 and above LN metastasis	0.570	0.399	0.409
ER	Negative	0.142	0.698	0.235
	Positive	0.549	0.511	0.380
PR	Negative	0.060	0.841	0.183
	Positive	0.401	0.799	0.784
HER2	Negative	0.189	0.827	0.833
	Positive	0.713	0.521	0.713
BloomRichardson score	≤5	NA	0.063	NA
	>5	NA	0.455	0.753
Mitotic index	Grade 1 and 2	NA	0.431	0.563
	Grade 3	NA	0.470	0.090
Nuclear pleomorphism	Grade 1 and 2	NA	0.545	0.528
	Grade 3	NA	0.563	0.247

Tubule formation	Score 1 and 2	NA	0.895	0.500
	Score 3	NA	0.905	0.705

4.8.1.2. Stromal cells

Table 4.17 Summary of the correlation between CSGalNAcT-1 stromal cells immunohistochemical staining (IRS, TPS, WAI) and mortality in every stratum of parameters in breast IDC. There is no significant correlation.

Clinicopathological parameters	Stratum	Immunoscoring		
		IRS 50	TPS 50	WAI 0.90
		P-value		
Age	≤50	0.927	0.927	0.760
	>50	0.903	0.903	0.590
Tumor size	≤30 mm	0.857	0.857	0.197
	>30mm	0.683	0.683	0.886
Histological grade	Grade 1 and 2	0.885	0.885	0.212
	Grade 3	0.902	0.902	0.579
Staging	Stage 1 and 2	0.955	0.955	0.609
	Stage 3	0.074	0.074	0.442
DCIS grade	None and low	0.751	0.751	0.379
	Intermediate and high	0.901	0.901	0.729
Lymph node involvement	Negative	0.808	0.808	0.507
	Positive	0.637	0.637	0.859
Lymph node stage	1-9 LN metastasis	0.548	0.548	0.110
	10 and above LN metastasis	0.494	0.494	0.207
ER	Negative	0.390	0.390	0.548
	Positive	0.271	0.271	0.166
PR	Negative	0.145	0.145	0.477
	Positive	0.381	0.381	0.215
HER2	Negative	0.670	0.670	0.347
	Positive	0.589	0.589	0.495
BloomRichardson score	≤5	NA	NA	0.513
	>5	0.594	0.594	0.789
Mitotic index	Grade 1 and 2	0.447	0.447	0.272
	Grade 3	0.830	0.830	0.971
Nuclear pleomorphism	Grade 1 and 2	0.416	0.416	0.205
	Grade 3	0.921	0.921	0.547
Tubule formation	Score 1 and 2	0.669	0.669	0.951
	Score 3	0.334	0.334	0.712

4.8.1.3. Diffuse stroma

Table 4.18 Summary of the correlation between CSGalNAcT-1 diffuse stroma immunohistochemical staining (IRS, TPS, WAI) and mortality in every stratum of parameters in breast IDC. P-value with asterisk represents statistically significant results.

Clinicopathological parameters	Stratum	Immunoscoring		
		IRS 100	TPS 20	WAI 1.0
		P-value		
Age	≤50	0.738	0.052	0.738
	>50	0.192	0.505	0.197
Tumor size	≤30 mm	NA	0.444	NA
	>30mm	0.667	0.816	0.679
Histological grade	Grade 1 and 2	NA	0.598	NA
	Grade 3	0.513	0.845	0.513
Staging	Stage 1 and 2	0.064	0.751	0.064
	Stage 3	NA	0.279	NA
DCIS grade	None and low	0.680	0.669	0.680
	Intermediate and high	0.723	0.779	0.721
Lymph node involvement	Negative	**0.042***	0.455	**0.044***
	Positive	NA	0.923	NA
Lymph node stage	1-9 LN metastasis	0.606	0.988	0.606
	10 and above LN metastasis	0.065	0.248	0.066
ER	Negative	NA	0.965	NA
	Positive	**0.017***	0.133	**0.018***
PR	Negative	NA	0.471	NA
	Positive	0.059	0.088	0.061
HER2	Negative	0.080	0.895	0.066
	Positive	0.713	0.193	0.713
BloomRichardson score	≤5	NA	0.127	NA
	>5	0.558	0.395	0.556
Mitotic index	Grade 1 and 2	0.743	0.552	0.743
	Grade 3	0.587	0.771	0.583
Nuclear pleomorphism	Grade 1 and 2	0.573	0.361	0.570
	Grade 3	NA	0.973	NA
Tubule formation	Score 1 and 2	NA	0.052	NA
	Score 3	0.573	0.290	0.573

Table 4.19 Summary of significant correlation between CSGalNAcT-1 immunostaining IRS and WAI in diffuse stroma and mortality in breast IDCs for clinicopathological parameters stratum.

Components	Immunoscores	Parameters	Stratum	Log Rank (Mantel-Cox)
Diffuse stroma	IRS 100	Lymph node involvement	No	0.042 (Patients with no lymph node involvement and low IRS have better survival)
		ER	Positive	0.017 (Patients with ER positive and low IRS have better survival)
	WAI 1.0	Lymph node involvement	No	0.044 (Patients with no lymph node involvement and low WAI have better survival)
		ER	Positive	0.018 (Patients with ER positive and low WAI have better survival)

Survival Functions

Lymph node involvement= No

P-value= 0.042*

Overall Survival (OS)
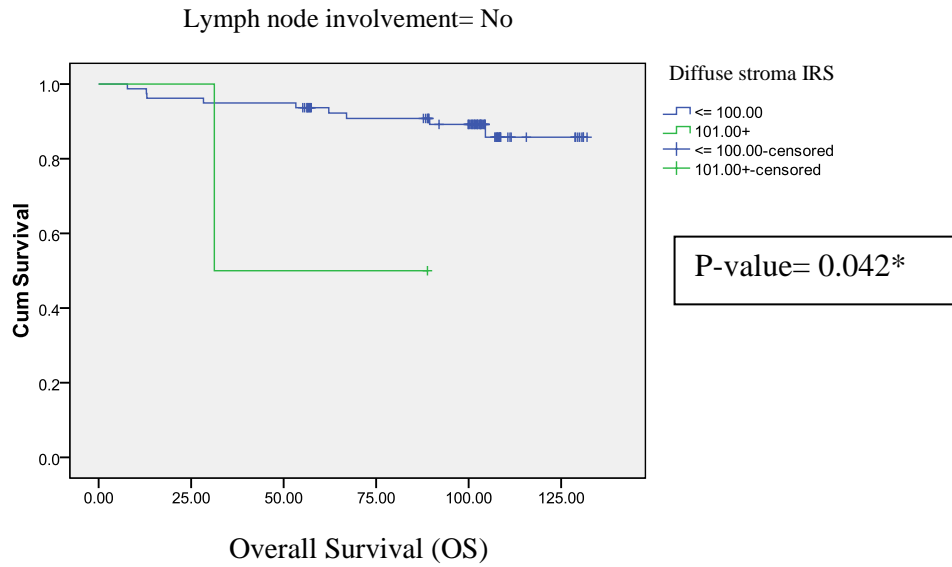
Figure 4.5 This is the Kaplan-Meier curve where the X-axis shows the OS timeline follow-up in months. Y-axis shows the proportion of patients who are still alive. Blue line shows diffuse stroma IRS staining ≤100; while green line is IRS staining >100. The curve shows the significance of mortality in patients with no lymph node involvement and low diffuse stroma IRS score (≤100), i.e. patients with no lymph node involvement and low IRS score have better survival.

Survival Functions

Estrogen receptor= Positive
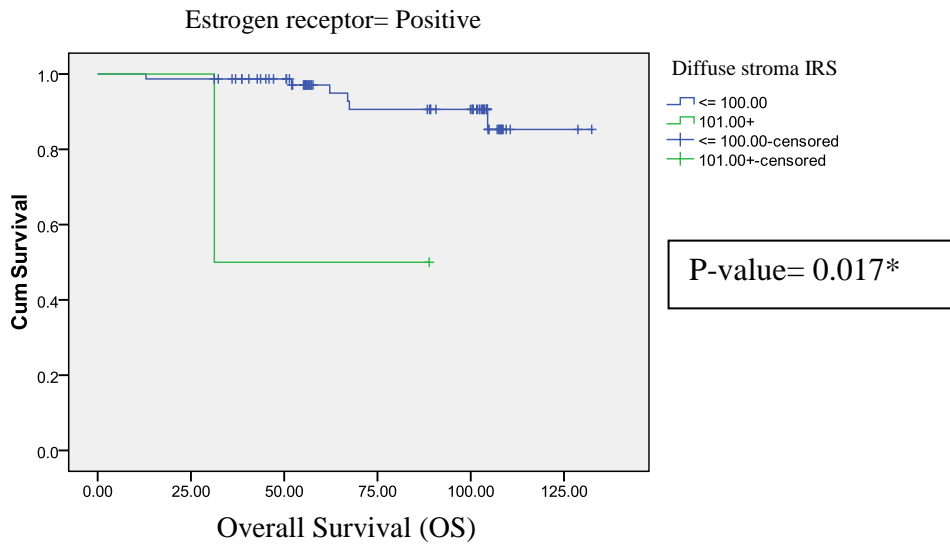
Figure 4.6 This is the Kaplan-Meier curve where the X-axis shows the OS timeline follow-up in months. Y-axis shows the proportion of patients who are still alive. Blue line shows diffuse stroma IRS staining ≤100; while green line is IRS staining >100. The curve shows the significance of mortality in patients with ER positive and low diffuse stroma IRS score (≤100), i.e. patients with ER positive and low IRS score have better survival.

Survival Functions

Lymph node involvement= No
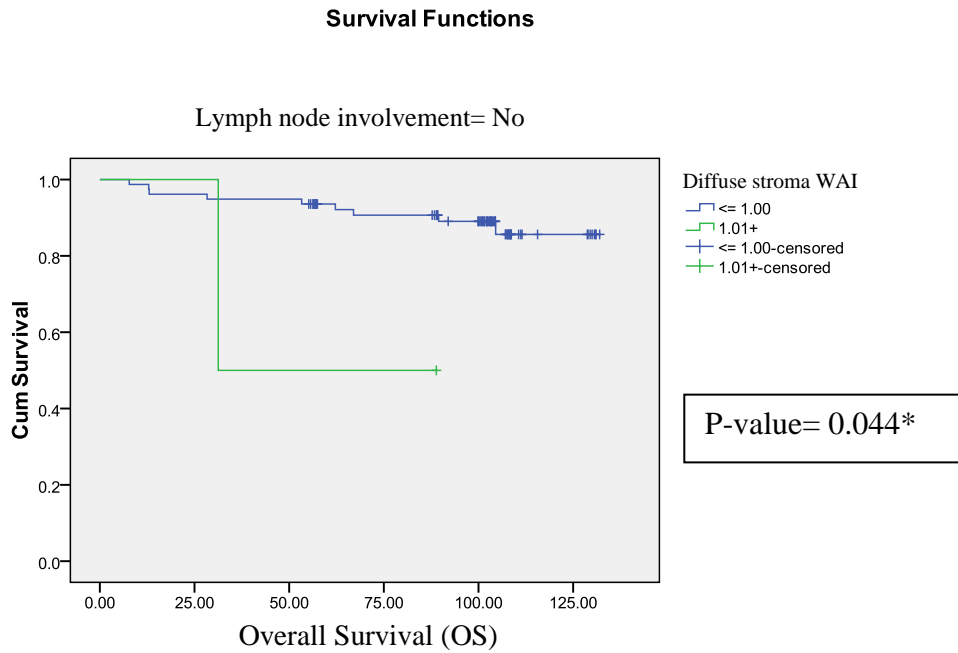
Figure 4.7 This is the Kaplan-Meier curve where the X-axis shows the OS timeline follow-up in months. Y-axis shows the proportion of patients who are still alive. Blue line shows diffuse stroma WAI staining ≤1.00; while green line is WAI staining >1.00. The curve shows the significance of mortality in patients with no lymph node involvement and low diffuse stroma WAI score (≤1.00), i.e. patients with no lymph node involvement and low WAI score have better survival.

Survival Functions

Estrogen receptor= Positive
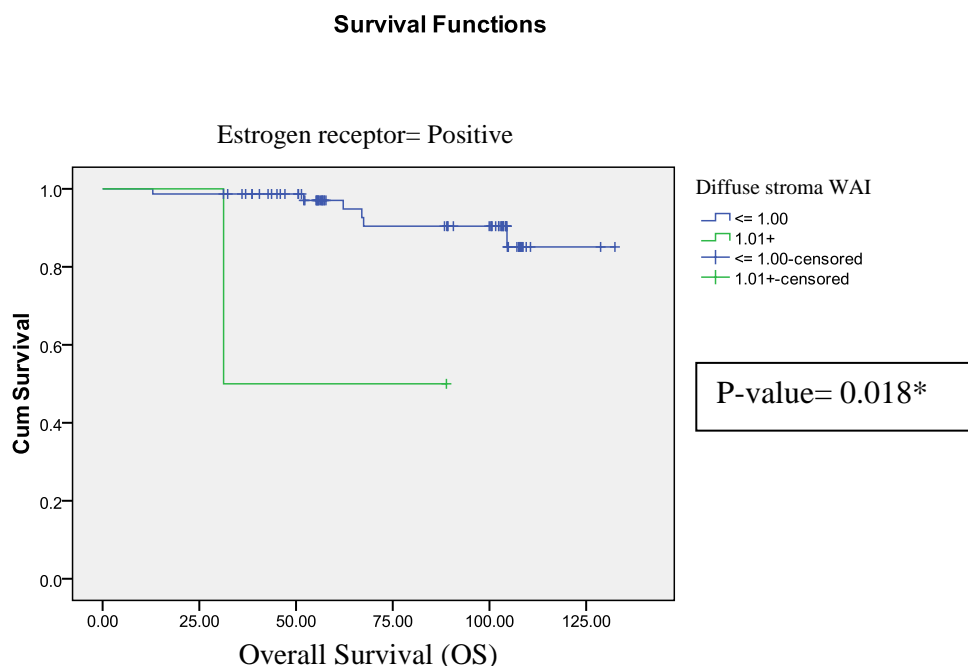
Figure 4.8 This is the Kaplan-Meier curve where the X-axis shows the OS timeline follow-up in months. Y-axis shows the proportion of patients who are still alive. Blue line shows diffuse stroma WAI staining ≤1.00; while green line is WAI staining >1.00. The curve shows the significance of mortality in patients with ER positive and low diffuse stroma WAI score (≤1.00), i.e. patients with ER positive and low WAI score have better survival.

4.8.2. Survival after recurrence (SAR)

Table 4.20 Summary of the correlation between CSGalNAcT-1 immunohistochemical staining and mortality in breast IDCs. There is no significant correlation.

Epithelial cells			
Parameters	IRS 150	TP 90	WAI 1.70
Log Rank (Mantel-Cox)	0.334	0.914	0.641
Stromal cells			
Parameters	IRS 50	TP 50	WAI 0.90
Log Rank (Mantel-Cox)	0.895	0.895	0.214
Diffuse stroma			
Parameters	IRS 100	TP 20	WAI 1.0
Log Rank (Mantel-Cox)	0.190	0.408	0.192

To exclude the confounding effect from the other clinicopathological parameters, survival analysis was carried out for different patient sub-strata. This was done for every stained component, i.e. epithelial cells, stromal cells, and diffuse stroma, with timeline SAR for the mortality data. The data was presented in Table 4.21 to Table 4.23. Significant relationship was found between immunoscoring of CSGalNAcT-1 in diffuse stroma (IRS) and IDC patients who are ER positive. The summary of the significant correlation is presented in Table 4.24 and the results were presented in Kaplan-Meier graphs in Figure 4.9.

4.8.2.1. Epithelial cells

Table 4.21 Summary of the correlation between CSGalNAcT-1 epithelial cells immunohistochemical staining (IRS, TPS, WAI) and mortality in every stratum of parameters in breast IDC. There is no significant correlation.

Clinicopathological parameters	Stratum	Immunoscoring		
		IRS 150	TPS 90	WAI 1.70
		P-value		
Age	≤50	0.704	0.742	0.639
	>50	0.117	0.774	0.601
Tumor size	≤30 mm	0.742	0.626	0.638
	>30mm	0.159	0.919	0.524
Histological grade	Grade 1 and 2	0.670	0.319	0.449
	Grade 3	0.074	0.594	0.208
Staging	Stage 1 and 2	0.375	0.968	0.906
	Stage 3	NA	0.400	0.205
DCIS grade	None and low	0.071	0.349	0.234
	Intermediate and high	0.675	0.450	0.459
Lymph node involvement	Negative	0.615	0.924	0.371
	Positive	0.121	0.818	0.558
Lymph node stage	1-9 LN metastasis	0.091	0.184	0.387
	10 and above LN metastasis	0.645	0.343	0.509
ER	Negative	0.136	0.811	0.356
	Positive	0.711	0.988	0.596
PR	Negative	0.062	0.788	0.157

	Positive	0.538	0.994	0.789
HER2	Negative	0.144	0.932	0.529
	Positive	0.752	0.564	0.752
BloomRichardson score	≤5	NA	0.317	NA
	>5	NA	0.547	0.962
Mitotic index	Grade 1 and 2	NA	0.382	0.611
	Grade 3	NA	0.510	0.811
Nuclear pleomorphism	Grade 1 and 2	NA	0.297	0.667
	Grade 3	NA	0.609	0.515
Tubule formation	Score 1 and 2	NA	0.833	0.514
	Score 3	NA	0.658	0.774

4.8.2.2. Stromal cells

Table 4.22 Summary of the correlation between CSGalNAcT-1 stromal cells immunohistochemical staining (IRS, TPS, WAI) and mortality in every stratum of parameters in breast IDC. There is no significant correlation.

Clinicopathological parameters	Stratum	Immunoscoring		
		IRS 50	TPS 50	WAI 0.90
		P-value		
Age	≤50	0.571	0.571	0.542
	>50	0.930	0.930	0.325
Tumor size	≤30 mm	0.953	0.953	0.173
	>30mm	0.663	0.663	0.559
Histological grade	Grade 1 and 2	0.893	0.893	0.143
	Grade 3	0.903	0.903	0.360
Staging	Stage 1 and 2	0.956	0.956	0.813
	Stage 3	0.205	0.205	0.442
DCIS grade	None and low	0.713	0.713	0.282
	Intermediate and high	0.807	0.807	0.380
Lymph node involvement	Negative	0.906	0.906	0.329
	Positive	0.864	0.864	0.964
Lymph node stage	1-9 LN metastasis	0.786	0.786	0.061
	10 and above LN metastasis	0.808	0.808	0.607
ER	Negative	0.493	0.493	0.750
	Positive	0.441	0.441	0.062
PR	Negative	0.075	0.075	0.442
	Positive	0.402	0.402	0.056
HER2	Negative	0.839	0.839	0.278
	Positive	0.647	0.647	0.705
BloomRichardson	≤5	NA	NA	NA

score	>5	0.521	0.521	0.812
Mitotic index	Grade 1 and 2	0.443	0.443	0.152
	Grade 3	0.743	0.743	0.767
Nuclear pleomorphism	Grade 1 and 2	0.476	0.476	0.100
	Grade 3	0.946	0.946	0.776
Tubule formation	Score 1 and 2	0.445	0.445	0.935
	Score 3	0.468	0.468	0.364

4.8.2.3. Diffuse stroma

Table 4.23 Summary of the correlation between CSGalNAcT-1 diffuse stroma immunohistochemical staining (IRS, TPS, WAI) and mortality in every stratum of parameters in breast IDC. P-value with asterisk represents statistically significant results.

Clinicopathological parameters	Stratum	Immunoscoring		
		IRS 100	TPS 20	WAI 1.0
		P-value		
Age	≤50	0.789	0.051	0.789
	>50	0.117	0.698	0.120
Tumor size	≤30 mm	NA	0.415	NA
	>30mm	0.361	0.933	0.368
Histological grade	Grade 1 and 2	NA	0.582	NA
	Grade 3	0.619	0.532	0.619
Staging	Stage 1 and 2	0.081	0.390	0.081
	Stage 3	NA	0.343	NA
DCIS grade	None and low	0.728	0.551	0.728
	Intermediate and high	0.768	0.802	0.767
Lymph node involvement	Negative	0.078	0.453	0.081
	Positive	NA	0.486	NA
Lymph node stage	1-9 LN metastasis	0.683	0.958	0.683
	10 and above LN metastasis	0.080	0.165	0.088
ER	Negative	NA	0.949	NA
	Positive	**0.011***	0.100	0.77
PR	Negative	NA	0.561	NA
	Positive	0.076	0.099	0.079
HER2	Negative	0.074	0.624	0.74
	Positive	0.752	0.143	0.752
BloomRichardson score	≤5	NA	0.317	NA
	>5	0.615	0.514	0.613
Mitotic index	Grade 1 and 2	0.773	0.521	0.773
	Grade 3	0.729	0.674	0.726

Nuclear pleomorphism	Grade 1 and 2	0.667	0.669	0.664
	Grade 3	NA	0.977	NA
Tubule formation	Score 1 and 2	NA	0.082	NA
	Score 3	0.683	0.367	0.683

Table 4.24 Summary of significant correlation between CSGalNAcT-1 immunoscoring IRS in diffuse stroma and mortality in breast IDCs for clinicopathological parameters stratum.

Components	Immunoscores	Parameters	Stratum	Log Rank (Mantel-Cox)
Diffuse stroma	IRS 100	ER	Positive	0.011 (Patients with ER positive and low IRS have better survival)

Survival Functions

Estrogen receptor= Positive

P-value= 0.011*
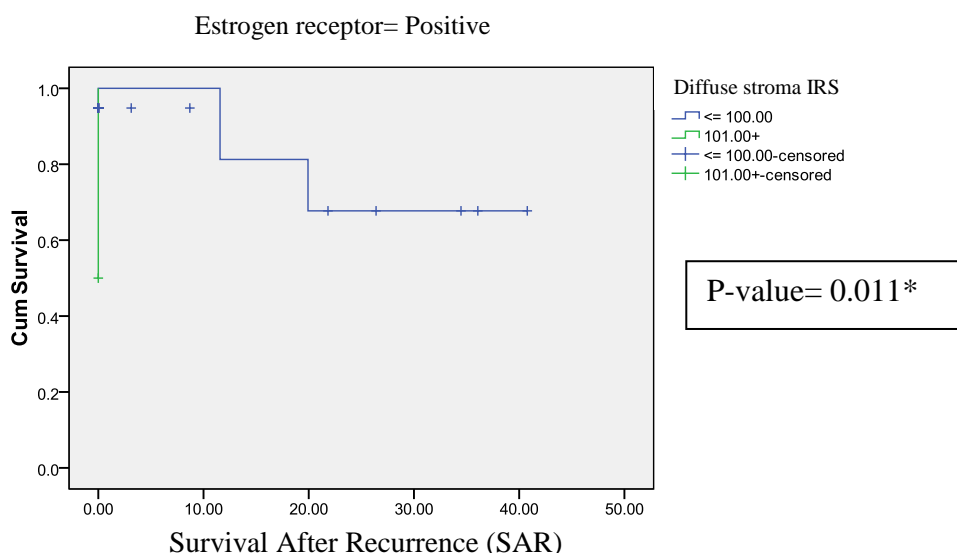
Figure 4.9 This is the Kaplan-Meier curve where the X-axis shows the SAR timeline follow-up in months. Y-axis shows the proportion of patients who are still alive. Blue line shows diffuse stroma IRS staining ≤100; while green line is IRS staining >100. This curve shows the significance of mortality in patients with ER positive and low diffuse stroma IRS score (≤100), i.e. patients with ER positive and low IRS score have better survival.

4.9. Timeline analysis of recurrence of disease in patients with breast invasive

ductal carcinoma

After correlating immunoscores with mortality of IDC, further statistical

analyses using Kaplan-Meier analysis were done to investigate if the

correlation exists in the aspect of tumor recurrence in patients, i.e. whether

increase or decrease in immunoscores contributes to the chances of recurrence

in IDC patients. The timeline disease free survival (DFS) was investigated.

Table 4.25 shows that there was no significant correlation between

CSGalNAcT-1 immunoscoring with the recurrence of breast invasive ductal

carcinoma in patients.

Table 4.25 Summary of the correlation between CSGalNAcT-1 immunohistochemical staining and recurrence in breast IDCs. There is no significant correlation.

Epithelial cells			
Parameters	IRS 150	TP 90	WAI 1.70
Log Rank (Mantel-Cox)	0.956	0.957	0.741
Stromal cells			
Parameters	IRS 50	TP 50	WAI 0.90
Log Rank (Mantel-Cox)	0.801	0.801	0.609
Diffuse stroma			
Parameters	IRS 100	TP 20	WAI 1.0
Log Rank (Mantel-Cox)	0.804	0.406	0.809

To exclude the confounding effect from the other clinicopathological

parameters, survival analysis was carried out for different patient sub-strata.

This was done for every stained component, i.e. epithelial cells, stromal cells,

and diffuse stroma, with DFS for the recurrence data. The data was presented

in Table 4.26 to Table 4.28. Significant correlation was found between

immunoscoring of CSGalNAcT-1 in diffuse stroma (TPS) and patients who

are ER positive, and have lower scoring of tubule formation. The summary of

the significant correlation is presented in Table 4.29 and results were

presented in Kaplan-Meier graphs in Figure 4.10 and 4.11.

4.9.1. Epithelial cells

Table 4.26 Summary of the correlation between CSGalNAcT-1 epithelial cells immunohistochemical staining (IRS, TPS, WAI) and recurrence in every stratum of parameters in breast IDC. There is no significant correlation.

Clinicopathological parameters	Stratum	Immunoscoring		
		IRS 150	TPS 90	WAI 1.70
		P-value		
Age	≤50	0.461	0.675	0.362
	>50	0.336	0.837	0.796
Tumor size	≤30 mm	0.487	0.732	0.353
	>30mm	0.565	0.993	0.922
Histological grade	Grade 1 and 2	0.512	0.562	0.241
	Grade 3	0.426	0.860	0.110
Staging	Stage 1 and 2	0.761	0.899	0.612
	Stage 3	NA	0.737	0.544
DCIS grade	None and low	0.413	0.876	0.103
	Intermediate and high	0.434	0.889	0.196
Lymph node involvement	Negative	0.426	0.975	0.186
	Positive	0.442	0.883	0.143
Lymph node stage	1-9 LN metastasis	0.720	0.839	0.851
	10 and above LN metastasis	0.526	0.764	0.360
ER	Negative	0.345	0.383	0.556
	Positive	0.459	0.341	0.284
PR	Negative	0.070	0.982	0.535
	Positive	0.270	0.983	0.465
HER2	Negative	0.362	0.924	0.889
	Positive	0.403	0.615	0.403
BloomRichardson score	≤5	NA	0.080	NA
	>5	NA	0.673	0.890
Mitotic index	Grade 1 and 2	NA	0.794	0.372
	Grade 3	NA	0.872	0.074
Nuclear pleomorphism	Grade 1 and 2	NA	0.706	0.426
	Grade 3	NA	0.859	0.492
Tubule formation	Score 1 and 2	NA	0.649	0.736
	Score 3	NA	0.665	0.572

4.9.2. Stromal cells

Table 4.27 Summary of the correlation between CSGalNAcT-1 stomal cells immunohistochemical staining (IRS, TPS, WAI) and recurrence in every stratum of parameters in breast IDC. There is no significant correlation.

Clinicopathological parameters	Stratum	Immunoscoring		
		IRS 50	TPS 50	WAI 0.90
		P-value		
Age	≤50	0.682	0.682	0.903
	>50	0.544	0.544	0.456
Tumor size	≤30 mm	0.709	0.709	0.690
	>30mm	0.354	0.354	0.440
Histological grade	Grade 1 and 2	0.725	0.725	0.944
	Grade 3	0.684	0.684	0.979
Staging	Stage 1 and 2	0.591	0.591	0.768
	Stage 3	0.544	0.544	0.320
DCIS grade	None and low	0.317	0.317	0.968
	Intermediate and high	0.766	0.766	0.408
Lymph node involvement	Negative	0.720	0.720	0.626
	Positive	0.872	0.872	0.642
Lymph node stage	1-9 LN metastasis	0.545	0.545	0.888
	10 and above LN metastasis	0.308	0.308	0.123
ER	Negative	0.671	0.671	0.596
	Positive	0.537	0.537	0.895
PR	Negative	0.578	0.578	0.787
	Positive	0.577	0.577	0.952
HER2	Negative	0.817	0.817	0.469
	Positive	0.221	0.221	0.089
BloomRichardson score	≤5	NA	NA	0.383
	>5	0.932	0.932	0.087
Mitotic index	Grade 1 and 2	0.895	0.895	0.445
	Grade 3	0.976	0.976	0.693
Nuclear pleomorphism	Grade 1 and 2	0.959	0.959	0.600
	Grade 3	0.949	0.949	0.482
Tubule formation	Score 1 and 2	0.132	0.132	0.188
	Score 3	0.175	0.175	0.600

4.9.3. Diffuse stroma

Table 4.28 Summary of the correlation between CSGalNAcT-1 diffuse stroma immunohistochemical staining (IRS, TPS, WAI) and recurrence in every stratum of parameters in breast IDC. P-value with asterisk represents statistically significant results.

Clinicopathological parameters	Stratum	Immunoscoring		
		IRS 100	TPS 20	WAI 1.0
		P-value		
Age	≤50	0.624	0.116	0.624
	>50	0.461	0.828	0.469
Tumor size	≤30 mm	NA	0.168	NA
	>30mm	0.921	0.621	0.906
Histological grade	Grade 1 and 2	NA	0.172	NA
	Grade 3	0.333	0.811	0.333
Staging	Stage 1 and 2	0.118	0.675	0.118
	Stage 3	NA	0.302	NA
DCIS grade	None and low	0.530	0.882	0.530
	Intermediate and high	0.546	0.527	0.544
Lymph node involvement	Negative	0.195	0.465	0.201
	Positive	NA	0.361	NA
Lymph node stage	1-9 LN metastasis	0.414	0.587	0.414
	10 and above LN metastasis	0.056	0.556	0.061
ER	Negative	NA	0.665	NA
	Positive	0.158	0.255	0.164
PR	Negative	NA	0.412	NA
	Positive	0.289	**0.047***	0.296
HER2	Negative	0.089	0.901	0.069
	Positive	0.403	0.144	0.403
BloomRichardson score	≤5	NA	0.475	NA
	>5	0.404	0.204	0.401
Mitotic index	Grade 1 and 2	0.635	0.249	0.635
	Grade 3	0.467	0.723	0.462
Nuclear pleomorphism	Grade 1 and 2	0.460	0.329	0.455
	Grade 3	NA	0.538	NA
Tubule formation	Score 1 and 2	NA	**0.013***	NA
	Score 3	0.441	0.581	0.441

Table 4.29 Summary of significant correlation between CSGalNAcT-1 immunoscoring WAI in diffuse stroma and recurrence in breast IDCs for clinicopathological parameters stratum.

Components	Immunoscores	Parameters	Stratum	Log Rank (Mantel-Cox)
Diffuse stroma	TPS 20	PR	Positive	0.047 (Patients with PR positive and low TPS have longer recurrence free period)
		Tubule formation	Score 1 and 2	0.013 (Patients with lower scoring of tubule formation and low TPS have longer recurrence free period)

Survival Functions

Progesterone receptor= Yes
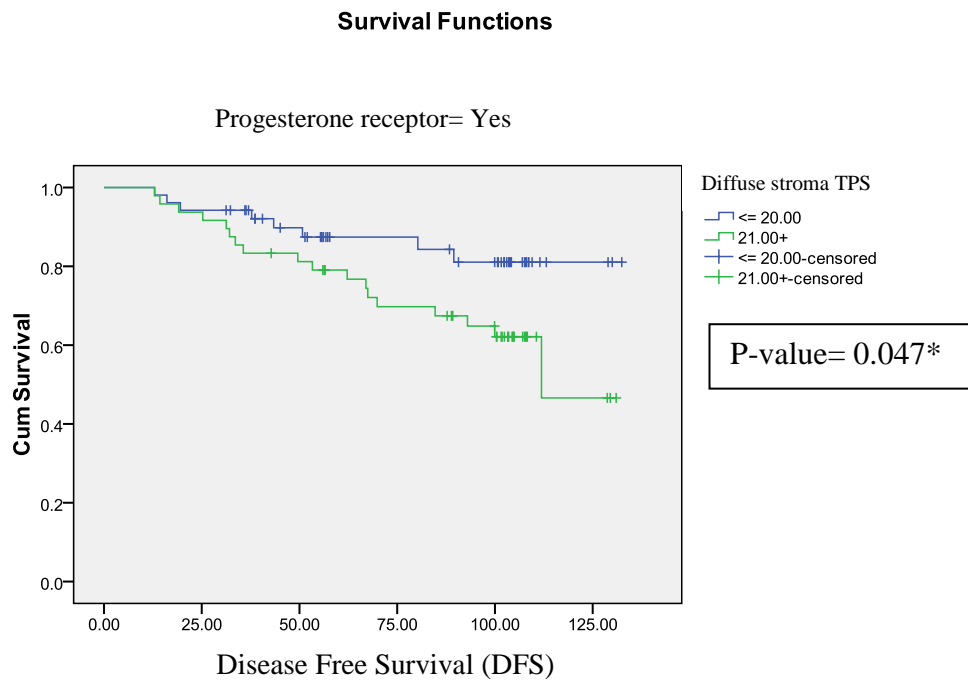
Figure 4.10 This is the Kaplan-Meier curve where the X-axis shows the DFS timeline follow-up in months. Y-axis shows the proportion of patients who have not had recurrence. Blue line shows diffuse stroma TPS staining ≤20; while green line is TPS staining >20. The curve shows the significance of recurrence in patients with positive PR and low diffuse stroma TPS score (≤20), i.e. patients with PR positive and low TP score have longer disease free period.

Survival Functions

Tubule formation score 1 and 2
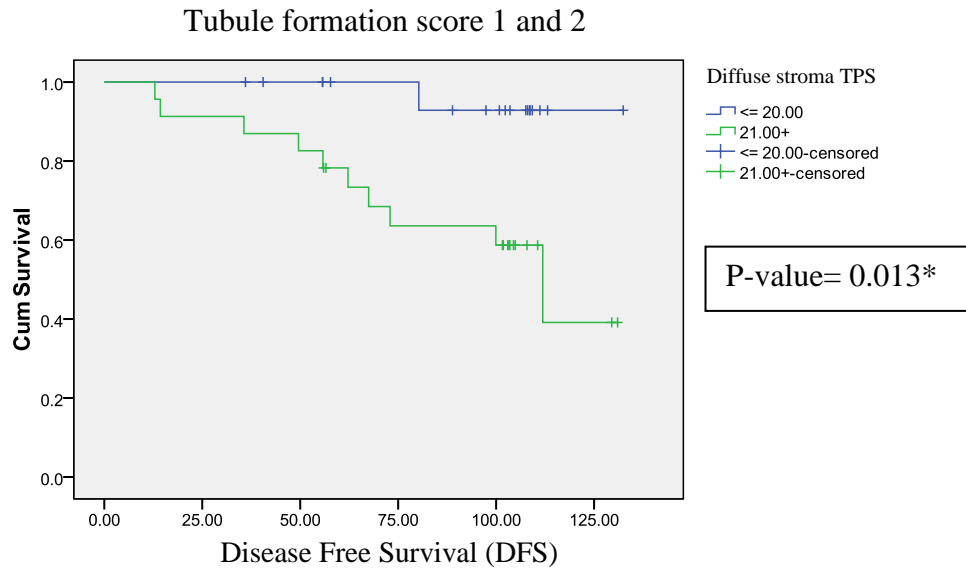
Figure 4.11 This is the Kaplan-Meier curve where the X-axis shows the DFS timeline follow-up in months. Y-axis shows the proportion of patients who have not had recurrence. Blue line shows diffuse stroma TPS staining ≤20; while green line is TPS staining >20. This curve shows the significance of recurrence in patients with low scoring of tubule formation (score 1 and 2) and low diffuse stroma TPS score (≤20), i.e. patients with lower scoring of tubule formation and low TPS score have longer recurrence free period.

CHAPTER 5

DISCUSSION

5. DISCUSSION

5.1. Expression and functional analysis of CSGalNAcT-1 in breast cell lines

5.1.1. Expression of *CSGalNAcT-1* in breast cell lines

This is the pilot study of *CSGalNAcT-1* in breast cancer. There are extensive studies of galactosaminoglycans and its proteoglycans in breast cancer and other cancer types but no study was found to correlate the enzyme that determines the synthesis of galactosaminoglycans with cancer, let alone the signaling pathway that CSGalNAcT-1 is involved in. In current study, it is interesting to know that the mRNA copy of *CSGalNAcT-1* was lower in all the breast cancer cell lines as compared with a normal breast cell line. This expression pattern gave a hint that *CSGalNAcT-1* could play a role in breast cancer malignancy. Hence, to explore the role of *CSGalNAcT-1*, this gene was silenced in normal breast cell line, MCF-12A; while over-expressed in breast cancer cell line, MCF7 and MDA-MB-231.

5.1.2. siRNA-mediated *CSGalNAcT-1* silencing and *CSGalNAcT-1* plasmid stable over-expression

siRNA-mediated silencing of *CSGalNAcT-1* was achieved optimally at 76% in MCF-12A (Figure 3.2). Dharmacon ON-TARGET*plus* SMARTpool siRNA comprises of four siRNA sequences in a single reagent was used in gene silencing. ON-TARGET*plus* SMARTpool siRNA is designed to reduce off-targets effect using dual-strand (sense and antisense) modification so that the potency and specificity of target gene knockdown are guaranteed (Jackson et al., 2006). The innovation of dual-strand modifications is demonstrated by modifying sense strand to prevent interaction with RNA-induced silencing

complex (RISC) and favor antisense strand uptake; and antisense strand seed region which most of the time contributes to off-target activity is also modified to impede off-target activity and enhance knockdown specificity (Jackson et al., 2006). The specificity of *CSGalNAcT-1* knockdown was proven as isoform *CSGalNAcT-2* did not exhibit significant change after *CSGalNAcT-1* knockdown (Figure 3.3).

On the contrary, *CSGalNAcT-1* was over-expressed in MCF7 and MDA-MB-231. Although GFP-tag was not cloned into the plasmid to serve as a report to the plasmid transfection efficiency, Neomycin G418 antibiotic serves as a specificity selection of cells that were successfully transfected with the plasmid.

Gene knockdown and over-expression of *CSGalNAcT-1* were validated at both gene transcript level via qRT-PCR and the protein level via western blotting and immunofluorescence technique (Figure 3.2, 3.4, 3.24 and 3.25).

5.1.3. Functional significance and signaling pathway of *CSGalNAcT-1* in breast cancer cell lines

Knocking down *CSGalNAcT-1* in normal breast cell line, MCF-12A, caused the cells to have increased migration, invasion, cell viability and apoptosis. On the contrary, over-expression of *CSGalNAcT-1* in breast cancer cell lines, MCF7 and MDA-MB-231, hampered the cancer phenotypes, i.e. decreased migration and invasion, reduced cell viability and affected adhesion. Interestingly, microarray screening of *CSGalNAcT-1* silenced MCF-12A

detected a few novel genes that could be the downstream targets of *CSGalNAcT-1*. These genes, which include *CXCL14*, *TRIM59*, *ONECUT2*, *APOL6* and *CDKN1C*, are plausible to be implicated in the phenotypic changes of *CSGalNAcT-1* knockdown and over-expression cells. A hypothetical diagram on the mechanisms of CSGalNAcT-1 role in MCF-12A was illustrated in Figure 5.1.

5.1.3.1. TRIM59

TRIM59 was discovered as the plausible early signal transducer in both RAS and SV40Tag oncogenic pathway in a study (Valiyeva et al., 2011). The tumor phenotypes acquired in *CSGalNAcT-1* knockdown MCF-12A could be attributed to the up-regulation of *TRIM59* interacting with effector molecules from RAS and SV40Tag oncogenic pathways.

TRIM59 is one of the members of the evolutionary conserved TRIM (*TRI*partite Motif) family (Khatamianfar et al., 2012). The functions of most of the TRIM family members, including *TRIM59*, are poorly understood but studies showed that some of the gene members are implicated in critical cellular process including immunity (Ozato et al., 2008, James et al., 2007, Keeble et al., 2008), proliferation (Gack et al., 2007, Short and Cox, 2006), transcriptional regulation (Ozato et al., 2008, Lerner et al., 2007), neuro-development (Balastik et al., 2008, Schwamborn et al., 2009), cell differentiation (Schwamborn et al., 2009) and cancer (Wang et al., 2009). In an immunohistochemical study, TRIM59 was shown to be a novel multiple cancer biomarker for detection of tumorigenesis (Khatamianfar et al., 2012).

In the study itself, TRIM59 was demonstrated to be up-regulated in early tumorigenesis of prostate intraepithelial neoplasia and grade 1 of renal cell carcinoma. The specificity of TRIM59 expression in tumor was proven by significantly low or negative TRIM59 immunohistochemistry signal in control and normal area. The highest expression of TRIM59 was identified in lung, breast, liver, skin, tongue and mouth (squamous cell cancer) and endometrial cancers.

Aberrant expression of TRIM59 in multiple cancer tissue revealed the implication of TRIM59 in tumorigenesis. Indeed, in a SV40 Tag oncogene-directed transgenic mouse prostate cancer models, *TRIM59* was shown to be upregulated in cDNA microarray analysis and was characterized to serve as a signaling pathway effector (Valiyeva et al., 2011). The function of *TRIM59* was elucidated by short hairpin RNA (shRNA)-mediated knockdown of the gene in human prostate cancer (CaP) cells. The CaP cells exhibited cell growth retardation and were arrested in S-phase. The proto-oncogenic function of *TRIM59* was further evident by its ability to induce tumorigenesis in prostate cancer transgenic mouse model with up-regulated TRIM59 expression at prostate-specific site. GeneChip analysis on the transgenic mice revealed that genes related to Ras/Braf/MEK/ERK signaling pathway were upregulated by 2- to 10-fold. Besides, some genes which are involved in both Ras/Braf/MEK/ERK and SV40 Tag/pRB/p53 pathways were identified. It was hypothesized that TRIM59 was transducing a novel signaling route, which served as a link between Ras and SV40 Tag/pRB/p53 oncogene signal pathways.

The RAS proteins are critical regulators in controlling signaling pathways of cellular growth in normal cellular function and during malignant transformation (Downward, 2003). Hence, a niche deregulation of the *RAS* genes or alterations in upstream or downstream signaling components could contribute to several aspects of the malignant phenotype. About 20% of all human tumors acquired activating point mutation in the *RAS*, most frequently in *KRAS* (Bos, 1989). Activated mutation of RAS prevented GTPase activating protein (GAP) from promoting hydrolysis of GTP to GDP thus locking RAS in the GTP-bound activated form (Downward, 2003). This mutation resulted in disordered tumor-cell growth, programmed cell death and invasion, as well as angiogenensis (Shields et al., 2000). Other mutations in RAS signaling pathways include GAP deletion (Weiss et al., 1999) and over-expression of growth factor receptor, such as epidermal growth factor receptor (EGFR) and ERBB2 (also known as HER2/neu) (Mendelsohn and Baselga, 2000). Over-expression of growth factor receptors are frequently found in many types of cancer, including breast, ovarian and stomach carcinomas. In addition, glioblastomas and some other tumor types harbor overacting truncated EGFR (Kuan et al., 2001). EGFR-family tyrosine kinases are commonly activated by autocrine production of EGF-like factors such as transforming growth factor-α (TGF-α) (Downward, 2003). BRAF, a serine/threonine kinase effector of RAS, which is responsible of activating downstream mitogen activated protein kinases (MAPK) is frequently activated by mutation in melanoma and colon carcinoma (Downward, 2003).

Simian virus 40 (SV40) is a DNA tumor virus which express dominant acting oncoproteins large T antigen (T antigen) and small T antigen (t antigen) (Ahuja et al., 2005). Studies have firmly established that T antigen's inhibition of p53 and Rb-family of tumor suppressors are important for SV40-induced transformation (Ahuja et al., 2005). E2F transcription factor regulates transcription of genes encoding proteins required for DNA replication, nucleotide metabolism, DNA repair and cell cycle progression and the activity of E2F is controlled by Rb-E2F interactions (Attwooll et al., 2004, Dimova and Dyson, 2005, Frolov and Dyson, 2004). By binding to Rb-proteins, Large T antigen hampered repressive Rb-E2F complexes, promoting transcription of E2F-dependent genes and progression into S-phase (Sullivan et al., 2000, Zalvide et al., 1998). p53 is a tumor suppressor which functions as a transcriptional activator, regulating expression of a number of genes mediated in cell cycle arrest and apoptosis (Ahuja et al., 2005). Large T antigen blocks p53 growth-suppressive functions by interacting with the DNA-binding surface of p53 and interfering with its ability to bind promoters and regulate gene expression (Barfonetti et al., 1992, Tevethia et al., 1997, Rushton et al., 1997).

5.1.3.2. ONECUT2

Transcription factor *one cut homeobox 2* (*ONECUT2*) is another proto-oncogene which could possibly contribute to the increased migration and invasion of *CSGalNAcT-1* silenced MCF-12A. ONECUT2 protein was substantially up-regulated in colorectal cancer tissues and the expression was negatively regulated by a tumor-suppressor miR-429 (Sun et al., 2014). In the

study describing the functional role of *ONECUT2* in colorectal cancer, *ONECUT2* was targeted by miR-429 to inhibit the initiation of epithelial-mesenchymal transition (EMT) and repress the expression of EMT-related markers found in TGF-β induced EMT pathway. TGF-β promotes EMT by regulating adherens junction either by interaction of TGF-β receptors and protein Par6 or by repressing E-cadherin transcription (Gregory et al., 2008). Besides, TGF-β also induced the expression of EMT inducing transcription factors such as ZEB1, ZEB2, SNAIL, and SLUG (Guarino, 2007, Thiery et al., 2009, Said and Williams, 2011). Taken together, transcription factor *ONECUT2* was involved in migration and invasion, which could explain the increased migration and invasion phenotypes obtained in MCF-12A after *CSGalNAcT-1* knockdown.

5.1.3.3. *APOL6, CDKN1C, GAS1* and BAD coordinately induce apoptosis in *CSGalNAcT-1* silenced MCF-12A

Interestingly, while proto-oncogenes were up-regulated in *CSGalNAcT-1* silenced MCF-12A, pro-apoptotic genes were up-regulated at the same time; and one of these is *Apoliproprotein L6* (*APOL6*). APOL6 was revealed as a novel pro-apoptotic Bcl-2 homology 3-only (BH3-only) protein (Liu et al., 2005). In the study, over-expression of wild type *APOL6* in p53-null colorectal cancer cells induced apoptosis via mitochondrial intrinsic pathway which was characterized by release of cytochrome c and Smac/DIABLO and activation of apoptosis initiator caspase caspase-8 and -9. The induction of apoptosis by APOL6 was accompanied with recruitment of and interaction with lipid/fatty acid components. BH3-only proteins belong to Bcl-2 family.

They have been shown to promote apoptosis by binding to Bcl-2 family members to inhibit their activity (Cory and Adams, 2002, Letai et al., 2002b) and pro-apoptotic family members to ameliorate their activity (Kuwana et al., 2002, Zong et al., 2001). To trigger a mitochondrial intrinsic apoptosis pathway, BH3-only proteins were shown to interact with voltage-dependent anion channel or the adenine nucleotide exchanger of the mitochondrial membrane proteins to induce mitochondrial dysfunction and cytochrome c release (Degli Esposti and Dive, 2003, Zamzami et al., 2000, Sugiyama et al., 2002). Importantly, the recruitment of and interaction with lipid/fatty acids components during apoptosis induction by APOL6 further emphasize the role of lipid messengers in inducing matrix metalloproteinase and initiating apoptosis (Klolesnick and Kronke, 1998, Esposti, 2002, Garcia-Ruiz et al., 2002).

Another tumor suppressor gene being up-regulated in *CSGalNAcT-1* silenced MCF-12A was *cyclin-dependent kinase inhibitor 1C* (*CDKNIC* or *p57^{KIP2}*). CDKN1C together with p27^{KIP1} and p21$^{CIP1/WAF1}$ are members of cyclin-dependent kinase (CDK) inhibitors Cip/Kip family (Matsuokam et al., 1995). Studies have demonstrated the implications of CDKN1C in the regulation of many cellular events, including cell cycle control, differentiation, apoptosis, and metastasis (Joseph et al., 2009, Vlachos et al., 2007, Vlachos and Joseph, 2009). The possible role of CDKN1C in the signaling pathway of *CSGalNAcT-1* silenced MCF-12A could be attributed to its role in regulating cell death. CDKN1C enhanced drug-induced cell death in HeLa cells through caspase-dependent mitochondrial pathways. (Vlachos et al., 2007, Samuelsson

et al., 2002). Another study showed that CDKN1C promoted anti-cancer drug induced apoptosis by inducing Bax, caspase-9 and -3 activities in mitochondrial intrinsic apoptosis pathway (Vlachos et al., 2007).

In current study, increased caspase 3/7 activity in *CSGalNAcT-1* silenced MCF-12A correlates with increased apoptosis (Section 3.2.6.1). Western blot examining the expression of a pro-apoptotic member of the Bcl-2 family, BAD, and its phosphorylated form (Downward, June 1999) in *CSGalNacT-1* silenced MCF-12A was conducted (Section 3.2.6.2). BAD is another BH3-only protein which promotes apoptosis by binding to anti-apoptotic Bcl-2 and Bcl-X_L so that the latter two are prevented from inhibiting Bax and related pro-apoptotic proteins to induce apoptosis (Yang et al., 1995). However, pro-apoptotic activity of BAD was interrupted when serine residues 112 and 136 of BAD were phosphorylated by protein kinase A (PKA) (Harada et al., 1999) and protein kinase B (PKB/Akt) (Datta et al., 1997, del Peso et al., 1997). Expression of total BAD was increased, though not significant, after *CSGalNAcT-1* knockdown in MCF-12A. Pro-apoptotic activity of *CSGalNAcT-1* silenced MCF-12A was reflected in the down-regulation of phosphorylated BAD (pBAD) and its relativity expression to total BAD (section 3.2.6.2). The de-phosphorylation of BAD is a consequent of the up-regulation of *growth arrest specific 1* (*GAS1*) from *CSGalNAcT-1* knockdown in MCF-12A. GAS1 protein induced growth arrest and apoptosis by inhibiting GDNF-α-receptors and its co-receptor RET (Schueler-Furman et al., 2006), hence impeded the activation of AKT (Dominguez-Monzon et al., 2009, Lopez-Ramirez et al., 2008), which in turn reduced the phosphorylation of

BAD. Hence BAD could translocate to the mitochondria to release cytochrome-c and trigger apoptosis (Zarco et al., 2012). The up-regulation of pro-apoptotic *APOL6*, *CDKN1C*, and *GAS1* in mRNA level as well as down-regulation of pBAD protein could have synergistically acted on mitochondrial intrinsic apoptosis pathway and resulted in the increased apoptosis in *CSGalNAcT-1* silenced MCF-12A.

5.1.4. F-actin staining reflects migration of *CSGalNAcT-1* silenced and over-expressed cells

The migratory changes in *CSGalNAcT-1* silenced MCF-12A were reflected in the F-actin immunofluorescence staining. In *CSGalNAcT*-1 silenced MCF-12A, F-actin immunofluorescence intensity was increased compared to negative control (Figure 3.6); while reduced F-actin immunofluorescence staining intensity was observed in *CSGalNAcT-1* over-expressed MCF7 and MDA-MB-231 compared to their empty vector clones, respectively (Figure 3.29 and 3.30). Actin filaments assembly is crucial for cell migratory. During cell migration, actin filaments assembly drives the formation of lamellipodia and filopodia to extend the cells forward and form protrusions to adhere to extracellular matrix with actin cytoskeleton. Finally, forward movement is completed by retracting actomyosin and disassembly of adhesion from the rear (Le Clainche and Carlier, 2008). In a paper published much earlier using Chinese hamster ovary cell mutants deficient in glycosaminoglycans, F-actin formation and focal adhesion on fibronectin substrata were compromised, indicating that glycosaminoglycans could possibly mediate the dynamic of cellular cytoskeleton formation and its interaction with extracellular matrix

components (LeBaron et al., 1988). However, the mechanism of how CSGalNAcT-1 regulates F-actin assembly and whether CSGalNAcT-1 directly or indirectly regulates F-actin assembly remain to be elucidated.

5.1.5. *CSGalNAcT-1 mediates cell adhesion to fibronectin and collagen I*

Metastasis of tumor cells begins with alteration in cell-to-cell adhesion and cell adhesion to extracellular matrix. Successful metastasis required the loss of cell-to-cell adhesion, causing dissemination of tumor cells from the primary tumor site (Albelda, 1993). This is usually accompanied with down-regulation of E-cadherins (MK et al., 2011), replacement of E-cadherins by N-cadherins (AM et al., 2011), and participation of integrins in activating the activity of ECM-degrading enzymes metalloproteinases (DM and YM, 2011). Then, the tumor cells require efficient cell-to-ECM interaction to reside the tumor cells in secondary site (Albelda, 1993). Collagen I and fibronectin are one of numerous components in extracellular matrix (DM and YM, 2011). Silencing *CSGalNAcT-1* in MCF-12A did not affect the adhesion of the cells to collagen I and fibronectin. Over-expression of *CSGalNAcT-1* in MCF7 reduced in adhesion to collagen I and fibronectin. This results showed that over-expression of *CSGalNAcT-1* reduced the potentiality of MCF7 to adhere to ECM before it metastasizes. The same result was observed in the reduced adhesion of MDA-MB-231 to collagen I. However, there was an increased of adhesion to fibronectin in *CSGalNAcT-1* over-expressed MDA-MB-231. The contradictory result could be due to the insufficiency of *CSGalNAcT-1* over-expression level to hamper the adhesion of the cells to fibronectin. It is possible that MDA-MB-231, a poorly differentiated grade III breast cancer

cell line requires higher expression level of *CSGalNAcT-1* to modulate the adhesion to fibronectin than differentiated breast cancer cell lines, MCF7.

5.1.6. CS*GalNAcT-1* signals downstream to *CXCL14* in cell behavioral changes

Microarray results of *CSGalNAcT-1* silenced MCF-12A picked up a number of genes which were up-regulated and down-regulated after the knockdown of *CSGalNAcT-1* (Table 3.2). A few genes that are plausibly implicated in the phenotypic changes of CSGalNAcT-1 knockdown MCF-12A were discussed in previous section. One of the up-regulated genes was chemokine *CXCL14*. CXCL14 belongs to the chemokines superfamily of CXC group (Zlotnik and Yoshie, 2000). CXCL14 is also known as breast and kidney expressed chemokine (BRAK) because of its ubiquitous and high expression in the kidney and breast tissue (Gu et al., 2012). CXCL14 expression is particularly more abundant in normal tissue than in malignant cell lines and cancerous tissues (Hromas et al., 1999, McKinnon et al., 2008); with the receptors yet to be identified (Kurth et al., 2001). The expression pattern of CXCL14 leads to the hypothesis of its role in regulating tumor progression (Frederick et al., 2000).

The microarray results showed that *CXCL14* expression was up-regulated by 2-fold in *CSGalNAcT-1* knockdown MCF-12A (Figure 3.15), this is later validated by qRT-PCR with the up-regulation of 1.8-fold in the knockdown cells and the protein expression was verified to be up-regulated by immunofluorescence (Figure 3.16). Silencing of *CSGalNAcT-1* changed the

normal breast cell line MCF-12A to acquire tumor phenotypes, i.e. became more invasive and proliferative (Section 3.2.3 to 3.2.5). Hence, it was hypothesized that the up-regulation of *CXCL14* was the downstream effect of *CSGalNAcT-1* knockdown and the phenotypic changes observed in *CSGalNAcT-1* knockdown MCF-12A could be attributed to the up-regulation of *CXCL14*. Hence to prove the hypothesis, double knockdown technique was employed. Double knockdown of *CSGalNAcT-1* and *CXCL14* was expected to restore the normal phenotypes of the MCF-12A. Above 90% silencing efficiency of *CXCL14* was achieved by 5nM Ambion Silencer Select® siRNA, two siRNAs were used for validation and one of them was selected for double knockdown experiment (Figure 3.17). The expression of *CSGalNAcT-1* in *CXCL14* silenced MCF-12A was verified not affected (Figure 3.18). Phenotypic assays were not done to assess the *CXCL14* silenced MCF-12A. This is because according to the hypothesis, *CXCL14* was hypothesized to promote *CSGalNAcT-1* silenced MCF-12A to acquire tumor phenotypes. Hence, knockdown of *CXCL14* in normal breast cell line MCF-12A is redundant.

Silencing efficiency of *CSGalNAcT-1* and *CXCL14* were above 90% in double knockdown experiment (Figure 3.19). Silencing efficiency of *CSGalNAcT-1* in the double silencing model remarkably improved from 76% (Figure 3.2) to 93% (Figure 3.19). In the double knockdown model, each single-gene silencing group was added with the non-targeting siRNA together with the targeted gene siRNA. In *CSGalNAcT-1* single silenced group, the same amount of Negative Control siRNA was added. Non-targeting siRNA serves as a negative control

as it is presumably not to target any gene and cause any effect. However, there was publication describing the effect of non-targeting siRNA that was transfected into 293T cells (Wei et al., 2012). Cells were at stress and received non-targeting toxicity due to the persistent activation of siRNA-RISC complex. Hence, the changes in the *CSGalNAcT-1* silencing efficiency in double knockdown model could be due to the interference of the non-targeting siRNA.

In double knockdown experiments, *CSGalNAcT-1* silenced MCF-12A had increased migration and invasion. This is in accordance to the results obtained from single silencing experiments although the magnitudes of changes were not as huge. This could be due to the interference of non-targeting siRNA added in the *CSGalNAcT-1* silenced group. *CXCL14* silenced MCF-12A revealed decrease in migration and invasion and double knockdown of *CSGalNAcT-1* and *CXCL14* brought down the migration and invasion which was as good as reverting the cells back to normal (Figure 3.20 and 3.21). No significant changes in proliferation were observed in any group of double knockdown model. The non-targeting siRNA in *CSGalNAcT-1* silenced group could have prevented the minimal changes in proliferation previously observed (Figure 3.8). In fibronectin adhesion assay, *CXCL14* silenced MCF-12A had increased adhesion but the change was not shown in double knockdown group. This could be due to the dampening effect brought by *CSGalNAcT-1* silenced group that did not harbor significant changes thus dampened the increased fibronectin adhesiveness of MCF-12A in double knockdown group. While in collagen I adhesion assay, both *CSGalNAcT-1* and *CXCL14* single silenced group had no significant changes; however, there

was an increase in adhesion to collagen I in double silenced group. The *CSGalNAcT-1* and *CXCL14* downstream molecules may act synergistically to increase adhesion to collagen I. Hence, from the phenotypic results obtained here, we can preliminarily conclude that *CXCL14* functions downstream of *CSGalNAcT-1* and *CXCL14* is pro-tumorigenic that contributes to the malignancy transformation of MCF-12A upon *CSGalNAcT-1* knockdown.

CXCL14, like other chemokines, has the immunological function to generate chemotaxis gradient and induce the migration in some immune cells, such as macrophages, natural killer cells and dendritic cells (Cao et al., 2000, Sleeman et al., 2000). In addition to the immunologic function of CXCL14, the biological roles of CXCL14 in tumorigenesis were extensively explored in recent years. In a study characterizing molecular and gene expression profile of the breast cancer tumor microenvironment, *CXCL14* was found to be over-expressed in myoepithelial cells and myofibroblasts and was able to promote the proliferation and invasiveness of breast cancer epithelial cells through paracrine effect (Allinen et al., 2004). In pancreatic cancer tissue, CXCL14 expression was up-regulated compared to chronic pancreatitis and normal pancreas tissue; besides, CXCL14 stimulation increased invasiveness of pancreatic cancer cells in Matrigel assay (Wente et al., 2008). Cancer-associated fibroblasts over-expressing CXCL14 were found in prostate cancer tissue. These fibroblasts promoted the growth of prostate cancer xenografts, and also increased tumor angiogenesis, macrophage infiltration; enhanced proliferation and migration of prostate cancer cells in vivo and in vitro, respectively (Augsten et al., 2009). While in colorectal cancer, CXCL14

expression levels were significantly associated with malignant clinicopathological parameters of the disease. High CXCL14 expression was associated to increased risk of recurrence in stage I/II patients and worse overall survival in advanced stage patients. In vitro knockdown of *CXCL14* impaired the tumorigenic behavior of colorectal carcinoma cells (Zeng et al., 2013).

The standard way of chemokines interacting with target cells is through binding to G-protein coupled receptors (Park et al., 2013). Chemokines can also regulate cellular activities through binding to polysaccharide-containing proteins, such as glycosaminoglycans, and lipids (Kuschert et al., 1999, Rybak et al., 1989). For example, CXCL10 was found to bind to heparin sulfate and heparin sulfate proteoglycan and interfere with cellular proliferation and migration (Jiang et al., 2010, Luster et al., 1995). CXCL14 was demonstrated to increase proliferation and migration of lung cancer cells by binding to cell surface heparin sulfate proteoglycans and sialic acids (Park et al., 2013). As CXCL14 could interact with heparin sulfate proteoglycans, there is high chance for CXCL14 to interact with chondroitin/ dermatan sulfate and/or respective proteoglycans and modulate cellular behaviors in normal biological process and/or in tumor progression. The likelihood of CXCL14 being pro-tumorigenic is highly possible. As mentioned earlier, CXCL14 could attract macrophages, traffic activated natural killer (NK) cells to sites of inflammation or malignancy (Starnes et al., 2006) and induce dendritic cells (DC) infiltration and maturation (Shurin et al., 2005), causing inflammation to happen. Tumor promoting inflammation has become an enabling characteristic

in the hallmark of cancer (Hanahan and Weinberg, 2011). Tumors were regarded by immune cells as wounds that never heal hence infiltrating inflammatory cells acts as a double-edged sword: tumor-antagonizing and tumor-promoting (Dvorak, 1986, Schafer and Werner, 2008). Tumor-promoting inflammatory cells, such as macrophage subtypes, mast cells, neutrophils, T and B lymphocytes (Coffelt et al., 2010, DeNardo et al., 2010, Egeblad et al., 2010, Johansson et al., 2008, Murdoch et al., 2008), release growth factor, cytokines and chemokines, proangiogenic and/or proinvasive factors to amplify the inflammation by recruiting more immune cells and promoted tumor progression eventually (Murdoch et al., 2008, Qian and Pollard, 2010). Moreover, inflammation may induce the production of reactive oxygen species and render surrounding normal cells and/or tumor cells to acquire genetic mutation (Grivennikov and Karin, 2010). Indeed in one breast cancer study, CXCL14 expression was up-regulated by ROS through novel signaling pathway and induced breast cancer cell invasiveness and proliferation (Pelicano et al., 2009).
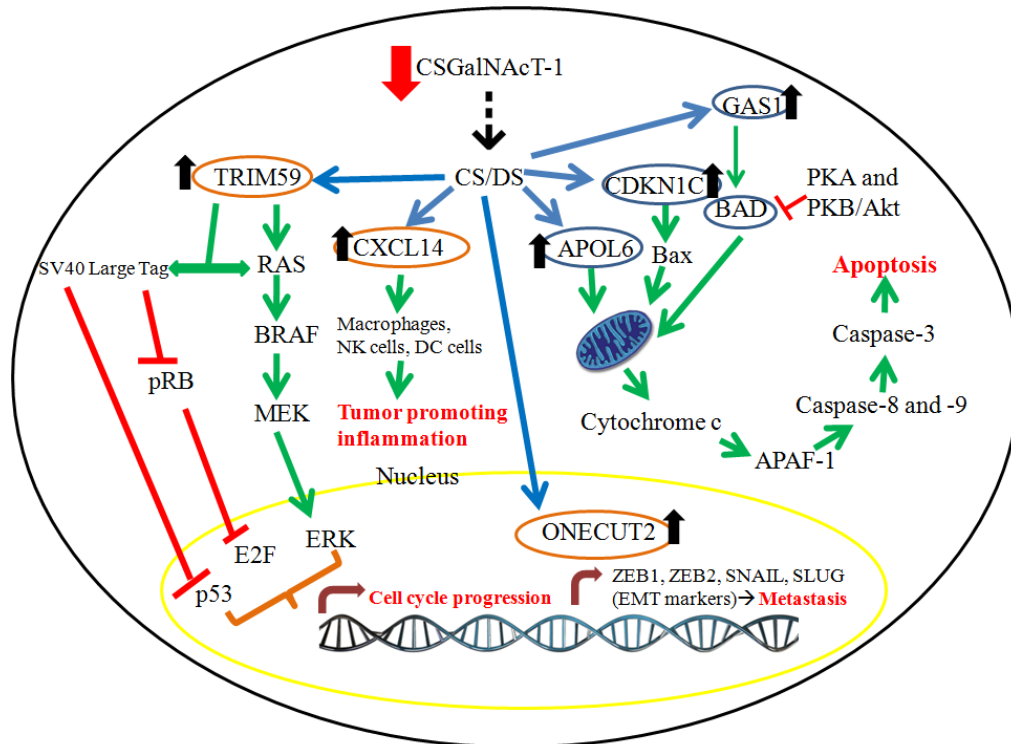
Figure 5.1 Hypothetical diagram on the signaling mechanisms of CSGalNAcT-1 in MCF-12A. Knockdown of *CSGalNAcT-1* in MCF-12A induced an up-regulation of proto-oncogene *CXCL14*, *TRIM59* and *ONECUT2*; and tumor-suppressor genes *APOL6*, *CDKN1C* and *GAS1*. Chemokine *CXCL14* attracts and activates macrophages, natural killer (NK) cells and dendritic cells which results in more tumor promoting inflammation to take place. *TRIM59* induces the expression of molecules in both RAS/BRAF/MEK/ERK and SV40 Tag/pRB/p53 pathways. *TRIM59* is hypothesized to serve a link between these two tumor promoting pathways. Another proto-oncogene which was up-regulated was *ONECUT2*. *ONECUT2* induces the transcription of epithelial-mesenchymal transition biomarkers and results in increased migration and invasion of the cells. The increased apoptosis in *CSGalNAcT-1* silenced MCF-12A was the results of the synergistic cooperation of *APOL6*, *CDKN1C*, *GAS1* and BAD via mitochondrial intrinsic apoptosis pathway.

5.2. CSGalNAcT-1 immunohistochemical analysis in invasive ductal

carcinoma (IDC)

Among different types of breast cancer, invasive ductal carcinoma is the most

common type of breast malignancy, predominating 60% to 80% of all breast

malignant lesions (Guinebretiere et al., 2005, Mallon et al., 2000). The

expression of CSGalNAcT-1 was investigated in invasive ductal carcinoma

tissue microarray in current study. The tissue microarray was constructed by

Department of Pathology, Singapore General Hospital, comprising 297 cases

from 1998 to 2004, among which 52 are normal tissue cases and 245 are IDC

cases. All the tissues were from Singaporean female, aged 23 to 89 years old.

In this study, CSGalNAcT-1 immunostaining was assessed based on three

kinds of scoring measurements, i.e. immunoreactivity score (IRS), total

percentage score (TPS) and weighted average intensity (WAI) of

CSGalNAcT-1 immunopositive cells. CSGalNAcT-1 was found to express in

cytoplasm of epithelial cells, stromal cells and diffuse stroma (Figure 4.1).

Expression pattern of CSGalNAcT-1 was investigated by comparing between

low histological grade (grade 1 and 2) and high histological grade (grade 3)

IDC (Figure 4.3). Although only WAI of stromal cells showed significant

difference, generally, all the three stained components had stronger expression

of CSGalNAcT-1 in low grade IDC as compared with high grade IDC. On top

of that, comparison of CSGalNAcT-1 expression between normal cases and

IDC cases was performed (Figure 4.2). In epithelial cells and stromal cells of

IDC cases, CSGalNAcT-1 had stronger staining compared to normal cases;

however, expression of CSGalNAcT-1 was weaker in diffuse stroma of IDC

cases compared to normal cases. These expression patterns showed that expression of CSGalNAcT-1 varied in different components of IDC and variably between normal and IDC cases and low grade and high grade IDC; this could mean that the implication and functional role of CSGalNAcT-1 in different components and IDC grade could vary in the pathogenesis of IDC.

This is a pilot study examining expression of CSGalNAcT-1 in invasive ductal carcinoma thus far; hence the data collected is preliminary. However, there were extensive immunohistochemistry and expression analysis study correlating the expression of chondroin/dermatan sulfate with the clinical outcome of breast cancer patients. In a immunohistochemical study, expression of stroma decorin was shown to have the highest in normal breast tissue, lower in DCIS and the lowest in breast invasive components (Oda et al., 2012). In another study which examined expression of lumican and decorin from node-negative invasive breast cancer by western blot analysis, low levels of both lumican and decorin correlated with aggressive clinicopathological parameters and associated with poor clinical outcome (Troup et al., 2003). These results supported the hypothesis that down-regulation of decorin and lumican facilitated the aggressiveness and progression of breast cancer.

Elevated expression of chondroitin sulfate in malignant cells of primary breast cancer patients was associated with poor overall survival and shorter relapse-free period (Svensson et al., 2011). In the case of versican, high relapse rate in patients is predicted by high versican level in peritumoral stroma of node-negative primary breast cancer (Ricciardelli et al., 2002, Suwiwat et al., 2004).

Hence, in contrast to decorin and lumican, chondroitin sulfate and versican exhibit pro-tumorigenic properties in breast tissue malignancies.

5.2.1. Prognostic value of CSGalNAcT-1 in invasive ductal carcinoma (IDC)

The significance of a molecule as a prognostic marker is its ability to predict the clinical outcome of disease in patients so that patients receive the most suitable and beneficial clinical management. Thus, it is useful to investigate the relevance of CSGalNAcT-1 expression with prognosis and survival of IDC patients.

Among the three stained components in IDC, only immunoscore of stromal cells showed significant correlation with some of the clinicopathological parameters. Weighted average intensity (WAI) was significantly associated with ethnicity (Chinese, Malay and Indian) and age. Besides, higher weighted average intensity, meaning stronger expression of CSGalNAcT-1 was associated with lower histological grade and mitotic index (Table 4.9). In concordance to Singapore cancer registry report of 2009-2013 (Lee et al., 2014), breast cancer was indeed the most common cancer among the three major ethnic groups in Singapore, i.e. Chinese, Malay and Indian. In the age per se, the incidence of cancer generally increases with age as gene mutations accumulate with the defect in repair mechanisms (Roses, 2005). The chance of a woman being diagnosed with breast cancer is 12.5% in her lifetime, and half of the risk happens after the age of 60 (Abeloff et al., 2004). Increasing age in IDC patients conferred to high expression of CSGalNAcT-1 in stromal cells. Histological grade has been used as a prognosis indicator to give an overview

of the differentiation of tumor (Dabbs, 2012). Nottingham grading system combines nuclear pleomorphism, tubule formation and mitotic rate index, which were formerly from Scarff-Bloom-Richardson (SBR) (Black et al., 1955); together with lymph node stage and tumor size to form a preferable and increasing popular grading system accepted by various international professional bodies (Tavassoli F, 2003, January 2005, Elston and Ellis, 1991). Mitotic rate index reflects the degree of proliferation of tumors and is examined from sections stained with hematoxylin and eosin (H&E) (Dabbs, 2012). In present IDC immunohistochemical study, high CSGalNAcT-1 expression in stromal cells correlated with low histological grade and low mitotic rate index. Hence, more CSGalNAcT-1 expression in stromal cells could possibly suggest a good prognosis in IDC patients.

Breast cancer is a heterogeneous disease which a number of factors are taken into account for the pathogenesis and progression of the malignancy (Di Cosimo and Baselga, 2010). To perform a more meaningful and more in depth association in breast IDC cases, multivariate test was used to take into consideration of the effect of other parameters simultaneously. Ethnicity was found to affect weighted average intensity (WAI) of CSGalNAcT-1 in stromal cells after adjusting for histological grade, mitotic index and age. Hence, ethnicity of patients along with the presence of its respective confounders may affect the staining of CSGalNAcT-1 in breast IDC.

In Kaplan-Meier survival analysis, low CSGalNAcT-1 immunopositivity (TPS) in diffuse stroma and lower scoring of tubule formation (score 1 and 2) was

shown to predict longer recurrence-free survival (Figure 4.11). Tubule formation is yet another prognostic marker from Nottingham grading system and it is a feature to reflect degree of tumor differentiation (Dabbs, 2012). Highly malignant breast cancer that deviates largely from the histological appearance of normal glandular tissue of the breast will be given the highest score of three. Besides, lower expression of CSGalNAcT-1 in diffuse stroma and cases with positive estrogen and progesterone receptor were shown to have longer overall survival and recurrence-free survival (Figure 4.6, 4.8, 4.9, and 4.10). Estrogen receptor and progesterone receptor are very strong predictive factors to the response of patients to endocrine therapy (Dabbs, 2012). Estrogen receptor is a nuclear transcription factor activated by estrogen hormone to regulate cell proliferation and differentiation of breast tissue (Clarke, 2003, Keen and Davidson, 2003, Fuqua SAW, 2004). Breast cancer cells are often over-proliferative via estrogen receptor signaling pathway and the consequence is detrimental to patients (Keen and Davidson, 2003, Fuqua SAW, 2004, Ellege RM, 2004). The expression of estrogen receptor serves as a powerful predictive factor for response to endocrine therapies, such as Tamoxifen and aromatase inhibitors (Ellege RM, 2004, Buzdar et al., 2004, Dowsett et al., 2005, Goss et al., 2007, Viale et al., 2007). The outcome of endocrine therapy in estrogen receptor positive patients is proven to be promising and effective (Ellege RM, 2004, Dahabreh et al., 2008, Fitzgibbons et al., 2000, Prat and Baselga, 2008). The expression of progesterone receptors is regulated by estrogen receptors; and as similar to estrogen receptors, progesterone receptors regulate cell proliferation when activated by progesterone hormone (Clarke, 2003, Ellege RM, 2004, Anderson, 2002,

Jacobsen et al., 2003). The response of progesterone receptor-positive cells to endocrine therapy is very effective with even very minimal (≥1%) of cells expressing the receptors (Mohsin et al., 2004, Love et al., 2002). Progesterone receptor-positive DCIS patients who received endocrine therapy after lumpectomy and radiation were proven to have reduced local recurrence (Allred et al., 2012). In sum, current IDC cases which had lower expression of CSGalNAcT-1 and positive hormone receptors resulted in a better outcome in patients. Lymph node involvement and lymph node metastases resulted breast cancer patients to acquire poor prognosis (Hortobagyi, 1998, Wilking et al., 1992). Negative lymph node involvement and lower expression of CSGalNAcT-1 in diffuse stroma also warranted IDC patients with better overall survival (Figure 4.5 and 4.7). Hence, from the Kaplan Meier survival analysis, lower expression of CSGalNAcT-1 in diffuse stroma together with less aggressive phenotypes conferred better prognosis.

In summary, the expression of CSGalNAcT-1 in stromal cells and diffuse stroma resulted in different implication to IDC malignancy. High expression of CSGalNAcT-1 in stromal cells correlated with less aggressive phenotypes in IDC patients, i.e. lower histological grade and mitotic index; but low expression of CSGalNAcT-1 in diffuse stroma conferred better prognosis in IDC patients. These results showed that the roles of CSGalNAcT-1 in IDC cancer depend on the compartment where the enzyme located as evident by the study of p27. The tumor suppressor p27 is a member of the CIP/KIP family of CKI. It is a tumor suppressor and an inhibitor of cell proliferation (Sherr and Robert, 2001). The anti-proliferative function of p27 was exerted in

the nucleus by inhibiting the interactions with cyclin-CDK enzymes (Russo et al., 1996). However, studies showed that relocation of p27 from nucleus to cytoplasm have been correlated with high tumor grade, poor clinical outcome and increased metastasis in carcinomas of breast, cervix, oesophagus, uterus and in some lymphomas and leukemia (Anayama et al., 1998, Dellas et al., 1998, Vrhovac et al., 1998, Kouvaraki et al., 2002, Watanabe et al., 2002). An explanation for these observations might be due to the role of p27 as a regulator of cytoskeletal structure and cell migration when located in the cytoplasm (McAllister et al., 2003). Hence, when p27 was located in cytoplasm, it inhibits apoptosis and stimulate cell migration by promoting the assembly and nuclear import of proliferation promoter cyclin D-CDK complexes (McAllister et al., 2003). Similar with p27, the roles of CSGalNAcT-1 in IDC is compartment-specific; however, the explanation for these observations needs further elucidation.

CHAPTER 6

CONCLUSIONS

AND

FUTURE WORK

6. CONCLUSIONS AND FUTURE WORK

Breast cancer is the leading cause of morbidity and mortality affecting female worldwide. Scientists put in a lot of effort to identify biomarkers and prognostic markers for the diagnosis of breast cancer and ultimately to seek the best therapeutic intervention for the patients. Since CSGalNAcT-1 is responsible in the biosynthesis of chondroitin sulfate and dermatan sulfate and the expression of this enzyme in normal breast cell line, MCF-12A, was found to be significantly higher than those of breast cancer cell lines, it is hypothesized that *CSGalNAcT-1* could be functionally implicated in breast cancer phenotypic changes. In order to prove this hypothesis, reciprocal knockdown and over-expression of *CSGalNAcT-1* were performed. *CSGalNAcT-1* silenced MCF-12A cells showed increase in migration, invasion, proliferation and apoptosis. On the other hand, over-expression of *CSGalNAcT-1* showed inhibition in migration, invasion, proliferation and mediate adhesion differently. In microarray analysis of *CSGalNAcT-1* silenced MCF-12A, it is interesting to reveal that bringing down the level of *CSGalNAcT-1* promoted the expression of both proto-oncogenes (*TRIM59* and *ONECUT2*) and tumor suppressor genes (*APOL6*, *CDKN1C* and *GAS1*). This explains the reason MCF-12A cells exhibited increased migration, invasion and proliferation but had increased apoptosis. Among the deregulated genes from *CSGalNAcT-1* silenced MCF-12A microarray analysis, *CXCL14* was selected for further study. Knockdown of *CSGalNAcT-1* in MCF-12A resulted in *CXCL14* up-regulation in the cells. Hence, it is postulated that *CXCL14* contributed to the behavioral changes in MCF-12A after *CSGalNAcT-1* was silenced. *CXCL14* was verified to work downstream of *CSGalNAcT-1* through

double knockdown of both genes in MCF-12A. When *CSGalNAcT-1* and *CXCL14* were silenced together, tumor phenotypes of MCF-12A gained through *CSGalNAcT-1* silencing were abolished.

CSGalNAcT-1 expression was determined in invasive ductal carcinoma by immunohistochemical study and found to localize in the cytoplasm of epithelial cells, stromal cells and diffuse stroma. The association of CSGalNAcT-1 immunostaining with clinicopathological parameters in all the stained components did not give much significant correlation, except in stromal cells. Direct association of CSGalNAcT-1 immunostaining in stromal cells with ethnicity (Chinese, Malay and Indian), patients older than 50 years old, low histological grade and low mitotic rate index were established. However, interesting findings were obtained from the association of CSGalNAcT-1 with clinical outcome of IDC patients. In summary, low expression of CSGalNAcT-1 together with less aggressive phenotypes, i.e. hormonal receptors positive, lower score in tubule formation, and negative lymph node involvement promised longer disease free survival and better overall survival. Thus, CSGalNAcT-1 could be a potential prognostic marker in specific group of patients harboring the biological characteristics as mentioned above. The results from in vitro and immunohistochemical study are summarized in Figure 6.1.
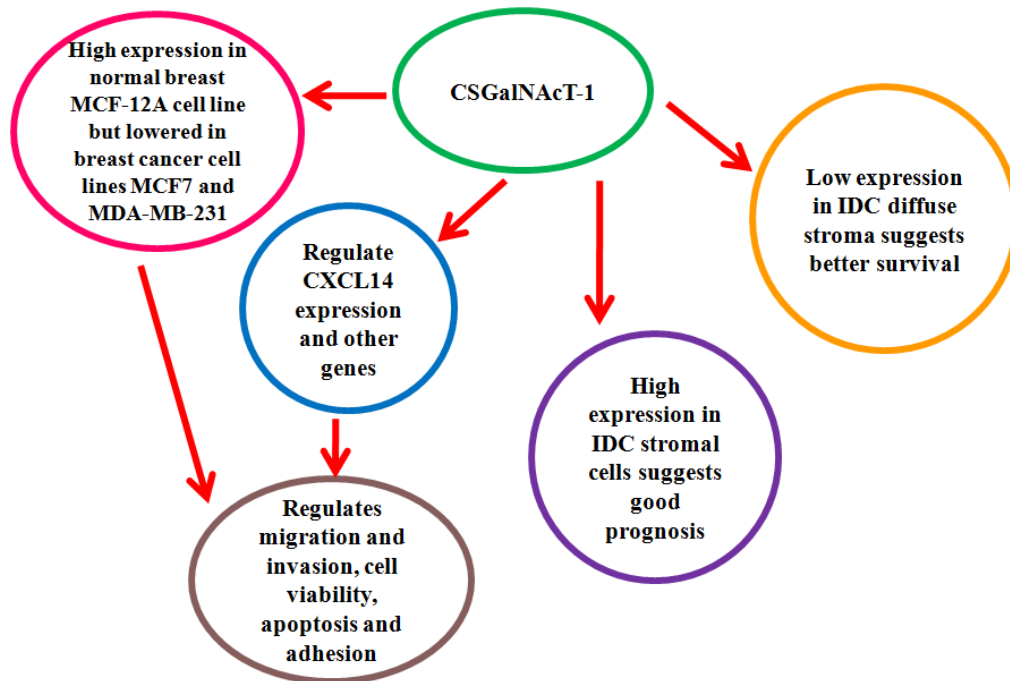
Figure 6.1 The result summary of functional role of CSGalNAcT-1 in mediating phenotypic changes of MCF-12A, MCF7 and MDA-MB-231 and the prognostic value of CSGalNAcT-1 in IDC in different compartments.

As CSGalNAcT-1 catalyzes the biosynthesis of chondroitin sulfate and dermatan sulfate, it is unsure whether the results obtained was an indirect effect via chondroitin/dermatan sulfate chain or it was a direct implication from CSGalNAcT-1 itself. Hence, to resolve this query, chondroitinases could be used to enzymatically degrade the chondroitin/dermatan sulfate chains in CSGalNAcT-1 over-expressed MCF7 and MDA-MB-231. If the phenotypic changes in the over-expression clones still exist, we could conclude that CSGalNAcT-1 is the effector molecule that directly mediates the phenotypic changes in the cells.

The molecular mechanism of which CSGalNAcT-1 interact with candidate downstream molecules, such as *CXCL14*, is still unknown. Immunoprecipitation could be employed to determine this interaction. The

functional role of *TRIM59*, *ONECUT2*, *APOL6*, *CDKN1C* and *GAS1* should be determined by experiments to confirm the roles of these genes with *CSGalNAcT-1* in the signaling pathway. To enhance the understanding of the functions of *CSGalNAcT-1* in breast cancer progression, stable *CSGalNAcT-1* over-expressed MCF7 and MDA-MB-231 cells could be delivered to animal model to investigate the function of *CSGalNAcT-1*.

The results obtained from immunohistochemical study here is still preliminary. From the multivariate analysis, ethnicity affects the expression of CSGalNAcT-1 in IDC; hence, sample population from different ethnicity could be included in future study to determine the relationship between ethnicity and CSGalNAcT-1 in IDC. Besides, larger sample size could be collected in future for validation of the prognostic value of CSGalNAcT-1 in IDC.

Reference List

1996. Breast cancer and hormonal contraceptives: collaborative reanalysis of individual data on 53 297 women with breast cancer and 100 239 women without breast cancer from 54 epidemiological studies. Collaborative Group on Hormonal Factors in Breast Cancer. *Lancet,* 347**,** 1713-27.

2010. *Breast Cancer* [Online]. Singapore. Available: http://www.hpb.gov.sg/HOPPortal/dandc-article/778 [Accessed 17 August 2013.

2012. Globocan 2012: Estimated Cancer Incidence, Mortality and Prevalance Worldwide in 2012. International Agency for Research on Cancer.

January 2005. Pathology reporting of breast disease. *A joint document incorporating the third edition of the NHS breast screening programme's guidelines for pathology reporting in breast cancer screening and the second edition of The Royal College of pathologists' minimum dataset for breast cancer histopathology.*

ABELOFF, M. D., ARMITAGE, J. O., NIEDERHUBER, J. E., KASTAN, M. B. & MCKENNA, W. G. 2004. *Clinical oncology*, Churchill Livingstone.

ACHARYYA, S., MATRISIAN, L., WELCH, D. R. & MASSAGUE, J. 2015. Invasion and metastasis. *The molecular basis of cancer.* 4 ed. Philadelphia, PA: Saunders/Elsevier.

AFRATIS, N., GIALELI, C., NIKITOVIC, D., TSEGENIDIS, T., KAROUSOU, E., THEOCHARIS, A. D., PAVAO, M. S., TZANAKAKIS, G. N. & KARAMANOS, N. K. 2012. Glycosaminoglycans: key players in cancer cell biology and treatment. *FEBS J,* 279**,** 1177-97.

AHUJA, D., SAENZ-ROBLES, M. & PIPAS, J. 2005. SV40 large T antigen targets multiple cellular pathways to elicit cellular transformation. *Oncogene,* 24.

AKHURST, R. J. & BALMAIN, A. 1999. Genetic events and the role of TGF beta in epithelial tumour progression. *J Pathol,* 187**,** 82-90.

ALBELDA, S. 1993. Role of integrins and other cell adhesion molecules in tumor progression and metastasis. *Lab investigation, Nature,* 68**,** 4-17.

ALINI, M. & LOSA, G. A. 1991. Partial characterization of proteoglycans isolated from neoplastic and nonneoplastic human breast tissues. *Cancer Res,* 51**,** 1443-7.

ALLINEN, M., BEROUKHIM, R., CAI, L., BRENNAN, C., LAHTI-DOMENICI, J., HUANG, H., PORTER, D., HU, M., CHIN, L., RICHARDSON, A., SCHNITT, S., SELLERS, W. R. & POLYAK, K. 2004. Molecular characterization of the tumor microenvironment in breast cancer. *Cancer Cell,* 6**,** 17-32.

ALLRED, D. C., ANDERSON, S. J., PAIK, S., WICKERHAM, D. L., NAGTEGAAL, I. D., SWAIN, S. M., MAMOUNAS, E. P., JULIAN, T. B., GEYER, C. E., JR., COSTANTINO, J. P., LAND, S. R. & WOLMARK, N. 2012. Adjuvant tamoxifen reduces subsequent breast cancer in women with estrogen receptor-positive ductal carcinoma in situ: a study based on NSABP protocol B-24. *J Clin Oncol,* 30**,** 1268-73.

ALTERI, R., BANDI, P., BRINTON, L., CASARES, C., COKKINIDES, V., GANSLER, T., GAPSTUR, S., GRAVES, K., KRAMER, J., MCNEAL, B., MAGRO, A., NISHADHAM, D., NEWMAN, L., NIEMEYER, D., RICHARDS, C., RUNOWICZ, C., SASLOW, D., SIMPSON, S., SMITH, R., SULLIVAN, K., WAGNER, D. & XU, J. 2011. *Breast Cancer Facts & Figures 2011-2012* [Online]. Atlanta, Georgia: American Cancer Society. Available: http://www.cancer.org/acs/groups/content/@epidemiologysurveilance/documents/document/acspc-030975.pdf [Accessed 20 August 2013.

AM, K., HIERHOLZER, A. & KEMLER, R. 2011. Replacement of E-cadherin by N-cadherin in the mammary gland leads to fibrocystic changes and tumor formation. *Breast Cancer Research,* 13.

ANAYAMA, T., FURIHATA, M., ISHIKAWA, T., OHTSUKI, Y. & OGOSHI, S. 1998. Positive correlation between p27Kip1 expression and progression in human esophageal squamous cell carcinoma. *International journal of cancer,* 79**,** 439-443.

ANDERSON, E. 2002. The role of oestrogen and progesterone receptors in human mammary development and tumorigenesis. *Breast Cancer Res,* 4**,** 197-201.

ARTEAGA, C. L., DUGGER, T. C. & HURD, S. D. 1996. The multifunctional role of transforming growth factor (TGF)-beta s on mammary epithelial cell biology. *Breast Cancer Res Treat,* 38**,** 49-56.

ASIMAKOPOULOU, A. P., THEOCHARIS, A. D., TZANAKAKIS, G. N. & KARAMANOS, N. K. 2008. The biological role of chondroitin sulfate in cancer and chondroitin-based anticancer agents. *In Vivo,* 22**,** 385-9.

ASPBERG, A., ADAM, S., KOSTKA, G., TIMPL, R. & HEINEGARD, D. 1999. Fibulin-1 is a ligand for the C-type lectin domains of aggrecan and versican. *J Biol Chem,* 274**,** 20444-9.

ATTWOOLL, C., DENCHI, E. & HELIN, K. 2004. The E2F family: specific functions and overlapping interests. *The EMBO Journal,* 23**,** 4709-4716.

AUGSTEN, M., HAGGLOF, C., OLSSON, E., STOLZ, C., TSAGOZIS, P., LEVCHENKO, T., FREDERICK, M. J., BORG, A., MICKE, P., EGEVAD, L. & OSTMAN, A. 2009. CXCL14 is an autocrine growth factor for fibroblasts and acts as a multi-modal stimulator of prostate tumor growth. *Proc Natl Acad Sci U S A,* 106**,** 3414-9.

BALASTIK, M., FERRAQUTI, F., PIRES-DA SILVA, A., LEE, T., ALVAREZ-BOLADO, G., LU, K. & GRUSS, P. 2008. Deficiency in ubiquitin ligase TRIM2 causes accumulation of neurofilament light chain and neurodegeration. *Proc Natl Acad Sci U S A,* 105**,** 12016-12021.

BALDIN, V. & DUCOMMUM, B. 1995. Subcellular localisation of human wee1 kinase is regulated during the cell cycle. *Journal of Cell Science,* 108**,** 2425-2432.

BARFONETTI, J., REYNISDOTTIR, I., FRIEDMAN, P. & PRIVES, C. 1992. Site-specific binding of wild-type p53 to cellular DNA is inhibited by SV40 T antigen and mutant p53. *Journal of Virology,* 71**,** 5620-5623.

BEDROSIAN, I., MICK, R., OREL, S. G., SCHNALL, M., REYNOLDS, C., SPITZ, F. R., CALLANS, L. S., BUZBY, G. P., ROSATO, E. F., FRAKER, D. L. & CZERNIECKI, B. J. 2003. Changes in the surgical management of patients with breast carcinoma based on preoperative magnetic resonance imaging. *Cancer,* 98**,** 468-73.

BERNSTEIN, L., HENDERSON, B. E., HANISCH, R., SULLIVAN-HALLEY, J. & ROSS, R. K. 1994. Physical exercise and reduced risk of breast cancer in young women. *J Natl Cancer Inst,* 86**,** 1403-8.

BLACK, M. M., OPLER, S. R. & SPEER, F. D. 1955. Survival in breast cancer cases in relation to the structure of the primary tumor and regional lymph nodes. *Surg Gynecol Obstet,* 100**,** 543-51.

BLOOM, H. J. & RICHARDSON, W. W. 1957. Histological grading and prognosis in breast cancer; a study of 1409 cases of which 359 have been followed for 15 years. *Br J Cancer,* 11**,** 359-77.

BOS, J. 1989. Ras oncogenes in human cancer: a review. *Cancer research,* 49**,** 4682-4689.

BOUDREAU, N. & BISSEL, M. 1998. Extracellular matrix signaling: integration of form and function in normal and malignant cells. *Current opinion in cell biology,* 10**,** 640-646.

BOYLE, P. 2005. Breast cancer control: signs of progress, but more work required. *Breast,* 14**,** 429-38.

BRAKEBUSCH, C., SEIDENBECHER, C. I., ASZTELY, F., RAUCH, U., MATTHIES, H., MEYER, H., KRUG, M., BOCKERS, T. M., ZHOU, X., KREUTZ, M. R., MONTAG, D., GUNDELFINGER, E. D. & FASSLER, R. 2002. Brevican-deficient mice display impaired hippocampal CA1 long-term potentiation but show no obvious deficits in learning and memory. *Mol Cell Biol,* 22**,** 7417-27.

BRINTON, L. A., SCHAIRER, C., HOOVER, R. N. & FRAUMENI, J. F., JR. 1988. Menstrual factors and risk of breast cancer. *Cancer Invest,* 6**,** 245-54.

BRUNELLE, J. & LETAI, A. 2009. Control of mitochondrial apoptosis by the Bcl-2 family. *Journal of Cell Science,* 122**,** 437-441.

BUZDAR, A. U., VERGOTE, I. & SAINSBURY, R. 2004. The impact of hormone receptor status on the clinical efficacy of the new-generation aromatase inhibitors: a review of data from first-line metastatic disease trials in postmenopausal women. *Breast J,* 10**,** 211-7.

CAO, X., ZHANG, W., WAN, T., HE, L., CHEN, T., YUAN, Z., MA, S., YU, Y. & CHEN, G. 2000. Molecular cloning and characterization of a novel CXC chemokine macrophage inflammatory protein-2 gamma chemoattractant for human neutrophils and dendritic cells. *J Immunol,* 165**,** 2588-95.

CAVALLARO, U. & CHRISTOFORI, G. 2004. Cell adhesion and signalling by cadherins and Ig-CAMs in cancer. *NAture Reviews Cancer,* 4**,** 118-132.

CERTO, M., DEL GAIZO MOORE, V., NISHINO, M. & AL., E. 2006. Mitochondria primed by death signals determine cellular addiction to antiapoptotic BCL-2 family members. *Cancer cell,* 9**,** 351-365.

CHEKENYA, M., ROOPRAI, H. K., DAVIES, D., LEVINE, J. M., BUTT, A. M. & PILKINGTON, G. J. 1999. The NG2 chondroitin sulfate proteoglycan: role in malignant progression of human brain tumours. *Int J Dev Neurosci,* 17**,** 421-35.

CHENG, E., WEI, M., WEILER, S. & AL., E. 2001. BCL-2, BCL-X(L) sequester BH3 domain-only molecules preventing BAX- and BAK-mediated mitochondrial apoptosis. *Molecular and Cell,* 8**,** 705-711.

CHENG, J., ZHOU, T., LIU, C., SHAPIRO, J., BRAUER, M., KIEFER, M., BARR, P. & MOUNTZ, J. 1994. Protection from Fas-mediated apoptosis by a soluble form of the Fas molecule. *Science,* 263**,** 1759-1762.

CLARKE, R. B. 2003. Steroid receptors and proliferation in the human breast. *Steroids,* 68**,** 789-94.

COFFELT, S. B., LEWIS, C. E., NALDINI, L., BROWN, J. M., FERRARA, N. & DE PALMA, M. 2010. Elusive identities and overlapping phenotypes of proangiogenic myeloid cells in tumors. *Am J Pathol,* 176**,** 1564-76.

COLLABORATIVE GROUP ON HORMONAL FACTORS IN BREAST, C. 2002. Breast cancer and breastfeeding: collaborative reanalysis of individual data from 47 epidemiological studies in 30 countries, including 50302 women with breast cancer and 96973 women without the disease. *Lancet,* 360**,** 187-95.

COONEY, C. A., JOUSHEGHANY, F., YAO-BORENGASSER, A., PHANAVANH, B., GOMES, T., KIEBER-EMMONS, A. M., SIEGEL, E. R., SUVA, L. J., FERRONE, S., KIEBER-EMMONS, T. & MONZAVI-KARBASSI, B. 2011. Chondroitin sulfates play a major role in breast cancer metastasis: a role for CSPG4 and CHST11 gene expression in forming surface

P-selectin ligands in aggressive breast cancer cells. *Breast Cancer Res,* 13**,** R58.

CORY, S. & ADAMS, J. 2002. The Bcl2 family: regulators of the cellular life-or-death switch. *Nature Reviews, Cancer.,* 2**,** 647-656.

DABBS, D. J. 2012. *Breast Pathology*, Elsevier/Saunders.

DAHABREH, I. J., LINARDOU, H., SIANNIS, F., FOUNTZILAS, G. & MURRAY, S. 2008. Trastuzumab in the adjuvant treatment of early-stage breast cancer: a systematic review and meta-analysis of randomized controlled trials. *Oncologist,* 13**,** 620-30.

DATTA, S. R., DUDEK, H., TAO, X., MASTERS, S., FU, H., GOTOH, Y. & GREENBERG, M. E. 1997. Akt phosphorylation of BAD couples survival signals to the cell-intrinsic death machinery. *Cell,* 91**,** 231-41.

DE LUCA, A., SANTRA, M., BALDI, A., GIORDANO, A. & IOZZO, R. V. 1996. Decorin-induced growth suppression is associated with up-regulation of p21, an inhibitor of cyclin-dependent kinases. *J Biol Chem,* 271**,** 18961-5.

DE WAARD, P., VLIEGENTHART, J. F., HARADA, T. & SUGAHARA, K. 1992. Structural studies on sulfated oligosaccharides derived from the carbohydrate-protein linkage region of chondroitin 6-sulfate proteoglycans of shark cartilage. II. Seven compounds containing 2 or 3 sulfate residues. *J Biol Chem,* 267**,** 6036-43.

DEEPA, S. S., UMEHARA, Y., HIGASHIYAMA, S., ITOH, N. & SUGAHARA, K. 2002. Specific molecular interactions of oversulfated chondroitin sulfate E with various heparin-binding growth factors. Implications as a physiological binding partner in the brain and other tissues. *J Biol Chem,* 277**,** 43707-16.

DEGLI ESPOSTI, M. & DIVE, C. 2003. Mitochondrial membrane permeabilisation by Bax/Bak. *Biochem Biophys Res Commun,* 304**,** 455-461.

DEL PESO, L., GONZALEZ-GARCIA, M., PAGE, C., HERRERA, R. & NUNEZ, G. 1997. Interleukin-3-induced phosphorylation of BAD through the protein kinase Akt. *Science,* 278**,** 687-9.

DELLAS, A., SCHULTHEISS, E., LEIVAS, M., MOCH, H. & TORHORST, J. 1998. Association of p27Kip1, cyclin E and c-myc expression with progression and prognosis in HPV-positive cervical neoplasms.

. *Anticancer Research,* 18**,** 3991-3998.

DENARDO, D. G., ANDREU, P. & COUSSENS, L. M. 2010. Interactions between lymphocytes and myeloid cells regulate pro- versus anti-tumor immunity. *Cancer Metastasis Rev,* 29**,** 309-16.

DI COSIMO, S. & BASELGA, J. 2010. Management of breast cancer with targeted agents: importance of heterogeneity. [corrected]. *Nat Rev Clin Oncol,* 7**,** 139-47.

DIMOVA, D. & DYSON, N. 2005. The E2F transcriptional network: old acquaintances with new faces. *Oncogene,* 24**,** 2810-2826.

DM, L. & YM, F. 2011. Signaling mechanism of cell adhesion molecules in breast cancer metastasis: potential therapeutic targets. *Breast Cancer Res Treat,* 128**,** 7-21.

DOEGE, K. J., GARRISON, K., COULTER, S. N. & YAMADA, Y. 1994. The structure of the rat aggrecan gene and preliminary characterization of its promoter. *J Biol Chem,* 269**,** 29232-40.

DOMCHEK, S. M., FRIEBEL, T. M., SINGER, C. F., EVANS, D. G., LYNCH, H. T., ISAACS, C., GARBER, J. E., NEUHAUSEN, S. L., MATLOFF, E., EELES, R., PICHERT, G., VAN T'VEER, L., TUNG, N., WEITZEL, J. N., COUCH, F. J., RUBINSTEIN, W. S., GANZ, P. A., DALY, M. B., OLOPADE, O. I., TOMLINSON, G., SCHILDKRAUT, J., BLUM, J. L. & REBBECK, T. R. 2010. Association of risk-reducing surgery in BRCA1 or BRCA2 mutation carriers with cancer risk and mortality. *JAMA,* 304**,** 967-75.

DOMINGUEZ-MONZON, G., BENITEZ, J., VERGARA, P., LORENZANA, R. & SEGOVIA, J. 2009. Gas1 inhibits cell proliferation and induces apoptosis of human primary gliomas in the absence of Shh. *International Journal of Developmental Neuroscience,* 27**,** 305-313.

DOURS-ZIMMERMANN, M. T. & ZIMMERMANN, D. R. 1994. A novel glycosaminoglycan attachment domain identified in two alternative splice variants of human versican. *J Biol Chem,* 269**,** 32992-8.

DOWNWARD, J. 2003. Targeting RAS singalling pathways in cancer therapy. *Nature Reviews, Cancer.,* 3**,** 11-22.

DOWNWARD, J. June 1999. How BAD phosphorylation is good for survival. *Nature cell Biology.*

DOWSETT, M., CUZICK, J., WALE, C., HOWELL, T., HOUGHTON, J. & BAUM, M. 2005. Retrospective analysis of time to recurrence in the ATAC trial according to hormone receptor status: an hypothesis-generating study. *J Clin Oncol,* 23**,** 7512-7.

DUFFY, S. W., TABAR, L., CHEN, H. H., HOLMQVIST, M., YEN, M. F., ABDSALAH, S., EPSTEIN, B., FRODIS, E., LJUNGBERG, E., HEDBORG-MELANDER, C., SUNDBOM, A., THOLIN, M., WIEGE, M., AKERLUND, A., WU, H. M., TUNG, T. S., CHIU, Y. H., CHIU, C. P., HUANG, C. C., SMITH, R. A., ROSEN, M., STENBECK, M. & HOLMBERG, L. 2002. The impact of organized mammography service screening on breast carcinoma mortality in seven Swedish counties. *Cancer,* 95**,** 458-69.

DUFFY, S. W., TABAR, L., OLSEN, A. H., VITAK, B., ALLGOOD, P. C., CHEN, T. H., YEN, A. M. & SMITH, R. A. 2010. Absolute numbers of lives saved and overdiagnosis in breast cancer screening, from a randomized trial and from the Breast Screening Programme in England. *J Med Screen,* 17**,** 25-30.

DVORAK, H. F. 1986. Tumors: wounds that do not heal. Similarities between tumor stroma generation and wound healing. *N Engl J Med,* 315**,** 1650-9.

EDGE, S. B., BYRD, D. R., COMPTON, C. C., FRITZ, A. G., GREENE, F. L. & TROTTI, A. 2011. *AJCC Cancer Staging Manual,* New York, Springer.

EGEBLAD, M., NAKASONE, E. S. & WERB, Z. 2010. Tumors as organs: complex tissues that interface with the entire organism. *Dev Cell,* 18**,** 884-901.

ELLEGE RM, A. D. 2004. *Diseases of the breast.,* Philadelphia, Lippincott Williams & Wilkins.

ELNEMR, A., OHTA, T., YACHIE, A., KAYAHARA, M., KITAGAWA, H., NINOMIYA, I., FUSHIDA, S., FUJIMURA, T., NISHIMURA, G., SHIMIZU, K. & MIWA, K. 2001. Human pancreatic cancer cells express non-functional Fas receptors and counterattack lymphocytes by expressing Fas ligand; a potential mechanism for immune escape. *International journal of oncology,* 18**,** 33-39.

ELSTON, C. W. & ELLIS, I. O. 1991. Pathological prognostic factors in breast cancer. I. The value of histological grade in breast cancer: experience from a large study with long-term follow-up. *Histopathology,* 19**,** 403-10.

ENGLISH, A. W. 2005. Enhancing axon regeneration in peripheral nerves also increases functionally inappropriate reinnervation of targets. *J Comp Neurol,* 490**,** 427-41.

ESPOSTI, M. 2002. Lipids, cardiolipin and apoptosis: a greasy licence to kill. *Cell death and differentiation,* 9**,** 234-236.

EVERS, M. R., XIA, G., KANG, H. G., SCHACHNER, M. & BAENZIGER, J. U. 2001. Molecular cloning and characterization of a dermatan-specific N-acetylgalactosamine 4-O-sulfotransferase. *J Biol Chem,* 276**,** 36344-53.

FEIG, S. A. 1994. Mammographic screening of women aged 40 to 49 years. Is it justified? *Obstet Gynecol Clin North Am,* 21**,** 587-606.

FISHER, L. W., TERMINE, J. D. & YOUNG, M. F. 1989. Deduced protein sequence of bone small proteoglycan I (biglycan) shows homology with proteoglycan II (decorin) and several nonconnective tissue proteins in a variety of species. *J Biol Chem,* 264**,** 4571-6.

FITZGIBBONS, P. L., PAGE, D. L., WEAVER, D., THOR, A. D., ALLRED, D. C., CLARK, G. M., RUBY, S. G., O'MALLEY, F., SIMPSON, J. F., CONNOLLY, J. L., HAYES, D. F., EDGE, S. B., LICHTER, A. & SCHNITT,

S. J. 2000. Prognostic factors in breast cancer. College of American Pathologists Consensus Statement 1999. *Arch Pathol Lab Med,* 124**,** 966-78.

FRANSSON, L. A., SILVERBERG, I. & CARLSTEDT, I. 1985. Structure of the heparan sulfate-protein linkage region. Demonstration of the sequence galactosyl-galactosyl-xylose-2-phosphate. *J Biol Chem,* 260**,** 14722-6.

FREDERICK, M. J., HENDERSON, Y., XU, X., DEAVERS, M. T., SAHIN, A. A., WU, H., LEWIS, D. E., EL-NAGGAR, A. K. & CLAYMAN, G. L. 2000. In vivo expression of the novel CXC chemokine BRAK in normal and cancerous human tissue. *Am J Pathol,* 156**,** 1937-50.

FREEDMAN, A. N., GRAUBARD, B. I., RAO, S. R., MCCASKILL-STEVENS, W., BALLARD-BARBASH, R. & GAIL, M. H. 2003. Estimates of the number of US women who could benefit from tamoxifen for breast cancer chemoprevention. *J Natl Cancer Inst,* 95**,** 526-32.

FROLOV, M. & DYSON, N. 2004. Molecular mechanisms of E2F-dependent activation and pRB-mediated repression. *Journal of Cell Science,* 117**,** 2173-2181.

FUKUTA, M., KOBAYASHI, Y., UCHIMURA, K., KIMATA, K. & HABUCHI, O. 1998. Molecular cloning and expression of human chondroitin 6-sulfotransferase. *Biochim Biophys Acta,* 1399**,** 57-61.

FUNDERBURGH, J. L. 2000. Keratan sulfate: structure, biosynthesis, and function. *Glycobiology,* 10**,** 951-8.

FUQUA SAW, S. S. 2004. *Diseases of the Breast.,* Lipincott Williams & Wilkins.

GACK, M., SHIN, Y., JOO, C., URANO, T., LIANG, C., SUN, L., TAKEUCHI, O., AKIRA, S., CHEN, Z., INOUE, S. & JUNG, J. 2007. TRIM25 RING-finger E3 ubiquitin ligase is essential for RIG-I-mediated antiviral activity. *Nature,* 446**,** 916-920.

GARCIA-RUIZ, C., COLELL, A., MORALES, A., CALVO, M., ENRICH, C. & FERNANDEZ-CHECA, J. 2002. Trafficking of ganglioside GD3 to mitochondria by tumor necrosis factor-alpha. *The journal of Biological Chemistry,* 277**,** 36443-36448.

GOSS, P. E., INGLE, J. N., MARTINO, S., ROBERT, N. J., MUSS, H. B., PICCART, M. J., CASTIGLIONE, M., TU, D., SHEPHERD, L. E., PRITCHARD, K. I., LIVINGSTON, R. B., DAVIDSON, N. E., NORTON, L., PEREZ, E. A., ABRAMS, J. S., CAMERON, D. A., PALMER, M. J., PATER, J. L. & NATIONAL CANCER INSTITUTE OF CANADA CLINICAL TRIALS GROUP, M. A. 2007. Efficacy of letrozole extended adjuvant therapy according to estrogen receptor and progesterone receptor status of the primary tumor: National Cancer Institute of Canada Clinical Trials Group MA.17. *J Clin Oncol,* 25**,** 2006-11.

GOTOH, M., SATO, T., AKASHIMA, T., IWASAKI, H., KAMEYAMA, A., MOCHIZUKI, H., YADA, T., INABA, N., ZHANG, Y., KIKUCHI, N., KWON, Y. D., TOGAYACHI, A., KUDO, T., NISHIHARA, S., WATANABE, H., KIMATA, K. & NARIMATSU, H. 2002a. Enzymatic synthesis of chondroitin with a novel chondroitin sulfate N-acetylgalactosaminyltransferase that transfers N-acetylgalactosamine to glucuronic acid in initiation and elongation of chondroitin sulfate synthesis. *J Biol Chem,* 277**,** 38189-96.

GOTOH, M., YADA, T., SATO, T., AKASHIMA, T., IWASAKI, H., MOCHIZUKI, H., INABA, N., TOGAYACHI, A., KUDO, T., WATANABE, H., KIMATA, K. & NARIMATSU, H. 2002b. Molecular cloning and characterization of a novel chondroitin sulfate glucuronyltransferase that transfers glucuronic acid to N-acetylgalactosamine. *J Biol Chem,* 277**,** 38179-88.

GRAHAM, R. A., LI, T. C., COOKE, I. D. & APLIN, J. D. 1994. Keratan sulphate as a secretory product of human endometrium: cyclic expression in normal women. *Hum Reprod,* 9**,** 926-30.

GREGORY, P., BERT, A., PATERSON, E., BARRY, S., TSYKIN, A., FARSHID, G., VADAS, M., KHEW-GOODALL, Y. & GOODALL, G. 2008. The miR-200 family and miR-205 regulate epithelial to mesenchymal transition by targeting ZEB1 and SP1. *Nature cell biology,* 10.

GRIVENNIKOV, S. I. & KARIN, M. 2010. Inflammation and oncogenesis: a vicious connection. *Curr Opin Genet Dev,* 20**,** 65-71.

GU, X. L., OU, Z. L., LIN, F. J., YANG, X. L., LUO, J. M., SHEN, Z. Z. & SHAO, Z. M. 2012. Expression of CXCL14 and its anticancer role in breast cancer. *Breast Cancer Res Treat,* 135**,** 725-35.

GUARINO, M. 2007. Epithelial–mesenchymal transition and tumour invasion. *The international journal of biochemistry and cell biology,* 39**,** 2153-2160.

GUINEBRETIERE, J. M., MENET, E., TARDIVON, A., CHEREL, P. & VANEL, D. 2005. Normal and pathological breast, the histological basis. *Eur J Radiol,* 54**,** 6-14.

GUO, W. & GIANCOTTI, F. 2004. Integrin signalling during tumour progression. *Nature Reviews Molecular Cell Biology,* 5**,** 816-826.

HAMAJIMA, N., HIROSE, K., TAJIMA, K., ROHAN, T., CALLE, E. E., HEATH, C. W., JR., COATES, R. J., LIFF, J. M., TALAMINI, R., CHANTARAKUL, N., KOETSAWANG, S., RACHAWAT, D., MORABIA, A., SCHUMAN, L., STEWART, W., SZKLO, M., BAIN, C., SCHOFIELD, F., SISKIND, V., BAND, P., COLDMAN, A. J., GALLAGHER, R. P., HISLOP, T. G., YANG, P., KOLONEL, L. M., NOMURA, A. M., HU, J., JOHNSON, K. C., MAO, Y., DE SANJOSE, S., LEE, N., MARCHBANKS, P., ORY, H. W., PETERSON, H. B., WILSON, H. G., WINGO, P. A., EBELING, K., KUNDE, D., NISHAN, P., HOPPER, J. L., COLDITZ, G.,

GAJALANSKI, V., MARTIN, N., PARDTHAISONG, T., SILPISORNKOSOL, S., THEETRANONT, C., BOOSIRI, B., CHUTIVONGSE, S., JIMAKORN, P., VIRUTAMASEN, P., WONGSRICHANALAI, C., EWERTZ, M., ADAMI, H. O., BERGKVIST, L., MAGNUSSON, C., PERSSON, I., CHANG-CLAUDE, J., PAUL, C., SKEGG, D. C., SPEARS, G. F., BOYLE, P., EVSTIFEEVA, T., DALING, J. R., HUTCHINSON, W. B., MALONE, K., NOONAN, E. A., STANFORD, J. L., THOMAS, D. B., WEISS, N. S., WHITE, E., ANDRIEU, N., BREMOND, A., CLAVEL, F., GAIRARD, B., LANSAC, J., PIANA, L., RENAUD, R., IZQUIERDO, A., VILADIU, P., CUEVAS, H. R., ONTIVEROS, P., PALET, A., SALAZAR, S. B., ARISTIZABEL, N., CUADROS, A., TRYGGVADOTTIR, L., TULINIUS, H., BACHELOT, A., LE, M. G., PETO, J., FRANCESCHI, S., LUBIN, F., MODAN, B., RON, E., WAX, Y., FRIEDMAN, G. D., HIATT, R. A., LEVI, F., BISHOP, T., KOSMELJ, K., et al. 2002. Alcohol, tobacco and breast cancer--collaborative reanalysis of individual data from 53 epidemiological studies, including 58,515 women with breast cancer and 95,067 women without the disease. *Br J Cancer,* 87**,** 1234-45.

HANAHAN, D. & WEINBERG, R. A. 2011. Hallmarks of cancer: the next generation. *Cell,* 144**,** 646-74.

HARADA, H., BECKNELL, B., WILM, M., MANN, M., HUANG, L. J., TAYLOR, S. S., SCOTT, J. D. & KORSMEYER, S. J. 1999. Phosphorylation and inactivation of BAD by mitochondria-anchored protein kinase A. *Mol Cell,* 3**,** 413-22.

HENDERSON, B. E., ROSS, R. K., JUDD, H. L., KRAILO, M. D. & PIKE, M. C. 1985. Do regular ovulatory cycles increase breast cancer risk? *Cancer,* 56**,** 1206-8.

HIRAOKA, N., NAKAGAWA, H., ONG, E., AKAMA, T. O., FUKUDA, M. N. & FUKUDA, M. 2000. Molecular cloning and expression of two distinct human chondroitin 4-O-sulfotransferases that belong to the HNK-1 sulfotransferase gene family. *J Biol Chem,* 275**,** 20188-96.

HORTOBAGYI, G. N. 1998. Treatment of breast cancer. *N Engl J Med,* 339**,** 974-84.

HROMAS, R., BROXMEYER, H. E., KIM, C., NAKSHATRI, H., CHRISTOPHERSON, K., 2ND, AZAM, M. & HOU, Y. H. 1999. Cloning of BRAK, a novel divergent CXC chemokine preferentially expressed in normal versus malignant cells. *Biochem Biophys Res Commun,* 255**,** 703-6.

HYNES, R. 2002. Integrins: bidirectional, allosteric signaling machines. 110**,** 673-687.

IIDA, J., WILHELMSON, K. L., NG, J., LEE, P., MORRISON, C., TAM, E., OVERALL, C. M. & MCCARTHY, J. B. 2007. Cell surface chondroitin sulfate glycosaminoglycan in melanoma: role in the activation of pro-MMP-2 (pro-gelatinase A). *Biochem J,* 403**,** 553-63.

IOZZO, R. V. 1998. Matrix proteoglycans: from molecular design to cellular function. *Annu Rev Biochem,* 67**,** 609-52.

IZUMIKAWA, T., KOIKE, T., SHIOZAWA, S., SUGAHARA, K., TAMURA, J. & KITAGAWA, H. 2008. Identification of chondroitin sulfate glucuronyltransferase as chondroitin synthase-3 involved in chondroitin polymerization: chondroitin polymerization is achieved by multiple enzyme complexes consisting of chondroitin synthase family members. *J Biol Chem,* 283**,** 11396-406.

JACKSON, A. L., BURCHARD, J., LEAKE, D., REYNOLDS, A., SCHELTER, J., GUO, J., JOHNSON, J. M., LIM, L., KARPILOW, J., NICHOLS, K., MARSHALL, W., KHVOROVA, A. & LINSLEY, P. S. 2006. Position-specific chemical modification of siRNAs reduces "off-target" transcript silencing. *RNA,* 12**,** 1197-205.

JACKSON, D. G. 2009. Immunological functions of hyaluronan and its receptors in the lymphatics. *Immunol Rev,* 230**,** 216-31.

JACOBSEN, B. M., RICHER, J. K., SARTORIUS, C. A. & HORWITZ, K. B. 2003. Expression profiling of human breast cancers and gene regulation by progesterone receptors. *J Mammary Gland Biol Neoplasia,* 8**,** 257-68.

JAMES, L., KEEBLE, A., KHAN, Z., RHODES, D. & TROWSDALE, J. 2007. Structural basis for PRYSPRY-mediated tripartite motif (TRIM) protein function. *Proceedings of the National Academy of Sciences of the United States of America,* 104**,** 6200-6205.

JIANG, D., LIANG, J., CAMPANELLA, G. S., GUO, R., YU, S., XIE, T., LIU, N., JUNG, Y., HOMER, R., MELTZER, E. B., LI, Y., TAGER, A. M., GOETINCK, P. F., LUSTER, A. D. & NOBLE, P. W. 2010. Inhibition of pulmonary fibrosis in mice by CXCL10 requires glycosaminoglycan binding and syndecan-4. *J Clin Invest,* 120**,** 2049-57.

JOHANSSON, M., DENARDO, D. G. & COUSSENS, L. M. 2008. Polarized immune responses differentially regulate cancer development. *Immunol Rev,* 222**,** 145-54.

JOSEPH, B., ANDERSSON, E., VLACHOS, P., SODERSTEN, E., LIU, L., TEIXEIRA, A. & HERMANSON, O. 2009. p57Kip2 is a repressor of Mash1 activity and neuronal differentiation in neural stem cells. *Cell death and differentiation,* 16**,** 1256-1265.

KAGESHITA, T., JOHNO, M., ONO, T., ARAO, T. & IMAI, K. 1985. Immunohistological detection of human malignant melanoma using monoclonal antibody to a melanoma-associated antigen. *Arch Dermatol Res,* 277**,** 334-6.

KALATHAS, D., THEOCHARIS, D. A., BOUNIAS, D., KYRIAKOPOULOU, D., PAPAGEORGAKOPOULOU, N., STAVROPOULOS, M. S. & VYNIOS, D. H. 2011. Chondroitin synthases I,

II, III and chondroitin sulfate glucuronyltransferase expression in colorectal cancer. *Mol Med Report,* 4**,** 363-8.

KANG, H. G., EVERS, M. R., XIA, G., BAENZIGER, J. U. & SCHACHNER, M. 2002. Molecular cloning and characterization of chondroitin-4-O-sulfotransferase-3. A novel member of the HNK-1 family of sulfotransferases. *J Biol Chem,* 277**,** 34766-72.

KARAMANOS, N. K., VANKY, P., TZANAKAKIS, G. N., TSEGENIDIS, T. & HJERPE, A. 1997. Ion-pair high-performance liquid chromatography for determining disaccharide composition in heparin and heparan sulphate. *J Chromatogr A,* 765**,** 169-79.

KAWASHIMA, H., ATARASHI, K., HIROSE, M., HIROSE, J., YAMADA, S., SUGAHARA, K. & MIYASAKA, M. 2002. Oversulfated chondroitin/dermatan sulfates containing GlcAbeta1/IdoAalpha1-3GalNAc(4,6-O-disulfate) interact with L- and P-selectin and chemokines. *J Biol Chem,* 277**,** 12921-30.

KAWASHIMA, H., HIROSE, M., HIROSE, J., NAGAKUBO, D., PLAAS, A. H. & MIYASAKA, M. 2000. Binding of a large chondroitin sulfate/dermatan sulfate proteoglycan, versican, to L-selectin, P-selectin, and CD44. *J Biol Chem,* 275**,** 35448-56.

KEEBLE, A., KHAN, Z., FORSTER, A. & JAMES, L. 2008. TRIM21 is an IgG receptor that is structurally, thermodynamically, and kinetically conserved. *Proc Natl Acad Sci U S A,* 105**,** 6045-6050.

KEEN, J. C. & DAVIDSON, N. E. 2003. The biology of breast carcinoma. *Cancer,* 97**,** 825-33.

KELLY, G. S. 1998. The role of glucosamine sulfate and chondroitin sulfates in the treatment of degenerative joint disease. *Altern Med Rev,* 3**,** 27-39.

KELSEY, J. L. & BERNSTEIN, L. 1996. Epidemiology and prevention of breast cancer. *Annu Rev Public Health,* 17**,** 47-67.

KERR, J., WINTERFORD, C. & HARMON, B. 1994. Apoptosis. Its significance in cancer and cancer therapy. *Cancer* 73**,** 2013-2026.

KHATAMIANFAR, V., VALIYEVA, F., RENNIE, P. S., LU, W. Y., YANG, B. B., BAUMAN, G. S., MOUSSA, M. & XUAN, J. W. 2012. TRIM59, a novel multiple cancer biomarker for immunohistochemical detection of tumorigenesis. *BMJ Open,* 2.

KITAGAWA, H., IZUMIKAWA, T., UYAMA, T. & SUGAHARA, K. 2003. Molecular cloning of a chondroitin polymerizing factor that cooperates with chondroitin synthase for chondroitin polymerization. *J Biol Chem,* 278**,** 23666-71.

KITAGAWA, H., UYAMA, T. & SUGAHARA, K. 2001. Molecular cloning and expression of a human chondroitin synthase. *J Biol Chem,* 276**,** 38721-6.

KLOLESNICK, R. & KRONKE, M. 1998. Regulation of ceramide production and apoptosis. *Annual review of physiology,* 60.

KOBAYASHI, M., SUGUMARAN, G., LIU, J., SHWORAK, N. W., SILBERT, J. E. & ROSENBERG, R. D. 1999. Molecular cloning and characterization of a human uronyl 2-sulfotransferase that sulfates iduronyl and glucuronyl residues in dermatan/chondroitin sulfate. *J Biol Chem,* 274**,** 10474-80.

KOUVARAKI, M., GORGOULIS, V., RASSIDAKIS, G., LIODIS, P., MARKOPOULOS, C., GOGAS, J. & KITTAS, C. 2002. High expression levels of p27 correlate with lymph node status in a subset of advanced invasive breast carcinomas. *Cancer,* 94**,** 2454-2465.

KOUVIDI, K., BERDIAKI, A., NIKITOVIC, D., KATONIS, P., AFRATIS, N., HASCALL, V. C., KARAMANOS, N. K. & TZANAKAKIS, G. N. 2011. Role of receptor for hyaluronic acid-mediated motility (RHAMM) in low molecular weight hyaluronan (LMWHA)-mediated fibrosarcoma cell adhesion. *J Biol Chem,* 286**,** 38509-20.

KUAN, C., WIKSTRAND, C. & BIGNER, D. 2001. EGF mutant receptor vIII as a molecular target in cancer therapy. *Endocrine-related cancer,* 8.

KURTH, I., WILLIMANN, K., SCHAERLI, P., HUNZIKER, T., CLARK-LEWIS, I. & MOSER, B. 2001. Monocyte selectivity and tissue localization suggests a role for breast and kidney-expressed chemokine (BRAK) in macrophage development. *J Exp Med,* 194**,** 855-61.

KUSCHERT, G. S., COULIN, F., POWER, C. A., PROUDFOOT, A. E., HUBBARD, R. E., HOOGEWERF, A. J. & WELLS, T. N. 1999. Glycosaminoglycans interact selectively with chemokines and modulate receptor binding and cellular responses. *Biochemistry,* 38**,** 12959-68.

KUWANA, T., MACKEY, M., PERKINS, G., ELLISMAN, M., LATTERICH, M., SCHNEITER, R., GREEN, D. & NEWMEYER, D. 2002. Bid, Bax, and lipids cooperate to form supramolecular openings in the outer mitochondrial membrane. *Cell* 111**,** 331-342.

LABROPOULOU, V. T., THEOCHARIS, A. D., RAVAZOULA, P., PERIMENIS, P., HJERPE, A., KARAMANOS, N. K. & KALOFONOS, H. P. 2006. Versican but not decorin accumulation is related to metastatic potential and neovascularization in testicular germ cell tumours. *Histopathology,* 49**,** 582-93.

LE CLAINCHE, C. & CARLIER, M. F. 2008. Regulation of actin assembly associated with protrusion and adhesion in cell migration. *Physiol Rev,* 88**,** 489-513.

LEBARON, R. G., ESKO, J. D., WOODS, A., JOHANSSON, S. & HOOK, M. 1988. Adhesion of glycosaminoglycan-deficient chinese hamster ovary cell mutants to fibronectin substrata. *J Cell Biol,* 106**,** 945-52.

LEBARON, R. G., ZIMMERMANN, D. R. & RUOSLAHTI, E. 1992. Hyaluronate binding properties of versican. *J Biol Chem,* 267**,** 10003-10.

LEE, H., L, C., KY, C., TT, K., EY, L. & W, H. 2014. Singapore Cancer Registry Interim Annual Registry Report- Trends in Cancer Incidence in Singapore 2009-2013.

LERNER, M., CORCORAN, M., CEPEDA, D., NIELSEN, M., ZUBAREV, R., PONTEN, F., UHLEN, M., HOBER, S., GRANDER, D. & SANGFELT, O. 2007. The RBCC gene RFP2 (Leu5) encodes a novel transmembrane E3 ubiquitin ligase invloved in ERAD. *Molecular biology of the cell,* 18**,** 1670-1682.

LETAI, A. 2008. Diagnosing and exploiting cancer's addiction to blocks in apoptosis. *Nature Reviews, Cancer.,* 8**,** 121-132.

LETAI, A., BASSIK, M., WALENSKY, L., SORCINELLI, M., WEILER, S. & KORSMEYER, S. 2002a. Distinct BH3 domains either sensitize or activate mitochondrial apoptosis, serving as prototype cancer therapeutics. *Cancer Cell,* 2**,** 183-192.

LETAI, A., BASSIK, M., WALENSKY, L., SORCINELLI, M., WEILER, S. & KORSMEYER, S. 2002b. Distinct BH3 domains either sensitize or activate mitochondrial apoptosis, serving as prototype cancer therapeutics. *Cancer cell,* 2**,** 183-192.

LI, Y., BARBASH, O. & DIEHL, J. A. 2015. Regulation of the cell cycle. *The molecular basis of cancer.* 4 ed. Phiadelphia, PA: Saunders/Elsevier.

LIU, Z., LU, H., JIANG, Z., PASTUSZYN, A. & HU, C. A. 2005. Apolipoprotein L6, a novel proapoptotic Bcl-2 homology 3-only protein, induces mitochondria-mediated apoptosis in cancer cells. *Mol Cancer Res,* 3**,** 21-31.

LOPEZ-RAMIREZ, M., DOMINGUEZ-MONZON, G., VERGARA, P. & SEGOVIA, J. 2008. Gas1 reduces Ret tyrosine 1062 phosphorylation and alters GDNF-mediated intracellular signaling. *International Journal of Developmental Neuroscience,* 26**,** 497-503.

LOVE, R. R., DUC, N. B., ALLRED, D. C., BINH, N. C., DINH, N. V., KHA, N. N., THUAN, T. V., MOHSIN, S. K., ROANH LE, D., KHANG, H. X., TRAN, T. L., QUY, T. T., THUY, N. V., THE, P. N., CAU, T. T., TUNG, N. D., HUONG, D. T., QUANG LE, M., HIEN, N. N., THUONG, L., SHEN, T. Z., XIN, Y., ZHANG, Q., HAVIGHURST, T. C., YANG, Y. F., HILLNER, B. E. & DEMETS, D. L. 2002. Oophorectomy and tamoxifen adjuvant therapy in premenopausal Vietnamese and Chinese women with operable breast cancer. *J Clin Oncol,* 20**,** 2559-66.

LUSTER, A. D., GREENBERG, S. M. & LEDER, P. 1995. The IP-10 chemokine binds to a specific cell surface heparan sulfate site shared with platelet factor 4 and inhibits endothelial cell proliferation. *J Exp Med,* 182**,** 219-31.

MACCARANA, M., OLANDER, B., MALMSTROM, J., TIEDEMANN, K., AEBERSOLD, R., LINDAHL, U., LI, J. P. & MALMSTROM, A. 2006. Biosynthesis of dermatan sulfate: chondroitin-glucuronate C5-epimerase is identical to SART2. *J Biol Chem,* 281**,** 11560-8.

MALAVAKI, C. J., THEOCHARIS, A. D., LAMARI, F. N., KANAKIS, I., TSEGENIDIS, T., TZANAKAKIS, G. N. & KARAMANOS, N. K. 2011. Heparan sulfate: biological significance, tools for biochemical analysis and structural characterization. *Biomed Chromatogr,* 25**,** 11-20.

MALLON, E., OSIN, P., NASIRI, N., BLAIN, I., HOWARD, B. & GUSTERSON, B. 2000. The basic pathology of human breast cancer. *J Mammary Gland Biol Neoplasia,* 5**,** 139-63.

MAO, Y., KELLER, E. T., GARFIELD, D. H., SHEN, K. & WANG, J. 2013. Stromal cells in tumor microenvironment and breast cancer. *Cancer Metastasis Rev,* 32**,** 303-315.

MARGOLIS, R. U. & MARGOLIS, R. K. 1997. Chondroitin sulfate proteoglycans as mediators of axon growth and pathfinding. *Cell Tissue Res,* 290**,** 343-8.

MAROUDAS, A., MUIR, H. & WINGHAM, J. 1969. The correlation of fixed negative charge with glycosaminoglycan content of human articular cartilage. *Biochim Biophys Acta,* 177**,** 492-500.

MATSUOKAM, S., MC, E., BAI, C., PARKER, S. H., ZHANG, P., BALDINI, A., HARPER, J. & ELLEDGE, S. 1995. p57KIP2, a structurally distinct member of the p21CIP1 Cdk inhibitor family, is a candidate tumor suppressor gene. *Genes & development,* 9.

MAZHAR, D. & WAXMAN, J. 2006. Dietary fat and breast cancer. *QJM,* 99**,** 469-73.

MCALLISTER, S., BECKER-HAPAK, M., PINTUCCI, G., PAGANO, M. & DOWDY, S. 2003. Overexpression of p27 induces cell scattering,

independently of its ability to bind the cyclin-CDK complex. Hepatocyte growth factor (HGF) stimulation induced p27 phosphorylation on Ser10 and its cytoplasmic translocation, which was required for cell scattering. *Molecular and cellular biology,* 23**,** 216-228.

MCKINNON, C. M., LYGOE, K. A., SKELTON, L., MITTER, R. & MELLOR, H. 2008. The atypical Rho GTPase RhoBTB2 is required for expression of the chemokine CXCL14 in normal and cancerous epithelial cells. *Oncogene,* 27**,** 6856-65.

MENDELSOHN, J. & BASELGA, J. 2000. The EGF receptor family as targets for cancer therapy. *Oncogene,* 19**,** 6550-6565.

MILITSOPOULOU, M., LAMARI, F. N., HJERPE, A. & KARAMANOS, N. K. 2002. Determination of twelve heparin- and heparan sulfate-derived disaccharides as 2-aminoacridone derivatives by capillary zone electrophoresis using ultraviolet and laser-induced fluorescence detection. *Electrophoresis,* 23**,** 1104-9.

MIYASHITA, T., KRAJEWSKI, S., KRAJEWSKA, M., WANG, H., LIN, H., LIEBERMANN, D., HOFFMANN, B. & REED, J. 1994. Tumor suppressor p53 is a regulator of bcl-2 and bax gene expression in vitro and in vivo. *Oncogene,* 9**,** 1799-1805.

MJAATVEDT, C. H., YAMAMURA, H., CAPEHART, A. A., TURNER, D. & MARKWALD, R. R. 1998. The Cspg2 gene, disrupted in the hdf mutant, is required for right cardiac chamber and endocardial cushion formation. *Dev Biol,* 202**,** 56-66.

MK, W., MA, T., BJ, S. & WP, S. 2011. Down-regulation of epithelial cadherin is required to initiate metastatic outgrowth of breast cancer. . *Molecular biology of the cell,* 22**,** 2423-2235.

MOHSIN, S. K., WEISS, H., HAVIGHURST, T., CLARK, G. M., BERARDO, M., ROANH LE, D., TO, T. V., QIAN, Z., LOVE, R. R. & ALLRED, D. C. 2004. Progesterone receptor by immunohistochemistry and clinical outcome in breast cancer: a validation study. *Mod Pathol,* 17**,** 1545-54.

MONZAVI-KARBASSI, B., STANLEY, J. S., HENNINGS, L., JOUSHEGHANY, F., ARTAUD, C., SHAAF, S. & KIEBER-EMMONS, T. 2007. Chondroitin sulfate glycosaminoglycans as major P-selectin ligands on metastatic breast cancer cell lines. *Int J Cancer,* 120**,** 1179-91.

MOSES, J., OLDBERG, A., CHENG, F. & FRANSSON, L. A. 1997. Biosynthesis of the proteoglycan decorin--transient 2-phosphorylation of xylose during formation of the trisaccharide linkage region. *Eur J Biochem,* 248**,** 521-6.

MOSES, J., OLDBERG, A. & FRANSSON, L. A. 1999. Initiation of galactosaminoglycan biosynthesis. Separate galactosylation and dephosphorylation pathways for phosphoxylosylated decorin protein and exogenous xyloside. *Eur J Biochem,* 260**,** 879-84.

MURDOCH, C., MUTHANA, M., COFFELT, S. B. & LEWIS, C. E. 2008. The role of myeloid cells in the promotion of tumour angiogenesis. *Nat Rev Cancer,* 8**,** 618-31.

NICOLA, V. 2006. *Chondroitin sulfate: structure, role and pharmacological activity*, Elsevier.

NIKITOVIC, D., ASSOUTI, M., SIFAKI, M., KATONIS, P., KRASAGAKIS, K., KARAMANOS, N. K. & TZANAKAKIS, G. N. 2008. Chondroitin sulfate and heparan sulfate-containing proteoglycans are both partners and targets of basic fibroblast growth factor-mediated proliferation in human metastatic melanoma cell lines. *Int J Biochem Cell Biol,* 40**,** 72-83.

NILSSON, I. & HOFFMANN, I. 2000. Cell cycle regulation by the Cdc25 phosphatase family. *Progress in cell cycle research,* 4**,** 107-114.

NISHIYAMA, A., DAHLIN, K. J., PRINCE, J. T., JOHNSTONE, S. R. & STALLCUP, W. B. 1991. The primary structure of NG2, a novel membrane-spanning proteoglycan. *J Cell Biol,* 114**,** 359-71.

ODA, G., SATO, T., ISHIKAWA, T., KAWACHI, H., NAKAGAWA, T., KUWAYAMA, T., ISHIGURO, M., IIDA, S., UETAKE, H. & SUGIHARA, K. 2012. Significance of stromal decorin expression during the progression of breast cancer. *Oncol Rep,* 28**,** 2003-8.

OHTAKE, S., ITO, Y., FUKUTA, M. & HABUCHI, O. 2001. Human N-acetylgalactosamine 4-sulfate 6-O-sulfotransferase cDNA is related to human B cell recombination activating gene-associated gene. *J Biol Chem,* 276**,** 43894-900.

OZATO, K., SHIN, D., CHANG, T. & 3RD, M. H. 2008. TRIM family proteins and their emerging roles in innate immunity. *Nature Reviews. Immunology.,* 8**,** 849-860.

OZERDEM, U., GRAKO, K. A., DAHLIN-HUPPE, K., MONOSOV, E. & STALLCUP, W. B. 2001. NG2 proteoglycan is expressed exclusively by mural cells during vascular morphogenesis. *Dev Dyn,* 222**,** 218-27.

P.O'MALLEY, F. & E.PINDER, S. 2006. *Breast Pathology,* Edinburgh, Elsevier.

PARK, C. R., YOU, D. J., KIM, D. K., MOON, M. J., LEE, C., OH, S. H., AHN, C., SEONG, J. Y. & HWANG, J. I. 2013. CXCL14 enhances proliferation and migration of NCI-H460 human lung cancer cells overexpressing the glycoproteins containing heparan sulfate or sialic acid. *J Cell Biochem,* 114**,** 1084-96.

PATEL, A. V., CALLEL, E. E., BERNSTEIN, L., WU, A. H. & THUN, M. J. 2003. Recreational physical activity and risk of postmenopausal breast cancer in a large cohort of US women. *Cancer Causes Control,* 14**,** 519-29.

PATEL, M., SHAH, T. & AMIN, A. 2007. Therapeutic opportunities in colon-specific drug-delivery systems. *Crit Rev Ther Drug Carrier Syst,* 24**,** 147-202.

PAULUS, W., BAUR, I., DOURS-ZIMMERMANN, M. T. & ZIMMERMANN, D. R. 1996. Differential expression of versican isoforms in brain tumors. *J Neuropathol Exp Neurol,* 55**,** 528-33.

PELICANO, H., LU, W., ZHOU, Y., ZHANG, W., CHEN, Z., HU, Y. & HUANG, P. 2009. Mitochondrial dysfunction and reactive oxygen species imbalance promote breast cancer cell motility through a CXCL14-mediated mechanism. *Cancer Res,* 69**,** 2375-83.

PENC, S. F., POMAHAC, B., WINKLER, T., DORSCHNER, R. A., ERIKSSON, E., HERNDON, M. & GALLO, R. L. 1998. Dermatan sulfate released after injury is a potent promoter of fibroblast growth factor-2 function. *J Biol Chem,* 273**,** 28116-21.

PETRINI, S., TESSA, A., CARROZZO, R., VERARDO, M., PIERINI, R., RIZZA, T. & BERTINI, E. 2003. Human melanoma/NG2 chondroitin sulfate proteoglycan is expressed in the sarcolemma of postnatal human skeletal myofibers. Abnormal expression in merosin-negative and Duchenne muscular dystrophies. *Mol Cell Neurosci,* 23**,** 219-31.

PEYROL, S., RACCURT, M., GERARD, F., GLEYZAL, C., GRIMAUD, J. A. & SOMMER, P. 1997. Lysyl oxidase gene expression in the stromal reaction to in situ and invasive ductal breast carcinoma. *Am J Pathol,* 150**,** 497-507.

PIKE, M. C., KRAILO, M. D., HENDERSON, B. E., CASAGRANDE, J. T. & HOEL, D. G. 1983. 'Hormonal' risk factors, 'breast tissue age' and the age-incidence of breast cancer. *Nature,* 303**,** 767-70.

PIKE, M. C., SPICER, D. V., DAHMOUSH, L. & PRESS, M. F. 1993. Estrogens, progestogens, normal breast cell proliferation, and breast cancer risk. *Epidemiol Rev,* 15**,** 17-35.

PLAAS, A. H., WONG-PALMS, S., ROUGHLEY, P. J., MIDURA, R. J. & HASCALL, V. C. 1997. Chemical and immunological assay of the nonreducing terminal residues of chondroitin sulfate from human aggrecan. *J Biol Chem,* 272**,** 20603-10.

PONDER, B. 2003. *In Hormones, Genes and Cancer.*, New York, Oxford University Press.

PRAT, A. & BASELGA, J. 2008. The role of hormonal therapy in the management of hormonal-receptor-positive breast cancer with co-expression of HER2. *Nat Clin Pract Oncol,* 5**,** 531-42.

PRYDZ, K. & DALEN, K. T. 2000. Synthesis and sorting of proteoglycans. *J Cell Sci,* 113 Pt 2**,** 193-205.

QIAN, B. Z. & POLLARD, J. W. 2010. Macrophage diversity enhances tumor progression and metastasis. *Cell,* 141**,** 39-51.

RECHT, A. 2009. Contralateral prophylactic mastectomy: caveat emptor. *J Clin Oncol,* 27**,** 1347-9.

REISS, M. & BARCELLOS-HOFF, M. H. 1997. Transforming growth factor-beta in breast cancer: a working hypothesis. *Breast Cancer Res Treat,* 45**,** 81-95.

RICCIARDELLI, C., BROOKS, J. H., SUWIWAT, S., SAKKO, A. J., MAYNE, K., RAYMOND, W. A., SESHADRI, R., LEBARON, R. G. & HORSFALL, D. J. 2002. Regulation of stromal versican expression by breast cancer cells and importance to relapse-free survival in patients with node-negative primary breast cancer. *Clin Cancer Res,* 8**,** 1054-60.

RICCIARDELLI, C., MAYNE, K., SYKES, P. J., RAYMOND, W. A., MCCAUL, K., MARSHALL, V. R. & HORSFALL, D. J. 1998. Elevated levels of versican but not decorin predict disease progression in early-stage prostate cancer. *Clin Cancer Res,* 4**,** 963-71.

ROSES, D. F. 2005. *Breast Cancer*, Elsevier.

RUSHTON, J., JIANG, D., SRINIVASAN, A., PIPAS, J. & ROBBINS, P. 1997. Simian virus 40 T antigen can regulate p53-mediated transcription independent of binding p53. *The Journal of Virology,* 71**,** 5620-5623.

RUSSO, A., JEFFREY, P., PATTERN, A., MASSAGUE, J. & PAVLETICH, N. 1996. Crystal structure of the p27KIP1 cylin dependent kinase inhibitor bound to the cyclin A-Cdk2 complex. . *Nature,* 382**,** 325-331.

RUSSO, J. 2004. *Molecular Basis of Breast Cancer,* Berlin; New York, Springer.

RYBAK, M. E., GIMBRONE, M. A., JR., DAVIES, P. F. & HANDIN, R. I. 1989. Interaction of platelet factor four with cultured vascular endothelial cells. *Blood,* 73**,** 1534-9.

SAID, N. & WILLIAMS, E. 2011. Growth factors in induction of epithelial–mesenchymal transition and metastasis. *Cells Tissues Organs,* 193**,** 85-97.

SAIGOH, K., IZUMIKAWA, T., KOIKE, T., SHIMIZU, J., KITAGAWA, H. & KUSUNOKI, S. 2011. Chondroitin beta-1,4-N-acetylgalactosaminyltransferase-1 missense mutations are associated with neuropathies. *J Hum Genet,* 56**,** 143-6.

SAKAI, K., KIMATA, K., SATO, T., GOTOH, M., NARIMATSU, H., SHINOMIYA, K. & WATANABE, H. 2007. Chondroitin sulfate N-acetylgalactosaminyltransferase-1 plays a critical role in chondroitin sulfate synthesis in cartilage. *J Biol Chem,* 282**,** 4152-61.

SAMUELSSON, M., PAZIRANDEH, A. & OKRET, S. 2002. A pro-apoptotic effect of the CDK inhibitor p57(Kip2) on staurosporine-induced apoptosis in HeLa cells. *Biochem Biophys Res Commun,* 296**,** 702-709.

SANDERSON, R. D. 2001. Heparan sulfate proteoglycans in invasion and metastasis. *Semin Cell Dev Biol,* 12**,** 89-98.

SANTRA, M., EICHSTETTER, I. & IOZZO, R. V. 2000. An anti-oncogenic role for decorin. Down-regulation of ErbB2 leads to growth suppression and cytodifferentiation of mammary carcinoma cells. *J Biol Chem,* 275**,** 35153-61.

SATO, T., GOTOH, M., KIYOHARA, K., AKASHIMA, T., IWASAKI, H., KAMEYAMA, A., MOCHIZUKI, H., YADA, T., INABA, N., TOGAYACHI, A., KUDO, T., ASADA, M., WATANABE, H., IMAMURA, T., KIMATA, K. & NARIMATSU, H. 2003. Differential roles of two N-acetylgalactosaminyltransferases, CSGalNAcT-1, and a novel enzyme, CSGalNAcT-2. Initiation and elongation in synthesis of chondroitin sulfate. *J Biol Chem,* 278**,** 3063-71.

SCHAFER, M. & WERNER, S. 2008. Cancer as an overhealing wound: an old hypothesis revisited. *Nat Rev Mol Cell Biol,* 9**,** 628-38.

SCHUELER-FURMAN, O., GLICK, E., SEGOVIA, J. & LINIAL, M. 2006. Is GAS1 a co-receptor for the GDNF family of ligands? *Trends in pharmacological sciences,* 27**,** 72-77.

SCHWAMBORN, J., BEREZIKOV, E. & KNOBLICH, J. 2009. The TRIM-NHL protein TRIM32 activates microRNAs and prevents self-renewal in mouse neural progenitors. *Cell,* 136**,** 913-925.

SEIDMAN, H., GELB, S. K., SILVERBERG, E., LAVERDA, N. & LUBERA, J. A. 1987. Survival experience in the Breast Cancer Detection Demonstration Project. *CA Cancer J Clin,* 37**,** 258-90.

SERRANO, M., LEE, H., CHIN, L. & AL., E. 1996. Role of the INK4a locus in tumor suppression and cell mortality. *Cell* 85**,** 27-37.

SHERR, C. & ROBERT, J. 1999. CDK inhibitors: positive and negative regulators of G1-phase progression. *Genes and development,* 13**,** 1501-1512.

SHERR, C. & ROBERT, J. 2001. CDK inhibitors: positive and negative regulators of G1-phase progression. *Genes and development,* 13**,** 1501-1512.

SHIELDS, J., PRUITT, K., MCFALL, A., SHAUB, A. & DER, C. 2000. Understanding Ras: 'it ain't over 'til it's over'. *Trends in Cell Biology,* 10**,** 147-154.

SHORT, K. & COX, T. 2006. Subclassification of the RBCC/TRIM superfamily reveals a novel motif necessary for microtubule binding. *The Journal of biological chemistry,* 281**,** 8970-8980.

SHURIN, G. V., FERRIS, R. L., TOURKOVA, I. L., PEREZ, L., LOKSHIN, A., BALKIR, L., COLLINS, B., CHATTA, G. S. & SHURIN, M. R. 2005. Loss of new chemokine CXCL14 in tumor tissue is associated with low infiltration by dendritic cells (DC), while restoration of human CXCL14 expression in tumor cells causes attraction of DC both in vitro and in vivo. *J Immunol,* 174**,** 5490-8.

SINGLETARY, K. W. & GAPSTUR, S. M. 2001. Alcohol and breast cancer: review of epidemiologic and experimental evidence and potential mechanisms. *JAMA,* 286**,** 2143-51.

SKANDALIS, S. S., KLETSAS, D., KYRIAKOPOULOU, D., STAVROPOULOS, M. & THEOCHARIS, D. A. 2006. The greatly increased amounts of accumulated versican and decorin with specific post-translational modifications may be closely associated with the malignant phenotype of pancreatic cancer. *Biochim Biophys Acta,* 1760**,** 1217-25.

SKANDALIS, S. S., LABROPOULOU, V. T., RAVAZOULA, P., LIKAKI-KARATZA, E., DOBRA, K., KALOFONOS, H. P., KARAMANOS, N. K. & THEOCHARIS, A. D. 2011. Versican but not decorin accumulation is related to malignancy in mammographically detected high density and malignant-appearing microcalcifications in non-palpable breast carcinomas. *BMC Cancer,* 11**,** 314.

SLEEMAN, M. A., FRASER, J. K., MURISON, J. G., KELLY, S. L., PRESTIDGE, R. L., PALMER, D. J., WATSON, J. D. & KUMBLE, K. D. 2000. B cell- and monocyte-activating chemokine (BMAC), a novel non-ELR alpha-chemokine. *Int Immunol,* 12**,** 677-89.

SMITH, F. O., RAUCH, C., WILLIAMS, D. E., MARCH, C. J., ARTHUR, D., HILDEN, J., LAMPKIN, B. C., BUCKLEY, J. D., BUCKLEY, C. V., WOODS, W. G., DINNDORF, P. A., SORENSEN, P., KERSEY, J., HAMMOND, D. & BERNSTEIN, I. D. 1996. The human homologue of rat NG2, a chondroitin sulfate proteoglycan, is not expressed on the cell surface of normal hematopoietic cells but is expressed by acute myeloid leukemia blasts from poor-prognosis patients with abnormalities of chromosome band 11q23. *Blood,* 87**,** 1123-33.

SMITH, R. A., SASLOW, D., SAWYER, K. A., BURKE, W., COSTANZA, M. E., EVANS, W. P., 3RD, FOSTER, R. S., JR., HENDRICK, E., EYRE, H. J., SENER, S., AMERICAN CANCER SOCIETY HIGH-RISK WORK, G., AMERICAN CANCER SOCIETY SCREENING OLDER WOMEN WORK, G., AMERICAN CANCER SOCIETY MAMMOGRAPHY WORK, G., AMERICAN CANCER SOCIETY PHYSICAL EXAMINATION WORK, G., AMERICAN CANCER SOCIETY NEW TECHNOLOGIES WORK, G. & AMERICAN CANCER SOCIETY BREAST CANCER ADVISORY, G. 2003. American Cancer Society guidelines for breast cancer screening: update 2003. *CA Cancer J Clin,* 53**,** 141-69.

STARNES, T., RASILA, K. K., ROBERTSON, M. J., BRAHMI, Z., DAHL, R., CHRISTOPHERSON, K. & HROMAS, R. 2006. The chemokine CXCL14 (BRAK) stimulates activated NK cell migration: implications for the downregulation of CXCL14 in malignancy. *Exp Hematol,* 34**,** 1101-5.

STAVROS, A. T., THICKMAN, D., RAPP, C. L., DENNIS, M. A., PARKER, S. H. & SISNEY, G. A. 1995. Solid breast nodules: use of sonography to distinguish between benign and malignant lesions. *Radiology,* 196**,** 123-34.

STEEG, P. & ZHOU, Q. 1998. Cyclins and breast cancer. *Breast Cancer Research and Treatment,* 52**,** 17-28.

SUGAHARA, K. & KITAGAWA, H. 2000. Recent advances in the study of the biosynthesis and functions of sulfated glycosaminoglycans. *Curr Opin Struct Biol,* 10**,** 518-27.

SUGAHARA, K., YAMASHINA, I., DE WAARD, P., VAN HALBEEK, H. & VLIEGENTHART, J. F. 1988. Structural studies on sulfated glycopeptides from the carbohydrate-protein linkage region of chondroitin 4-sulfate proteoglycans of swarm rat chondrosarcoma. Demonstration of the structure Gal(4-O-sulfate)beta 1-3Gal beta 1-4XYL beta 1-O-Ser. *J Biol Chem,* 263**,** 10168-74.

SUGIYAMA, T., SHIMUZU, S., MATSUOKA, Y., YONEDA, Y. & TSUJIMOTO, Y. 2002. Activation of mitochondrial voltage-dependent anion channel by apro-apoptotic BH3-only protein Bim. *Oncogene,* 21**,** 4944-4956.

SULLIVAN, C., TREMBLAY, J., FEWELL, S., LEWIS, J., BRODSKY, J. & PIPAS, J. 2000. Species-specific elements in the large T-antigen J domain are required for cellular transformation and DNA replication by simian virus 40. *Molecular and Cellular Biology,* 20**,** 5749-5757.

SUN, Y., SHEN, S., LIU, X., TANG, H., WANG, Z., YU, Z., LI, X. & WU, M. 2014. miR-429 inhibits cells growth and invasion and regulates EMT-related marker genes by targeting Onecut2 in colorectal carcinoma. *Molecular and cellular biochemistry,* 390**,** 19-30.

SUWIWAT, S., RICCIARDELLI, C., TAMMI, R., TAMMI, M., AUVINEN, P., KOSMA, V. M., LEBARON, R. G., RAYMOND, W. A., TILLEY, W. D. & HORSFALL, D. J. 2004. Expression of extracellular matrix components versican, chondroitin sulfate, tenascin, and hyaluronan, and their association with disease outcome in node-negative breast cancer. *Clin Cancer Res,* 10**,** 2491-8.

SVENSSON, K. J., CHRISTIANSON, H. C., KUCHARZEWSKA, P., FAGERSTROM, V., LUNDSTEDT, L., BORGQUIST, S., JIRSTROM, K. & BELTING, M. 2011. Chondroitin sulfate expression predicts poor outcome in breast cancer. *Int J Oncol,* 39**,** 1421-8.

TAIT, S. & GREEN, D. 2010. Mitochondria and cell death: outer membrane permeabilization and beyond. *Nature Reviews Molecular Cell Biology,* 11**,** 621-632.

TAVASSOLI F, D. P. 2003. Pathology and genetics of tumours of the breast and female genital organs.

TEN DAM, G. B., VAN DE WESTERLO, E. M., PURUSHOTHAMAN, A., STAN, R. V., BULTEN, J., SWEEP, F. C., MASSUGER, L. F., SUGAHARA, K. & VAN KUPPEVELT, T. H. 2007. Antibody GD3G7 selected against embryonic glycosaminoglycans defines chondroitin sulfate-E domains highly

up-regulated in ovarian cancer and involved in vascular endothelial growth factor binding. *Am J Pathol,* 171**,** 1324-33.

TERRY, M. B., ZHANG, F. F., KABAT, G., BRITTON, J. A., TEITELBAUM, S. L., NEUGUT, A. I. & GAMMON, M. D. 2006. Lifetime alcohol intake and breast cancer risk. *Ann Epidemiol,* 16**,** 230-40.

TEVETHIA, M., BONNEAU, R., GRIFFITH, J. & MYLIN, L. 1997. A simian virus 40 large T-antigen segment containing amino acids 1 to 127 and expressed under the control of the rat elastase-1 promoter produces pancreatic acinar carcinomas in transgenic mice. *The Journal of Virology,* 71**,** 8157-8166.

THEOCHARIS, A. D., TSOLAKIS, I., TZANAKAKIS, G. N. & KARAMANOS, N. K. 2006. Chondroitin sulfate as a key molecule in the development of atherosclerosis and cancer progression. *Adv Pharmacol,* 53**,** 281-95.

THEOCHARIS, A. D., VYNIOS, D. H., PAPAGEORGAKOPOULOU, N., SKANDALIS, S. S. & THEOCHARIS, D. A. 2003. Altered content composition and structure of glycosaminoglycans and proteoglycans in gastric carcinoma. *Int J Biochem Cell Biol,* 35**,** 376-90.

THIERY, J., ACLOQUE, H., HUANG, R. & NIETO, M. 2009. Epithelial–mesenchymal transition in development and disease. *Cell* 139**,** 871-890.

TIMPL, R. & BROWN, J. C. 1996. Supramolecular assembly of basement membranes. *Bioessays,* 18**,** 123-32.

TOOLE, B. P. 2001. Hyaluronan in morphogenesis. *Semin Cell Dev Biol,* 12**,** 79-87.

TRALHAO, J. G., SCHAEFER, L., MICEGOVA, M., EVARISTO, C., SCHONHERR, E., KAYAL, S., VEIGA-FERNANDES, H., DANEL, C., IOZZO, R. V., KRESSE, H. & LEMARCHAND, P. 2003. In vivo selective and distant killing of cancer cells using adenovirus-mediated decorin gene transfer. *FASEB J,* 17**,** 464-6.

TROUP, S., NJUE, C., KLIEWER, E. V., PARISIEN, M., ROSKELLEY, C., CHAKRAVARTI, S., ROUGHLEY, P. J., MURPHY, L. C. & WATSON, P. H. 2003. Reduced expression of the small leucine-rich proteoglycans, lumican, and decorin is associated with poor outcome in node-negative invasive breast cancer. *Clin Cancer Res,* 9**,** 207-14.

TROWBRIDGE, J. M. & GALLO, R. L. 2002. Dermatan sulfate: new functions from an old glycosaminoglycan. *Glycobiology,* 12**,** 117R-25R.

TURLEY, E. A., NOBLE, P. W. & BOURGUIGNON, L. Y. 2002. Signaling properties of hyaluronan receptors. *J Biol Chem,* 277**,** 4589-92.

TUTTLE, T. M., HABERMANN, E. B., GRUND, E. H., MORRIS, T. J. & VIRNIG, B. A. 2007. Increasing use of contralateral prophylactic mastectomy

for breast cancer patients: a trend toward more aggressive surgical treatment. *J Clin Oncol,* 25**,** 5203-9.

TUTTLE, T. M., JAROSEK, S., HABERMANN, E. B., ARRINGTON, A., ABRAHAM, A., MORRIS, T. J. & VIRNIG, B. A. 2009. Increasing rates of contralateral prophylactic mastectomy among patients with ductal carcinoma in situ. *J Clin Oncol,* 27**,** 1362-7.

UENO, M., YAMADA, S., ZAKO, M., BERNFIELD, M. & SUGAHARA, K. 2001. Structural characterization of heparan sulfate and chondroitin sulfate of syndecan-1 purified from normal murine mammary gland epithelial cells. Common phosphorylation of xylose and differential sulfation of galactose in the protein linkage region tetrasaccharide sequence. *J Biol Chem,* 276**,** 29134-40.

UYAMA, T., KITAGAWA, H., TAMURA, J. & SUGAHARA, K. 2002. Molecular cloning and expression of human chondroitin N-acetylgalactosaminyltransferase - The key enzyme for chain initiation and elongation of chondroitin/dermatan sulfate on the protein linkage region tetrasaccharide shared by heparin/heparan sulfate. *Journal of Biological Chemistry,* 277**,** 8841-8846.

UYAMA, T., KITAGAWA, H., TANAKA, J., TAMURA, J., OGAWA, T. & SUGAHARA, K. 2003. Molecular cloning and expression of a second chondroitin N-acetylgalactosaminyltransferase involved in the initiation and elongation of chondroitin/dermatan sulfate. *J Biol Chem,* 278**,** 3072-8.

VALIYEVA, F., JIANG, F., ELMAADAWI, A., MOUSSA, M., YEE, S. P., RAPTIS, L., IZAWA, J. I., YANG, B. B., GREENBERG, N. M., WANG, F. & XUAN, J. W. 2011. Characterization of the oncogenic activity of the novel TRIM59 gene in mouse cancer models. *Mol Cancer Ther,* 10**,** 1229-40.

VIALE, G., REGAN, M. M., MAIORANO, E., MASTROPASQUA, M. G., DELL'ORTO, P., RASMUSSEN, B. B., RAFFOUL, J., NEVEN, P., OROSZ, Z., BRAYE, S., OHLSCHLEGEL, C., THURLIMANN, B., GELBER, R. D., CASTIGLIONE-GERTSCH, M., PRICE, K. N., GOLDHIRSCH, A., GUSTERSON, B. A. & COATES, A. S. 2007. Prognostic and predictive value of centrally reviewed expression of estrogen and progesterone receptors in a randomized trial comparing letrozole and tamoxifen adjuvant therapy for postmenopausal early breast cancer: BIG 1-98. *J Clin Oncol,* 25**,** 3846-52.

VIJAYAGOPAL, P., FIGUEROA, J. E. & LEVINE, E. A. 1998. Altered composition and increased endothelial cell proliferative activity of proteoglycans isolated from breast carcinoma. *J Surg Oncol,* 68**,** 250-4.

VLACHOS, P. & JOSEPH, B. 2009. The Cdk inhibitor p57(Kip2) controls LIM-kinase 1 activity and regulates actin cytoskeleton dynamics. *Oncogene,* 28**,** 4175-4188.

VLACHOS, P., NYMAN, U., HAJJI, N. & JOSEPH, B. 2007. The cell cycle inhibitor p57(Kip2) promotes cell death via the mitochondrial apoptotic pathway. *Cell death and differentiation,* 14**,** 1497-1507.

VLODAVSKY, I., FOLKMAN, J., SULLIVAN, R., FRIDMAN, R., ISHAI-MICHAELI, R., SASSE, J. & KLAGSBRUN, M. 1987. Endothelial cell-derived basic fibroblast growth factor: synthesis and deposition into subendothelial extracellular matrix. *Proc Natl Acad Sci U S A,* 84**,** 2292-6.

VOGEL, K. G. & HEINEGARD, D. 1985. Characterization of proteoglycans from adult bovine tendon. *J Biol Chem,* 260**,** 9298-306.

VOGEL, K. G., PAULSSON, M. & HEINEGARD, D. 1984. Specific inhibition of type I and type II collagen fibrillogenesis by the small proteoglycan of tendon. *Biochem J,* 223**,** 587-97.

VOGEL, V. G., COSTANTINO, J. P., WICKERHAM, D. L., CRONIN, W. M., CECCHINI, R. S., ATKINS, J. N., BEVERS, T. B., FEHRENBACHER, L., PAJON, E. R., WADE, J. L., 3RD, ROBIDOUX, A., MARGOLESE, R. G., JAMES, J., RUNOWICZ, C. D., GANZ, P. A., REIS, S. E., MCCASKILL-STEVENS, W., FORD, L. G., JORDAN, V. C., WOLMARK, N., NATIONAL SURGICAL ADJUVANT, B. & BOWEL, P. 2010. Update of the National Surgical Adjuvant Breast and Bowel Project Study of Tamoxifen and Raloxifene (STAR) P-2 Trial: Preventing breast cancer. *Cancer Prev Res (Phila),* 3**,** 696-706.

VRHOVAC, R., DELMER, A., TANG, R., MARIE, J., ZITTOUN, R. & AJCHENBAUM-CYMBALISTA, F. 1998. Prognostic significance of the cell cycle inhibitor p27Kip1 in chronic B-cell lymphocytic leukemia. *Blood,* 91**,** 4694-4700.

WALTER-YOHRLING, J., CAO, X., CALLAHAN, M., WEBER, W., MORGENBESSER, S., MADDEN, S. L., WANG, C. & TEICHER, B. A. 2003. Identification of genes expressed in malignant cells that promote invasion. *Cancer Res,* 63**,** 8939-47.

WANG, L., HEIDT, D., LEE, C., YANG, H., LOGSDON, C., ZHANG, L., FEARON, E., LJUNGMAN, M. & SIMEONE, D. 2009. Oncogenic function of ATDC in pancreatic cancer through Wnt pathway activation and β-catenin stabilization. *Cancer cell,* 15**,** 207-219.

WATANABE, J., SATO, H., KANAI, T., KAMATA, Y., JOBO, T., HATA, H., FUJISAWA, T., OHNO, E., KAMEYA, T. & KURAMOTO, H. 2002. Paradoxical expression of cell cycle inhibitor p27 in endometrioid adenocarcinomas of the uterine corpus with proliferation and clinicopathological parameters. *Btritish Journal of Cancer,* 87**,** 81-85.

WATANABE, Y., TAKEUCHI, K., HIGA ONAGA, S., SATO, M., TSUJITA, M., ABE, M., NATSUME, R., LI, M., FURUICHI, T., SAEKI, M., IZUMIKAWA, T., HASEGAWA, A., YOKOYAMA, M., IKEGAWA, S., SAKIMURA, K., AMIZUKA, N., KITAGAWA, H. & IGARASHI, M. 2010.

Chondroitin sulfate N-acetylgalactosaminyltransferase-1 is required for normal cartilage development. *Biochem J,* 432**,** 47-55.

WATERS, E. A., CRONIN, K. A., GRAUBARD, B. I., HAN, P. K. & FREEDMAN, A. N. 2010. Prevalence of tamoxifen use for breast cancer chemoprevention among U.S. women. *Cancer Epidemiol Biomarkers Prev,* 19**,** 443-6.

WEGROWSKI, Y. & MAQUART, F. X. 2004. Involvement of stromal proteoglycans in tumour progression. *Crit Rev Oncol Hematol,* 49**,** 259-68.

WEI, M., ZONG, W., CHENG, E. & AL., E. 2001. Proapoptotic BAX and BAK: a requisite gateway to mitochondrial dysfunction and death. *Science,* 292**,** 727-730.

WEI, P. C., LO, W. T., SU, M. I., SHEW, J. Y. & LEE, W. H. 2012. Non-targeting siRNA induces NPGPx expression to cooperate with exoribonuclease XRN2 for releasing the stress. *Nucleic Acids Res,* 40**,** 323-32.

WEISS, B., BOLLAG, G. & SHANNON, K. 1999. Hyperactive Ras as a therapeutic target in neurofibromatosis type 1. *American journal of medical genetics,* 89**,** 14-22.

WENTE, M. N., MAYER, C., GAIDA, M. M., MICHALSKI, C. W., GIESE, T., BERGMANN, F., GIESE, N. A., BUCHLER, M. W. & FRIESS, H. 2008. CXCL14 expression and potential function in pancreatic cancer. *Cancer Lett,* 259**,** 209-17.

WHITE, E., GREEN, D. R. & LETAI, A. G. 2015. Apoptotis, necrosis and autophagy. *The molecular basis of cancer.* 4 ed. Philadelphia, PA: Saunders/Elsevier.

WILKING, N., RUTQVIST, L. E., CARSTENSEN, J., MATTSSON, A. & SKOOG, L. 1992. Prognostic significance of axillary nodal status in primary breast cancer in relation to the number of resected nodes. Stockholm Breast Cancer Study Group. *Acta Oncol,* 31**,** 29-35.

WILLIS, S., FLETCHER, J., KAUFMANN, T. & AL., E. 2007. Apoptosis initiated when BH3 ligands engage multiple Bcl-2 homologs, not Bax or Bak. *Science,* 315**,** 856-859.

WILSON, B. S., RUBERTO, G. & FERRONE, S. 1983. Immunochemical characterization of a human high molecular weight--melanoma associated antigen identified with monoclonal antibodies. *Cancer Immunol Immunother,* 14**,** 196-201.

WOLF, B. & GREEN, D. 1999. Suicidal tendencies: apoptotic cell death by caspase family proteinases. *The Journal of Biological Chemistry,* 274**,** 20049-20052.

WOLF, K. & FRIEDL, P. 2006. Molecular mechanisms of cancer cell invasion and plasticity. *British journal of dermatology,* 154**,** 11-15.

XU, T., BIANCO, P., FISHER, L. W., LONGENECKER, G., SMITH, E., GOLDSTEIN, S., BONADIO, J., BOSKEY, A., HEEGAARD, A. M., SOMMER, B., SATOMURA, K., DOMINGUEZ, P., ZHAO, C., KULKARNI, A. B., ROBEY, P. G. & YOUNG, M. F. 1998. Targeted disruption of the biglycan gene leads to an osteoporosis-like phenotype in mice. *Nat Genet,* 20**,** 78-82.

YADA, T., SATO, T., KASEYAMA, H., GOTOH, M., IWASAKI, H., KIKUCHI, N., KWON, Y. D., TOGAYACHI, A., KUDO, T., WATANABE, H., NARIMATSU, H. & KIMATA, K. 2003. Chondroitin sulfate synthase-3. Molecular cloning and characterization. *J Biol Chem,* 278**,** 39711-25.

YAMAGATA, M., SAGA, S., KATO, M., BERNFIELD, M. & KIMATA, K. 1993. Selective distributions of proteoglycans and their ligands in pericellular matrix of cultured fibroblasts. Implications for their roles in cell-substratum adhesion. *J Cell Sci,* 106 (Pt 1)**,** 55-65.

YAMAGUCHI, Y., MANN, D. M. & RUOSLAHTI, E. 1990. Negative regulation of transforming growth factor-beta by the proteoglycan decorin. *Nature,* 346**,** 281-4.

YAMAUCHI, S., MITA, S., MATSUBARA, T., FUKUTA, M., HABUCHI, H., KIMATA, K. & HABUCHI, O. 2000. Molecular cloning and expression of chondroitin 4-sulfotransferase. *J Biol Chem,* 275**,** 8975-81.

YANG, E., ZHA, J., JOCKEL, J., BOISE, L. H., THOMPSON, C. B. & KORSMEYER, S. J. 1995. Bad, a heterodimeric partner for Bcl-XL and Bcl-2, displaces Bax and promotes cell death. *Cell,* 80**,** 285-91.

YIP, G. W., SMOLLICH, M. & GOTTE, M. 2006. Therapeutic value of glycosaminoglycans in cancer. *Mol Cancer Ther,* 5**,** 2139-48.

ZALVIDE, J., STUBDAL, H. & DECAPRIO, J. 1998. The J Domain of Simian Virus 40 Large T Antigen Is Required To Functionally Inactivate RB Family Proteins. *Molecular and Cellular Biology,* 18**,** 1408-1415.

ZAMZAMI, N., EL HAMEL, C., MAISSE, C., BRENNER, C., MUNOZ-PINEDO, C., BELZACQ, A., COSTANTINI, P., VIEIRA, H., LOEFFLER, M., MOLLE, G. & KOROEMER, G. 2000. Bid acts on the permeability transition pore complex to induce apoptosis. *Oncogene,* 19**,** 6342-6350.

ZARCO, N., GONZALEZ-RAMIREZ, R., GONZALEZ, R. & SEGOVIA, J. 2012. GAS1 induces cell death through an intrinsic apoptotic pathway. *Apoptosis,* 17**,** 627-635.

ZENG, J., YANG, X., CHENG, L., LIU, R., LEI, Y., DONG, D., LI, F., LAU, Q. C., DENG, L., NICE, E. C., XIE, K. & HUANG, C. 2013. Chemokine

CXCL14 is associated with prognosis in patients with colorectal carcinoma after curative resection. *J Transl Med,* 11**,** 6.

ZHANG, S. M., LEE, I. M., MANSON, J. E., COOK, N. R., WILLETT, W. C. & BURING, J. E. 2007. Alcohol consumption and breast cancer risk in the Women's Health Study. *Am J Epidemiol,* 165**,** 667-76.

ZIMMERMANN, D. R., DOURS-ZIMMERMANN, M. T., SCHUBERT, M. & BRUCKNER-TUDERMAN, L. 1994. Versican is expressed in the proliferating zone in the epidermis and in association with the elastic network of the dermis. *J Cell Biol,* 124**,** 817-25.

ZLOTNIK, A. & YOSHIE, O. 2000. Chemokines: a new classification system and their role in immunity. *Immunity,* 12**,** 121-7.

ZONG, W., LINDSTEN, T., ROSS, A., MACGREGOR, G. & THOMPSON, C. 2001. BH3-only proteins that bind pro-survival Bcl-2 family members fail to induce apoptosis in the absence of Bax and Bak. *Genes & Development,* 15**,** 1481-1486.